COUNTERCURRENT CHROMATOGRAPHY OF PROTEINS USING AQUEOUS TWO – PHASE SYSTEMS

A thesis submitted for the degree of Doctor of Philosophy

By

Emma Catherine Bourton

Brunel Institute for Bioengineering
Brunel University
April 2008

Abstract

The biotechnology industry requires high – capacity protein manufacturing processes that retain protein functionality. Large – scale countercurrent J – type centrifuges have been developed by the Brunel Institute for Bioengineering that successfully purify small organic molecules using aqueous – organic phase systems. Aqueous two – phase systems (ATPS) have been used historically to purify bio-molecules whilst retaining their biological function. This thesis focuses on extending CCC to the separation of proteins, using a model ATPS of PEG-1000 and potassium dihydrogen phosphate to separate a mixture of lysozyme and myoglobin.

Initial studies were on the behaviour of this phase system in a J – type CCC centrifuge fitted with a multilayer column; the variable parameters examined were centrifuge rotational speed, mobile phase flow rate and direction, and type of mobile phase. A set of optimum conditions were identified that gave good retention and stability of the phases in the column.

These conditions were applied to separate a mixture of the proteins lysozyme and myoglobin in the same centrifuge. However, the proteins did not elute as predicted from their equilibrium distribution ratios. It appears that the wave – like mixing and settling behaviour of the phases in the centrifuge was insufficient for the proteins to achieve equilibrium partitioning.

A centrifugal partition chromatography (CPC) centrifuge was introduced to the study. This provided full protein separation, credited to the cascade phase mixing created by this design of centrifuge. The experimental parameters were used in an experiment on a pilot – scale CPC instrument.

The CPC study was extended to the isolation of a target protein (phosphomannose isomerase) from a fermentation supernatant. CPC gave partial purification of the protein with retention of enzyme activity.

This thesis demonstrates the importance of phase mixing in CCC, which has led to a new column design by BIB with the potential of industrial – scale protein purifications.

Contents

Acknowledgements

A PhD thesis is, by definition, the product of work done by one individual. However, the process would be that much more difficult for the student without the guidance and support of other people – and it has certainly been so in my case. I would like to thank Professors Derek Fisher and Ian Sutherland for their invaluable suggestions and guidance regarding the direction of the project, and for tuition on the science and engineering aspects involved. My colleagues at Brunel Institute for Bioengineering also deserve a mention, especially: Mrs Margaret Pearce, for organisational and moral support; Dr Ian Garrard, for all things laboratory, especially regarding HPLC; Dr Hugh Guan, for many interesting discussions on the work; Mr David Hawes, for patiently making another CCC coil after I had wrecked the original during one of my less successful experiments.
Syngenta were the industrial sponsors of the project, and thanks are given to the staff at Jealott's Hill International Research Centre, Berkshire, especially: Mr Peter Massey, for overall project management and advice; Dr Daniel Fox, for guidance with the protein aspects of the project; Mrs Sheila Attenborough, for practical help with the PMI work.
The Division of Biosciences at Brunel kindly allowed me free rein on many pieces of their equipment in relation to my work. Mr Derek Barnes (Technician, Division of Biosciences) happily provided his expertise with the protein assays in the project. Dr Christopher Parris, acting as an unofficial (but very welcome) extra supervisor, provided invaluable scientific insights into the work, not to mention much – needed encouragement when the going got tough.
My parents have exhibited infinite patience towards me during the last three years. In particular I have to thank them for always preparing an evening meal for me, despite them never knowing exactly what time it would be consumed.
Lastly, I'd like to thank Ms Louise Baddeley for personal guidance that has undoubtedly helped me complete my studies, and Dr Stephen Vaughan-Smith; without his unfailing support over the last 15 years I would not be where I am today.

Abbreviations and Nomenclature

ACN	Acetonitrile
ATPS	Aqueous two – phase system
BIB	Brunel Institute for Bioengineering
BSA	Bovine serum albumin
CCC	Countercurrent chromatography
CCD	Countercurrent distribution
CPC	Centrifugal partition chromatography
CV	Column volume
D	Distribution ratio
DE	Dynamic Extractions Limited
DNA	Deoxyribonucleic acid
HPLC	High performance liquid chromatography
K	Partition coefficient
K_2HPO_4	Dipotassium hydrogen phosphate
LP	Lower phase
MP	Mobile phase
PEG	Polyethylene glycol
PFA	Perfluoralkoxy
PTFE	Polytetrafluoroethylene (Teflon®)
r	Radius of the planetary bobbin
R	Radius of the main (sun) rotor
rpm	Revolutions per minute
SDS	Sodium dodecyl sulphate
Sf	Stationary phase retention
SP	Stationary phase
Tris	Trishydroxymethylaminomethane
UP	Upper phase
UV	Ultraviolet (light)
β	Ratio of r/R

Chapter 1 – Introduction

1.1. Aqueous Two – Phase Systems

1.1.1. History of Aqueous Two – Phase Systems

Aqueous two – phase systems (ATPS) were first reported by the Dutch microbiologist Beijerinck, who had observed that aqueous solutions of gelatine and agar (starch) formed two liquid phases when mixed together (Beijerinck, 1896). The phenomenon was then largely overlooked until the Swedish biochemist Per-Åke Albertsson experimented with polyethylene glycol (PEG) in an attempt to desorb chloroplast particles from hydroxylapatite grains suspended in potassium phosphate buffer during a chromatography experiment. Albertsson noted that the hydroxylapatite had been purged of chloroplasts, and that the PEG and salt buffer had formed two liquid layers. The chloroplasts themselves had concentrated in the liquid layer present on top of the phosphate buffer layer. This was the first experiment in which an aqueous liquid – liquid polymer two – phase system had been used for the partition of cell particles. Albertsson conducted further experiments using this PEG – potassium phosphate system with microorganisms (*e.g. Serratia marcescens* and *Chlorella pyrenoidosa*) and various types of plant cell particles (*e.g.* starch grains and chloroplast fragments). He observed that partition was selective, and that the particles collected in one of the two phases or at the interface (Albertsson, 1956a, 1956b).

Over the following two decades, Albertsson and collaborators developed and applied several types of aqueous liquid – liquid polymer two – phase systems to separating viruses, cells, and cell organelles. The partitioning of proteins in these phase systems was also investigated; a successful countercurrent distribution (CCD) experiment using a PEG – dextran system was carried out, opening the way for ATPS purification of proteins (Albertsson and Nyns, 1959, 1961) (refer to Section 1.3.1 for an explanation of CCD).

Work was also conducted during this period on elucidating the factors governing partition, such as molecular weight of the polymers (Albertsson, 1958a, 1958b), ionic composition (Albertsson and Nyns, 1959, 1961), and the relationship between the partition coefficient and the surface area of proteins and viruses (Albertsson, 1958b, 1962b; Albertsson and Frick, 1960). It was discovered that small changes in the ratio of ions within a system caused large shifts in the

partition of proteins, nucleic acids and cell particles. It had been assumed that in a polymer – polymer system (such as PEG – dextran) the salts partitioned equally between the phases. Work by Johansson (1970a) showed some salts partitioned more equally than others; this inequality in distribution of ions created a small electrical potential between the phases (Albertsson, 1971a) that had a strong influence on the partition of charged entities such as proteins, nucleic acids and cell particles.

Researchers during this period also noted the potential of scaling – up the partitioning process. A PEG – dextran system was used to purify a DNA polymerase from a bacterial cell extract (Okazaki and Kornberg, 1964); this example was used as a model for large – scale biotechnological application of phase partition to enzyme purification. The experiments on chloroplasts and cells demonstrated that the phase systems used are mild towards fragile organelles and cells. This is due to their high water content, low interfacial tension (Rydén and Albertsson, 1971), and a general protective effect of the polymers.

By the early 1970s, the basic knowledge of ATPS had sufficiently developed for the method to be applied in the fields of biochemistry, molecular biology, cell biology and biotechnology (refer to Section 1.1.3). Research into the fundamentals of these systems continued, covering such areas as the role of water structure on phase separation (Gupta *et al*, 2002), the kinetics of phase separation (Kaul *et al*, 1995; Solano-Castillo and Rito-Palomares, 2000), the thermodynamics of phase separation (Großmann and Maurer, 1995; Großmann *et al*, 1995; Zafarani-Moattar and Sadeghi, 2001), and how temperature affected phase equilibrium (Hartounian *et al*, 1993). Physicochemical properties of phase systems were also reported, such as interfacial tension (Mishima *et al*, 1998), phase composition, viscosity, and density (Snyder *et al*, 1992).

1.1.2. Definition and Examples of Aqueous Two – Phase Systems

Aqueous two – phase systems can be defined as a mixture of two polymers (or one polymer and a salt) present above certain concentrations in an aqueous medium that separates into two phases (Hatti-Kaul, 2000). These systems can be further subdivided, depending on the nature of the polymer(s) and the identity of the salt and are extensive in number and type; some examples are given in Table 1.1.2a.

Table 1.1.2a: Examples of aqueous two – phase systems (Albertsson, 1971b).

Type of Phase System	Examples
Non – ionic polymer: Non – ionic polymer	(1) Polyethylene glycol: Dextran (2) Methylcellulose: Dextran
Polyelectrolyte: Non – ionic polymer	Sodium carboxymethyldextran: Polyvinylalcohol
Polyelectrolyte: Polyelectrolyte	Sodium dextran sulphate: Sodium carboxymethylcellulose
Polymer: Low Molecular Weight Component	(1) Polyethylene glycol: Potassium phosphate (2) Polypropylene glycol: Glucose

In recent years, particular attention has been given to the use of thermosensitive polymers *e.g.* poly(ethylene oxide) (PEO) and poly(propylene oxide) (PPO). The PEO – PPO random copolymer has a decreased solubility in water at higher temperatures. When heated above the lower critical solution temperature (LCST), this system will form into two layers: a lower layer consisting of PEO – PPO, and an aqueous upper layer. The temperature at which this occurs is known as the cloud point (CP) of the polymer. Using these systems has several advantages. The low salt concentrations involved reduces the risk of salting out the protein, the polymers can be recycled, and the target protein is recovered in an aqueous solution, which facilitates downstream processing (Li and Peeples, 2004). Examples of these systems are given in Table 1.1.2b.

Table 1.1.2b: Examples of the use of ATPS containing thermosensitive polymers.

Phase System(s)	Protein(s)	Reference
PEO-4000: dextran, Ucon 50-HB-5100: dextran	Ribonuclease A, Myoglobin	Carlsson *et al* (1993)
$EO_{20}PO_{80}$: dextran T-500	Glucose-6-phosphate dehydrogenase, Hexokinase, 3-phosphoglycerate kinase	Alred *et al* (1994)
Ucon 50-HB-5100: hydroxypropyl starch, $EO_{30}PO_{70}$: hydroxypropyl starch	Bovine serum albumin, Lysozyme, β-lactoglobulin A, Myoglobin, Cytochrome *c*	Berggren *et al* (1995)
$EO_{30}PO_{70}$: dextran T-500, Ucon 50-HB-5100: dextran T-500	Bovine serum albumin, Lysozyme	Johansson *et al* (1996)
5.0% $EO_{50}PO_{50}$: 5.0% HM-EOPO (hydrophobically modified copolymer of EO and PO)	Bovine serum albumin, Lysozyme, Apolipoprotein A-1	Persson *et al* (1999)
$EO_{20}PO_{80}$: Na_2HPO_4	β-xylosidase	Pan and Li (2001)
7.1% dextran: 6.8% $EO_{30}PO_{70}$ 9.0% dextran: 9.0% $EO_{30}PO_{70}$	α-Chymotrypsinogen A, Cytochrome *c*, Ribonuclease-A, α-Lactalbumin, Lysozyme, Myoglobin, α-Chymotrypsin	Berggren *et al* (2002)
7.1% dextran: 6.8% $EO_{30}PO_{70}$	Lactate dehydrogenase	Fexby and Bülow (2002)
Ucon 50-HB-5100 (random copolymer of 50% EO + 50% PO): polyvinyl alcohol, Ucon 50-HB-5100: hydroxypropyl starch, Ucon 50-HB-5100: $(NH_4)_2SO_4$	Endo-polygalacturonase	Pereira *et al* (2003)
20.0% PEO-PPO-2500: 7.0-15.0% $(NH_4)_2SO_4$	Recombinant thermostable α-amylase (MJA1)	Li and Peeples (2004)
Random copolymer EOPO: maltodextrin	Bovine serum albumin, Lysozyme, Trypsin	Bolognese *et al* (2005)

The theoretical basis of phase separation is complex. In polymer – polymer systems, it is attributed to the high molecular weight of the polymers combined with interaction between the segments of these molecules (Flory, 1953;

Albertsson, 1986). The phase separation that occurs is driven by the change in enthalpy when the polymers interact (Flory, 1953).

In polymer – salt systems, phase behaviour in strongly influenced by the type of salt and its concentration; addition of a salt to a single polymer in solution will induce phase separation to yield a salt – rich, polymer – poor lower phase and a salt – poor, polymer – rich upper phase (Albertsson, 1986, Walter *et al*, 1985, and Abbot *et al*, 1990). The relative effectiveness of various salts in creating phase separation follows the Hofmeister series – a classification of ions based on their salting – out ability (Ananthapadmanabhan and Goddard, 1987). The Hofmeister series is based on the nature of the salt anion. Small multivalent anions with high – charge density (*e.g.* sulphate and phosphate) do not interact closely with the polymer molecules. This leads to regions around the polymer molecules that do not contain salt ions; these regions are the basis for the formation of the two – phase system (Abbot *et al*, 1990; Huddleston *et al*, 1991).

Some typical polymer – salt systems used in protein purification are shown in Table 1.1.2c.

Table 1.1.2c: Selected examples of typical polymer – salt ATPS used in protein purification.

Phase System(s)	Protein(s)	Reference
10.3% w/w PEG-1450: 12.01% w/w potassium phosphate (in the ratio 18:7 w/w K_2HPO_4: KH_2PO_4)	α-amylase, Bovine serum albumin, α-chymotrypsin, Cytochrome *c*, Lysozyme, Myoglobin, Ribonuclease-A	de Belval *et al* (1998)
10-30% w/v PEG-1500: 20% w/v $MgSO_4$ 10-30% w/v PEG-1500: 20% w/v $(NH_4)_2SO_4$ 25-30% w/v PEG-1500: 20% w/v NaH_2PO_4 25-30% w/v PEG-1500: 20% w/v Na_2HPO_4	β-xylosidase	Pan *et al* (2001)
PEG-1500: K_2HPO_4 PEG-4000: K_2HPO_4 PEG-1500: Na_2SO_4 PEG-4000: Na_2SO_4 (Compositions = various % w/w)	Lysozyme, Bovine serum albumin, α-amylase	Haghtalab *et al* (2003)
20% w/w PEG-2000: 15% w/w $(NH_4)_2SO_4$ 10% w/w PEG-2000: 18% w/w $(NH_4)_2SO_4$	Recombinant thermostable α-amylase (MJA1)	Li and Peeples (2004)

PEG – salt systems are preferred for protein extraction, both for economic reasons and because they tend to be more selective than polymer – polymer systems (Vernau and Kula, 1990). The use of phosphates and sulphates has led to high concentrations in effluent discharge, and hence to environmental concerns. One approach is to utilise citrate salts, as they are biodegradable and non – toxic (Vernau and Kula, 1990), and research into phase systems using these salts has been conducted (refer to Table 1.1.2d).

Recycling the chemicals from aqueous two – phase systems has also been investigated as a means of lessening the environmental impact of these phase systems (Hustedt, 1986; Papamichael *et al*, 1992).

Table 1.1.2d: Examples of the use of ATPS containing citrate salts.

Phase System(s)	Protein(s)	Reference
PEG-(400, 1550, 4000, 6000, 12000, 20000): sodium citrate	Alcohol dehydrogenase, Glucose-6-phosphate dehydrogenase, Alanine dehydrogenase, Leucine dehydrogenase, Oxynitrilase	Vernau and Kula (1990)
PEG-1500: sodium citrate	BSA	Franco *et al* (1995)
PEG-(1500, 4000): sodium citrate	Thaumatin derivatives	Miranda *et al* (1996)
PEG-(1000, 3350): sodium citrate	Penicillin acylase	Marcos *et al* (1998)
PEG-(600, 1450, 3350): sodium citrate	Porcine insulin	Alves *et al* (2000)
PEG-4000: sodium citrate	α-amylase, Amyloglucosidase, BSA, α-Chymotrypsinogen A, Conalbumin, Invertase, α-Lactalbumin, Lysozyme, Ovalbumin, Subtilisin, Thaumatin, Trypsin inhibitor	Andrews *et al* (2005)
PEG-4000: sodium citrate	α-amylase	Zhi *et al* (2005)
PEG-(1000, 1450, 3350): sodium citrate	BSA, α-Lactoalbumin, α-1 Antitrypsin, β-Lactoglobulin	Boaglio *et al* (2006)
PEG-1500: sodium citrate	Lysozyme	Su and Chiang (2006)
PEG-2000: potassium citrate	Not applicable*	Jayapal *et al* (2007)
PEG-(600, 1000, 1450, 3350, 8000): sodium citrate	Trypsin, α-Chymotrypsin	Tubío *et al* (2007)

* This was a study of the liquid – liquid equilibrium of this phase system and did not involve proteins.

1.1.3. Applications and Advantages of Aqueous Two – Phase Systems

Aqueous two – phase systems have a number of advantages over conventional extraction processes that have resulted in their use in a number of biological applications. The aqueous nature of both phases creates a gentle, non – denaturing environment for biomaterials (when compared with aqueous – organic solvent systems). Interfacial tension is low, typically 0.0001 to 0.1 dyne cm^{-1} (compared with 1 to 20 dyne cm^{-1} for aqueous – organic solvent systems). This creates a high interfacial contact area when the phases are mixed, and thus efficient mass transfer of bioparticles. Low interfacial tension also minimises denaturation of proteins, allowing proteins to retain structure and function. The polymers themselves are known to have a stabilising influence on particle structure and biological activities (Albertsson, 1986).

ATPS has, since the early 1970s, become a powerful tool in a number of applications:

1) The fractionation of cells into subpopulations (Walter *et al*, 1985, Walter and Johansson, 1994).

2) Determining the surface hydrophobicity and the isoelectric point of proteins (by cross – partitioning) (Walter and Johansson, 1994, Chapter 20).

3) Detection and quantification of biochemical reactions (Backman, 2000). These techniques rely on the fact that the free and bound forms of the interacting molecules (reagents and products) will partition differently in the two phases of an ATPS. By measuring the concentrations of these molecules in each phase, information on the stoichiometry of the reaction can be obtained. This technique has been used to characterise the binding of calmodulin to non – erythroid spectrin (Björk *et al*, 1995).

4) Concentration and purification of biomolecules, including soluble and membrane – bound proteins, viruses, amino acids and nucleic acids *e.g.* DNA (Hatti-Kaul, 2000).

5) In extractive bioconversion, where a biochemical reaction takes place in one phase and the product is extracted into the other. Suitable partitioning of enzyme, substrate and product can shift the equilibrium of the reaction positively, making a high degree of conversion possible. Disadvantages include contamination of the product with the phase components, and reduction of the reaction rate if the these components are present in high concentrations (Hustedt *et al*, 1985).

Extractive bioconversion has been used to produce glucose-6-phosphate from glucose by the reaction of hexokinase in a PEG – dextran system (Yamazaki and Suzuki, 1979). A PEG – phosphate system has been used to support the conversion of the amino acid N-acetyl-L-methionine to L-methionine by acylase (Kuhlmann *et al*, 1980).

6) In environmental remediation, where ATPS is used to remove environmentally – harmful substances from industrial discharge (Hatti-Kaul, 2000).

7) The application of ATPS that has attracted the most interest in biotechnology is its use in the isolation of proteins from crude feedstocks (Table 1.1.3a).

Table 1.1.3a: Selected examples of the use of ATPS in the isolation of proteins from crude feedstocks.

Phase System(s)	Protein(s)	Type of Feedstock	Reference
4.8%-26.2% w/w PEG-6000: 5.5%-12.0% w/w potassium phosphate	β-galactosidase	Cell lysate of *E. coli*	Veide *et al* (1983)
PEG-(400, 1550, 4000, 6000, 12000, 20000): sodium citrate	Alcohol dehydrogenase, Glucose-6-phosphate dehydrogenase, Alanine dehydrogenase, Leucine dehydrogenase, Oxynitrilase	Bakers' yeast (*S. cerevisiae*) preparation. *B. cereus* cell fermentation. Almond bran (Plazenta *A. amararum* pulv.)	Vernau and Kula (1990)
7.0% w/v PEG-6000: phosphate, 1.2M NaCl, pH 7	Thaumatin	Cell lysate of *E. coli*	Cascone *et al* (1991)
PEG (600, 1450, 4000, 6000): sodium/potassium phosphate	IgG	Murine hybridoma culture supernatant	Andrews *et al* (1996)
PEG (1000, 3350): sodium citrate	Penicillin acylase	Cell lysate of *E. coli*	Marcos *et al* (1998)
5.0% $EO_{50}PO_{50}$: 5.0% HM-EOPO (hydrophobically modified copolymer of EO and PO)	Bovine serum albumin, Lysozyme, Apolipoprotein A-1	*E. coli* fermentation solution	Persson *et al* (1999)
7.0% w/w PEG-8000: 7.0% w/w Dextran T500	β-glucosidase	Fermentation supernatant from various strains of the fungi *Aspergillus*	Brumbauer *et al* (2000)
27.0% w/w PEG-1000: 14.0% w/w K_2HPO_4, pH 9.0	Fumarase Pyruvate Bulk protein	Brewers' yeast suspension (disrupted)	Rito-Palomares and Lyddiatt (2000)
$EO_{20}PO_{80}$: Na_2HPO_4	β-xylosidase	Fermentation supernatant from the fungi *Trichoderma koningii*	Pan and Li (2001)

Table 1.1.3a: Continued

Phase System(s)	Protein(s)	Type of Feedstock	Reference
10-30% w/v PEG-1500: 20% w/v $MgSO_4$ 10-30% w/v PEG-1500: 20% w/v $(NH_4)_2SO_4$ 25-30% w/v PEG-1500: 20% w/v NaH_2PO_4 25-30% w/v PEG-1500: 20% w/v Na_2HPO_4	β-xylosidase	Fermentation supernatant from the fungi *Trichoderma koningii*	Pan *et al* (2001)
Detergent – based polymers *e.g.* Triton X114	Cutinase	Culture broth of *S. cerevisiae*	Rodenbrock *et al* (2001)
Ucon 50-HB-5100 (random copolymer of 50% EO + 50% PO): polyvinyl alcohol, Ucon 50-HB-5100: hydroxypropyl starch, Ucon 50-HB-5100: $(NH_4)_2SO_4$	Endo – polygalacturonase	Fermentation broth of the yeast *K. marxianus*	Pereira *et al* (2003)
20% w/w PEG-2000: 15% w/w $(NH_4)_2SO_4$ 10% w/w PEG-2000: 18% w/w $(NH_4)_2SO_4$ 20.0% PEO-PPO-2500: 7.0-15.0% $(NH_4)_2SO_4$	Recombinant thermostable α-amylase (MJA1)	Cell lysate of *E. coli*	Li and Peeples (2004)
4.4% w/w PEG-8000: 6.0% w/w Dextran T500	Glucosyltransferase	Cell lysate of *Streptococcus mutans*	Yanagida *et al* (2004)
PEG-4000: sodium citrate	α-amylase	Cultivation supernatant of *Bacillus subtilis*	Zhi *et al* (2005)

1.1.4. Limitations of Aqueous Two – Phase Systems in Protein Purification

Despite its many advantages, ATPS is not widely employed in protein purification for a number of reasons:

1) There remains a generally poor understanding of the mechanisms of partitioning, making method development an empirical exercise, although some progress has been made in this field (Johansson *et al*, 1998).

2) The amount of protein that can be dissolved in a phase system is usually limited to 1.0 $mgml^{-1}$ to 5.0 $mgml^{-1}$ (Table 1.1.4a). Saturation behaviour is observed as the protein concentration reaches this limit; further increase in protein

concentration causes the protein to precipitate at the interface, leading to reduced recovery (Engel *et al*, 2000). Both PEG and salt solutions are frequently used to precipitate proteins, however, under certain conditions, some proteins can be present in phase systems at relatively high concentrations without precipitating (refer to Table 1.1.4a).

Table 1.1.4a: Selected examples of protein concentrations present in ATPS.

Phase System(s)	Protein(s)	Protein Conc^{n} (mgml^{-1})*	Reference
4.8%-26.2% w/w PEG-6000: 5.5%-12.0% w/w potassium phosphate	β-galactosidase	2.3	Veide *et al* (1983)
1) 20% w/w Dextran T500: 70% w/w PEG-6000 2) 80% w/w Dextran T500: 20% w/w polyvinyl alcohol 3) 20% w/w Dextran sulphate: 70% w/w PEG-6000 4) 40% w/w Dextran sulphate: 48% w/w methylcellulose 5) 40% w/w Dextran sulphate: 20% w/w polyvinyl alcohol	Feline Leukaemia Virus proteins: gp70 (outer envelope protein) and p27 (a gag protein)	1) 31.0 2) 26.0 3) 9.3 4) 17.4 5) 22.7	Hammar *et al* (1989)
7.0% w/v PEG-6000: phosphate, 1.2M NaCl, pH 7	Thaumatin	40.0	Cascone *et al* (1991)
PEO-4000: dextran Ucon 50-HB-5100: dextran	Ribonuclease A, Myoglobin	0.2 – 0.5	Carlsson *et al* (1993)
1.0% w/w hydroxyethyl cellulose: 4.0% w/w poly(ethyleneimine)	BSA, Myoglobin, Lactate dehydrogenase	3.0 0.5 0.2	Dissing and Mattiasson (1994)
10.0% w/w PEG-4000: 11.5% w/w phosphate with 3% NaCl at pH 7	α-amylase	12.3	Schmidt *et al* (1994)
15.0% w/w PEG-1450: 14.0% w/w sodium/potassium phosphate, 12.0% w/w NaCl, pH 7	IgG	1.0	Andrews *et al* (1996)
PEG-1450: potassium phosphate PEG-1000: potassium phosphate	BSA, Ovalbumin, Lysozyme, Cytochrome *c*, Ribonuclease A, Myoglobin, α-amylase, α-chymotrypsin, Bovine methaemoglobin	3.0	Huddleston *et al* (1996)

Table 1.1.4a: Continued

Phase System(s)	Protein(s)	Protein Conc^{n} (mgml^{-1})*	Reference
6.0% w/w PEG-4000: 5.8% dextran T500 6.0% EO30/PO70: 5.0% dextran T500	BSA, Lysozyme	0.5	Johansson *et al* (1996)
10.3% w/w PEG-1450: 12.01% w/w potassium phosphate (in the ratio 18:7 w/w K_2HPO_4: KH_2PO_4)	α-amylase, Bovine serum albumin, α-chymotrypsin, Cytochrome *c*, Lysozyme, Myoglobin, Ribonuclease-A	1.0 (each protein)	de Belval *et al* (1998)
$EO_{20}PO_{80}$: Na_2HPO_4	β-xylosidase	1.12	Pan and Li (2001)
10-30% w/v PEG-1500: 20% w/v $MgSO_4$ 10-30% w/v PEG-1500: 20% w/v $(NH_4)_2SO_4$ 25-30% w/v PEG-1500: 20% w/v NaH_2PO_4 25-30% w/v PEG-1500: 20% w/v Na_2HPO_4	β-xylosidase	1.08	Pan *et al* (2001)
12.5% w/w polyethyleneoxide-maleic acid: 12.5% w/w potassium phosphate	Lysozyme, Conalbumin, Ovalbumin	1.0	Kajiuchi *et al* (2002)
PEG-1500: K_2HPO_4 PEG-4000: K_2HPO_4 PEG-1500: Na_2SO_4 PEG-4000: Na_2SO_4 (Compositions = various % w/w)	Lysozyme, Bovine serum albumin, α-amylase	2.0	Haghtalab *et al* (2003)
10.0% w/w PEG-1540: 14.8% w/w KH_2PO_4 /K_2HPO_4 with 2 mol kg^{-1} NaCl	Horseradish peroxidase	2.0 – 4.0 (total protein)	Magri *et al* (2003)
PEG-1500/4000/6000: ammonium carbamate	BSA, Trypsin, Lysozyme	1.0	Dallora *et al* (2007)

* There is a considerable quantity of literature on enzyme purification using ATPS that reports protein (enzyme) concentration in terms of Umg^{-1} and/or as specific activity (*e.g.* as μmol mg^{-1} min^{-1}). Concentrations of non – enzymatic proteins are frequently reported as partition coefficients, rather than in terms of mass per unit volume.

In addition, many protein concentrations reported are given for the concentration of protein in one of the two phases, rather than the complete phase system. For ease of comparison, only protein concentrations reported in mgml^{-1} (or equivalent) for complete phase systems are included in Table 1.1.4a.

1.1.5. Phase Diagrams for Aqueous Two – Phase Systems

In an aqueous mixture of two polymers, or a polymer and a salt, two phases will only form if these components are present above certain concentrations (Albertsson, 1971b). These concentrations at which phase separation occurs can be represented in a phase diagram, such as in Figure 1.1.5a, which shows a phase system of polymer P and salt S.

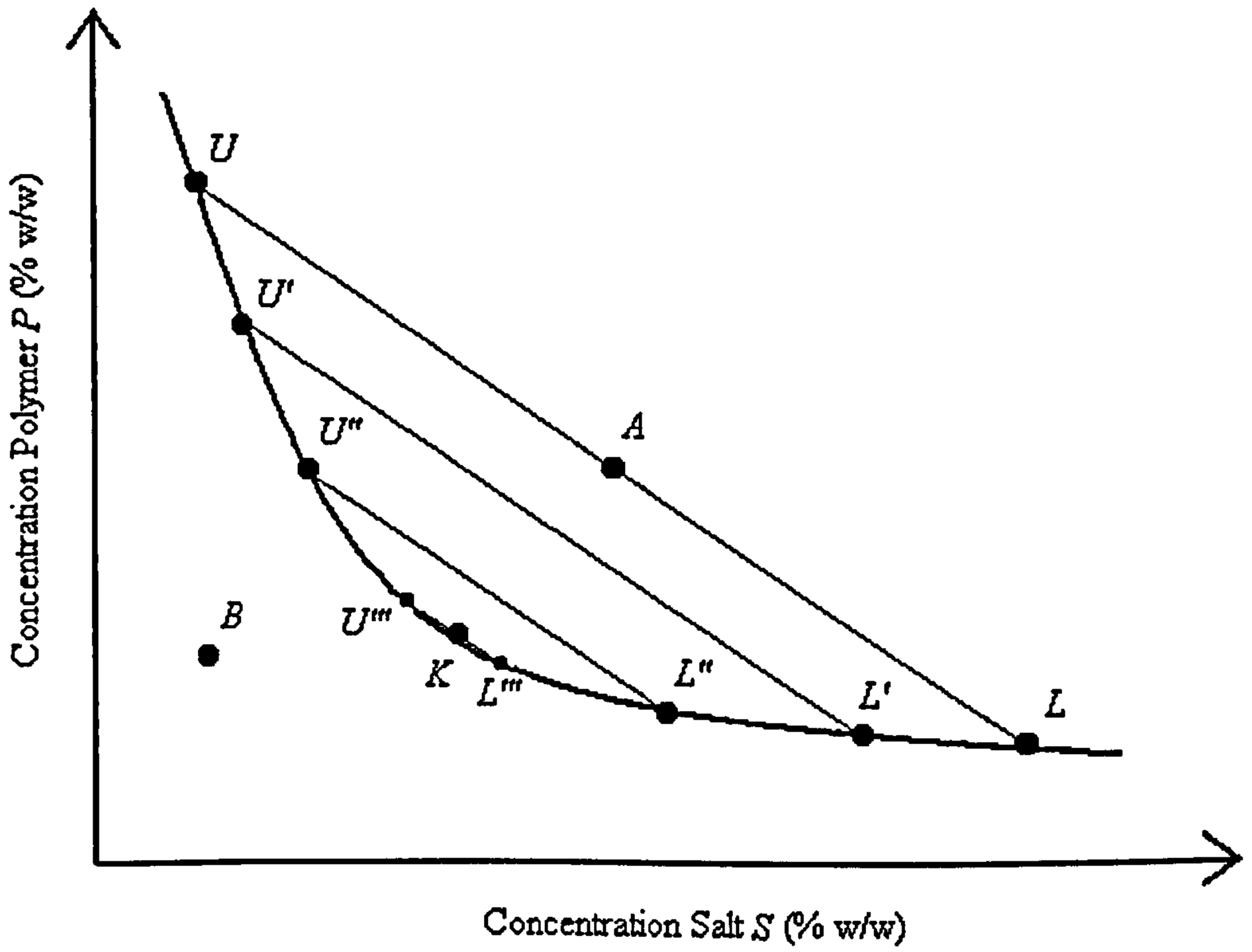

Figure 1.1.5a: Example of a phase diagram for an ATPS.

Conventionally, the component enriched in the top phase is plotted on the vertical axis; the component enriched in the bottom phase is plotted on the horizontal axis. The concentrations of each component are typically given in terms of percentage weight – for – weight (% w/w). The concentrations above which two phases form are represented by a line (usually a curve) called the binodal. A mixture of the two components whose concentrations lie on or above the line will form two phases; a mixture that lies below the line will remain as a homogenous solution *e.g.* in Figure 1.1.5a, a mixture at point *A* will form two phases; a mixture at point *B* will remain as a single phase.

The concentration of polymer and salt in the single phase solution *B* can be obtained from the graph axes. Point *A* on the diagram represents the total

composition of a solution that will separate into two phases. The composition of the upper phase is given at point *U* on the binodal, and that of the lower phase at point *L*. Points *U* and *L* are termed nodes. The line drawn joining the nodes together and passing through point *A* is called a tie – line. Any systems with a total composition that falls on this tie – line will separate into two phases with compositions defined by *U* and *L*. The lever arm rule states that the relative volumes of the top and bottom phases will differ, however, since the ratio of the weights (approximately equal to the volumes) of the upper and lower phases is given by the ratio of the lengths of *AL* to *AU*.

A series of tie – lines drawn to approach the binodal (*U'L'* and *U"L"* in Figure 1.1.5a) will eventually reach the critical point (*K* in Figure 1.1.5a). A system at the critical point will just separate into two phases of equal volume and composition, and be represented by a vanishingly small tie – line. All compositions at the binodal are also critical compositions; however it is only at the critical point that the volume ratio of upper and lower phase equals 1.

The constituents of a phase diagram, namely the binodal, nodes and tie – line, are determined experimentally (Albertsson, 1971b) by analysing the composition of the upper and lower phases. Techniques used include: refractive index measurement, polarimetry (for optically active polymers *e.g.* dextran), radioactive labelling of the polymer(s) and total carbon measurement (*e.g.* for PEG). Salt ion concentrations can be determined by ion chromatography and conductivity measurements (Walter *et al*, 1985). Also employed are wet weight measurements such as turbidometric titration and the cloud point method (Kaul, 2000). These techniques determine the binodal by recording the mass of stock solutions of known concentration required to produce the formation of, respectively, a one – phase system and a two – phase system.

Aqueous two – phase systems are temperature – dependent, therefore a phase system must be prepared under temperature – controlled conditions. Likewise, determination of the constituents of the phases must take place under temperature control, and the resulting phase diagram should report that temperature.

1.1.6. Preparation of Aqueous Two – Phase Systems

The preparation of polymer – polymer and polymer – salt aqueous two – phase systems is quite straightforward. Typically, stock solutions of the phase components are prepared and mixed in appropriate amounts (by weight) in a separating funnel. The system is allowed to attain the required temperature then mixed thoroughly to form an emulsion. Separation into the two phases also occurs in temperature – controlled conditions either under gravity or by centrifugation (Hatti-Kaul, 2000). For PEG – salt systems, an "all – in – one" method can be adopted, where the polymer, dry salt and water are measured into one vessel in proportions that are present in the phase system overall. They are then allowed to separate under temperature – controlled conditions. A phase system is quicker to produce by this method, however it is not generally suitable for systems that include dextran. This is for two reasons: dextran is generally not a dry material, and therefore the concentration in a stock solution must first be determined by polarimetry in the absence of other components; dextran can require warming to dissolve into solution, and it is preferable not to have the other components of the phase system present.

After separation, the phases can be stored using a refrigerator or freezer, but must be brought to operational temperature before use.

1.1.7. Physicochemical Properties of Aqueous Two – Phase Systems

Aqueous two – phase systems possess a number of physiochemical properties, the measurement of which can provide insight into the mechanisms responsible for the partition behaviour observed. In addition, such measurements can be used as a quality control procedure when working with batch quantities of a phase system to ensure the reproducibility of a phase system is maintained (Brooks and Norris-Jones, 2000).

Measurement of the interfacial tension between the phases is a popular method for quality control, as this property is very sensitive to the composition of the phases (Ryden and Albertsson, 1971). Other physicochemical properties that can be measured include: electrostatic potential difference between the phases; phase viscosity; phase density.

1.1.8. Single – Step Partitioning of Proteins in Aqueous Two – Phase Systems

The partitioning of a protein between the two phases of an ATPS is determined by the interactions between the protein and the phase components (Albertsson *et al*, 1990). The factors that determine partition of a protein are as follows:

A) Properties of the protein:

1) The molecular mass or surface area of the protein

2) The protein surface charge

3) Hydrophobicity of the protein – a relatively hydrophobic protein will favour the more hydrophobic of the phases

4) Biospecificity – the attraction between certain sites on the surface of the protein and affinity ligands localised in one phase *e.g.* PEG – ligands in a PEG – rich phase

5) Conformation of the protein (including the chiral form)

B) Properties of the phase system:

1) Concentration and molecular weight of the polymers used

2) Concentration and identity of the salts used (these will also determine the pH of the system, which in turn will influence protein partitioning)

3) Electrochemical potential between the phases

The molecular and chemical features important in PEG – salt aqueous two – phase partition are summarised in Figure 1.1.8a.

The partition of a protein in an ATPS is described by the partition coefficient, *K*. This is defined as:

$$K = \frac{\text{Concentration of the Protein in Upper Phase}}{\text{Concentration of the Protein in the Lower Phase}} \qquad \text{[Equation 1.1.8a]}$$

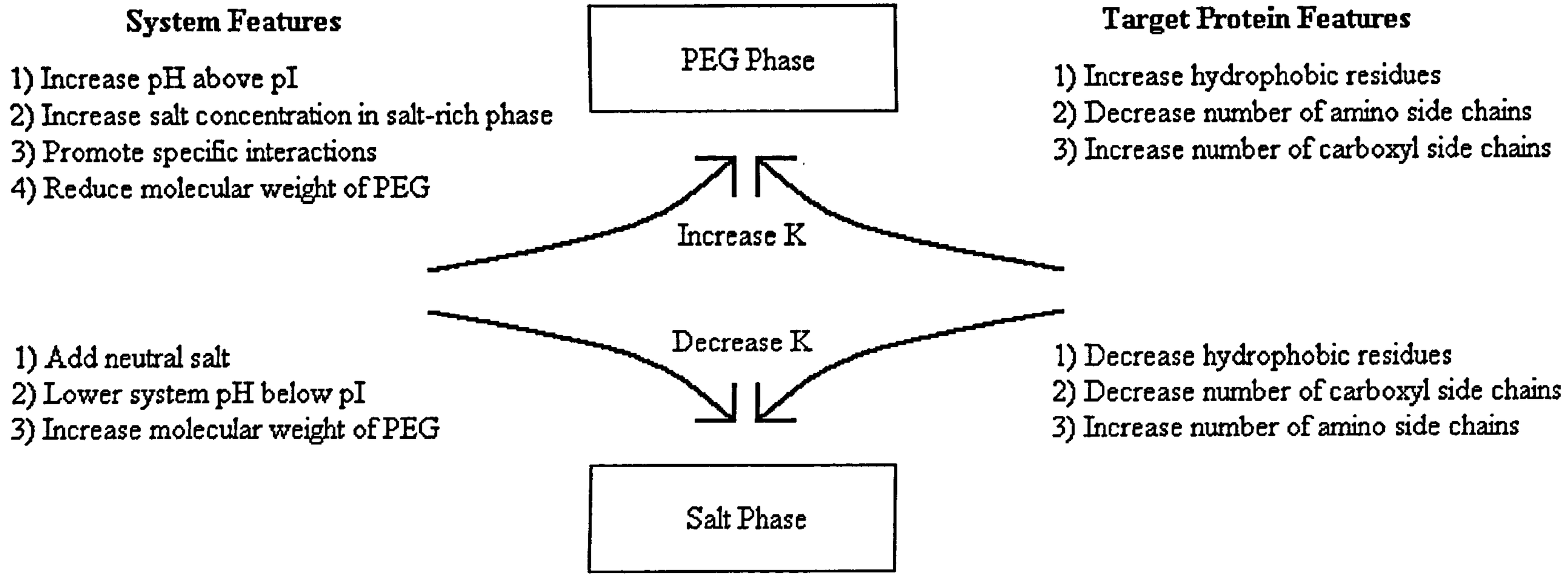

Figure 1.1.8a: Summary of the molecular features important in PEG – salt aqueous two – phase partition (adapted from Huddleston *et al*, 1991).

A number of proteins have been subjected to the single – step partition process, using a variety of ATPS (refer to Table 1.1.8a).

Table 1.1.8a: More recent examples of the use of ATPS in single – step partition to purify proteins.

Phase System(s)	Protein(s)	Reference
PEG-(400, 1550, 4000, 6000, 12000, 20000): sodium citrate	Alcohol dehydrogenase, Glucose-6-phosphate dehydrogenase, Alanine dehydrogenase, Leucine dehydrogenase, Oxynitrilase	Vernau and Kula (1990)
7.0% w/v PEG-6000: phosphate, 1.2M NaCl, pH 7	Thaumatin	Cascone *et al* (1991)
PEO-4000: dextran, Ucon 50-HB-5100: dextran	Ribonuclease A, Myoglobin	Carlsson *et al* (1993)
$EO_{20}PO_{80}$: dextran T-500	Glucose-6-phosphate dehydrogenase, Hexokinase, 3-phosphoglycerate kinase	Alred *et al* (1994)
10.0% w/w PEG-4000: 11.5% w/w phosphate with 3% NaCl at pH 7	α-amylase	Schmidt *et al* (1994)
Ucon 50-HB-5100: hydroxypropyl starch, $EO_{30}PO_{70}$: hydroxypropyl starch	Bovine serum albumin, Lysozyme, β-lactoglobulin A, Myoglobin, Cytochrome *c*	Berggren *et al* (1995)
PEG-1500: sodium citrate	BSA	Franco *et al* (1995)
PEG-(600, 1450, 4000, 6000): sodium/potassium phosphate	IgG	Andrews *et al* (1996)
$EO_{30}PO_{70}$: dextran T-500, Ucon 50-HB-5100: dextran T-500	Bovine serum albumin, Lysozyme	Johansson *et al* (1996)
PEG-(1500, 4000): sodium citrate	Thaumatin derivatives	Miranda *et al* (1996)
PEG-(1000, 3350): sodium citrate	Penicillin acylase	Marcos *et al* (1998)
5.0% $EO_{50}PO_{50}$: 5.0% HM-EOPO (hydrophobically modified copolymer of EO and PO)	Bovine serum albumin, Lysozyme, Apolipoprotein A-1	Persson *et al* (1999)
PEG-(600, 1450, 3350): sodium citrate	Porcine insulin	Alves *et al* (2000)
$EO_{20}PO_{80}$: Na_2HPO_4	β-xylosidase	Pan and Li (2001)

Table 1.1.8a: Continued

Phase System(s)	Protein(s)	Reference
10-30% w/v PEG-1500: 20% w/v $MgSO_4$ 10-30% w/v PEG-1500: 20% w/v $(NH_4)_2SO_4$ 25-30% w/v PEG-1500: 20% w/v NaH_2PO_4 25-30% w/v PEG-1500: 20% w/v Na_2HPO_4	β-xylosidase	Pan *et al* (2001)
7.1% dextran: 6.8% $EO_{30}PO_{70}$ 9.0% dextran: 9.0% $EO_{30}PO_{70}$	α-Chymotrypsinogen A, Cytochrome *c*, Ribonuclease-A, α-Lactalbumin, Lysozyme, Myoglobin, α-Chymotrypsin	Berggren *et al* (2002)
7.1% dextran: 6.8% $EO_{30}PO_{70}$	Lactate dehydrogenase	Fexby and Bülow (2002)
PEG-1500: K_2HPO_4 PEG-4000: K_2HPO_4 PEG-1500: Na_2SO_4 PEG-4000: Na_2SO_4 (Compositions = various % w/w)	Lysozyme, Bovine serum albumin, α-amylase	Haghtalab *et al* (2003)
Ucon 50-HB-5100 (random copolymer of 50% EO + 50% PO): polyvinyl alcohol, Ucon 50-HB-5100: hydroxypropyl starch, Ucon 50-HB-5100: $(NH_4)_2SO_4$	Endo – polygalacturonase	Pereira *et al* (2003)
20% w/w PEG-2000: 15% w/w $(NH_4)_2SO_4$ 10% w/w PEG-2000: 18% w/w $(NH_4)_2SO_4$ 20.0% PEO-PPO-2500: 7.0-15.0% $(NH_4)_2SO_4$	Recombinant thermostable α-amylase (MJA1)	Li and Peeples (2004)
PEG-4000: sodium citrate	α-amylase, Amyloglucosidase, BSA, α-Chymotrypsinogen A, Conalbumin, Invertase, α-Lactalbumin, Lysozyme, Ovalbumin, Subtilisin, Thaumatin, Trypsin inhibitor	Andrews *et al* (2005)

Table 1.1.8a: Continued

Phase System(s)	Protein(s)	Reference
Random copolymer EOPO: maltodextrin	Bovine serum albumin, Lysozyme, Trypsin	Bolognese *et al* (2005)
PEG-(1000, 1450, 3350): sodium citrate	BSA, α-Lactoalbumin, α-1 Antitrypsin, β-Lactoglobulin	Boaglio *et al* (2006)
PEG-1500: sodium citrate	Lysozyme	Su and Chiang (2006)
PEG-1500/4000/6000: ammonium carbamate	BSA, Trypsin, Lysozyme	Dallora *et al* (2007)
PEG-(600, 1000, 1450, 3350, 8000): sodium citrate	Trypsin, α-Chymotrypsin	Tubío *et al* (2007)

1.2. Chromatographic Theory

1.2.1. Definition of Chromatography

Chromatography is an analytical and preparative method used for the separation and determination of the proportions of chemical components in complex mixtures (Skoog *et al*, 1994). All chromatography methods involve the use of a stationary phase and a mobile phase. Components of a mixture are carried through the stationary phase by the flow of a gaseous or liquid mobile phase, separations being based on differences in migration rates among the sample components.

A chromatogram (refer to Figure 1.2.1a) is a graphical illustration of some function of solute concentration versus elution time or elution volume, and is useful in both qualitative and quantitative analysis. The positions of the peaks on the time or elution volume axis can be used to identify the components of the sample when compared with reference materials that have been subjected to chromatography under identical conditions to the sample. The areas under the peaks provide a quantitative measure of the amount of each species.

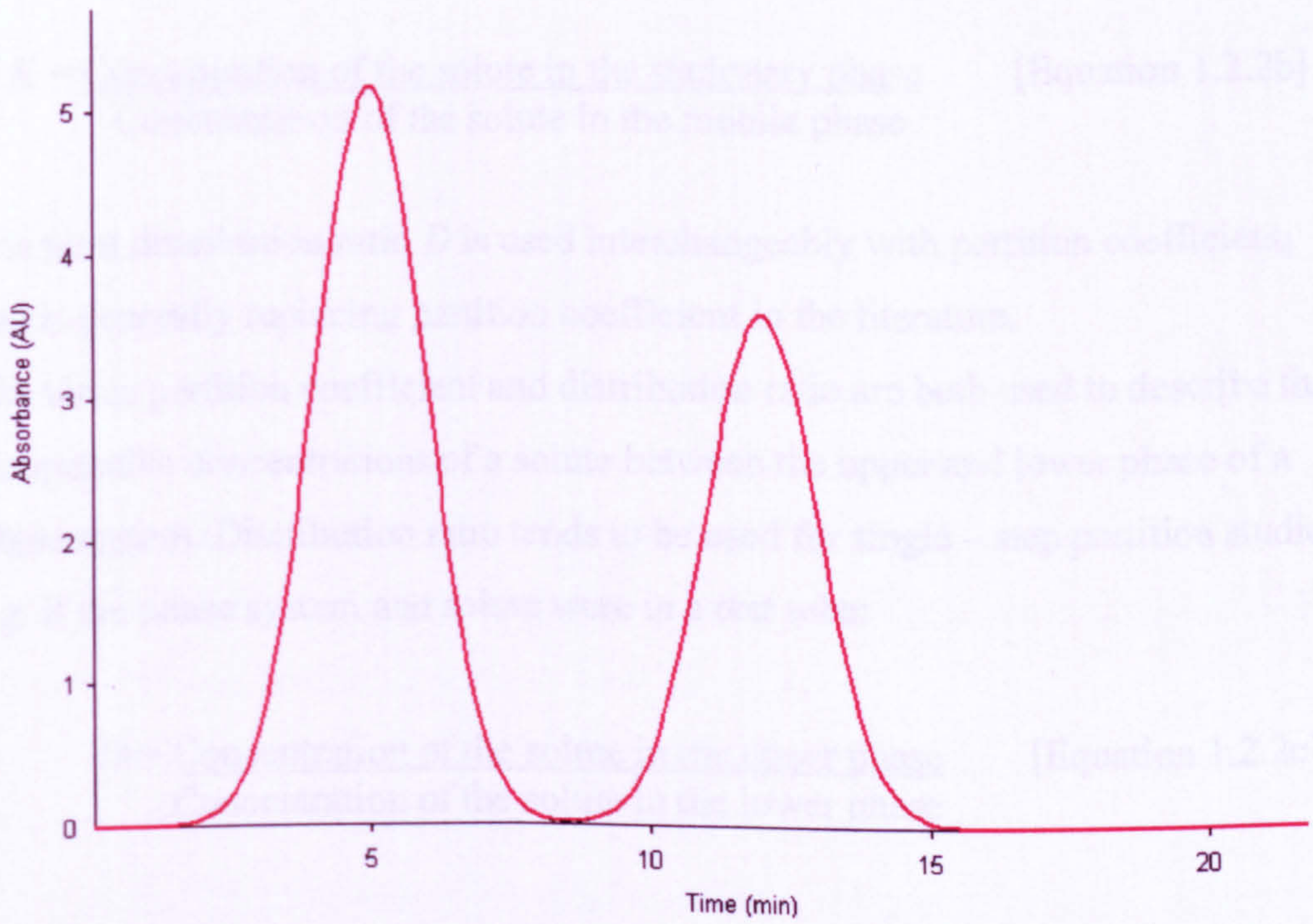

Figure 1.2.1a: Example of a chromatogram.

1.2.2. The Partition Ratio and Distribution Ratio in Liquid – Liquid Chromatography

All chromatographic separations are based on differences in the extent to which solutes are partitioned between mobile and stationary phases (Skoog *et al*, 1994). For the solute species *A*, the equilibrium is:

$$A_{\text{mobile}} \leftrightarrow A_{\text{stationary}} \qquad \text{[Equation 1.2.2a]}$$

Liquid – liquid chromatography employs two immiscible liquids to act as the stationary and mobile phases. It is governed by the same mathematical relationships found in chromatography in general. However, the absence of a solid stationary phase means that adsorption does not contribute to solute retention; separation is determined only by the partition coefficient of the solute in the solvent system used (Conway, 1990).

Therefore, the partition coefficient *K* is defined as:

$$K = \frac{\text{Concentration of the solute in the stationary phase}}{\text{Concentration of the solute in the mobile phase}} \qquad \text{[Equation 1.2.2b]}$$

The term distribution ratio *D* is used interchangeably with partition coefficient, and is generally replacing partition coefficient in the literature.

The terms partition coefficient and distribution ratio are both used to describe the comparative concentrations of a solute between the upper and lower phase of a phase system. Distribution ratio tends to be used for single – step partition studies *e.g.* if the phase system and solute were in a test tube:

$$D = \frac{\text{Concentration of the solute in the upper phase}}{\text{Concentration of the solute in the lower phase}} \qquad \text{[Equation 1.2.2c]}$$

1.2.3. Retention of Solutes in Countercurrent Chromatography

Countercurrent chromatography is a form of liquid – liquid chromatography (refer to Section 1.3). The chromatographic process in countercurrent chromatography involves the solutes present in a sample undergoing a number of transitions between the stationary phase liquid and the mobile phase liquid contained within a column (Berthod, 2002). The column can be visualised (for example) as a length of tubing, with the stationary phase held immobile within it, whilst the solutes enter and exit the column in the mobile phase. The solutes separate due to their differing affinities for the stationary phase. Those solutes with little affinity for the stationary phase will spend most time in the mobile phase, and exit the column fairly rapidly; those solutes with greater affinity for the stationary phase will spend comparatively more time in the stationary phase, and hence exit the column later. Hence a mixture of different solutes that enter the column simultaneously and as a mixture will exit it in a sequential fashion as single entities over a specific time period.

Retention of a particular solute in the column can be given in terms of volume or time. The solute retention volume V_R is given by:

$$V_R = V_M + K \times V_S \qquad \text{[Equation 1.2.3a]}$$

V_M and V_S are the mobile and stationary phase volumes, respectively, inside the column, and K is the distribution ratio of that solute in that phase system.

If the flow rate of the mobile phase is known (in addition to the values for V_M, V_S and K), it is possible to calculate the retention time of the solute or conversely the time at which it is expected to elute from the column.

The volume of a liquid – liquid chromatography column is always a known quantity; this value is either supplied by the manufacturer of the instrument or can be calculated by filling the system entirely with one phase of an (immiscible) two – phase system, and then displacing this phase with the other phase into a measuring cylinder – the system volume will be the volume of the first phase emerging from the column. The column volume V_C can be defined as:

$$V_C = V_M + V_S \qquad \text{[Equation 1.2.3b]}$$

The stationary phase volume retention ratio, *Sf*, is given by:

$$Sf = V_S/V_C \qquad \text{[Equation 1.2.3c]}$$

In percentage terms:

$$Sf = V_S/V_C \times 100 \qquad \text{[Equation 1.2.3d]}$$

Using equations [1.2.3b] and [1.2.3c], equation [1.2.3a] can be rewritten as:

$$V_R = V_C + (K-1) \times V_S \qquad \text{[Equation 1.2.3e]}$$

and

$$V_R = V_C + [1 + (K-1) \times Sf] \qquad \text{[Equation 1.2.3f]}$$

The phase volumes inside the column and the stationary phase volume retention ratio (*Sf*) can be easily measured, hence these equations can be used to predict the position of the peak corresponding to a particular solute (providing its distribution coefficient *K* is known). Conversely, the *K* value of a solute can be calculated if its retention volume V_R is known.

If the distribution ratio (*K*) of a solute equals one (1), it has equal affinity for the mobile and stationary phase, and will partition equally between the two phases. This situation is equivalent to the column being filled with one phase only (or another solvent), and so the retention volume of the solute is the same as the column volume (V_C).

If the distribution ratio (*K*) of a solute is less than 1, the solute favours the mobile phase, and so the corresponding peak will be located before the $K = 1$ peak.

If the distribution ratio (*K*) of a solute is greater than 1, the solute favours the stationary phase, and so the corresponding peak will be located after the $K = 1$ peak.

1.2.4. Column Efficiency in Countercurrent Chromatography

The efficiency of a chromatographic column is related to the width of a peak on a chromatogram, and is described in quantitative terms by the rate theory of chromatography (Skoog *et al*, 1994). Qualitatively, the rate theory encompasses the random nature of the behaviour of each solute molecule whilst in the column, in terms of how much time is spend in each phase, and the path taken by it down the column. Some molecules will travel rapidly through the column, eluting first, because they have spent most of their time in the mobile phase. Conversely, those molecules spending most time in the stationary phase will travel slowly through the column, eluting last. The result of this random behaviour is a symmetrical spread of velocities around the mean value (seen as a Gaussian peak on the chromatogram) which represents the behaviour of the average solute molecule. Band broadening (the peaks become non – Gaussian) can occur if:

- Too concentrated a sample is loaded onto the column
- Too great a volume of sample is loaded onto the column

As the sample molecules travel down the column, they diffuse outwards from a more concentrated part of the solution to a more dilute part. Therefore in the centre of the peak the concentration of sample molecules is high, at the two edges of the peak, the sample molecule concentration is approaching zero. Molecules from a large and/or concentrated sample will move outwards into the column more than molecules from a small and/or dilute sample, thus leading to band broadening.

Band breadth increases as it moves down the column, because more time is allowed for spreading by these various mechanisms to occur. Therefore, the width of a band is directly related to residence time in the column, and inversely related to the mobile phase flow rate.

1.2.5. Column Resolution in Countercurrent Chromatography

The resolution factor, *Rs*, quantifies the quality of a separation. A resolution factor value of 1.5 or above means that two adjacent peaks are fully separated (the detector response has returned to the baseline) (Figure 1.2.5a).

A resolution factor of less than 1.5 indicates some overlapping of the peaks (Figure 1.2.5b).

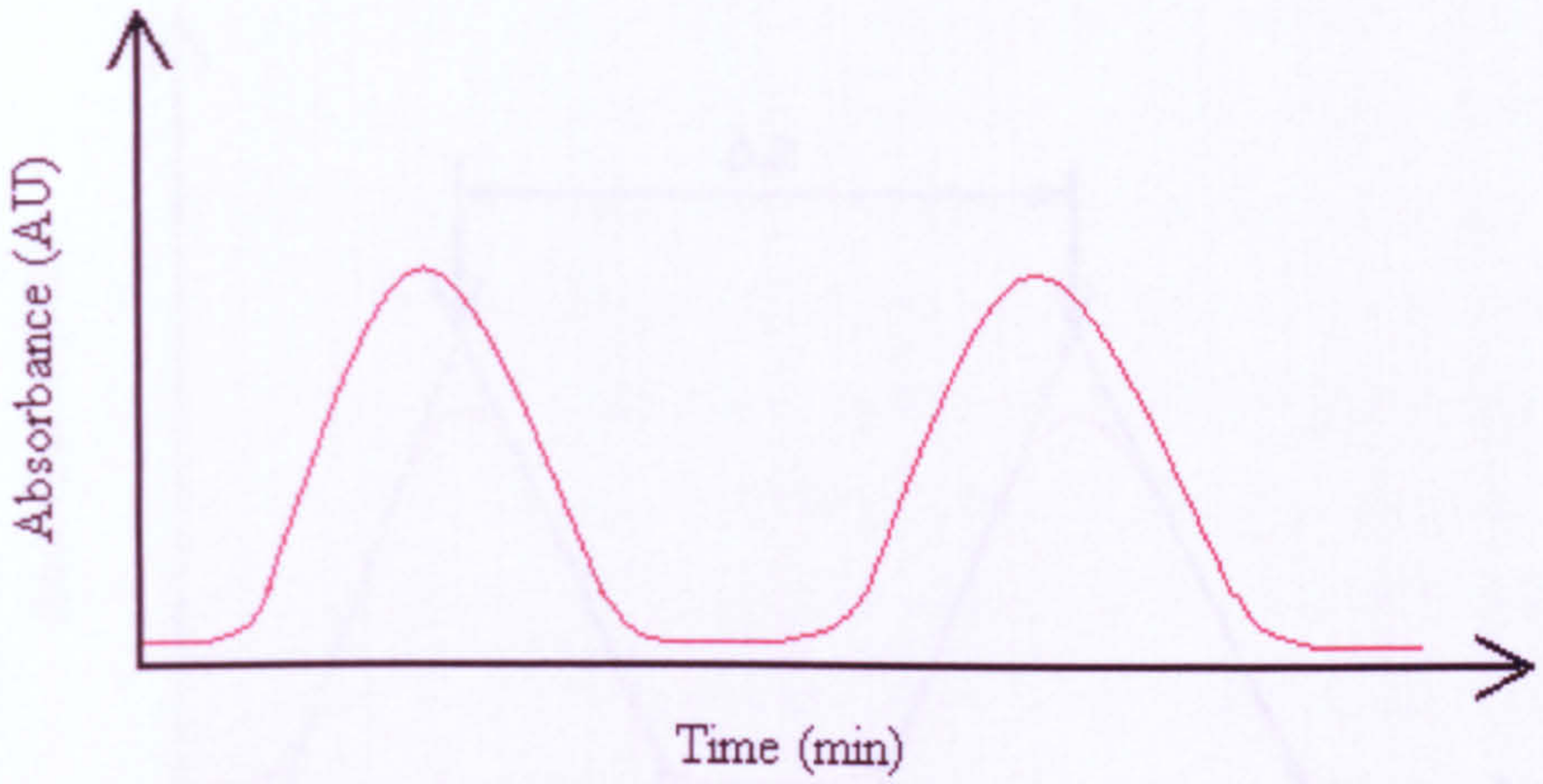

Figure 1.2.5a: Example of a chromatogram of resolution ≥ 1.5.

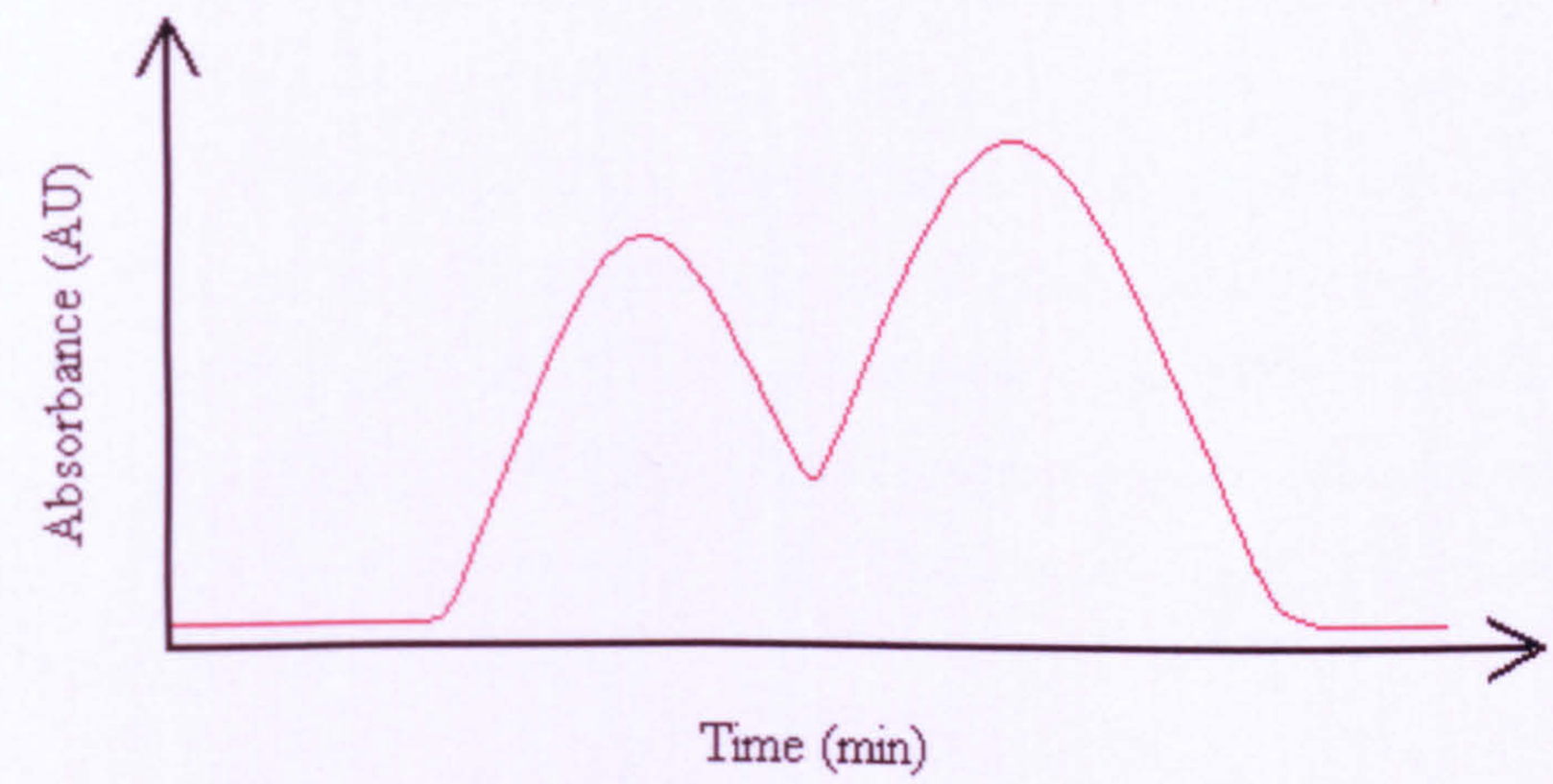

Figure 1.2.5b: Example of a chromatogram of resolution ≤ 1.5.

The resolution factor is calculated using the following equation:

$$Rs = \frac{2 \times \Delta Z}{W_1 + W_2}$$ [Equation 1.2.5a]

The values for ΔZ, W_1 and W_2 can be measured directly from the chromatogram:

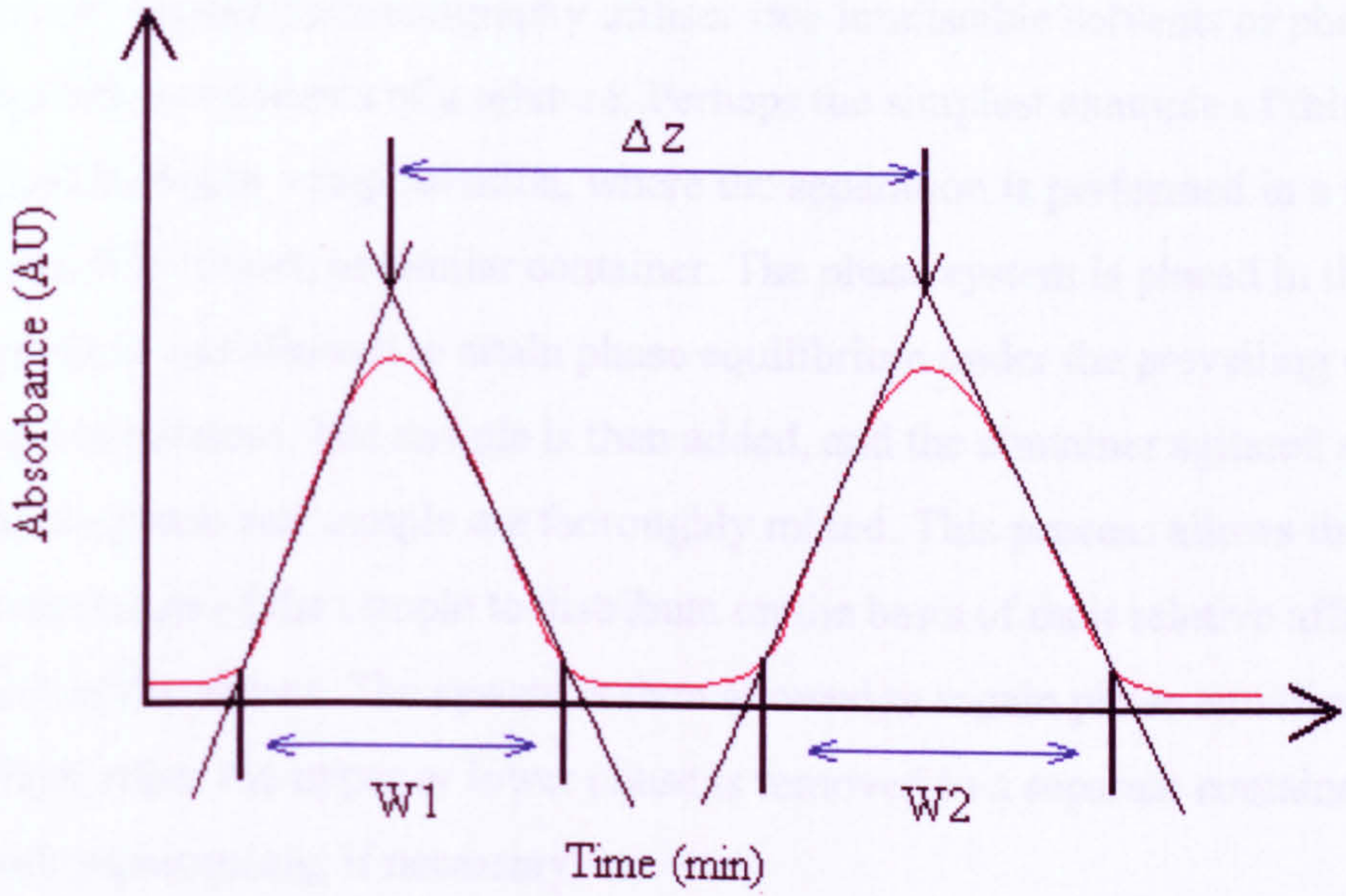

Figure 1.2.5c: Example of a chromatogram showing parameters used to calculate the resolution factor, *Rs*.

1.3. Liquid – Liquid Chromatography

1.3.1. Countercurrent Distribution

Liquid – liquid chromatography utilises two immiscible solvents or phases to separate components of a mixture. Perhaps the simplest example of this process is found in single – step partition, where the separation is performed in a test tube, separating funnel, or similar container. The phase system is placed in the container and allowed to attain phase equilibrium under the prevailing conditions *e.g.* temperature. The sample is then added, and the container agitated so that the phase system and sample are thoroughly mixed. This process allows the components of the sample to distribute on the basis of their relative affinities for each of the phases. The system is then allowed to regain phase equilibrium, after which either the upper or lower phase is removed to a separate container for further processing, if necessary.

Countercurrent distribution (CCD) is a multistage process based on a number of single – step partitions. It was pioneered in the 1950s by Lyman Craig, who devised several CCD instruments. In its simplest form, CCD comprises a series of test tubes. The process can best be explained with an example (Albertsson, 1986). A substance of mass 100 mg is distributed in a two – phase system in which its partition coefficient equals 1. The volume ratio of the system is also 1. At equilibrium, the amount of substance in the upper phase equals that in the lower phase *i.e.* 50 mg in the upper phase and 50 mg in the lower phase (tube 0 at transfer 0^{th} in Figure 1.3.1a).

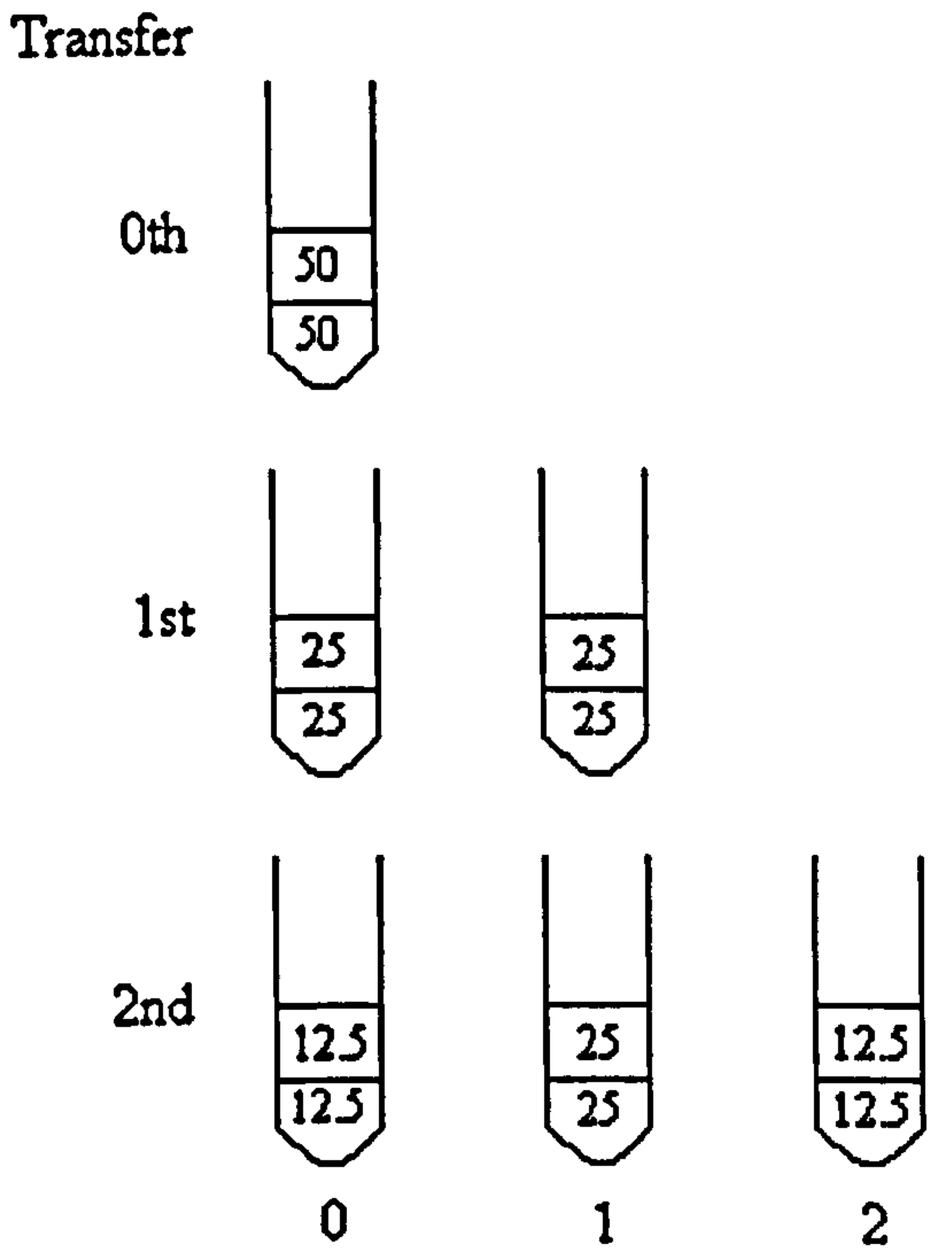

Figure 1.3.1a: Example of the CCD process using test tubes (according to Craig and adapted from Albertsson, 1986). Numbers inside the test tubes are the mass of substance in milligrams (mg).

The upper phase of tube 0 is transferred to tube 1, containing fresh lower phase of equal volume. In addition, fresh upper phase of equal volume is added to the lower phase of tube 0. The two tubes are shaken, and after equilibrium is obtained, the substance will be distributed as in the second row of Figure 1.3.1a *i.e.* 25% of the original amount of the substance is in each phase. One transfer is now completed.

The second transfer involves the upper phase of tube 1 being transferred to fresh lower phase in tube 2; the upper phase of tube 0 is transferred to tube 1, and fresh upper phase is added to tube 0. After equilibrium the substance will distribute as shown in the third row of Figure 1.3.1a.

This procedure may be repeated many times; with each transfer, the number of tubes increases by 1.

When the sample contains two species with different partition coefficients for the phase system used, countercurrent distribution can be considered a form of chromatography. Each step in CCD involves the thorough mixing of all components, with the sample molecules transferring between the two phases,

before equilibrium is attained. If the sample includes macromolecules such as proteins, this thorough mixing greatly reduces problems such as with mass transfer (the inhibition of molecules to move between the phases due to their molecular size). The thorough mixing demonstrated in each CCD step also increases the rate of transfer of the sample molecules between the two phases; therefore equilibrium is attained much faster than if the phases were subjected to gentle mixing. CCD is perhaps the technique that allows the greatest exhibition of ideal, or theoretical, behaviour of the phase system and the sample molecules. For this reason, it is frequently used as a model of ideal behaviour when comparing the behaviour of countercurrent chromatography systems.

A thin – layer CCD apparatus was developed by Albertsson that consisted of 60 chambers cut out of a circular piece of Perspex (Albertsson, 1965). The advantage of the thin – layer design was that experimentally acceptable phase separation times (generally 5 to 10 minutes) could be achieved with PEG – dextran systems; these systems took considerably longer to separate in more conventional containers, such as test tubes.

1.3.2. Countercurrent Distribution of Proteins

CCD has been employed several times in the study of protein behaviour in aqueous two – phase systems (refer to Table 1.3.2a).

Table 1.3.2a: Selected examples of the use of CCD with ATPS to purify proteins.

Phase System(s)	Protein(s)	Reference
5.0% w/w PEG-(6500, 8000): 7.0% w/w Dextran T500	Hexokinase, Glucose-6-phosphate dehydrogenase, Phosphofructokinase, Glyceraldehydephosphate dehydrogenase, 3-Phosphoglycerate kinase, Phosphoglycerate mutase, Enolase, Alcohol dehydrogenase	Johansson *et al* (1984)

Table 1.3.2a: Continued

Phase System(s)	Protein(s)	Reference
(Hydroxypropylstarch polymer = PPT) 14.0% w/w PPT: 5.0% w/w PEG-8000 14.0% w/w PPT: 5.0% w/w PEG-20000 8.0% w/w Dextran T500: 6.0% w/w PEG-8000 8.0% w/w Dextran T500: 6.0% w/w PEG-20000	Catalase, β-galactosidase	Tjerneld *et al* (1986)
10.8% w/w PEG-8000: 2.3% w/w Dextran T500 12.6% w/w PEG-8000: 2.7% w/w Dextran T500 14.5% w/w PEG-8000: 3.1% w/w Dextran T500 16.2% w/w PEG-8000: 4.5% w/w Dextran T500 18.0% w/w PEG-8000: 4.9% w/w Dextran T500 19.8% w/w PEG-8000: 5.4% w/w Dextran T500	β-glucosidase	Johansson and Reczey (1998)
20.0% w/w PEG-8000: 4.0% w/w Dextran T500	Cellulase, β-glucosidase	Brumbauer *et al* (1999)
7.0% w/w PEG-8000: 7.0% w/w Dextran T500	β-glucosidase	Brumbauer *et al* (2000)
PEG-(600, 1000): potassium phosphate	Alpha-1-antitrypsin	Reh *et al* (2002)

1.3.3. Countercurrent Chromatography: Introduction and Background

Countercurrent distribution has proved to be an effective method of protein separation. However, such step – wise processes do not lend themselves well to large – scale operations; historically those instruments built for this purpose were fragile and inconvenient to use (Mandava and Ito, 1988). The discrete, individual nature of the process means that even small – scale separations are time – consuming to perform.

An instrument that allows a continuous form of liquid – liquid chromatography was first reported by Ito and co – workers in 1966 (Ito *et al*, 1966). The diverse techniques that evolved from these early experiments were collectively termed countercurrent chromatography (CCC), and several different instruments have

subsequently been designed (Conway, 1990). Common between them all is the use of immiscible liquids that are subjected to gravitational or centrifugal forces inside the instrument (Mandava and Ito, 1988).

CCC can be subdivided into hydrodynamic CCC and hydrostatic CCC (Berthod and Talabardon, 1999). Historically, many hydrodynamic machines were developed by Ito, whilst most hydrostatic machines were designed and marketed by the Japanese company Sanki Engineering Limited. The technique name chosen and registered by Sanki was centrifugal partition chromatography (CPC). This acronym is also used in the field to refer to the coil planet centrifuge; however, in this work, CPC will refer exclusively to centrifugal partition chromatography, and will be addressed in Section 1.3.6.

This project initially utilised a particular type of hydrodynamic instrument called the Brunel/DE J – type CCC centrifuge. The design of this instrument is addressed in Section 1.3.5.

1.3.4. Hydrodynamic CCC: Basic Theory

Hydrodynamic CCC uses a rotating coiled tube to produce a hydrodynamic equilibrium between the two immiscible phases contained within it (Ito, 1988). The theory of this is best explained using a coiled tube. The tube is filled with water, and an air bubble and a glass bead are introduced. Both ends of the tube are sealed, and the tube is rotated about a horizontal axis (Figure 1.3.4a).

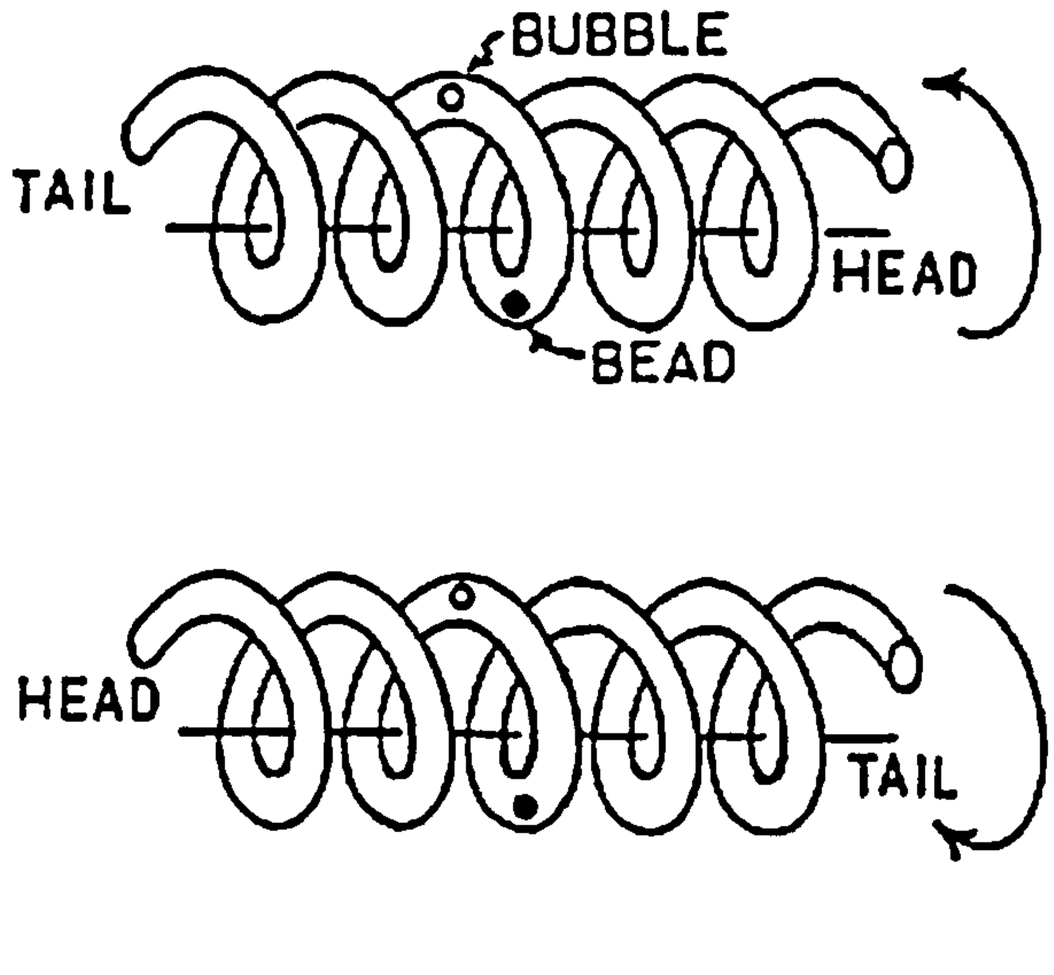

Figure 1.3.4a: Helical coils filled with water and each containing one bubble (white circle) and one bead (black circle). Rotation of the coils in the direction indicated will cause both bubble and bead to move to one end of the coil – an example of the Archimedean Screw Effect (adapted from Conway, 1990).

If the coil is then rotated in the direction shown by the arrow, both the air bubble and the bead will travel along the coil in the same direction towards one end of the coil. This end is designated the "Head" and the other end the "Tail". If the direction of rotation of the coil is reversed, the position of the "Head" and "Tail" is also reversed. This motion of bubble and bead within the water – filled coil is an example of the Archimedean Screw Effect, and is exhibited in both a helical coil (shown in Figure 1.3.4a) and a spiral coil (shown in Figure 1.3.4b).

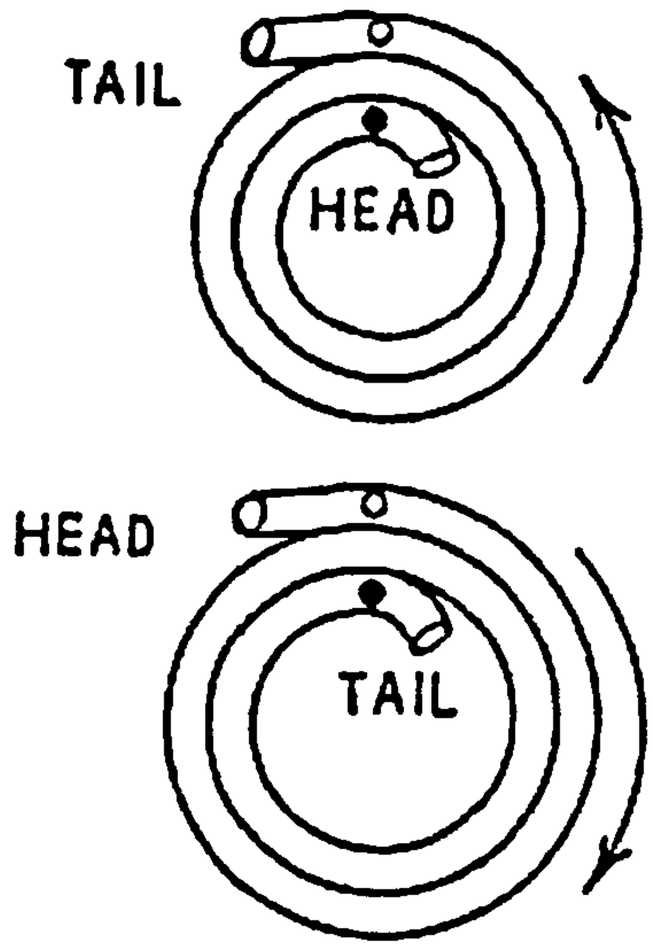

Figure 1.3.4b: Spiral coils filled with water and each containing one bubble (white circle) and one bead (black circle). Rotation of the coils in the direction indicated will cause both bubble and bead to move to one end of the coil – an example of the Archimedean Screw Effect (adapted from Conway, 1990).

If an identical coil is filled with equal volumes of two immiscible liquids, the ends sealed and the coil rotated as before, an equilibrium will be reached where each turn of the coil contains equal amounts of each phase (Figure 1.3.4c).

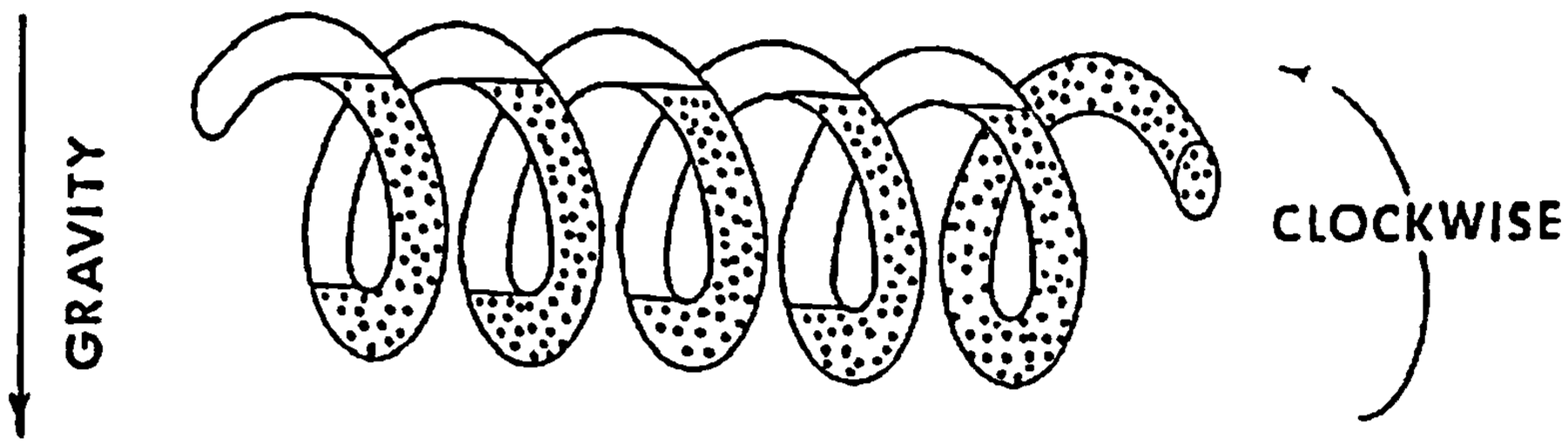

Figure 1.3.4c: Distribution of phases at equilibrium in a helical coil containing equal volumes of heavy phase (shaded area) and light phase (clear area) (adapted from Conway, 1990).

The coil is then emptied and refilled with unequal volumes of the two immiscible liquids *e.g.* one – third is filled with the heavy phase and two – thirds with the lighter phase. When it is rotated as before, the heavy phase (present in lesser amount) will half fill the coil turns at the "Head" end, with the lighter phase filling the remaining volume. The excess of the lighter phase will therefore completely

fill the turns at the "Tail" end of the coil. If the proportions of heavy and light phase are reversed, the distribution of the liquids will also be reversed.
To summarise, the phase present in the lesser amount, whether lighter or heavier, will travel to the "Head" of the coil, where it occupies half of each of a sufficient number of turns, and the excess of the other phase, either lighter or heavier, will remain at the "Tail". The behaviour of the liquids is analogous to that of the bubble and bead in the water – filled coil; the bubble/bead can be regarded as a very small amount of one phase which always moves to the "Head".
This type of phase distribution, typically observed at slow rotational speed and characterised by alternating segments of heavy and light phase, is termed segmented or Archimedean distribution (Conway, 1990).

A slowly – rotating coil containing equal volumes of two immiscible phases is allowed to reach equilibrium. The ends of the coil are then opened to allow one of the phases (designated the mobile phase) to be pumped into the "Head" end; the phases will be distributed as in Figure 1.3.4d.

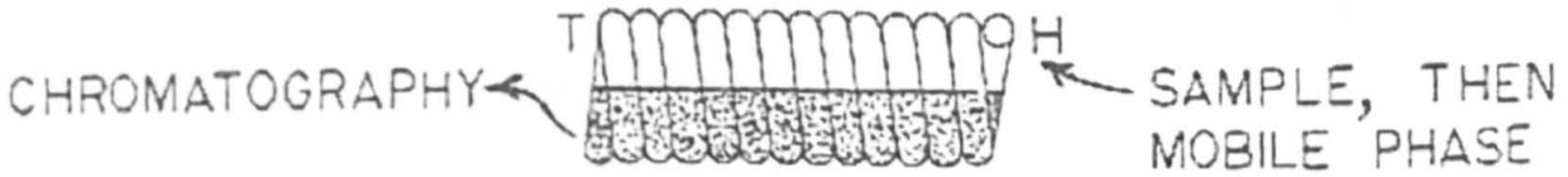

Figure 1.3.4d: Helical coil containing heavy phase (shaded area) and light phase (clear area) being utilised for chromatography (adapted from Conway, 1990).

Since the amount pumped in will constitute an excess of that phase, it will be carried by the rotating coil to the "Tail" end (Conway, 1990). The mobile phase is prevented from flushing the stationary phase from the column by the Archimedean Screw Force, which carries the stationary phase towards the "Head", against the flow of the mobile phase. Interfacial frictional force does operate in the direction of mobile phase flow; however, in reality, a dynamic equilibrium is reached inside the coil, which depends on rotational speed, mobile phase flow rate, viscosity of the two phases, and other factors.
Either phase can act as the mobile phase. However it must be pumped from "Head" to "Tail"; pumping "Tail" – to – "Head" would cooperate with the Archimedean Screw Force and flush the stationary phase from the coil. This

feature of the system can be used to empty the coil of stationary phase, if necessary.

If a small volume of sample is introduced to the coil in the mobile phase, it will undergo partition between the two phases present in each turn of the coil, and its constituents will undergo chromatographic separation on the basis of their distribution ratios in that particular phase system. Every turn of the coil could be visualised as a single extraction stage (equivalent to one transfer in CCD), and the number of theoretical plates calculated from elution profile could be approximated to the number of turns in the coil. However, this only applies if there is 100% mixing and mass transfer efficiency in each mixing and settling stage, which rarely occurs in CCC or CPC.

The fluid dynamics described so far occur when the coil is rotated at very slow speeds (<10 rpm). As the rotational speed increases to approximately 100 rpm, the heavy phase will move to the "Head" end of the coil; this is called unilateral distribution. When the rate of column rotation is increased further, so that the effect of gravity is negligible compared with that of the radial centrifugal force field, a uniform phase distribution occurs (Figure 1.3.4e). It is this type of phase distribution that occurs in the Brunel/DE J – type CCC centrifuge.

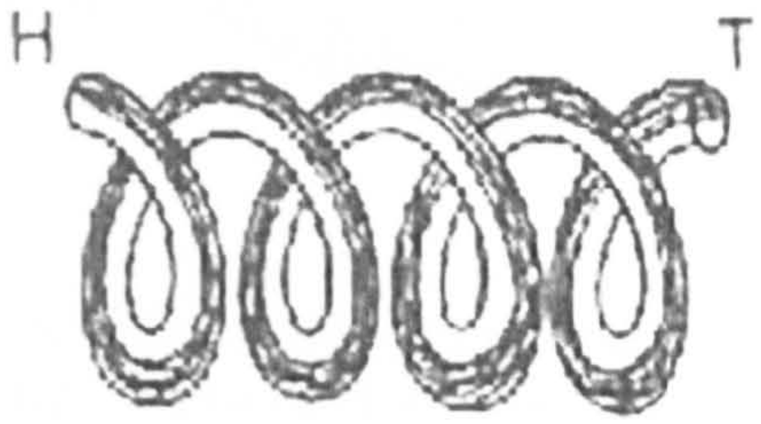

Figure 1.3.4e: Helical coil showing the distribution of heavy phase (shaded area) and light phase (clear area) when uniform phase distribution is attained (adapted from Conway, 1990).

1.3.5. Design of the Brunel/DE J – Type CCC Centrifuge

The Brunel/DE J – type CCC centrifuges are classified as planetary coaxial instruments. Most coils used with these machines are multilayer; the tubing that forms the column is wound on a bobbin as cotton thread is wound on a cotton reel, with the ends of the tubing emerging from the bobbin centre. The bobbin is

attached to a rotor (called the sun rotor), and in the case of the smallest machines (MILLI/MINI), the tubing ends are fed into the centre of the rotor, to emerge from the rear of the machine (Figure 1.3.5a). The "flying leads" are those sections of tubing external to the bobbin; the letter J shape they form as they exit the bobbin and enter the sun rotor gives the centrifuge its name.

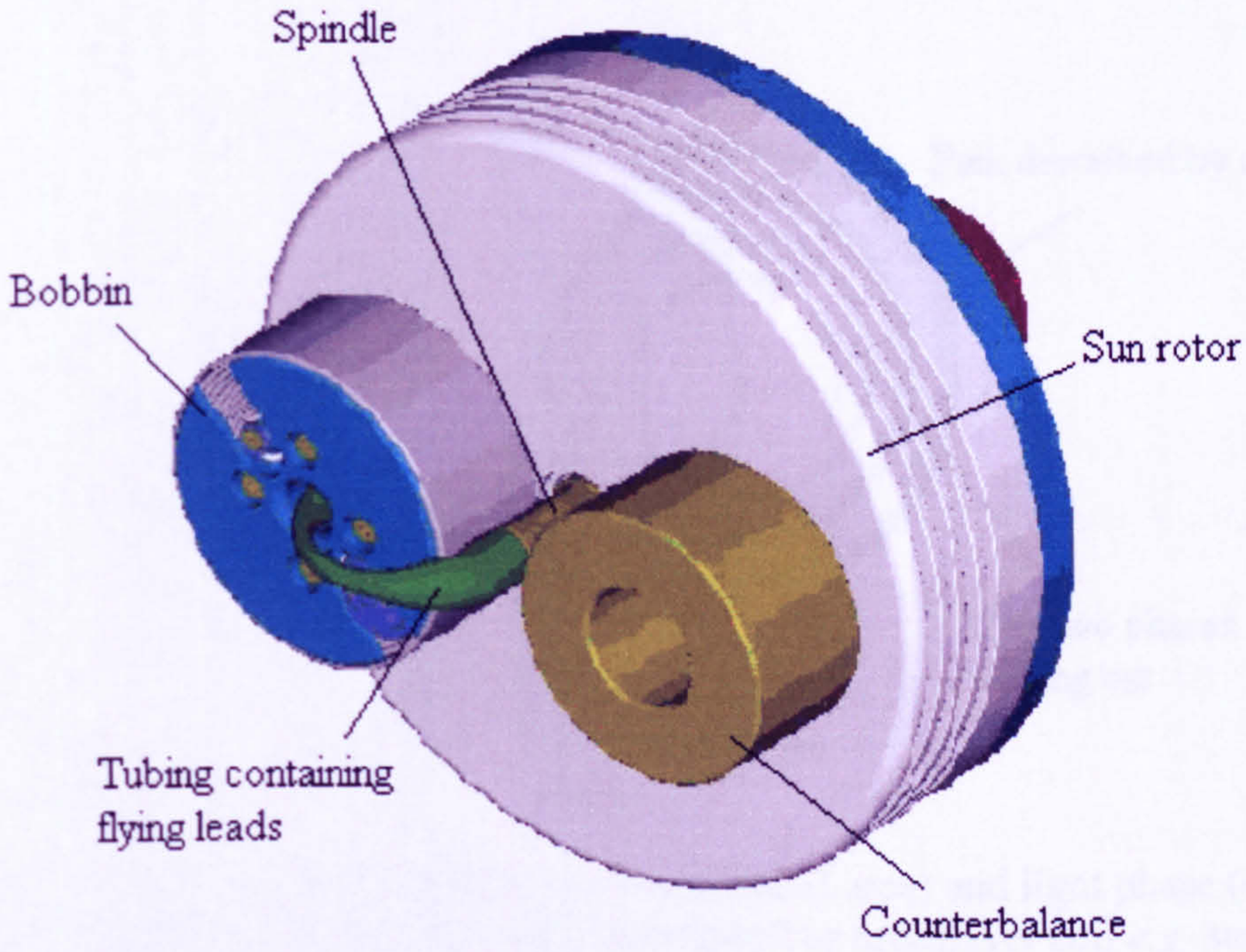

Figure 1.3.5a: DE-MINI CCC centrifuge rotor assembly showing location of bobbin, counterbalance, flying leads and spindle (adapted from Figure 3.8.4.3 of DE Mini Centrifuge Instruction Manual, Revision 2, April 2005, courtesy of D. Hawes/Dynamic Extractions Ltd).

The bobbin is fixed to the sun rotor so that it is able to rotate around its own axis, and on the MILLI/MINI version, a counterbalance is attached to the rotor to provide stability when the assembly is rotated. The larger centrifuges (MIDI and MAXI) have two bobbins that counterbalance one another, and these centrifuges can be operated utilising one bobbin (parallel operation) or both bobbins (series operation).

When the centrifuge is in operation, the sun rotor, carrying the bobbin, rotates in a clockwise direction. The bobbin, in addition to rotating with the sun rotor, also rotates in a clockwise direction around its own axis; this type of movement is described as planetary motion. There is one rotation of the bobbin for one rotation of the sun rotor.

Planetary motion produces a non – uniform centrifugal force field which agitates the immiscible liquid phases in one section of each loop of the coil. The liquid in the remainder of the loop exhibits uniform distribution (Figure 1.3.5b).

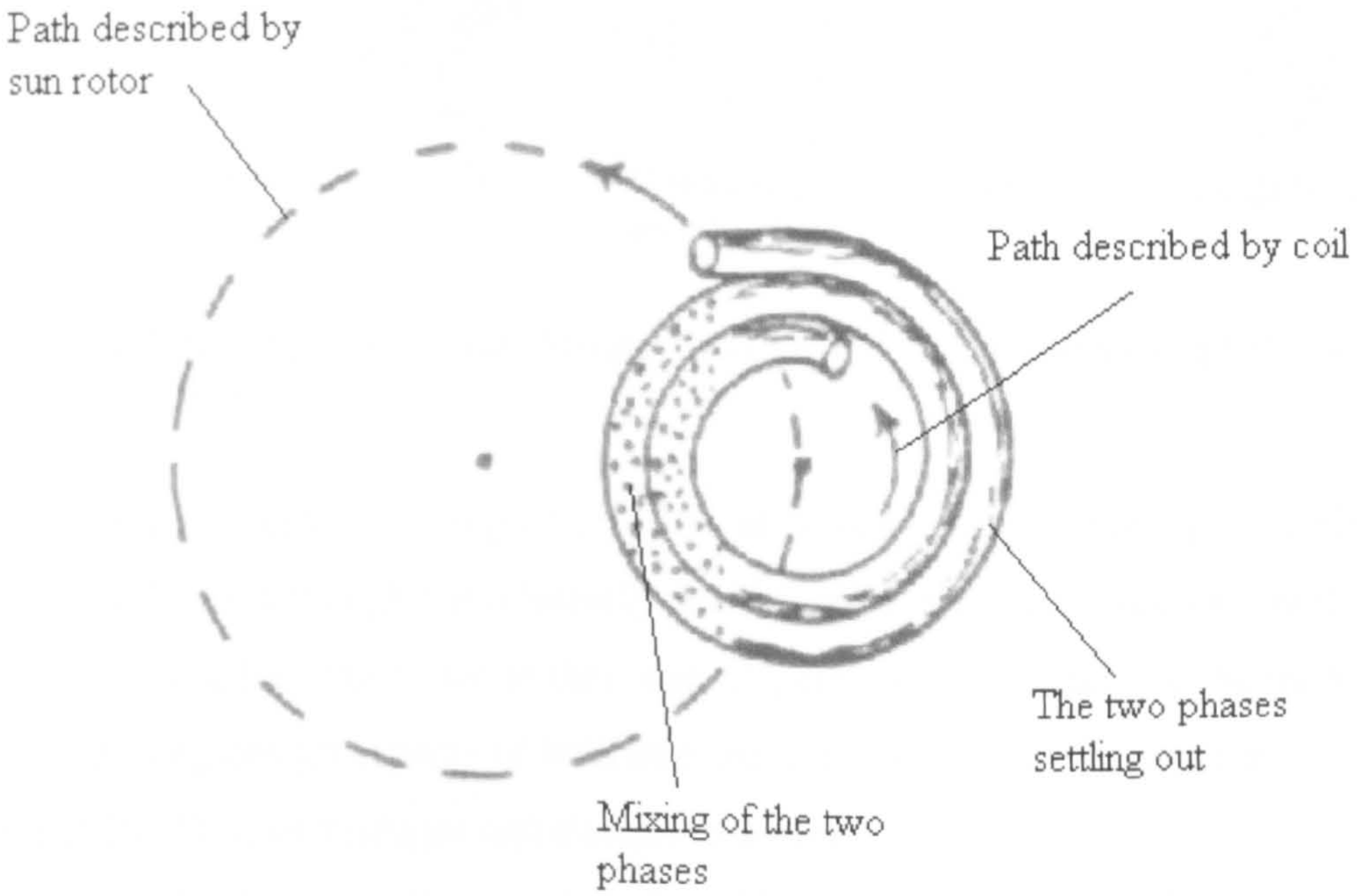

Figure 1.3.5b: Distribution of heavy phase (shaded area) and light phase (clear area) inside a planetary coaxial single layer spiral or multilayer coil *e.g.* such as is used on the Brunel/DE J – type CCC centrifuges. The diagram illustrates the point in the rotation pathway where mixing of the two phases occurs (dotted area) and where the two phases separate out (adapted from Conway, 1990).

Hence in each loop of the coil there is a zone where mixing of the two phases occurs, followed by a zone where the two phases separate out. During a CCC separation, mobile phase is flowing through the coil, carrying the multi – component sample. At a single point in time, a specific volume of mobile and stationary phase, together with the sample components, will undergo the mixing process in each loop of the coil. The mobile phase constituent of this volume will then immediately enter the settling step, before undergoing a repeat process in the next loop. One mixing and settling step is equivalent to one transfer in CCD, with

the associated separation of the sample components. The liquids in the coil have been described as exhibiting waves of mixing and settling, and several visualisation studies have been undertaken of this behaviour (Conway and Ito, 1984; Sutherland and Wood, 1999; Wood, 2002).

Central to the performance of the CCC centrifuge is the design of the column.

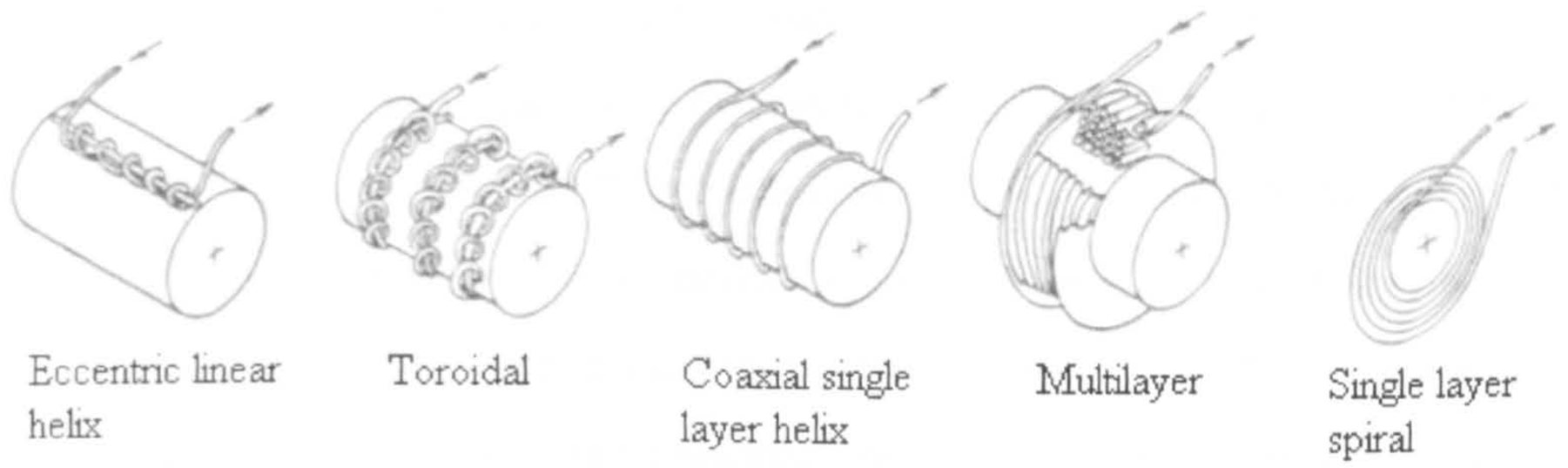

Figure 1.3.5c: Typical column designs used in CCC centrifuges (adapted from Conway, 1990).

The simplest columns are single layer helical coils and single layer spiral coils (Figure 1.3.5c), although the relatively small volume and short column length of these coils is a limiting factor in their use. Capacity of these coils can be increased by combining design aspects of both into the multilayer coil (fitted to the Brunel/DE CCC centrifuges and described above).

The toroidal column is often employed in CCC centrifuges, and is formed by winding the tubing onto a flexible core, which is in turn coiled onto the column holder or bobbin (Conway, 1990). The first centrifuge to use such a column was patented in 1977 (Ito, 1977) and was subsequently employed to separate a variety of biological molecules and cells using aqueous two – phase systems: two different strains of *E. coli* (Sutherland and Ito, 1978; Sutherland *et al*, 1987); cell membrane fragments (Flanagan *et al*, 1984); rat liver cell organelles (Heywood-Waddington *et al*, 1984; Sutherland *et al*, 1984; Sutherland *et al*, 1985; Heywood-Waddington *et al*, 1986; Heywood-Waddington *et al*, 1988). It was discovered that phase system behaviour within toroidal coils differed considerably from that in other coils; unusually, for a column consisting of a coiled tube, the phases were described as exhibiting hydrostatic, rather than hydrodynamic, behaviour.

1.3.6. Hydrostatic CCC: Basic Description

Droplet CCC (DCCC) is an established technique where droplets of mobile phase pass through a vertical column of stationary phase under unit gravity (Tanimura *et al*, 1970). Centrifugal partition chromatography, first introduced in 1982 (Murayama *et al*, 1982), can be viewed as a logical progression from DCCC. The vertical column is replaced by a number of chambers serially connected by narrower ducts that are placed in the rotor of a centrifuge (Berthod and Talabardon, 1999). A CPC instrument possesses a single axis of rotation that produces a constant centrifugal force field which maintains the stationary phase in the chambers. This compares with the structure of the CCC instruments designed by Ito and others; open plastic tubes coiled in spools subjected to a changing and cyclic centrifugal force field produced by a rotational motion with two or more axes of gyration. In both cases, the stationary phase is held in position by these forces while the mobile phase is pumped through it. In CPC, the mobile phase is driven by an external pump whilst in the ducts, but travels through the chambers under the influence of the centrifugal force field (Marchal *et al*, 2002a).

CPC centrifuges have two operating modes: descending and ascending (Figure 1.3.6a).

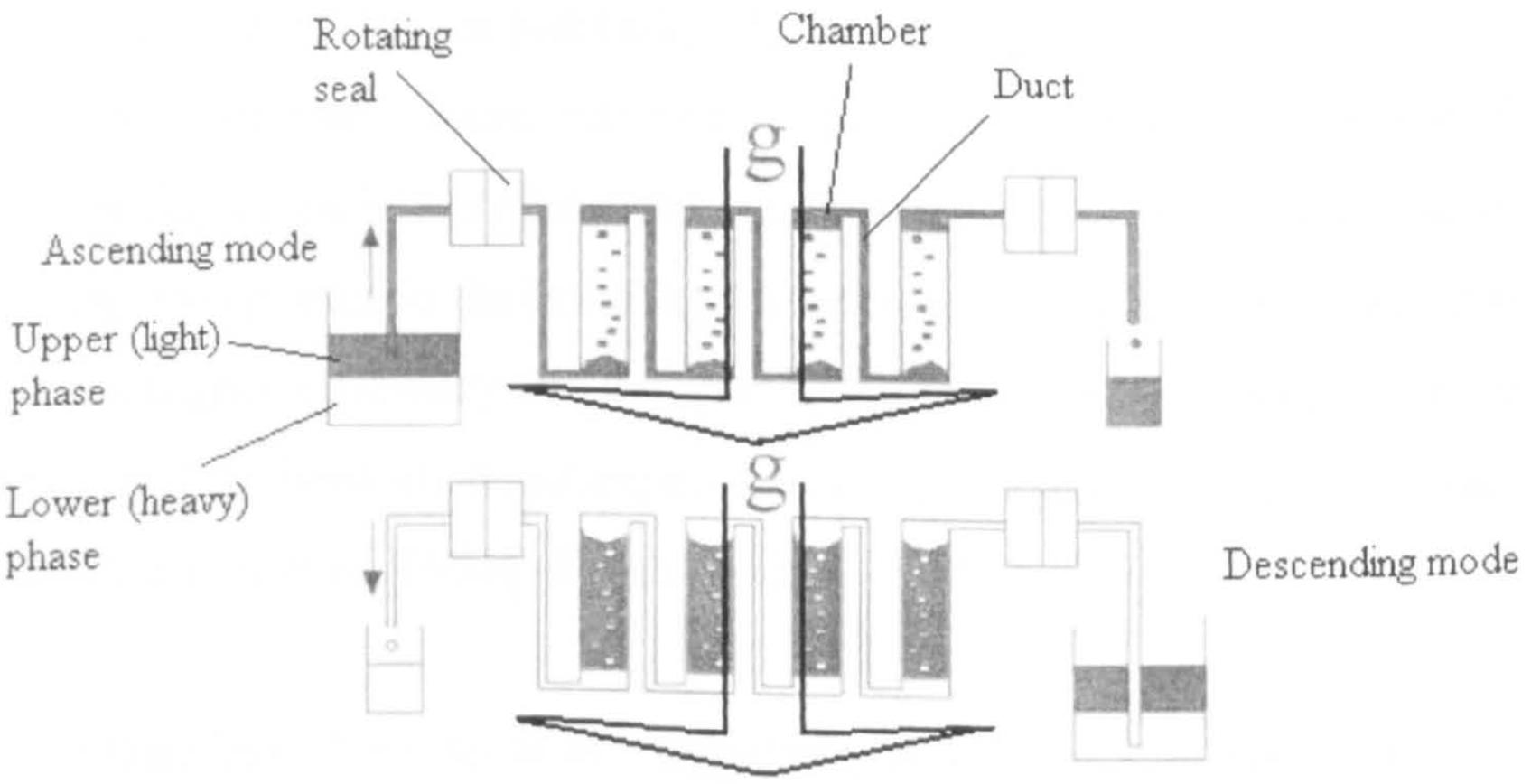

Figure 1.3.6a: Simplified diagram of the arrangement of chambers and ducts in a CPC centrifuge. The diagram shows the centrifuge operating in ascending mode (upper phase mobile) and descending mode (lower phase mobile), with the droplets of mobile phase passing through the stationary phase in each chamber. The large arrows indicate the direction of the gravitational force field (adapted from Marchal *et al*, 2002a).

The descending mode is chosen if the mobile phase is the lower (denser) phase of the liquid two – phase system. The mobile phase is pumped into one end of the column and forms into droplets under the influence of the constant centrifugal force field. These droplets of phase descend through the stationary phase, before exiting at the other end of the column.

The ascending mode is chosen if the mobile phase is the upper (less dense) phase of the liquid two – phase system. The mobile phase is pumped into the "Tail" of the column, where it forms into droplets that ascend through the stationary phase, before exiting at the "Head" of the column.

There have been several studies on fluid dynamics in CPC centrifuges. Droplet velocity has been shown to be dependent only on the interfacial tension of the phase system, and the viscosity of each phase, not on the centrifugal force field or mobile phase flow rate (Menet *et al*, 1994). However, in a constant force field, droplet velocity is dictated by droplet size, which is dependent on the centrifugal force field strength (higher force field strength produces smaller droplets). Increasing the rate at which the mobile phase is pumped does not increase the droplet velocity either; instead it increases the number of mobile phase droplets created. This factor explains why the stationary phase retention decreases as mobile phase flow rate increases; more droplets of mobile phase mean that there is less available space for the stationary phase to occupy.

In summary, if rotational speed and mobile phase flow rate are both increased, droplet size decreases but droplet number increases. Therefore, the interfacial area between the two phases in the centrifuge increases, leading to easier mass transfer of particles, higher efficiency of the column, and better separation of components. These points have been observed experimentally for aqueous – organic phase systems (Foucault *et al*, 1992a; Foucault *et al*, 1992b).

Several studies have been made of the hydrodynamics and kinetics of phase mixing in CPC centrifuges using stroboscopic photography. By colouring the mobile phase with a dye, van Buel *et al* (1998) were able to observe that the mobile phase occurred as droplets at relatively low flow rates and low rotational speeds, but formed a jet when either the flow rate or the rotational speed was increased above a critical value. The behaviour of the two phases has been filmed (Marchal *et al*, 2000; Marchal *et al*, 2002b); visualisation that confirmed the

importance of the Coriolis force on mobile phase flow shape. The Coriolis force acts upon the mobile phase flow, causing it to deviate sideways (across the chamber), rather than follow a straight path downwards or upwards through the chamber. These visual records made by Marchal *et al* gave rise to the statement that the chromatographic efficiency of CPC centrifuges was largely due to good mixing of the phases within each chamber (Marchal *et al*, 2002b).This group also filmed the behaviour of a 17.4% w/w PEG-3550: 10.6% w/w dipotassium hydrogen phosphate ATPS in a CPC centrifuge (Marchal *et al*, 2002a), with the lower phase designated as the mobile phase. The authors attributed the flow pattern of the mobile phase (described as a non – oscillating sheet) to the relatively high viscosity, low interfacial tension and low density difference of this phase system. The effect of the Coriolis force on the separation of mixtures in a Sanki (Kyoto, Japan) CPC centrifuge has also been studied (Ikehata *et al*, 2004). Experimental results showed that the direction of column rotation (clockwise or anticlockwise) was critical in obtaining good separations using both aqueous – organic and aqueous – aqueous phase systems.

Results from the comprehensive study using visualisation methods by Marchal *et al* (2002a) produced some redesigns of chamber geometry. One example of this is seen in the Partitron 25, a 25 litre capacity CPC centrifuge made by PARTUS Technologies in collaboration with Couturier SAS and the University of Reims (Margraff *et al*, 2005). This production scale instrument attempted to satisfy the demands of industry, including reliability, biocompatibility, and short separation times. To achieve the latter, high mobile phase flow rates would have to be used, creating high pressures within the instrument. The chambers of the Partitron 25 were filled with tampons of knitted metal wire to increase mass transfer efficiency.

The manufacturer states:

"The Partitron 25 has been designed to enable good manufacturing practice (GMP) compliance, and is currently validated in commercial pharmaceutical processes. More information on the complete cleaning of all cells between cycles will be the subject of coming publications." (Margraff *et al*, 2005).

However, it is likely that such inserts proved problematic when thorough cleaning of the machine became necessary. Information from the manufacturer on this aspect of the Partitron 25 is still awaited.

1.3.7. Design of the Armen CPC Centrifuge

The CPC centrifuge used in this study was purchased from Armen Instrument (Vannes, France). An advance in chamber design by Armen was demonstrated in the double chamber system incorporated into this model of centrifuge (Sutherland *et al*, 2008). The double chamber helps maximise efficiency by allowing two mixing and settling steps to occur where previous designs allowed only one mixing and settling event per chamber. The chambers and ducts of the Armen CPC centrifuges are engraved into metal discs (Figure 1.3.7a). Each double chamber consists of two cavities joined together by a very short section of duct. The discs are then stacked together to form a cylinder (the rotor) which is rotated in a single axis during the operation of the centrifuge. Further details of this CPC centrifuge are given in Section 2.4.1.

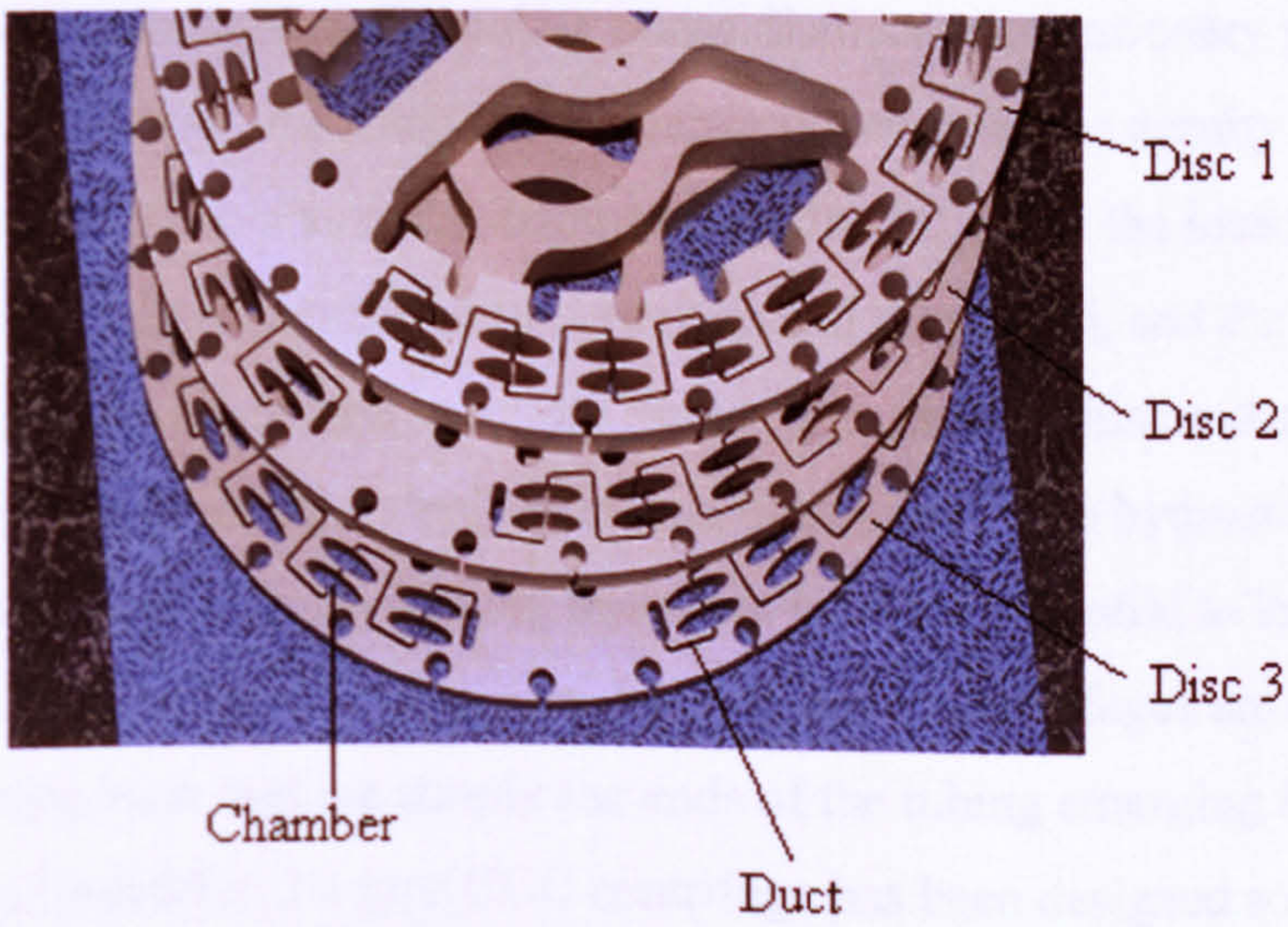

Figure 1.3.7a: Photograph of three discs from the Armen 12.5 litre CPC centrifuge, showing the chambers and connecting ducts (courtesy of I.A. Sutherland, 2007).

There are a number of differences between hydrodynamic CCC (as demonstrated in a J – type centrifuge) and hydrostatic CCC (as demonstrated in a CPC centrifuge):

1) The behaviour of the phases differs when the mobile phase pump is stopped but the rotation of the centrifuge is continued. In hydrodynamic CCC, the heavy and light phases move to opposite ends of the tubing, whereas in hydrostatic CCC the stationary phase remains trapped in the chambers.
2) The interaction of the two phases in each process is also different. In hydrodynamic centrifuges, both phases are in contact throughout the length of the column, and gentle, wave – like mixing is observed, whereas the design of hydrostatic centrifuges creates zones (the ducts that connect chambers) where only mobile phase is present. The two phases only interact in the chambers, where a vigorous cascade mixing is seen.
3) There is a contrast in the operating pressure of each type of instrument. A hydrostatic pressure difference is created in each chamber of a hydrostatic CCC centrifuge as the mobile phase displaces the stationary phase. The magnitude of this pressure difference depends on the density difference between each phase, the distance from the inflow to the interface in each chamber, the strength of the gravitational force field, and the number of chambers connected in series (Sutherland, 2007). This moderate level of pressure is absent in hydrodynamic centrifuges. The hydrostatic centrifuges possess rotating seals that have the potential to leak under this internal pressure, whereas the hydrodynamic centrifuges are equipped with flying leads that are simply the ends of the tubing emerging from the coil; the Brunel/DE J – type CCC centrifuge has been designed so that the flying leads do not become tangled during the operation of the centrifuge.

1.3.8. Protein Separation using Hydrodynamic and Hydrostatic CCC

Numerous examples of protein separation using both hydrodynamic and hydrostatic CCC centrifuges have been reported, and the use of ATPS in CCC for protein separation has recently been reviewed (Sutherland, 2007). The literature reveals that many researchers have employed the same, or very similar, phase

systems and proteins in their studies of instrument performance. This allows the reviewer to make more direct comparisons between the different centrifuges. A typical model aqueous two – phase system is 12.5% w/w PEG-1000: 12.5% w/w dipotassium hydrogen phosphate, with the lower phase employed as the mobile phase. Typical model proteins include: myoglobin, lysozyme, cytochrome *c* and bovine serum albumin (BSA). It is difficult to make absolute comparisons between different centrifuges, as the individual designs necessitated the use of different operating conditions. However, Table 1.3.8a details some studies using this model phase system and proteins in a range of CCC centrifuges.

Separations using the model ATPS and proteins mentioned above have been achieved with J – type coil planet centrifuges. Some of the column (coil) configurations used were:

- The column holder accommodates four identical multilayer coils arranged symmetrically around the column holder shaft. The coils are connected in series (Ito and Oka, 1988).
- The column holder accommodates three identical eccentric coil assemblies. Each assembly consists of eight coil units; each unit is prepared by winding a single piece of 1.6mm tubing into a 12cm long, double layer helical coil (Shibusawa and Ito, 1991).
- The column is a spiral disk assembly consisting of nine polyethylene disks, each of which has had grooves cut into its surface. The disks are sandwiched together to form a continuous column (Ito *et al*, 2003).

Other proteins have been purified using J – type centrifuges. Horseradish peroxidase was purified using a 10.0% w/w PEG-1540: 14.8% w/w phosphate buffer in a synchronous coil planet centrifuge fitted with three coaxial multilayer columns (Magri *et al*, 2003). α-amylase was purified using both a 13.0% w/w PEG-1000: 14.0% w/w phosphate buffer ATPS and a 13.0% w/w PEG-1000: 14.0% w/w citrate ATPS in a HSCCC instrument fitted with three multilayer columns (Zhi *et al*, 2005). Both proteins were purified from complex starting materials: horseradish peroxidase from horseradish root extract; α-amylase from the fermentation supernatant of *Bacillus subtilis*. Importantly, enzyme assays were conducted by both research groups to ascertain the level of post – purification

enzyme activity. In the case of α-amylase, it was found that when the PEG-1000: citrate system containing 2.0% sodium chloride and supplemented with 0.56% w/w calcium chloride was used, recovery of enzyme activity increased from around 30% to 73.1%. The authors suggest that the Ca^{2+} ion acts as a protective agent for the enzyme when it is subjected to solutions of high ionic strength. Recovery of enzyme activity is vital when considering a purification technique. In addition, both research groups used SDS-PAGE as a technique to confirm the results obtained from the enzyme assays. This is in contrast to the research groups using the model ATPS and protein systems (refer to Table 1.3.8a), who often rely solely on an online spectrophotometer to visualise results.

Despite these successes with the J – type centrifuges, in some quarters the opinion remained that these instruments did not give sufficient stationary phase retention when used with aqueous two – phase systems to allow for protein separation (Shinomiya *et al*, 1998). These problems had been anticipated previously, with the cross – axis coil planet centrifuge (X – type CPC) suggested as a design that may solve them (Ito, 1987). These centrifuges are similar to the J – type, except that the bobbin position is altered so that it rotates at a 90° angle to the rotational plane of the sun rotor. Rotating the bobbin in this position creates a complex, three – dimensional gravitational force field, which is thought to enhance mixing of more viscous phases within the column. Some of the column (coil) configurations used were:

- Eccentric coil assemblies (Shinomiya *et al*, 1993; Shinomiya *et al*, 1996a; Shinomiya *et al*, 1996b; Shinomiya *et al*, 1998; Shinomiya *et al*, 1999).
- Toroidal coil assemblies (Shinomiya *et al*, 1998; Shinomiya *et al*, 1999).
- Multilayer coil assemblies (Shibusawa and Ito, 1991; Shinomiya *et al*, 1993).
- Single layer helical coil assemblies (Shinomiya *et al*, 1993).
- Spiral coil assemblies (Shinomiya *et al*, 2002).

A cross – axis coil planet centrifuge fitted with eccentric coils has been used in conjunction with a 4.0% w/w PEG-8000: 5.0% w/w dextran T500 ATPS (buffered with potassium phosphate) to separate lysozyme and myoglobin

(Shinomiya *et al*, 2000). Some proteins exhibit superior solubility in PEG – dextran phase systems with low salt concentrations than in PEG – salt phase systems with high salt concentrations. Sodium chloride was added to the PEG – dextran phase system in varying concentrations to increase the partition coefficients of the lysozyme and myoglobin. In this case, it also increased the separation factor between the two proteins; the best resolution was obtained with the phase system containing the highest sodium chloride concentration. However, this peak resolution value of 1.3 was much less than the resolution value of 1.8 obtained by the same researchers using identical conditions but a 12.5% w/w PEG-1000: 12.5% w/w dipotassium hydrogen phosphate ATPS.

Purification of the enzyme maltose binding protein tagged – histone deacetylase (MBP-HDAC) from *E. coli* cell lysate has been achieved recently using a cross – axis coil planet centrifuge (Shibusawa *et al*, 2007). A PEG – dextran phase system was used, and the CCC fractions collected were analysed by both a HPLC – based deacetylation assay and by SDS-PAGE. PEG and dextran were removed from the fractions by ultrafiltration; this was to prevent band smearing during SDS-PAGE. The authors compared the performance of the CCC process with that of affinity chromatography. They found that most of the MBP-HDAC had passed through the affinity chromatography column in the cell lysate, and recovery was consequentially poor. By contrast, good purification and recovery of the target enzyme was achieved using CCC.

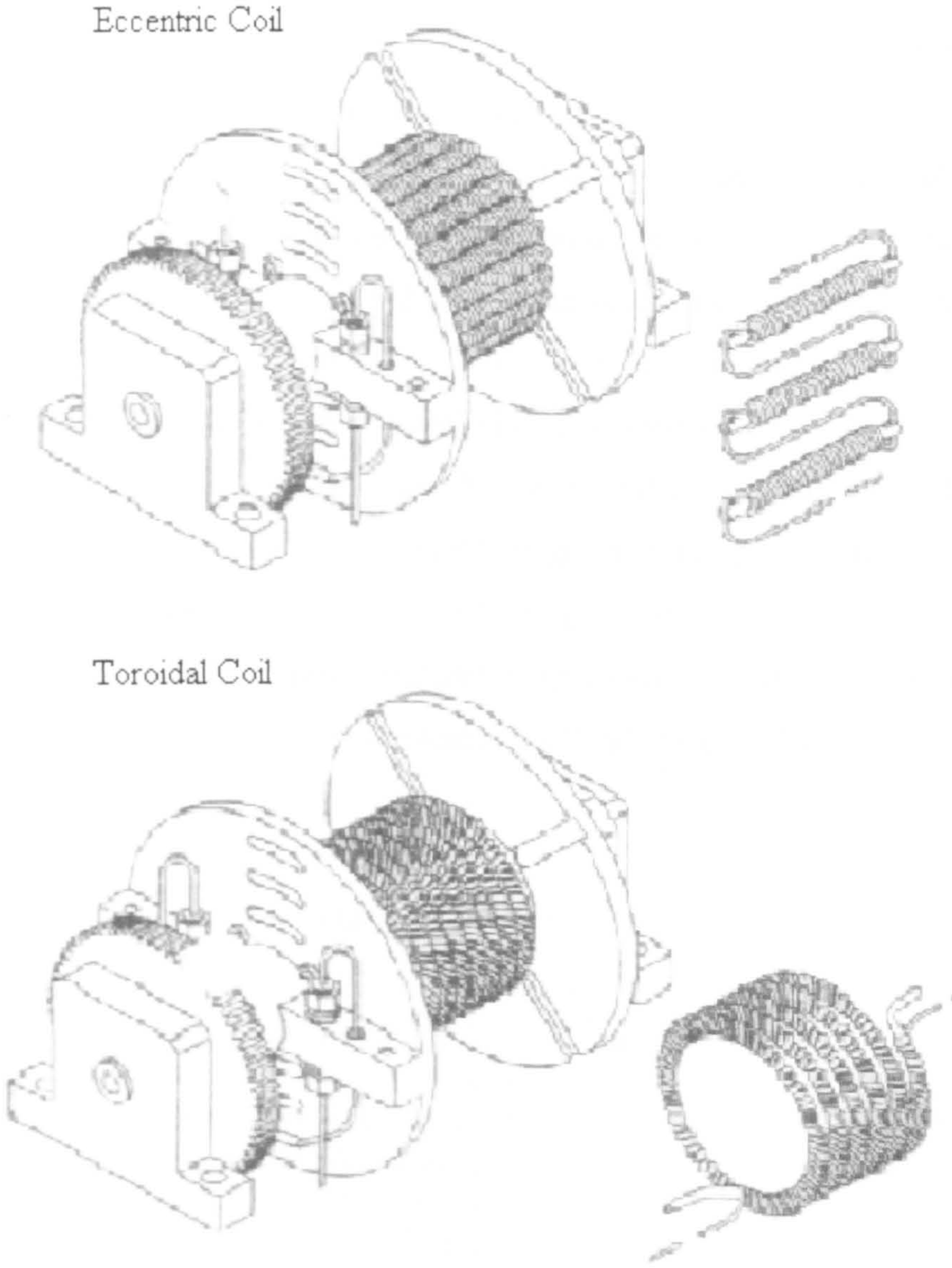

Figure 1.3.8a: Schematic drawing of two different types of coiled columns: an eccentric coil and a toroidal coil (taken from Shinomiya *et al*, 1999).

The non – synchronous coil planet centrifuge was introduced in 1979 (Ito *et al*, 1979) and like the J – type coil planet centrifuge, both rotor and bobbin have the same plane of rotation. Unlike the J – type, the bobbin and rotor have different rotational speeds (typically in the range 0 to 60 rpm and 600 to 1000 rpm respectively). Rotor and bobbin (independent of one another) can rotate in a clockwise or anticlockwise fashion. The gravitational force field strength is determined by the rotor speed, whilst the degree of phase mixing is determined by the bobbin speed. The centrifuges can be fitted with both multilayer and eccentric coils (Shinomiya *et al*, 2003); the multilayer coil obtained a separation of

resolution 1.83 for lysozyme and myoglobin. The eccentric coil was less effective (resolution was reduced to 0.97), although the authors do not postulate on the reason for this difference in the resolution.

The cascade mixing typical of CPC is also seen in some toroidal coil CCC centrifuges, where the tubing has been wound in such a way that the stationary phase can become trapped and the process is a hydrostatic (rather than a hydrodynamic) one (Sutherland, 2007). Protein separations have been achieved with toroidal coil CCC centrifuges (Ito *et al*, 1998).

A Sanki CPC centrifuge, model LLN, was used with a PEG-8000: dextran ATPS to purify recombinant tissue – plasminogen activator, achieving a two – fold purification with 50% recovery of the target protein (Grunfeld *et al*, 1992).

Lysozyme and BSA were separated using another Sanki CPC centrifuge, model LLBM, with a total internal volume of 230 ml (refer to Table 1.3.8a).

Table 1.3.8a: Selected examples where CCC centrifuges have been used to separate the proteins myoglobin, lysozyme, cytochrome *c* and bovine serum albumin (BSA) with a 12.5% w/w PEG-1000: 12.5% w/w K_2HPO_4 ATPS (LP = MP) (from Sutherland, 2007).

Column & Centrifuge Type	Column Volume (ml)	Sample Loaded (%CV)	Column Diameter (mm)	Column Length (m)	Rotational Speed (rpm)	MP Flow Rate ($mlmin^{-1}$)	Resolution			Reference
							Rs12	Rs23	Rs13	
Toroidal coil centrifuge	13	—	0.55	60	1200	0.05	1.56	1.50	2.58	Ito *et al*, 1998
	13	—	0.55	60	1200	0.10	0.97	1.19	1.97	
	13	—	0.55	60	1200	0.20	0.77	0.79	1.39	
High speed CCC	200	—	1.6	100	800	1.00	—	—	2.60	Ito and Oka, 1988
High speed CCC	220	—	1.6	109	800	0.50	2.22	—	—	Shibusawa and Ito, 1991
	220	—	1.6	109	800	0.70	1.43	—	—	
	220	—	1.6	109	800	1.10	0.73	—	—	
Co – axial non – synchronous CCC	39	2.6	0.8	78	800/10	0.20	1.62	1.83	3.18	Shinomiya *et al*, 2003
Eccentric non – synchronous CCC	20	5.0	0.8	40	800/10	0.20	0.53	0.97	1.51	Shinomiya *et al*, 2003
Eccentric non – synchronous CCC	20	5.0	0.8	40	800CCW /40CW	0.2	1.20	1.50	—	Shinomiya and Ito, 2004
Eccentric X – type coil planet centrifuge	28	3.6	1.0	36	800	0.20	0.91	—	—	Shinomiya *et al*, 1996b
Eccentric X – type coil planet centrifuge	27	3.7	1.0	34	800	0.20	—	1.21	—	Shinomiya *et al*, 1999

Table 1.3.8a: Continued

Column & Centrifuge Type	Column Volume (ml)	Sample Loaded (%CV)	Column Diameter (mm)	Column Length (m)	Rotational Speed (rpm)	MP Flow Rate ($mlmin^{-1}$)	Resolution			Reference
							Rs12	Rs23	Rs13	
Toroidal X – type coil planet centrifuge	29	3.4	1.0	37	800	0.20	—	1.70	—	Shinomiya *et al*, 1999
Centrifugal partition chromatograph	230	0.4	—	—	1200	0.80	1.73	—	—	*Chen *et al*, 1999

%CV: Percentage of column volume
1: Cytochrome *c* or Bovine serum albumin (BSA)
2: Myoglobin
3: Lysozyme
* Phase system used consisted of PEG-6000: KH_2PO_4/K_2HPO_4

1.3.9. The Scale – Up of Hydrodynamic and Hydrostatic CCC

Whilst the majority of separations have been achieved on analytical scale centrifuges, there has been some progress made in the scale – up of CCC.

One of the disadvantages of many analytical – scale centrifuge designs (in particular the cross – axis coil planet centrifuges) is that their complexity makes it difficult to produce a functional and reliable large – scale version.

Larger capacity hydrodynamic J – type centrifuges have been designed and produced by the Brunel University team. Models used include the "Quattro", fitted with two multilayer bobbins connected in series, with total capacity 928 ml (Sutherland *et al*, 2001a). Initial studies focused on the theoretical aspects of scale – up, specifically how the hydrodynamic, engineering and chromatographic variables affected the process (Sutherland *et al*, 2001b). Experimental work compared the performance of smaller versions (capacities of 25 ml and 95 ml) with that of the 928 ml capacity "Quattro". The centrifuges all the same planetary radius (R) of 110 mm and were rotated at 800 rpm. An aqueous – organic phase system consisting of heptane/ethyl acetate/methanol/water was used to separate a mixture of benzyl alcohol and 2-phenyl-ethanol. These studies were assisted by the production of the computer program "C.H.E.S.S." (Sutherland *et al*, 2003). This modelled a given CCC process on the basis of an eluting CCD model, and allowed factors such as peak width and efficiency to be predicted.

One important overall conclusion from the theoretical and experimental studies was the linear nature and therefore predictability of the scaling – up process. A further study revealed that stationary phase retention increased significantly with increased tubing bore, and resolution can be maintained even if the mobile phase flow rate was increased 20 – fold (Sutherland *et al*, 2001c). This confirmed that not only could hydrodynamic CCC be performed on a large scale, but that doing so did not sacrifice the effectiveness of the separation process.

This centrifuge was subsequently used in the purification of a range of biomolecules, including: erythromycin A (from its analogues) (Booth *et al*, 2003) and from a fermentation broth (Booth *et al*, 2004); the glucosinolate glucoraphanin (Fisher *et al*, 2005); DNA plasmids (Al-Marzouqi, 2006).

A Pharma-Tech planetary centrifuge was also used in both semi – preparative (capacity 325 ml) and preparative (capacity 850 ml) modes to purify glucoraphanin (Fahey *et al*, 2003).

Interest and funding from the biotechnology industry (in partnership with the EPSRC) for pilot – scale CCC centrifuges led to the design and production of the "Brunel DE-MAXI" J – type centrifuge by the Brunel team. This centrifuge has a rotor radius of 300 mm, and rotational speed range of 100 to 850 rpm, a 4.6 litre capacity, with tubing of 10 mm bore and 60 m in length wound onto two bobbins, which can be operated either in series or in parallel (Sutherland *et al*, 2005). This was used in the manufacture of a 1 kg quantity of glucoraphanin (Ignatova *et al*, unpublished results) following the successful production of 53 g using the "Brunel DE-MIDI" centrifuge (Fisher *et al*, 2005).

A preparative scale multilayer coil (575 ml capacity) was used in a cross – axis coil planet centrifuge to separate cytochrome *c*, myoglobin, ovalbumin and haemoglobin (Shinomiya *et al*, 1993). The centrifuge was also fitted with analytical – scale eccentric coils (volumes of 35.4 ml and 34.0 ml), and so could not be classified as a true pilot scale machine.

Partitron 25, the 25 litre capacity, pilot – scale CPC centrifuge (Margraff *et al*, 2005) (refer to Section 1.3.6) has been operated with a 12.5% w/w PEG-1000: 12.5% w/w dipotassium hydrogen phosphate ATPS. Although a reasonably good stationary phase retention value of 74% was obtained, the loading sample consisted of just the one protein, myoglobin, therefore it is difficult to draw a conclusion of the effectiveness of this instrument in protein separation.

1.4. Conclusions

Aqueous two – phase systems have advantages over conventional extraction processes in the purification of many biomolecules, including proteins. The aqueous nature of these systems creates a non – denaturing environment, and the polymers used have a stabilising effect on protein structure. They have been employed in a diverse range of applications in the last 40 years, and some work has been undertaken to understand their intrinsic properties.

Aqueous two – phase systems have been employed in liquid – liquid chromatography, from single – step partition experiments up to medium scale research using countercurrent chromatography centrifuges.

There have been a number of different designs of these centrifuges, encompassing both hydrostatic and hydrodynamic CCC. Each design has advantages and disadvantages; however, there are few that are designed to operate on a truly large scale. Recent advances in the manufacture of proteins present challenges to downstream processing stages, specifically a need for high – capacity techniques that allow the proteins to retain their biological function. The Brunel/DE J – type CCC centrifuges have purified small organic molecules, using aqueous – organic phase systems, on a scale from mg to kg quantities.

The challenge of this study was to combine this technology with aqueous two – phase systems to explore the feasibility of protein purification on a large scale, focussing on a protein of commercial interest.

1.5. Aims and Objectives of the Research

The primary aim of this thesis was to develop protein separations on the Brunel/DE J – type CCC centrifuges (an example of hydrodynamic CCC). The Armen CPC centrifuge (an example of hydrostatic CCC) was also used in the study, and this allowed comparisons between hydrodynamic and hydrostatic CCC to be made.

The following objectives were to be addressed during the study:

- To gain an understanding of how aqueous two – phase systems behave in both the Brunel/DE J – type CCC centrifuges, and in the Armen CPC centrifuge, in particular how stationary phase retention varies with rotational speed, mobile phase flow rate, mode of operation (lower or upper phase as the mobile phase) and column bore (J – type CCC centrifuges only).
- To use both types of centrifuge to perform a chromatographic separation of two model proteins and phase system chosen from the literature.
- To use both types of centrifuge to purify from fermentation supernatant at least one plant – based protein that is of commercial interest to our industrial partner Syngenta, and to investigate the degree of biological activity retained by this protein during the separation process.

Chapter 2 – General Materials and Methods

2.1. Overview of Chapter

This chapter details the general experimental methods relevant to this thesis, such as the reagents, equipment and experimental protocols used. It contains the methods and results of peripheral experiments that were conducted, such as the measurement of the physicochemical properties of the phase system, and the measurement of the distribution ratio of the proteins lysozyme and myoglobin, and experiments to determine the solubility of these proteins.

The chapter also contains details of how certain chromatographic parameters were calculated in the chapters on the separation of lysozyme and myoglobin using CCC and CPC centrifuges.

2.2. Aqueous Two – Phase Systems (ATPS)

2.2.1. Preparation of the 12.5% w/w PEG-1000: 12.5% w/w Dipotassium Hydrogen Phosphate ATPS

Polyethylene glycol (PEG) of average molecular weight 1000 Daltons and the anhydrous salt dipotassium hydrogen phosphate (K_2HPO_4) were obtained from Sigma-Aldrich (Poole, Dorset, UK). Deionised water of purity 1.0 $M\Omega cm^{-1}$ was obtained from the in – house water purifier (Purite, Thame, Oxfordshire, UK).

Stock solutions of 100 g, 200 g, 400 g, 700 g or 1400 g 40% w/w PEG-1000 were made by combining liquid PEG (melted in a 50°C oven for 3 hours) with water in a weight to weight ratio of 4:6 (PEG:water). Stock solutions of 40% w/w dipotassium hydrogen phosphate were made by combining the salt with water in the same weight to weight ratios.

The ATPS was made in batches, created by combining the PEG and salt stock solutions with water in the quantities shown in Table 2.2.1a.

All reagents were weighed out into glass bottles of appropriate capacity. A balance with accuracy of 0.01 g was used to measure weights between 10 g and 1000 g. A balance with accuracy of 0.1 g was used to measure weights greater than 1000 g.

Table 2.2.1a: Quantities of 40% w/w PEG-1000 stock solution, 40% dipotassium hydrogen phosphate stock solution and water used to produce varying quantities of a 12.5% w/w PEG-1000: 12.5% w/w dipotassium hydrogen phosphate ATPS.

Mass of ATPS (g)	Mass of 40% w/w PEG-1000 Stock Solution (g)	Mass of 40% w/w K_2HPO_4 Stock Solution (g)	Mass of Water (g)
10	3.13	3.13	3.74
100	31.25	31.25	37.50
200	62.50	62.50	75.00
600	187.50	187.50	225.00
1000	312.50	312.50	375.00
2000	625.00	625.00	750.00
4000	1250.0	1250.0	1500.0

The ATPS was poured into a separating funnel of appropriate capacity and allowed to attain temperature equilibrium in a 30°C incubator. The funnel contents were then shaken thoroughly and allowed to separate for at least three hours, typically overnight. The majority of the lower phase was run off into a glass bottle. The liquid around the interface, consisting of approximately 1.0 ml of each phase, was run off and discarded, as it contained contaminants that had collected at the interface during phase separation. The majority of the upper phase was decanted into another bottle. Both phases were stored at 4°C. Measurements were taken at this point or shortly afterwards of physiochemical properties such as volume ratio, density, pH, viscosity and interfacial tension.

2.2.2. Measurement of the Volume Ratio of a 12.5% w/w PEG-1000: 12.5% w/w Dipotassium Hydrogen Phosphate ATPS

The volume of the upper and lower phases at 30°C was determined with the use of measuring cylinders as the phases were decanted from the separating funnel. Only phase systems of total mass 2000 g were used. A small amount of each phase (≤ 2 ml) was lost from each phase system; this was because contaminants from the reagents collected at the interface during phase separation, and so a small volume of phase either side of the interface was discarded as waste.

A total of seven phase systems were measured. The volume ratios (UP:LP) were between 1:1.3 and 1:1.4; the mean volume ratio was 1:1.36.

2.2.3. Measurement of the Density of a 12.5% w/w PEG-1000: 12.5% w/w Dipotassium Hydrogen Phosphate ATPS

The densities of the upper and lower phases were determined gravimetrically using a 10 ml density flask and a balance of readability 0.0001 g. Measurements were made in triplicate at a temperature of 30°C ± 2.5°C.

A total of five phase systems were measured and the densities of each are shown in Table 2.2.3a.

Table 2.2.3a: Densities of the upper and lower phases of selected 12.5% w/w PEG-1000: 12.5% w/w dipotassium hydrogen phosphate aqueous two – phase systems made during the course of this study.

Phase	Density of Individual Phase Systems (gml^{-1})					Average Density (gml^{-1})
UP	1.0571	1.0796	1.0775	1.0634	1.0821	1.0719
LP	1.1491	1.1247	1.1250	1.1239	1.1240	1.1293

2.2.4. Measurement of the pH of a 12.5% w/w PEG-1000: 12.5% w/w Dipotassium Hydrogen Phosphate ATPS

The pH value of each phase was measured using a Mettler Toledo "SevenEasy" pH meter (Mettler-Toledo Ltd, Leicester, UK). Measurements were made at a temperature of 30°C ± 2.5°C. Prior to measurements being taken, the pH meter underwent a three – point calibration (at pH values 4.01, 7.00 and 9.21) using buffer solutions provided by the manufacturer.

A total of five phase systems were measured and the pH values of each are shown in Table 2.2.4a.

Table 2.2.4a: Densities of the upper and lower phases of selected 12.5% w/w PEG-1000: 12.5% w/w dipotassium hydrogen phosphate aqueous two – phase systems made during the course of this study.

Phase	pH of Individual Phase Systems					Average pH
UP	9.30	9.27	9.35	9.34	9.26	9.30
LP	9.16	9.23	9.30	9.23	9.11	9.21

2.2.5. Measurement of the Viscosity of a 12.5% w/w PEG-1000: 12.5% w/w Dipotassium Hydrogen Phosphate ATPS

The viscosity of each phase was determined using an Anton Paar "AMVn" automated microviscometer (Anton Paar, Graz, Austria). A photograph of the model used is shown in Figure 2.2.5a.

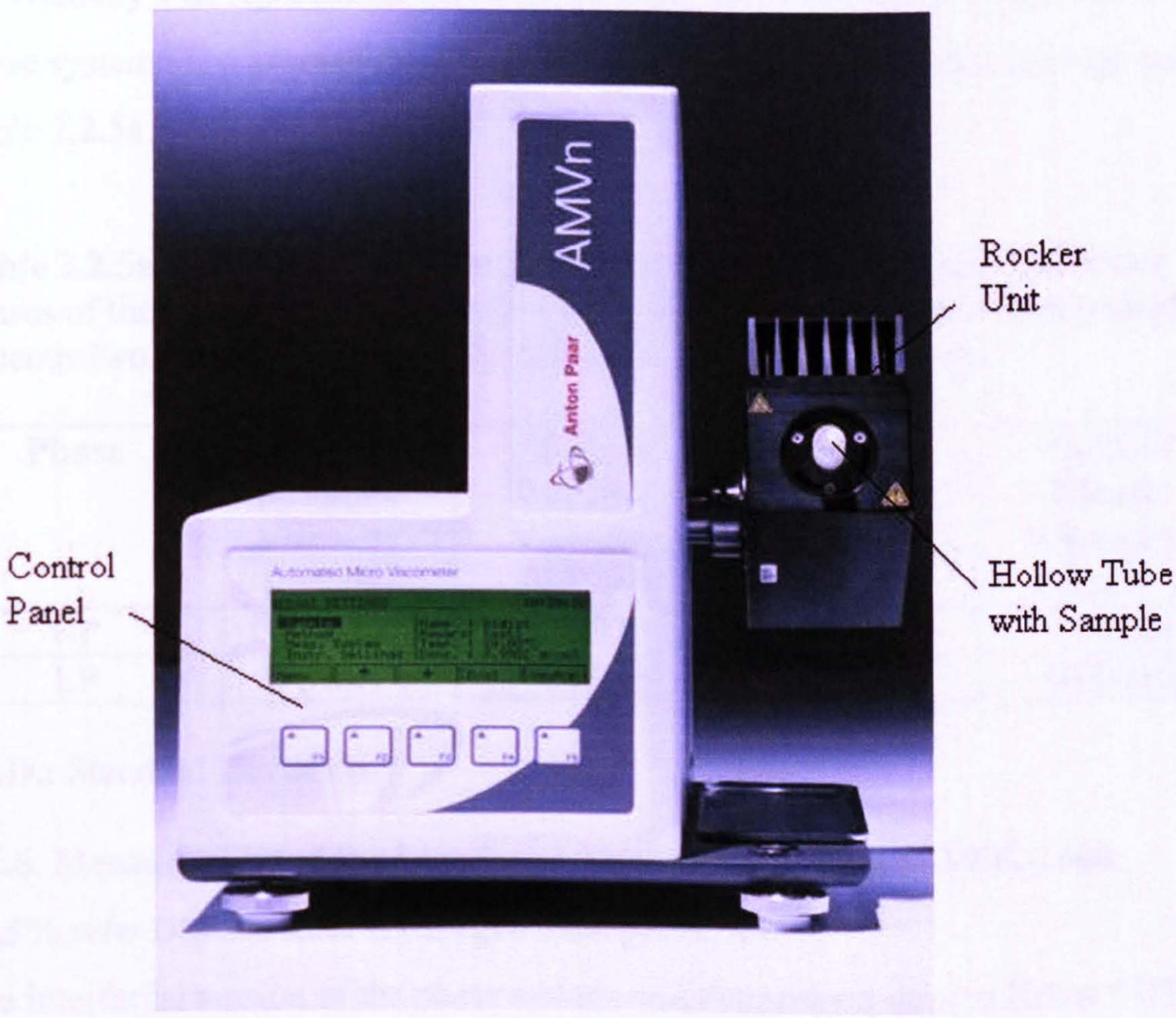

Figure 2.2.5a: Photograph of the viscometer model used in the measurement of the viscosity of each phase from the 12.5% w/w PEG-1000: 12.5% w/w dipotassium hydrogen phosphate ATPS.

This viscometer used the "rolling ball" principle to measure the viscosity of the phases. The instrument consisted of a hollow glass tube, permanently sealed at one end, which was housed in a temperature – controlled rocker unit; the unit can rotate through a range of angles inclined to the horizontal plane. The hollow tube was filled with the phase under measurement, a small ball bearing added, and the end sealed. The tube was placed in the temperature – equilibrated rocker unit and the measurement program initiated. The rocker unit rotated through to the pre – set incline angle, and then rotated back to the starting position. The ball bearing moved up and down the liquid – filled tube as the rocker unit rotated. A sensor

within the unit measured the time taken by the ball bearing to travel from one end of the tube to the other through the liquid. Integral software then calculated the dynamic and kinematic viscosity of the phase.

In this study, one phase system was used for all measurements, at a temperature of 29.25°C for the lower phase and 29.0°C for the upper phase. The measurement of the viscosity was repeated six times for both the upper and lower phases of the phase system. The average dynamic and kinetic viscosities for each are reported in Table 2.2.5a.

Table 2.2.5a: Average dynamic and kinetic viscosities of the upper and lower phases of the 12.5% w/w PEG-1000: 12.5% w/w dipotassium hydrogen phosphate aqueous two – phase systems made during the course of this study.

Phase	Average Dynamic Viscosity (mPa•s)	*S.D. of Dynamic Viscosity (mPa•s)	Average Kinetic Viscosity (mm^2s^{-1})	*S.D. of Kinetic Viscosity (mm^2s^{-1})
UP	4.8350	0.00029	4.5467	0.00028
LP	1.7104	0.00018	1.5219	0.00016

***S.D.:** Standard Deviation

2.2.6. Measurement of the Interfacial Tension a 12.5% w/w PEG-1000: 12.5% w/w Dipotassium Hydrogen Phosphate ATPS

The interfacial tension of the phase system was determined using a Krüss "SITE 04" spinning – drop tensiometer (Krüss, Hamburg, Germany).

Spinning – drop tensiometers are used when the value for the interfacial tension of a system is very small, in the order of 1×10^{-5} to 1×10^{-6} mNm^{-1}. The first reported use of these tensiometers with ATPS was with PEG – dextran systems (Ryden and Albertsson, 1971). The instrument consisted of a horizontal capillary tube (open at both ends) that can be rotated at high speed. The capillary tube was surrounded by an oil bath that gave good temperature control. The temperature of the system was maintained at 30°C ± 2°C. The central section of the capillary tube was observed using a measuring – microscope with a graduated field of view. The capillary tube was filled with the denser of the two phases and brought to a steady rotational speed. A microsyringe was used to inject droplets of the less dense upper phase into the rotating cylinder; by opening the outlet valve of the

capillary tube a single droplet was brought into the microscope field of vision. The diameter of the drop was then measured using the microscope.

The diameter of three different droplets was measured; each droplet was measured at rotational speeds of 2000 rpm, 3000 rpm and 4000 rpm. The average diameter of the droplets at each rotational speed was then calculated, and these values used to determine the interfacial tension at each value of rotational speed, using the Vonnegut equation (Vonnegut, 1942):

$$\sigma = \frac{1}{4} r^3 \Delta\rho \omega^2 \qquad \text{[Equation 2.2.6a]}$$

σ = Interfacial tension ($N \cdot m^{-1}$)
r = Radius of droplet (m)
$\Delta\rho$ = Density difference between the two phases ($kg \cdot m^{-3}$)
ω = Angular velocity ($rad \cdot s^{-1}$)

The Vonnegut equation is valid providing the length of the droplet is at least four times its diameter. The interfacial tension was determined at rotational speeds of 2000 rpm, 3000 rpm and 4000 rpm, and the average of these values taken. This data is reported in Table 2.2.6a.

Table 2.2.6a: Interfacial tension of one 12.5% w/w PEG-1000: 12.5% w/w dipotassium hydrogen phosphate aqueous two – phase system made during the course of this study.

Rotational Speed (rpm)	2000	3000	4000	Average
Interfacial Tension (mNm^{-1})	0.096	0.085	0.095	0.092

2.3. Design and Operation of the CCC Centrifuges and Ancillary Equipment

2.3.1. The CCC Centrifuges and Coils

The centrifuges and coils used were prototypes (Brunel Institute for Bioengineering, Brunel University, Uxbridge, UK), the design and fundamental principles of which were described earlier (refer to Section 1.3.5). Details of the centrifuges and coils used in this study are given in Table 2.3.1a.

Table 2.3.1a: Details of the J – type CCC centrifuges and coils used in this study.

Centrifuge	Overall Dimensions h × w × d (cm)	Diameter of Bobbins (cm)	Coil Name	Column Volume (ml)	Column Bore (mm)	Column Length (m)	Tubing Material	R Value (mm)	r Value (mm)	β Value
MILLI #1	35 × 35 × 42	8.5	SBRI-CCC	10.8	1.6	5.3	PTFE	50	33.5-36.8	0.67-0.74
MILLI #1	35 × 35 × 42	8.5	DEM-PRO #1	46.3	2.7	8.0	PTFE	50	26.7-36.6	0.53-0.73
MILLI #1	35 × 35 × 42	8.5	DEM-PRO #2	45.1	2.7	7.9	PTFE	50	26.7-36.6	0.53-0.73
SMART-MIDI	52 × 63 × 52	19.0	SMART - MIDI	431.0	4.0	34.3	PFA	110	71.0-98.0	0.65-0.89

The centrifuges and associated ancillary equipment used in this project were organised into self – contained "rigs". Each rig consisted of a portable trolley holding the centrifuge, plus the ancillary equipment: liquid – handling pumps, UV detector, fraction collector, water bath and computer equipment (computer, monitor, keyboard, mouse). Those instruments wholly or partly controlled by software were connected to the computer via an interface box. The instruments were connected using PTFE tubing of bore 0.8 mm or 1.6 mm. Valves were included in the tubing system to facilitate the handling of the various liquids involved in the experiments (Upchurch Scientific, Anachem, Luton, Bedfordshire, UK). A diagram of a typical rig layout is shown in Figure 2.3.1a and Figures 2.3.1b, 2.3.1c and 2.3.1d are annotated photographs showing the equipment *in situ*.

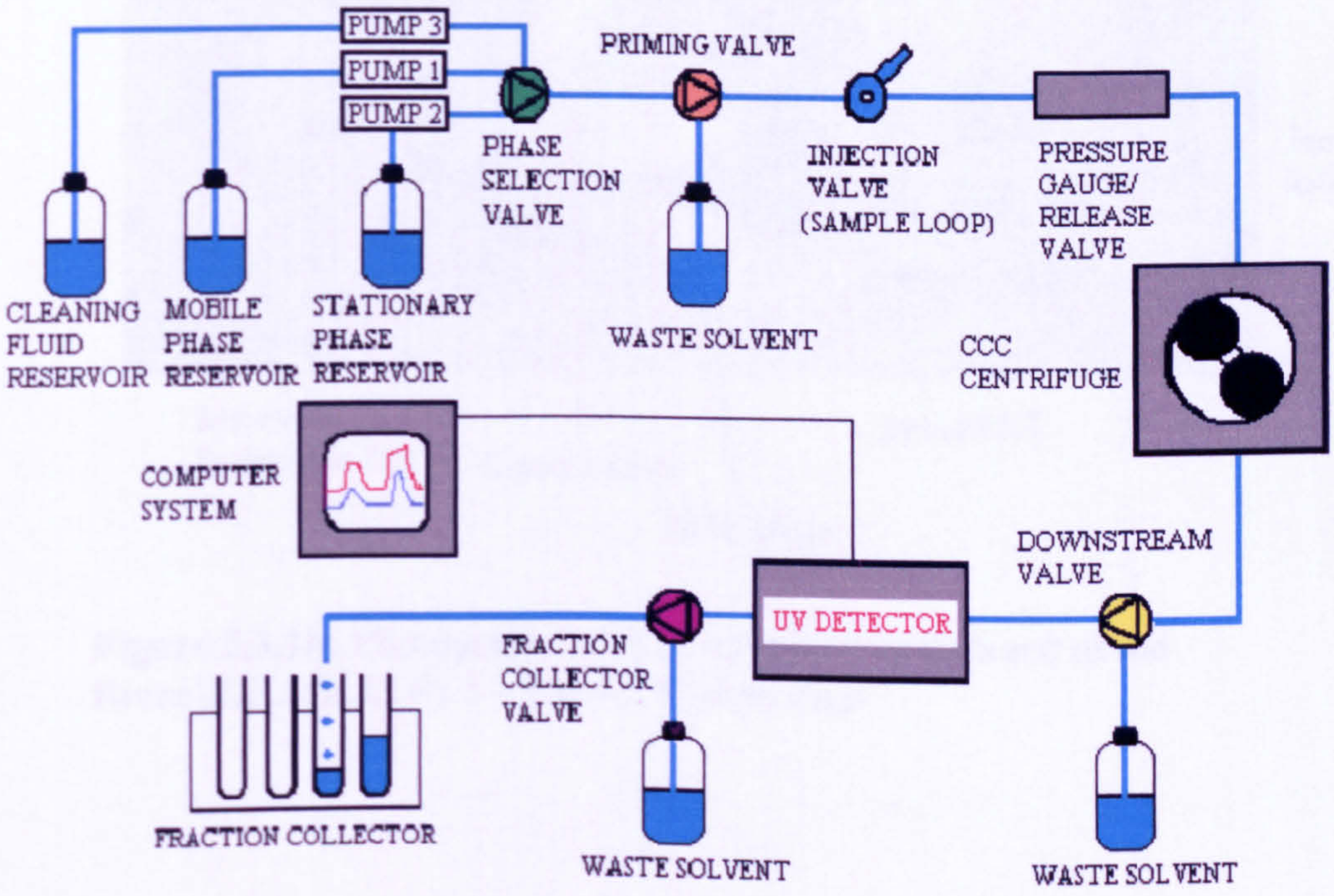

Figure 2.3.1a: A typical Brunel CCC rig showing the position of the centrifuge and ancillary equipment.

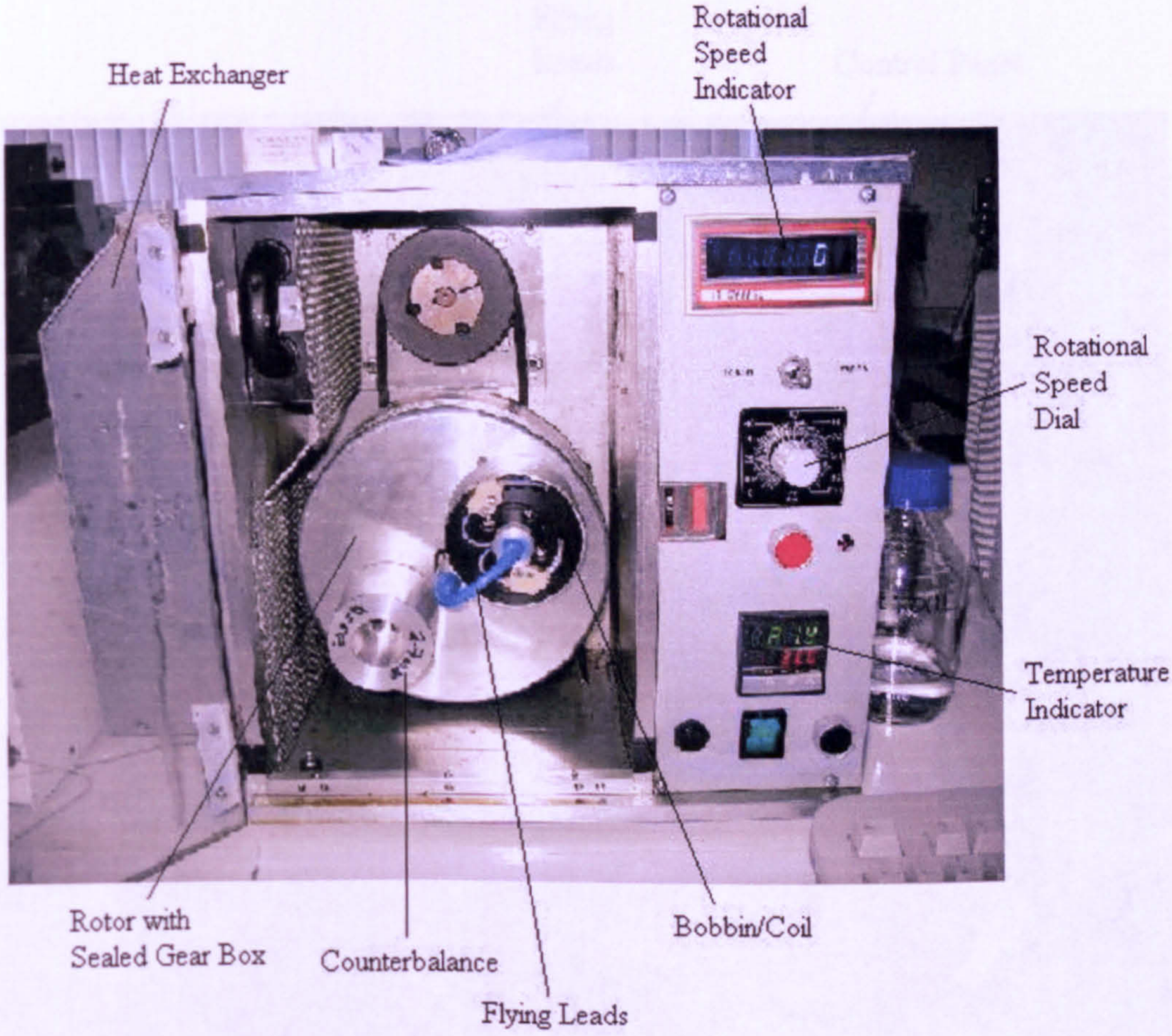

Figure 2.3.1b: Photograph (with descriptive annotations) of the Brunel/DE MILLI #1 J – type CCC centrifuge.

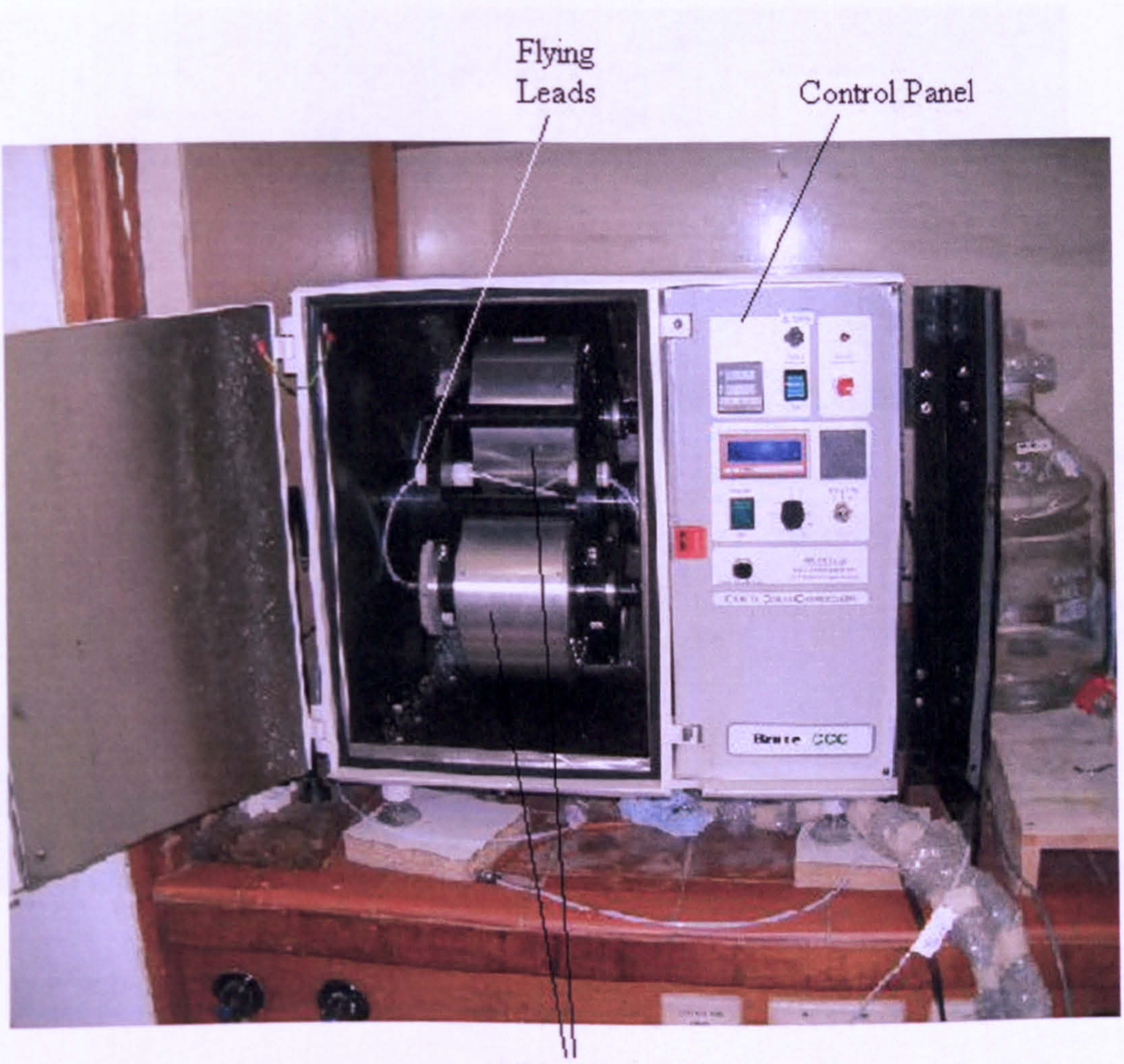

Figure 2.3.1c: Photograph (with descriptive annotations) of the Brunel/DE SMART-MIDI J – type CCC centrifuge.

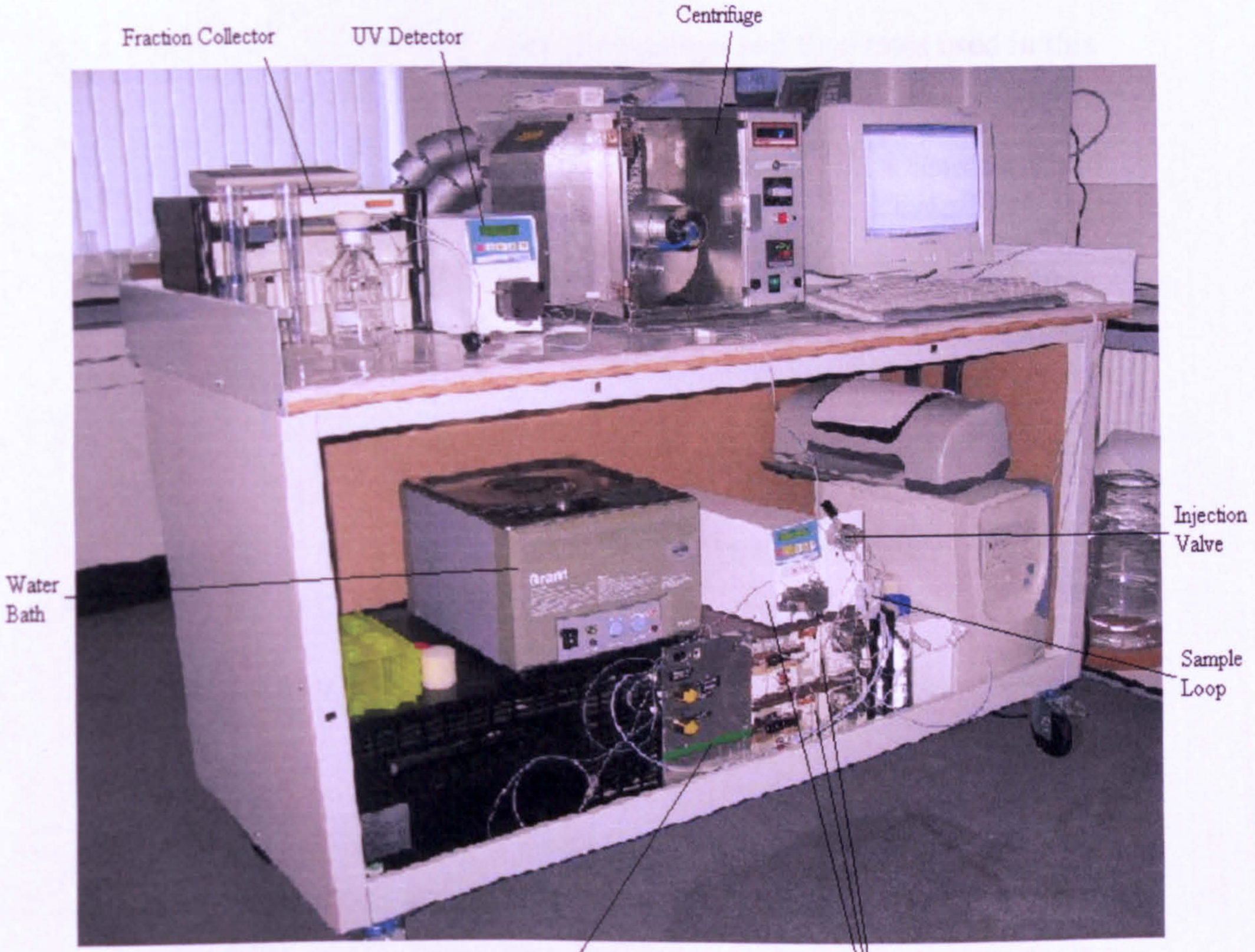

Figure 2.3.1d: Photograph (with descriptive annotations) of the MILLI #1 centrifuge and its ancillary equipment mounted on a trolley.

2.3.2. Liquid – Handling Pumps

Liquid – handling pumps were used to deliver stationary phase, mobile phase and a cleaning solution into the system. Details of the pumps used are given in Table 2.3.2a.

Table 2.3.2a: Details of the liquid – handling pumps and flow rates used in this study.

Rig	Stationary Phase Pump/Flow Rate ($mlmin^{-1}$)	Mobile Phase Pump (Flow Rates Variable)	Cleaning Fluid Pump/Flow Rate ($mlmin^{-1}$)
MILLI #1	Gilson[1] 303 10.0 $mlmin^{-1}$	Knauer[2] WellChrom HPLC-Pump K-501	Gilson[1] 303 10.0 $mlmin^{-1}$
SMART-MIDI	Gilson[1] 303 25.0 $mlmin^{-1}$	Rainin[3] Dynamax Model SD-1	Rainin[3] Dynamax Model SD-1 100.0 $mlmin^{-1}$

[1] Gilson Inc (Middleton, WI, USA)
[2] Knauer (Berlin, Germany)
[3] Rainin (Woburn, MA, USA)

2.3.3. UV Detectors

The UV detector used on the MILLI #1 rig was a Knauer model 2501 fitted with an analytical cell and set at wavelength 280 nm.
The UV detector used on the SMART-MIDI rig was a Gilson model 151 fitted with a preparative cell (path length 0.2 mm, volume 0.7 µl) and set at wavelength 280 nm.

2.3.4. Fraction Collector

A Gilson model 201 fraction collector was used for some experiments on the MILLI #1 rig, however in most cases fractions were collected by hand.

2.3.5. Computer Hardware and Software

Computers running the Knauer "Eurochrom® for Windows Basic Edition V3.05" software were present on both rigs, where they were connected to the mobile phase pump, injection valve and detector via an interface box (Knauer model IF2). The system was configured so that data from the detector was recorded as a chromatogram as soon as the injection valve was switched to "Inject" mode. In

many experiments, but not all, this occurred just after the start of the mobile phase pump. These so – called "blank injections" allowed the recording of data from the start of the mobile phase flow to the end of the experiment, capturing important events on the chromatogram such as the time that the mobile phase first eluted from the column. If a blank injection was made, the injection valve was reset and subsequently used to inject the loading sample.

2.3.6. Miscellaneous Ancillary Equipment

- Water baths: the MILLI #1 rig was equipped with a Grant (Keison Products, Chelmsford, Essex, UK) SUB14 water bath. The SMART-MIDI rig was equipped with a Grant Y22 water bath. Unless otherwise specified, the water baths were maintained at 30°C, ± 2°C, verified with a mercury thermometer.
- Chilling units: these were used to maintain the internal temperature of the centrifuges. MILLI #1 was connected to a portable chilling unit. The SMART-MIDI centrifuge was connected to the in – house chilling system (ICS, Hampshire, UK) fitted to the Advanced Bioprocessing Centre laboratories.
- Pressure gauges and pressure release valves: pressure gauges (Ametek-USG, Meerbusch, Germany) were used to monitor the pressure created in the system. An increase of pressure, often caused by a blockage in the system, could cause the column to burst. Pressure release valves rated at 100 psi (Upchurch Scientific) were fitted to the system to release excess pressure.

2.3.7. Operating Procedure for the CCC Centrifuges and Ancillary Equipment

A protocol was devised to operate the equipment for each experiment in a standard way. The protocol is detailed in Table 2.3.7a.

Table 2.3.7a: Details of the step – wise procedure used for the operation of the CCC centrifuges and ancillary equipment.

Step Number	Operation
1	Bottles of phase were placed in the water bath and brought to temperature equilibration. Pump inlet tubes were placed in the phase solutions.
2	MP & SP pumps were primed with the appropriate phase solution.
3	The column was filled with SP, pumping from "Tail" to "Head" (*i.e.* in the direction of the Archimedean Screw Force) whilst the column was rotated slowly (approximately 200 rpm). This allowed any air trapped in the column to be removed; air bubbles could adversely affect the separation process.
4	Centrifuge rotation was started and the centrifuge unit allowed to reach the required temperature.
5	The MP pump was started and data recording initiated by performing a "blank injection". SP started eluting from the column; this eluent was collected in a measuring cylinder and its volume noted at timed intervals.
6	The system was allowed to equilibrate. This occurred when MP first eluted from the column. The eluent (now a mixture of SP and MP) continued to be collected in the measuring cylinder; this would provide information that would allow the SP retention to be calculated at the MP breakthrough point.
7	The loading sample was injected into the sample loop and then onto the column. Fraction collection (if required) was started, with the fractions being collected in graduated plastic tubes.
8	The centrifuge was run until the proteins loaded had eluted from the column.
9	Fraction/eluent collection, data recording, the mobile phase pump and the centrifuge were stopped.
10	The system contents were evacuated with nitrogen gas or air being pumped from "Tail" to "Head" and the coil rotated slowly. The post – separation column contents were important as they gave the volume of SP retained during the experiment, and also contained any proteins that did not elute in the duration of the experiment.
11	The system was cleaned by pumping through six to eight system volumes of distilled water, followed by the same volume of methanol. The system was left in a solution of 70% methanol/30% water to prevent microbial growth.

2.4. Design and Operation of the CPC Centrifuge and Ancillary Equipment

2.4.1. The CPC Centrifuge

An Armen "Elite" CPC centrifuge was supplied by Armen Instrument (Vannes, France). It consists of two 500 ml columns that can be operated either in series (total volume 1000 ml) or separately (500 ml). The basic design of the centrifuge columns was described in Section 1.3.7. Each 500 ml column comprises 42 stacked discs with a total of 1008 cells (24 per disc). Each cell has a volume of 0.424 ml, giving a total active volume of 429.0 ml. The total volume of the interconnecting ducts is 71.0 ml.

The external dead volume is 1.0 ml, and was taken as negligible.

Integral to the design of the centrifuge were the following:

- Liquid – handling pumps, consisting of two elution pumps (one for the upper phase and one for the lower phase), and two injection pumps.
- A sample loop and injection port.
- A pressure gauge that monitors the internal pressure of the system. If the pressure reaches 70 bar (1050 psi) (set by the manufacturer), the pumps automatically stop. This prevents damage to the rotor plates and gaskets.
- Armen "Elite Glider" software that controls instrument functions such as rotational speed, flow rate of pumps, mode of injection and operational mode.

Samples can be loaded onto to the column either by filling a sample loop with a syringe (via the injection port), or by using the injection pumps. A sample loop was used for all injections made in this study.

Gas – operated valves are used to control functions such as operational mode (ascending or descending) and selection of the appropriate pumps. The valves were operated using an online compressed air supply of pressure 4 bar (60 psi). An annotated photograph showing the CPC centrifuge used in this study is shown in Figure 2.4.1a.

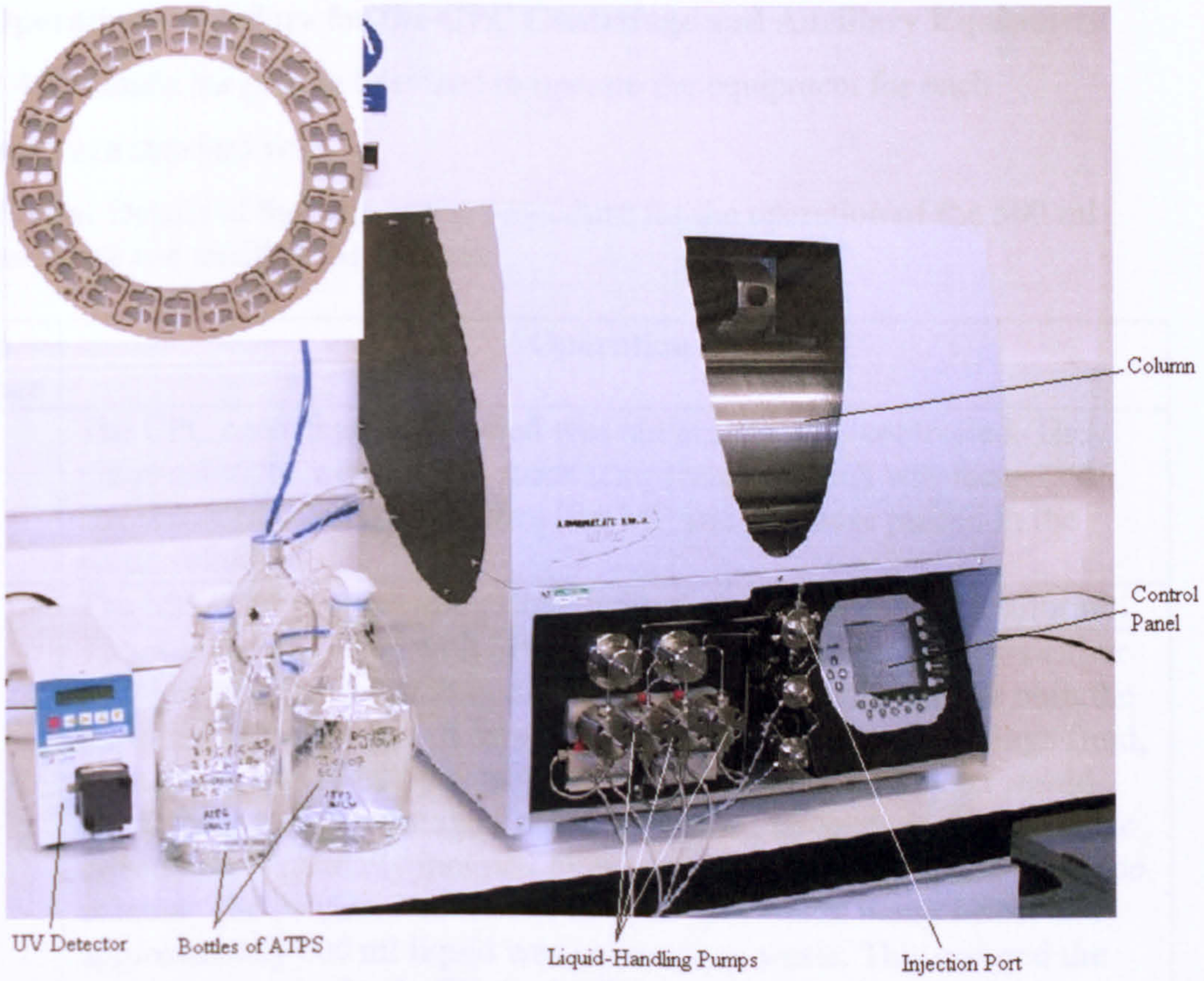

Figure 2.4.1a: Photograph (with descriptive annotations) of the CPC centrifuge. The insert shows one of the disks that comprise the column.

2.4.2. UV Detector

The UV detector used was a Knauer model 2501 fitted with a preparative cell and set at wavelength 280 nm.

2.4.3. Computer Hardware and Software

A computer running the "Picolog for Windows" software (Pico Technology Ltd, St Neots, Cambridgeshire, UK) was connected to the UV detector and used for data collection. The signal from the detector was plotted against time to produce a chromatogram. Data collection was usually initiated a few minutes before the start of the mobile phase pump.

2.4.4. Miscellaneous Ancillary Equipment

Back pressure regulators: these were fitted to the system between the column exit and the UV detector, and were used in some experiments to determine the effect that post – column back pressure had on stationary phase retention and protein resolution.

2.4.5. Operating Procedure for the CPC Centrifuge and Ancillary Equipment

Table 2.4.5a details the protocol devised to operate the equipment for each experiment in a standard way.

Table 2.4.5a: Details of the step – wise procedure for the operation of the 500 ml CPC centrifuge and ancillary equipment.

Step Number	Operation
1	The CPC centrifuge as supplied was not temperature controlled. The phase solutions were kept at room temperature (which was measured and recorded). Pump inlet tubes (for MP and SP) were placed in the phase solutions.
2	The MP & SP pumps were primed with the appropriate phase solution.
3	The column was filled with SP as follows. The storage fluid was either 100% distilled water or 70% distilled water/30% methanol. As both the upper and lower phases of this ATPS were denser than the storage fluid, the column was filled by rotating in the ascending mode. This would allow the less dense storage fluid to be pushed upwards in the cells (the direction it is naturally inclined to go) until it eventually eluted from the column. The column was rotated at 1000 rpm whilst being filled, and approximately 600 ml liquid was collected as waste. This ensured the column was completely filled with SP.
4	The operating conditions for the experiment were set *i.e.* the rotor speed and MP flow rate were selected. The operation mode was selected according to the following rationale: • If the UP = SP & the LP = MP: the MP is denser than the SP, and when entering the cells will fall through the liquid; therefore the operation mode is descending. • If the LP = SP & the UP = MP: the MP is less dense than the SP, and when entering the cells will pass upwards through the liquid; therefore the operation mode is ascending.
5	A file was created on the computer to record and save the data from the UV detector. Data recording was started.
6	The loading sample was injected into the sample loop. The next stage of the experiment could be done in one of two ways: • The Sandwich Injection Method. The MP pump was started and the sample was injected onto the column simultaneously. • The Pre – Equilibration Method. The MP pump was started, and the column was allowed to reach equilibrium before the sample was loaded onto the column. Equilibrium normally occurred shortly after MP breakthrough was observed, and was indicated by a steady baseline on the chromatogram. In both cases, fraction collection (if required) started as soon as the sample was injected. Fractions were collected in graduated 15 ml plastic centrifuge tubes. This allowed the volume of each phase in each fraction to be accurately recorded, and the volume of displaced stationary phase to be calculated.

Table 2.4.5a: Continued

Step Number	Operation
7	The centrifuge was run until the proteins loaded had eluted from the column.
8	Fraction collection, data recording, the mobile phase pump and the centrifuge rotor were stopped.
9	The design of the CPC centrifuge, with its channels and ducts, meant that the column contents could not be evacuated with gas; distilled water was used instead. The phase system present in the column at the end of the experiment was denser than water, and so the system was emptied by rotating the column at 1000 rpm in descending mode.
10	The system was cleaned by pumping through six to eight system volumes of distilled water. If not to be used for some time, the system was then filled (in descending mode) with a solution of 70% distilled water/30% methanol to prevent microbial growth.

2.5. Protein Sample Preparation, Detection and Quantification

2.5.1. Preparation of Lysozyme and Myoglobin Loading Samples

Lysozyme from chicken egg white and myoglobin from horse skeletal muscle were obtained from Sigma-Aldrich (Poole, Dorset, UK). Both proteins were supplied in lyophilized powder form.

Lysozyme and myoglobin loading samples were used in both the CCC and CPC studies, and were prepared as follows. Similar quantities of lysozyme and myoglobin were weighed out into a glass vial, and equal volumes of the upper and lower phases of a 12.5% w/w PEG-1000: 12.5% w/w K_2HPO_4 ATPS were added. The vial was inverted to mix the contents, and the sample filtered using a MILLEX®-HV PVDF 33 mm diameter, 0.45 µm pore syringe driven filter unit (Millipore, Watford, Hertfordshire, UK). A filter made of PVDF (polyvinylidene fluoride) was used due to the low protein binding properties of this material. Filtering was considered necessary to prevent the narrow bore of the sample loop used on the J – type CCC centrifuges from blocking. The manufacturer of the CPC centrifuge advised that filtering was necessary with that instrument to prevent the narrow interconnecting ducts from blocking.

Unless otherwise stated, the loading samples were prepared to be of concentration 2.2 $mgml^{-1}$ lysozyme and 2.2 $mgml^{-1}$ myoglobin (± 0.2 $mgml^{-1}$ each protein) in equal volumes of the upper and lower phases of the 12.5% w/w PEG-1000: 12.5% w/w K_2HPO_4 ATPS. These concentrations were reduced by the filtering process, which was necessary to prevent any undissolved protein from blocking the CCC and CPC systems.

2.5.2. Determining the Distribution Ratios of Lysozyme and Myoglobin

All chromatographic separations are based on differences in the extent to which solutes are partitioned between mobile and stationary phases (Skoog *et al*, 1994). The distribution ratio is a quantitative measure of these differences, and is give by the equation:

$$D = \frac{\text{Concentration of the solute in the upper phase}}{\text{Concentration of the solute in the lower phase}} \qquad \text{[Equation 2.5.2a]}$$

The first stage in the separation process was to determine the distribution ratio of each protein in the phase system. This information was used later when designing the experiments involving CCC and CPC, specifically in deciding which phase would act as the mobile phase, and which would act as the stationary phase.

The distribution ratio of lysozyme and myoglobin in a 12.5% w/w PEG-1000: 12.5% w/w K_2HPO_4 ATPS was determined as follows.

The separated phases were brought to 25°C in a water bath. Exactly 30.0 mg lysozyme and 30.0 mg myoglobin were weighed out into separate centrifuge tubes, then 3.0 ml each of lower phase and upper phase was added to each tube. The tubes were inverted to mix the solutions, and placed in the 25°C water bath until phase separation had occurred.

Triplicate 200 µl samples were taken of the upper and lower phases from both the lysozyme and myoglobin phase systems, and each was diluted with 800 µl distilled water (purity 1.0 $M\Omega cm^{-1}$). The absorbance at wavelength 280 nm of each sample was determined using single – sample cuvettes in a Hitachi U-1800 spectrophotometer (Hitachi, Wokingham, Berkshire UK), with pure samples of upper and lower phase used as blank solutions.

The results are shown in Section 4.3.2.

2.5.3. Initial Methods used for Lysozyme and Myoglobin Detection and Quantification in CCC Fractions

Initially, protein detection and quantification in the samples collected during CCC experiments involving lysozyme and myoglobin was done by measuring absorbance at wavelength 280 nm using single – sample cuvettes in a Hitachi U-1800 spectrophotometer. However, this proved to be unsatisfactory for a number of reasons:

- A typical quantity of total protein used in the loading samples was 0.1 mg. This would be distributed between several fractions during the CCC process; each fraction would therefore contain insufficient amounts of protein to allow accurate detection and quantification using this method.
- It is a laborious method as it only allows for one sample to be analysed at any one time, and an automated alternative was not available.
- The presence of different proteins cannot be detected.

An alternative method was then devised using HPLC. Spectrophotometry using a single cuvette was reserved for detection of certain proteins by their biological activity *e.g.* the assay for phosphomannose isomerase (refer to Chapter 6).

2.5.4. HPLC Method for Lysozyme and Myoglobin Detection and Quantification

Solutions of lysozyme and myoglobin in distilled water were made, each of concentration 1.0 $mgml^{-1}$. A Perkin Elmer (Beaconsfield, Buckinghamshire, UK) MultiPROBE II Plus liquid – handling robot was used to prepare standard solutions of concentrations: 0.1 $mgml^{-1}$, 0.2 $mgml^{-1}$, 0.5 $mgml^{-1}$, 0.7 $mgml^{-1}$, and 1.0 $mgml^{-1}$. Distilled water was from the in – house water purifier, and had a purity of 1.0 $M\Omega cm^{-1}$.

The solutions were analysed using a Waters (Elstree, Hertfordshire, UK) 2695 HPLC separations module, equipped with a Waters 2996 photodiode array detector and operated using Waters Empower™ software. The column used was a YMC (Kyoto, Japan) ODS – AQ, particle size S-5 μm, pore size 20 nm, length 150 mm and internal diameter 4.6 mm. The running conditions were as follows:

- Injection volume: 10.0 μl
- Run time: 15 minutes
- Flow rate: 1.0 $mlmin^{-1}$
- Column temperature: 40.0°C ± 5.0°C
- Time held at final conditions: 1 minute
- Gradient: 30% ACN → 55% ACN over 10 minutes
- Detector wavelength range: 210.0 nm to 600.0 nm ("MaxPlot"), resolution 1.2 nm

The software created calibration plots, plotting peak area (y – axis) against mass of protein (x – axis). The resulting straight line graphs gave values for the constants m (gradient of the line) and c (intercept of the line on the y axis) from the equation of a straight line ($y = m \times x + c$). These constants were used in subsequent experiments to determine the quantity and concentration of protein in fractions collected during the CCC and CPC experiments.

2.5.5. Utilisation of the HPLC Method for Lysozyme and Myoglobin Detection and Quantification in the Analysis of CCC and CPC Fractions

The fractions collected during the CCC and CPC experiments consisted mainly of lower phase (the mobile phase) and a small volume of upper phase (the stationary phase). The presence of small quantities of upper (stationary) phase was due to stationary phase "stripping" from the column during the experiment. The lysozyme and myoglobin in each fraction were partitioned between these two phases according to their individual distribution ratios. To obtain a sample that contained proportionate amounts of each protein as they were present in the fraction overall, each fraction was mixed by inversion, a 0.8 ml aliquot transferred to a HPLC vial, and 0.2 ml water (purity 18.2 $M\Omega cm^{-1}$) added. Addition of the 0.2 ml water "breaks" the phase system, producing a one phase solution.

The volume of each CCC/CPC fraction was recorded, and subsequently the mass of each protein in each fraction was calculated. The concentration and mass of lysozyme and myoglobin species in the CCC/CPC loading sample was also determined by HPLC analysis, following this method.

The results from the HPLC analysis of the fractions collected during each experiment were analysed to yield information on the recovery of the myoglobin species and lysozyme from the CCC/CPC process.

For each experiment, the total mass of lysozyme, apomyoglobin and myoglobin in the collected fractions was obtained, and compared with the mass of these proteins present in the loading sample. The values were then used to obtain a percentage recovery value for each protein in each experiment, according to the equation:

$$\% \text{ Recovery} = \frac{\text{Total Mass of the Protein in the Fractions}}{\text{Total Mass of the Protein in the Loading Sample}} \times 100 \quad \text{[Equation 2.5.5a]}$$

2.5.6. Solubility Studies of Lysozyme and Myoglobin

One aim of the study was to maximise throughput of proteins in the separation process by working with samples at their highest limits of concentration. It was therefore considered important to gain an understanding of the degree of solubility of lysozyme and myoglobin in the 12.5% w/w PEG-1000: 12.5% w/w K_2HPO_4 ATPS before the separation studies on the CCC and CPC centrifuges were undertaken. Ito

and his co – workers (Ito *et al*, 2003) reported using these proteins in this phase system at total protein concentrations of 20.0 $mgml^{-1}$. However, a review of the literature on the solubility of proteins in aqueous two – phase systems showed that more typical protein concentrations are in the range 1 to 5 $mgml^{-1}$. The variation between these reported solubilities prompted an investigation of the solubility of lysozyme and myoglobin in this phase system.

Standard solutions of lysozyme and myoglobin in distilled water (purity = 1.0 $M\Omega cm^{-1}$) were prepared by serial dilution. The concentrations were in the range 0 to 1.0 $mgml^{-1}$ at 0.1 $mgml^{-1}$ intervals. The absorbance at wavelength 280 nm of each solution was measured using single – sample cuvettes in a Hitachi U-1800 spectrophotometer. Standard curves were created for both proteins of absorbance at wavelength 280 nm against protein concentration. The resulting straight line graphs gave values for the constants m (gradient of the line) and c (intercept of the line on the y axis) from the equation of a straight line ($y = m \times x + c$); these were used in the following analysis of solutions of unknown protein concentrations.

Solutions each of volume 2.0 ml were created separately for lysozyme and myoglobin, using the upper and lower phases of a 12.5% w/w PEG-1000: 12.5% w/w K_2HPO_4 ATPS. The concentrations of protein in each were: 2.5; 5.0; 7.5; 10.0 $mgml^{-1}$.

The solutions were incubated in a 30°C water bath for 15 minutes, centrifuged in a "Heraeus Biofuge Pico" microcentrifuge (Thermo Scientific, Basingstoke, UK) at 13 000 rpm for five minutes, and the supernatant removed. A 1:20 dilution of each supernatant was made using the appropriate phase solution. The absorbance at wavelength 280 nm of each solution was obtained using single – sample cuvettes in a Hitachi U-1800 spectrophotometer, and the absorbance values multiplied by a factor of 20 to give the absorbance of the undiluted solutions. The observed concentrations of protein in the undiluted solutions were calculated using the standard curves produced earlier, and these were plotted against the theoretical protein concentrations; a variation between the theoretical and observed protein concentration for a particular sample would show that some protein has been lost during the centrifugation step. This would indicate that the solution had exceeded the saturation point, and therefore contained undissolved protein, which would sediment either at the bottom of the tube or at the interface.

The standard curves of absorbance at wavelength 280 nm against protein concentration for lysozyme and myoglobin in distilled water are shown in Figures 2.5.6a and 2.5.6b.

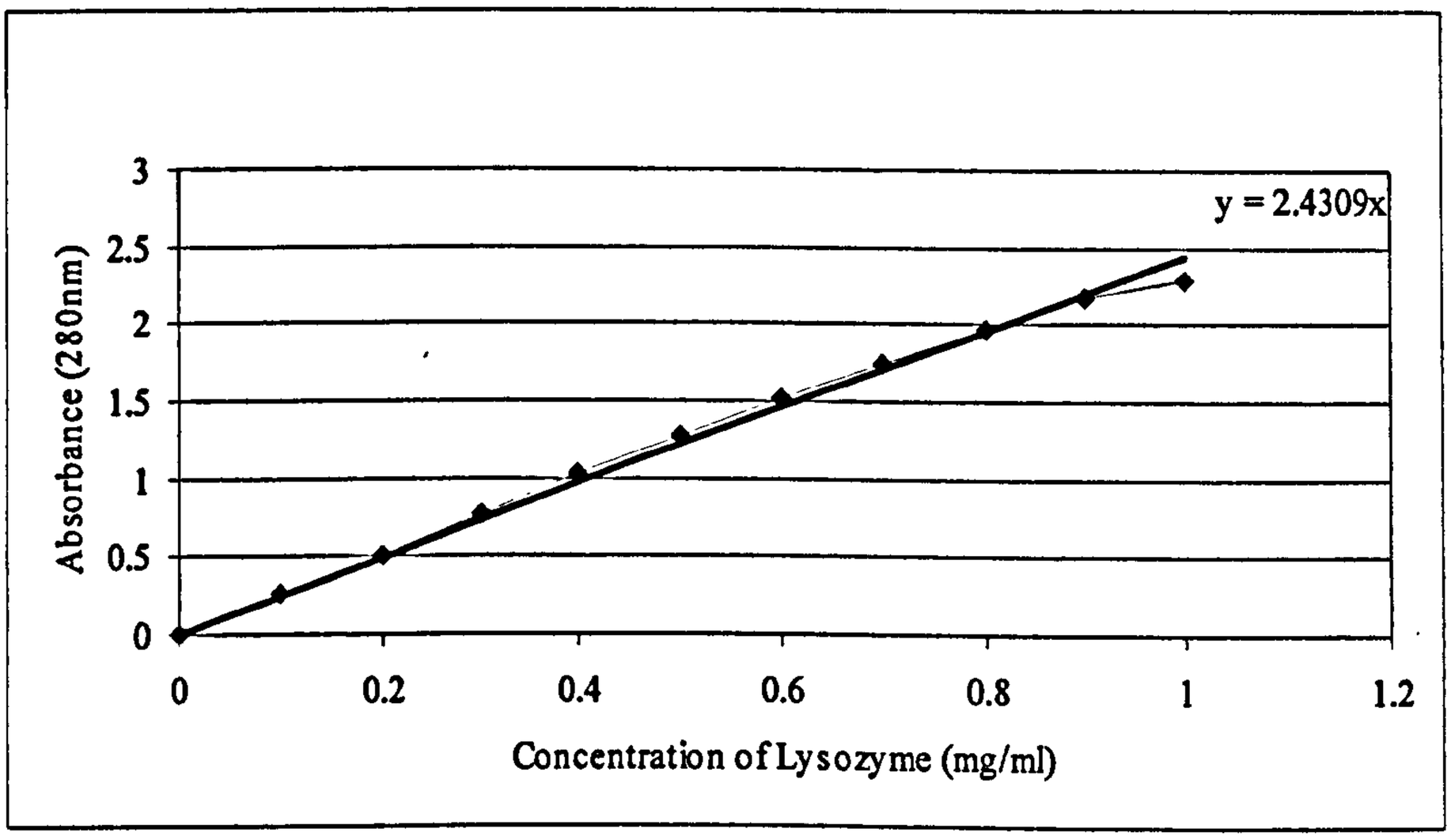

Figure 2.5.6a: Standard curve of absorbance at wavelength 280 nm against protein concentration for lysozyme in distilled water.

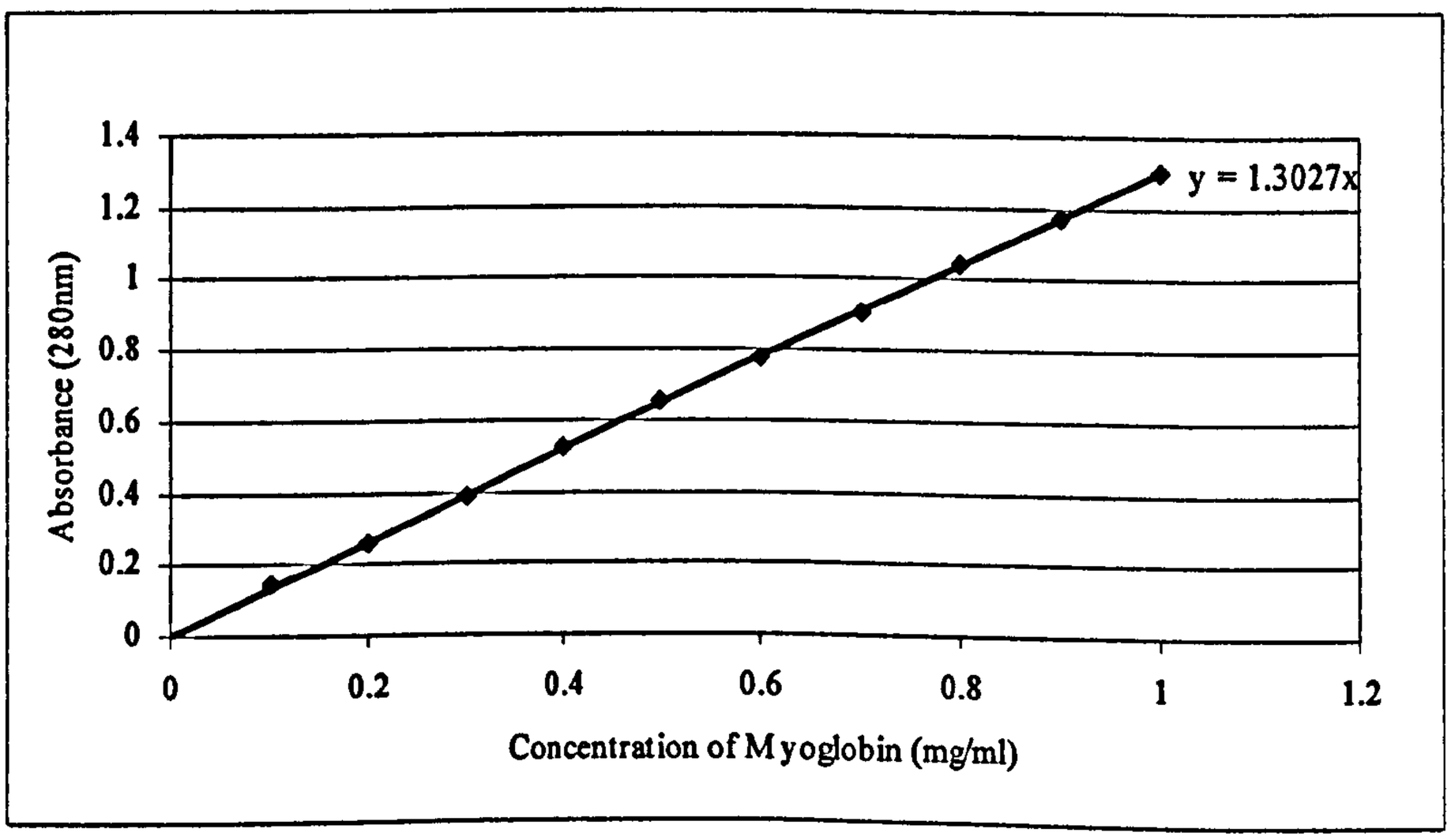

Figure 2.5.6b: Standard curve of absorbance at wavelength 280 nm against protein concentration for myoglobin in distilled water.

Dilutions in the order of 1:20 were made of the solutions of lysozyme and myoglobin in upper and lower phase. The absorbance of the diluted solutions at wavelength 280 nm was measured and the absorbance of the undiluted solutions calculated. These

values were then used to determine the observed concentrations of the protein in the solutions, using the equations:

$$\text{Concentration of Lysozyme } (mgml^{-1}) = \frac{\text{Absorbance at 280 nm}}{2.4309} \quad \text{[Equation 2.5.6a]}$$

$$\text{Concentration of Myoglobin } (mgml^{-1}) = \frac{\text{Absorbance at 280 nm}}{1.3027} \quad \text{[Equation 2.5.6b]}$$

The theoretical and observed protein concentrations for each solution are reported in Table 2.5.6a and shown graphically in Figure 2.5.6c.

Table 2.5.6a: The theoretical and observed protein concentrations for each solution used in the solubility studies of lysozyme and myoglobin in a 12.5% w/w PEG-1000: 12.5% w/w K_2HPO_4 ATPS.

Protein	Phase from ATPS	Theoretical Conc^n of Protein ($mgml^{-1}$)	Observed Conc^n of Protein ($mgml^{-1}$)	Difference in the Theoretical & Observed Conc^n of Protein ($mgml^{-1}$)
Lysozyme	Lower	2.5	2.7	(−) 2
Lysozyme	Lower	5.0	4.5	0.5
Lysozyme	Lower	7.5	6.3	1.2
Lysozyme	Lower	10.0	7.9	2.1
Lysozyme	Upper	2.5	2.4	0.1
Lysozyme	Upper	5.0	4.2	0.8
Lysozyme	Upper	7.5	5.7	1.8
Lysozyme	Upper	10.0	7.5	2.5
Myoglobin	Lower	2.5	2.7	(−) 2
Myoglobin	Lower	5.0	4.9	0.1
Myoglobin	Lower	7.5	7.3	0.2
Myoglobin	Lower	10.0	9.4	0.6
Myoglobin	Upper	2.5	2.5	0
Myoglobin	Upper	5.0	4.8	0.2
Myoglobin	Upper	7.5	7.2	0.3
Myoglobin	Upper	10.0	8.8	1.2

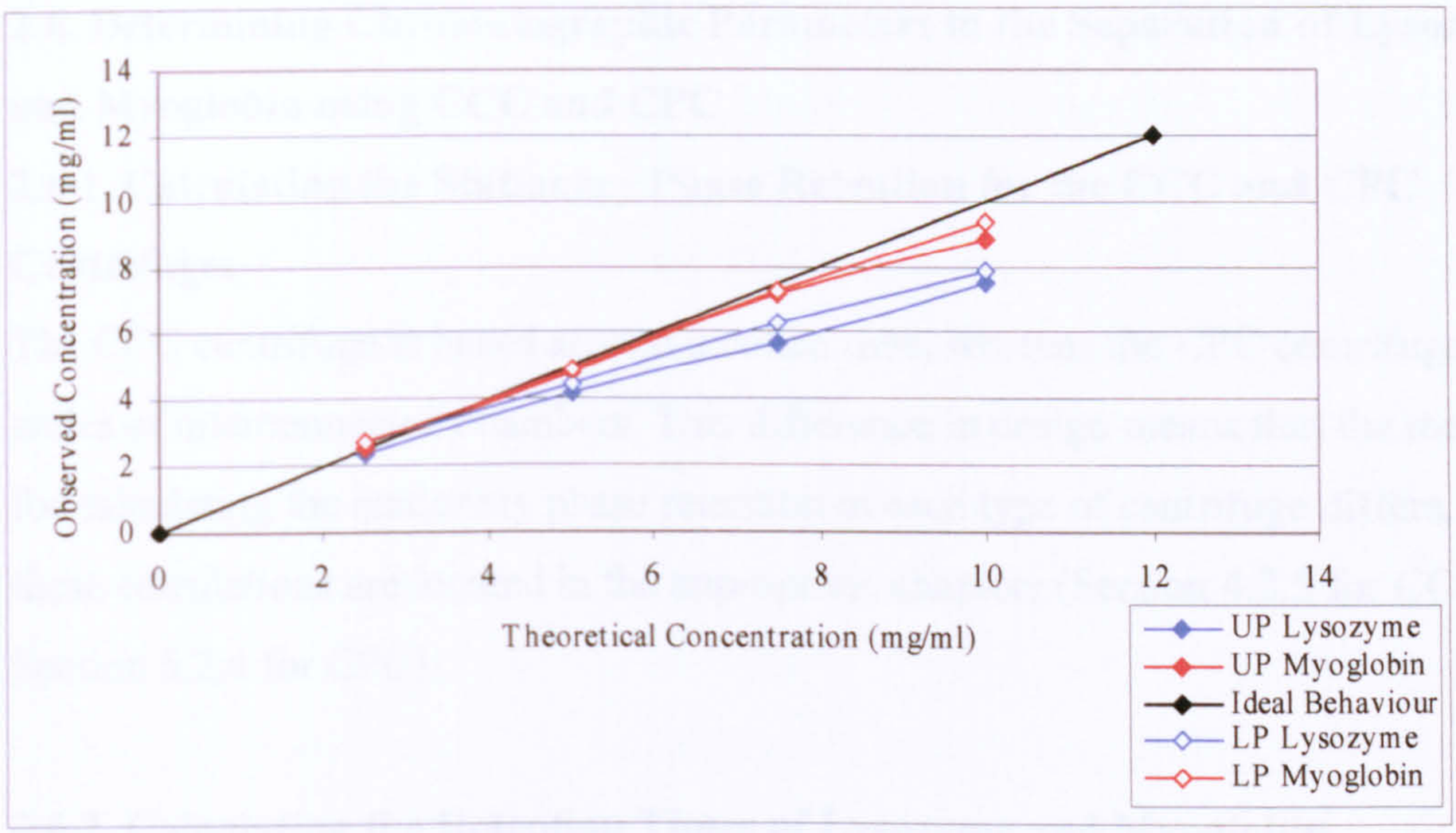

Figure 2.5.6c: Theoretical concentrations against observed concentrations of lysozyme and myoglobin in the upper and lower phases of a 12.5% w/w PEG-1000: 12.5% w/w K_2HPO_4 ATPS.

The results in Table 2.5.6a and Figure 2.5.6c show that above a theoretical concentration of 2.5 $mgml^{-1}$ the observed concentrations of lysozyme and myoglobin in both upper and lower phases of the phase system are less than the theoretical values. It would appear that these solutions contained undissolved protein that was lost during the centrifugation step of the experiment.

It was therefore decided that for the separation studies on the CCC and CPC centrifuges the concentration of total protein in the loading samples would be in the range 2.0 to 2.5 $mgml^{-1}$. A study of the effect of increasing the mass of protein on the CCC/CPC process would be achieved by increasing the volume of the loading sample, rather than its total protein concentration.

2.6. Determining Chromatographic Parameters in the Separation of Lysozyme and Myoglobin using CCC and CPC

2.6.1. Calculating the Stationary Phase Retention for the CCC and CPC Centrifuges

The CCC centrifuge is based around a coiled tube, whereas the CPC centrifuge is a series of interconnected chambers. This difference in design means that the method for calculating the stationary phase retention in each type of centrifuge differs, and so these calculations are located in the appropriate chapters (Section 4.2.5 for CCC and Section 5.2.4 for CPC).

2.6.2. Calculating the Retention Times of Lysozyme and Myoglobin

The concept of the solute retention volume (V_R) was introduced in Section 1.2.3, and with the partition coefficient (K) it can be used to predict when a particular solute (in this case a protein) will elute from the column.

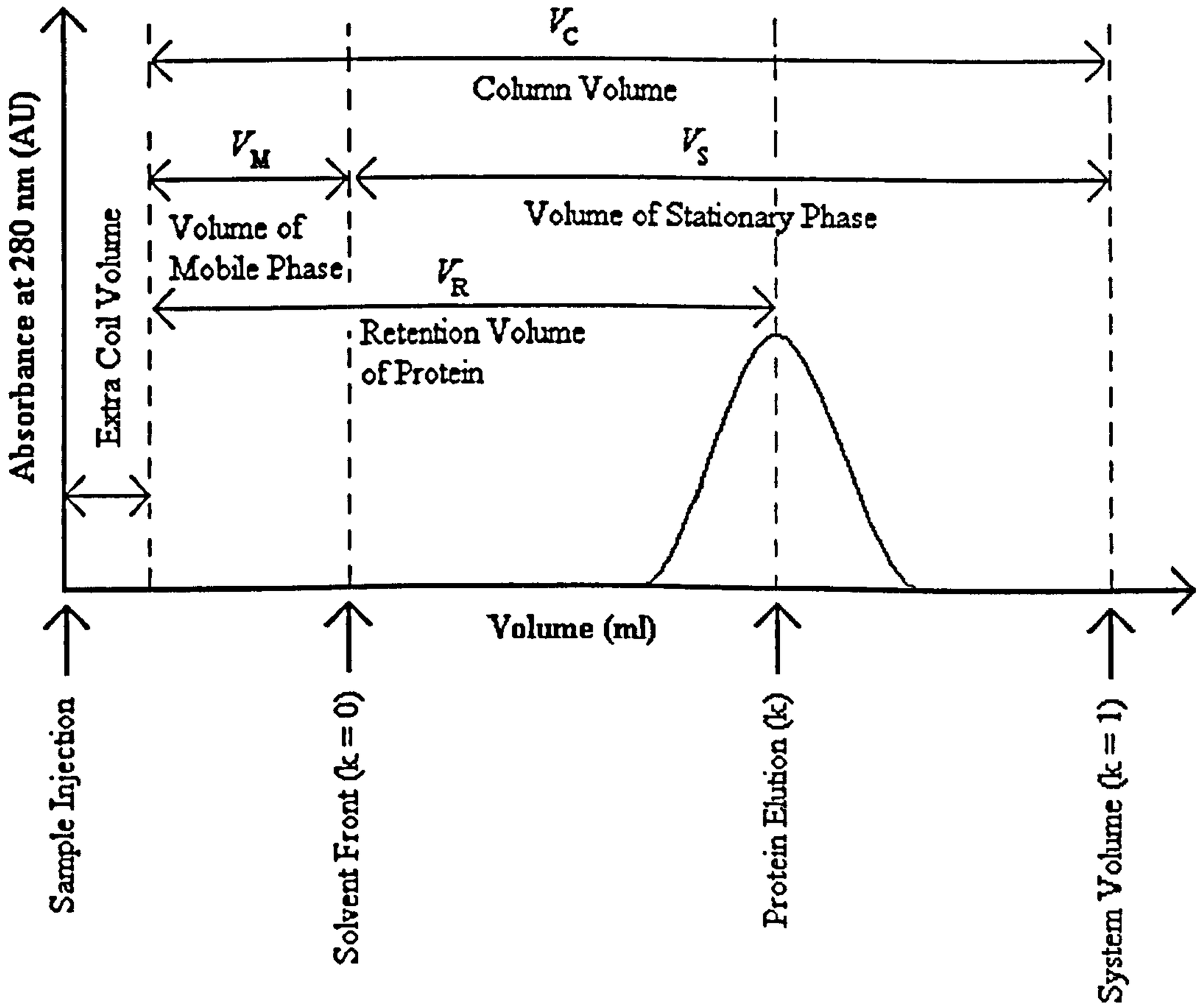

Figure 2.6.2a: Illustration of a chromatogram annotated to show the theoretical volumes associated with the chromatographic process.

Figure 2.6.2a shows how the retention volume of a protein is related to the volumes occupied by the stationary and mobile phases in a liquid – liquid chromatographic column. The x – axis is usually denoted in units of volume, or it can be converted into units of time if the mobile phase flow rate is known.

The process is best explained by describing the progress (in terms of volume) of a single pure protein sample through the column. The protein sample is injected at volume = 0, and is carried with the mobile phase through the extra or dead coil volume. The next region on the graph, labelled V_M or Volume of Mobile Phase, represents the volume of mobile phase that the sample must pass through before emerging at the solvent front. If the protein has a partition coefficient of zero ($K = 0$) it will not interact with the stationary phase at all, but will remain exclusively in the mobile phase, to elute at the solvent front. If the protein has a partition coefficient of one ($K = 1$) it shows no preference for either phase, and will behave as if the column is filled with one phase only. Its retention volume will therefore be the same as the Column Volume (V_C). If the protein has a partition coefficient of between zero and one, it has some affinity with the stationary phase, but not as much as with the mobile phase, and so will elute between the $K = 0$ and $K = 1$ points. If the protein has a partition coefficient of more than one, it has greater affinity with the stationary phase than with the mobile phase, and so will elute after the $K = 1$ point.

The factors shown in Figure 2.6.2a are related by the equation:

$$V_R = V_M + K \times V_S \qquad \text{[Equation 2.6.2a]}$$

V_R = Retention volume (ml)
V_M = Volume of mobile phase in column (ml)
V_S = Volume of stationary phase in column (ml)
K = Partition coefficient of protein(s)

This equation was used to calculate the $K = 1$ point for each experiment in the chapters concerning the separation of lysozyme and myoglobin by CCC and CPC. It was calculated initially as the retention *volume* and then (as the mobile phase flow rate was known) converted to the retention *time*.

The chromatograms in each chapter were annotated with this value. However, in theory neither protein will elute at the $K = 1$ point, due to the distribution ratios of the

proteins. If the lower phase is used as the mobile phase, $K = 1.9$ (lysozyme) and $K = 0.6$ (myoglobin); therefore myoglobin should elute at some point before and lysozyme at some point after the $K = 1$ point. If the upper phase is used as the mobile phase, $K = 0.5$ (lysozyme) and $K = 1.7$ (myoglobin); therefore lysozyme should elute at some point before and myoglobin at some point after the $K = 1$ point.

The exact retention volume of each protein depends on what volume of stationary phase has been retained in the column as the proteins enter it. The stationary phase retention values depend on the experimental parameters used, and so the retention volume of each protein will vary for experiment to experiment. In the lysozyme/myoglobin separation experiments, the volumes of mobile phase and stationary phase are taken to be those at:

- The mobile phase breakthrough point when calculating the retention time of the first protein to elute. This is because the partition behaviour of the first protein to elute is governed by the volume composition of mobile phase and stationary phase in the column at the mobile phase breakthrough point.
- The end of the experiment when calculating the retention time of the second (last) protein to elute. This is because the partition behaviour of the last protein to elute is governed by the volume composition of mobile phase and stationary phase in the column towards the end of the experiment, when a degree of stationary phase "stripping" has occurred.

The predicted and observed retention volumes (as retention times) for each protein in each experiment were calculated and reported in Table 4.3.2a (for the CCC experiments) and in Table 5.3.2a (for the CPC experiments). The *predicted* retention times are calculated using the data for the stationary phase retention volume obtained during that particular experiment, whereas the *observed* retention times are those that actually occurred; a comparison can therefore be made between the two values. A difference between the predicted and observed retention times of a protein would indicate that the protein in the column has not achieved the same partition between the two phases that was attained in the single – tube partition experiments.

Note that elution positions are reported as times, rather than volumes. This is because the chromatograms in these chapters were recorded over a time course, and so the x – axis of each will be in units of time.

Retention time is related to retention volume by the equation:

$$\text{Retention time} = \frac{\text{Retention volume}}{\text{MP flow rate}} \qquad \text{[Equation 2.6.2b]}$$

In all cases, the retention time of a protein is the time between the injection of the protein(s) onto the column and the apex of the elution peak for that protein on the chromatogram.

2.6.3. Calculating the Lysozyme and Myoglobin Resolution Values

Protein resolution factors were calculated using the following equation:

$$Rs = \frac{2 \times \Delta Z}{W_1 + W_2} \qquad \text{[Equation 2.6.3a]}$$

The values for ΔZ, W_1 and W_2 were measured directly from the chromatograms:

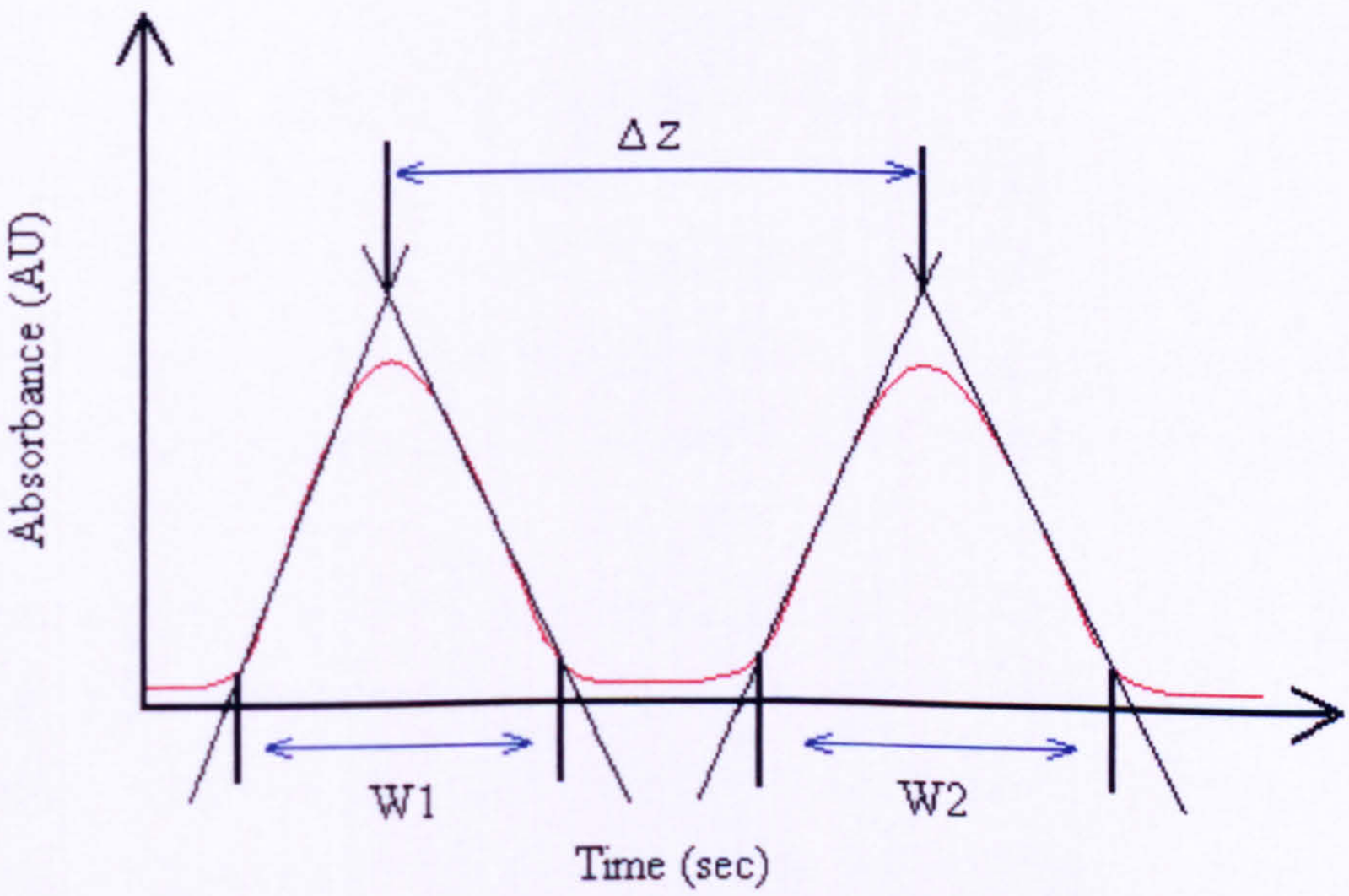

Figure 2.6.3a: Illustration of a chromatogram showing parameters used to calculate the resolution factor, *Rs*.

Resolution was calculated between both lysozyme and myoglobin, and between lysozyme and apomyoglobin. The apomyoglobin molecule is differs from the myoglobin molecule in that the former is minus a haem group. One factor that governs protein partitioning in aqueous two – phase systems is the pH of the system and the isoelectric point of the protein (Johansson, 1985). The isoelectric point is a consequence of the identity and nature of the amino acids on the surface of the protein. Therefore, the partitioning behaviour of apomyoglobin and myoglobin should indicate whether or not the surface amino acids are the same in both molecules. Thus it was felt appropriate to calculate and record the resolution between lysozyme and *both* forms of the myoglobin species.

Chapter 3 – Stationary Phase Retention Studies on J – Type CCC Centrifuges

3.1. Introduction

The initial focus of this project was to compare the performance of the multilayer column fitted to a Brunel/DE J – type CCC centrifuge with the results obtained by Ito *et al* who used a spiral disk assembly fitted to a similar type of centrifuge (Ito *et al*, 2003). Ito and his co – workers employed the spiral design of column to test the chromatographic resolution and stationary phase retention of three different two – phase solvent systems: 1-butanol/acetic acid/water, PEG-1000/dipotassium hydrogen phosphate and PEG-8000/Dextran T500. The model system used by Ito and co – workers that was chosen for study consisted of a 12.5% w/w PEG-1000: 12.5% w/w dipotassium hydrogen phosphate ATPS; the loading sample comprising of 10.0 mg lysozyme plus 10.0 mg myoglobin in a solution of 0.5 ml upper phase plus 0.5 ml lower phase from this phase system. Of the two aqueous two – phase systems, the PEG – salt was favoured over the PEG – dextran; use of the dextran – rich lower phase in the Brunel/DE J – type CCC centrifuges would be difficult to use because of its high viscosity. Ito *et al* showed that a partial separation of these proteins was obtained in the spiral disk assembly, and therefore this was considered to be an ideal model system on which to begin the study of the multilayer J – type CCC column.

In chromatography, good resolution of two or more compounds relies on several factors, such as column length, distribution ratios of the compounds, good interaction between the mobile and stationary phases, and satisfactory stationary phase retention (Berthod and Talabardon, 1999). It is the last of these that is the focus of this chapter.

The starting point of this study was to fit the Brunel/DE MILLI #1 CCC centrifuge with a particular multilayer column, and obtain values for the stationary phase retention at the mobile phase breakthrough point and subsequent loss of stationary phase after this point (stationary phase "stripping") for different operational parameters including: rotational speed; mobile phase flow rate; direction of mobile phase flow; lower phase as mobile phase; upper phase as mobile phase. The set of operational parameters that yielded the greatest

stationary phase retention and the least stationary phase "stripping" would then be used in the later experiments to separate the proteins lysozyme and myoglobin. Several studies have been conducted on how the distribution of the phases within a column varies with the nature of the phase system. Ito considered how phase systems classified as hydrophobic (*e.g.* hexane/water), hydrophilic (*e.g.* butanol/acetic acid/water) and intermediate between hydrophobic and hydrophilic (*e.g.* ethyl acetate/acetic acid/water) distributed in a number of rotating coils (Ito, 1992). He concluded that for hydrophobic phase systems, the more dense phase moved to the "Tail" of the column, for hydrophilic phase systems the more dense phase moved to the "Head" and the more dense phase could move either way for the intermediate phase systems. Another study by Sutherland and others employed a similar range of phase systems, but the columns used were of a larger bore than that used by Ito (Sutherland *et al*, 2000). This study concluded that for these phase systems, the lower phase always goes to the "Tail" when the "Tail" is at the periphery of a coil planet centrifuge.

The effect of variable parameters on the retention of stationary phase in the column has also been extensively studied in aqueous – organic solvent systems. In general, stationary phase retention increases with an increase in rotational speed and with a decrease in mobile phase flow rate (Maryutina *et al*, 2003).

This chapter investigates how the 12.5% w/w PEG-1000: 12.5% w/w dipotassium hydrogen phosphate ATPS behaves in a multilayer column fitted to a Brunel/DE J – type CCC centrifuge operated at different experimental parameters, and specifically whether its behaviour correlates to that predicted by these previous investigations.

3.2. Materials and Methods

3.2.1. Preparation of the Aqueous Two – Phase System

The phase system used in these experiments was the 12.5% w/w PEG-1000: 12.5% w/w K_2HPO_4 ATPS. Appropriate quantities were prepared as required following the procedure in Section 2.2.1.

3.2.2. Preparation and Use of the Brunel/DE MILLI #1 J – Type CCC Centrifuge

The Brunel/DE MILLI #1 CCC centrifuge was fitted with the SBRI-CCC coil (bore 1.6 mm, length 5.3 m and capacity 10.8 ml). The experimental apparatus was arranged as shown in Figure 2.3.1a, with the following modifications:

- The sample loop was not required in these experiments, and so the injection valve was set in the closed position.
- The eluent from the column passed through the UV detector, but the signal was not recorded as a chromatogram.
- The fraction collector was replaced by a 50 ml burette clamped in an upright position with the tap at the bottom of the burette closed.

The dead volume of the system was defined as the volume of the tubing connecting the liquid – handling pumps to the entrance of the column, plus the volume of the tubing from the exit of the column to the burette. The length of this tubing was determined using a tape measure, and with the cross – sectional area of the tubing known, the dead volume was calculated to be 2.2 ml.

The system temperature in all experiments was 30°C ± 1.0°C.

The protocol for the operation of the centrifuge in these experiments is given in Table 3.2.2a.

Table 3.2.2a: Step – wise procedure for the operation of the MILLI #1 CCC centrifuge and ancillary equipment in the stationary phase retention studies.

Step Number	Operation
1	Bottles of phase were placed in the water bath and brought to temperature equilibration. Pump inlet tubes were placed in the phase solutions.
2	MP & SP pumps were primed with the appropriate phase solution.
3	The column was filled with SP, pumping from "Tail" to "Head" (*i.e.* in the direction of the Archimedean Screw Force) whilst the coil was rotated slowly (approximately 200 rpm). This allowed any air trapped in the column to be removed; air bubbles could adversely affect the behaviour of the phases in the column.
4	Centrifuge rotation was started and the centrifuge unit allowed to reach the required temperature.
5	The end of the tubing from the UV detector was placed in the top of the (empty) burette and secured in place.
6	The MP pump and stopwatch were started simultaneously. SP started eluting from the column; a note of the volume of SP collecting in the burette was made at set time intervals (this verified that the flow rate set on the pump was accurate).
7	The system was allowed to equilibrate. This occurred when MP first eluted from the column. A note was made of the time this happened and the volume of SP that had been collected at this point.
8	The eluent (now a mixture of SP and MP) continued to be collected in the burette, and the volumes of each were recorded at set time points as the experiment continued. This detected any further loss of SP from the column.
9	Data recording, the mobile phase pump and the centrifuge were stopped at an appropriate time point.
10	The system contents were evacuated with nitrogen gas or air being pumped from "Tail" to "Head" and the coil rotated slowly. The post – experiment column contents were important as they allowed cross – checking with the eluted volume values obtained earlier in the experiment. This in turn allowed calculation of the SP volume retained in the column during the experiment.
11	The system was cleaned by pumping through six to eight system volumes of distilled water, followed by the same volume of methanol. The system was left in a solution of 70% methanol/30% water to prevent microbial growth.

Direction of Centrifuge Rotation

The centrifuge was always rotated in a clockwise direction, as observed by the operator through the door of the centrifuge. This direction of rotation orientates the "Head" of the column at the centre of the coil and the "Tail" at the periphery. It is possible to rotate the centrifuge anticlockwise, however the engineers who designed the centrifuge and coils recommended that the centrifuge be rotated in a clockwise direction for optimum performance. Optimum performance of these centrifuges is obtained when the Archimedean Screw Force (the hydrodynamic force) and the hydrostatic force are aligned and acting in the same direction. The direction of rotation has implications for the behaviour of the phase system within the column, however addressing this area was considered to be beyond the scope of this study. However, research was being conducted at the same time as this study on the behaviour of a PEG – potassium phosphate ATPS in a spiral coil (Guan *et al*, 2007). Results from this work confirmed that rotating the centrifuge in a clockwise direction would produce superior stationary phase retention.

Conditions for the Pumping of the Mobile Phase

Four pumping conditions were investigated:

- UP as the MP, pumped "Head" to "Tail"
- UP as the MP, pumped "Tail" to "Head"
- LP as the MP, pumped "Head" to "Tail"
- LP as the MP, pumped "Tail" to "Head"

Selecting the Mobile Phase Flow Rate

Initial experiments were conducted at a flow rate of 1.0 $mlmin^{-1}$. However, this caused the complete loss of stationary phase from the column. Subsequently, two (slower) flow rates were used at each pump condition: 0.25 $mlmin^{-1}$ and 0.50 $mlmin^{-1}$. The selection of these flow rates was based on previous work using aqueous – organic solvent systems with this column.

The duration of the experiments with a mobile phase flow rate of 0.25 $mlmin^{-1}$ was 80 minutes, and for those with a mobile phase flow rate of 0.5 $mlmin^{-1}$ was 40 minutes.

Defining the "Head" and "Tail" of the Column

The direction in which the coil is rotated determines whether the "Head" of the column is located at the centre or the periphery of the coil. The flying leads are attached to both ends of the column; therefore one flying lead extends from the "Head" of the column whilst the other extends from the "Tail". To determine which flying lead is the "Head" and which is the "Tail", the column was filled with a mixture of air and water, and the centrifuge rotated clockwise at approximately 200 rpm. The action of the Archimedean Screw Effect will force the water towards the "Head"; the inclusion of air in the column allows the operator to observe the elution of the water from the "Head" as fast – moving droplets (termed "spitting"). The other flying lead is therefore the "Tail" of the column. Note that if the coil is rotated in an anticlockwise fashion, the positions of the "Head" and "Tail" are reversed.

Selecting the Rotational Speed of the Coil

For each flow rate at each pump condition, the following rotational speeds were used: 800 rpm, 1300 rpm and 1800 rpm.

A comparison between two types of column can only be made if the acceleration due to gravitational force exerted on the column contents is the same for both systems.

Acceleration due to gravity is given in terms of metres per second per second ($msec^{-2}$). The acceleration due to gravity on Earth (unit gravity or 1G) is 9.81 $msec^{-2}$.

The acceleration due to gravitational force exerted on the column is quoted in terms of number of unit gravities, and is given by the equation:

$$G = \frac{R \times \theta^2}{9.81} \qquad \text{[Equation 3.2.2a]}$$

R is the radius of the main (sun) rotor in metres.

θ is the rotational speed of the coil in radians per second.

In the 2003 paper by Ito *et al*, R had a value of 10 cm ≡ 0.1 m.

The rotational speed used was 800 rpm ≡ $[(800 \times 2\pi)/60]^2$ radians per second.

Therefore, the acceleration due to gravitational force exerted on this column was:

$$G = \frac{0.1 \times [(800 \times 2\pi)/60]^2}{9.81}$$

$$G = 71.5\ G \qquad (701.8\ msec^{-2})$$

To exert the same acceleration due to gravitational force on the SBRI-CCC coil (R = 0.05 m), the rotational speed required was calculated as:

$$71.5 \times 9.81 = 0.05 \times [(\text{Rotational speed} \times 2\pi)/60]^2$$

Rotational speed = **1131 rpm**

The experiments were used as an opportunity to gain insight into the effect of rotational speed on the stationary phase retention of an ATPS in a J – type CCC centrifuge. The engineers who designed the centrifuge advised that the maximum safe rotational speed for this coil on this centrifuge was 1800 rpm. An appropriate minimum rotational speed of 800 rpm was recommended; 1300 rpm was chosen as the mid – range rotational speed, as this speed produced a gravitational force approximate to that produced in the Ito experiments (Ito *et al*, 2003).

3.3. Results

Table 3.3a reports the stationary phase retention values obtained at the mobile phase breakthrough point and at the end of each experiment. The table also shows the amount of stationary phase lost from the column between the mobile phase breakthrough point and the end of the experiment (stationary phase "stripping"). All stationary phase values are reported as percentages of the total column volume.

Figure 3.3a is a graphical representation of how stationary phase retention at the mobile phase breakthrough point in each experiment varies with rotational speed. The experiments are grouped according to the identity of the mobile phase (upper or lower phase), the mobile phase flow rate and the direction of mobile phase flow.

Figure 3.3b is a graphical representation of how stationary phase retention at the end of each experiment varies with rotational speed. The experiments are grouped according to the identity of the mobile phase (upper or lower phase), the mobile phase flow rate and the direction of mobile phase flow.

Figure 3.3c is a graphical representation of how stationary phase "stripping" varies with rotational speed. The experiments are grouped according to the identity of the mobile phase (upper or lower phase), the mobile phase flow rate and the direction of mobile phase flow.

Figure 3.3d is a graphical representation of how stationary phase retention at the mobile phase breakthrough point and at the end of the experiment varied with rotational speed, and how the stationary phase "stripping" varied with rotational speed under the following experimental conditions: MP = LP; direction of MP flow = "Tail" to "Head"; MP flow rate = 0.25 $mlmin^{-1}$. These conditions gave the largest stationary phase retention values at the two time points mentioned, but also gave the largest stationary phase "stripping" values, indicating a high level of phase instability within the column during the experiment.

Figure 3.3e is a graphical representation of how stationary phase retention at the mobile phase breakthrough point and at the end of the experiment varied with rotational speed, and how the stationary phase "stripping" varied with rotational speed under the following experimental conditions: MP = LP; direction of MP flow = "Head" to "Tail"; MP flow rate = 0.25 $mlmin^{-1}$. These conditions gave moderate stationary phase retention values at the two time points mentioned, but

gave the smallest stationary phase "stripping" values, indicating a high level of phase stability within the column during the experiment.

The data used in Figures 3.3a, 3.3b and 3.3c is reported in Table 3.3a.

Table 3.3a: The variation in the stationary phase retention at the mobile phase breakthrough point and at the end of the experiment, and the loss ("stripping") of stationary phase (all as a percentage of the total column volume) obtained using a 1.6 mm bore, 5.3 m long, 10.8 ml capacity column fitted to the MILLI #1 CCC centrifuge and rotated in a clockwise direction ("Head" at centre; "Tail" at periphery). Solvent system: 12.5% w/w PEG-1000: 12.5% w/w K_2HPO_4 ATPS.

Identity of Mobile Phase	Direction of MP Flow	MP Flow Rate ($mlmin^{-1}$)	Rotational Speed (rpm)	*Sf* at MP b/p (%CV)	*Sf* at e/e (%CV)	Stripping SP (%CV)
UP	H to T	0.25	800	32.41	28.70	3.70
UP	H to T	0.25	1300	38.89	36.11	2.78
UP	H to T	0.25	1800	37.96	34.26	3.70
UP	H to T	0.5	800	23.15	21.30	1.85
UP	H to T	0.5	1300	30.56	27.78	2.78
UP	H to T	0.5	1800	36.11	31.48	4.63
UP	T to H	0.25	800	4.63	2.78	1.85
UP	T to H	0.25	1300	4.63	0.93	3.70
UP	T to H	0.25	1800	4.63	3.24	1.39
UP	T to H	0.5	800	3.24	1.39	1.85
UP	T to H	0.5	1300	2.78	1.39	1.39
UP	T to H	0.5	1800	4.63	3.24	1.39
LP	H to T	0.25	800	27.78	11.57	16.20
LP	H to T	0.25	1300	41.67	27.78	13.89
LP	H to T	0.25	1800	50.93	43.98	6.94
LP	H to T	0.5	800	23.15	9.26	13.89
LP	H to T	0.5	1300	32.41	20.83	11.57
LP	H to T	0.5	1800	42.59	41.67	0.93
LP	T to H	0.25	800	61.11	27.78	33.33
LP	T to H	0.25	1300	74.07	55.56	18.52
LP	T to H	0.25	1800	79.63	55.56	24.07
LP	T to H	0.5	800	43.52	11.57	31.94
LP	T to H	0.5	1300	66.67	32.41	34.26
LP	T to H	0.5	1800	76.39	27.78	48.61

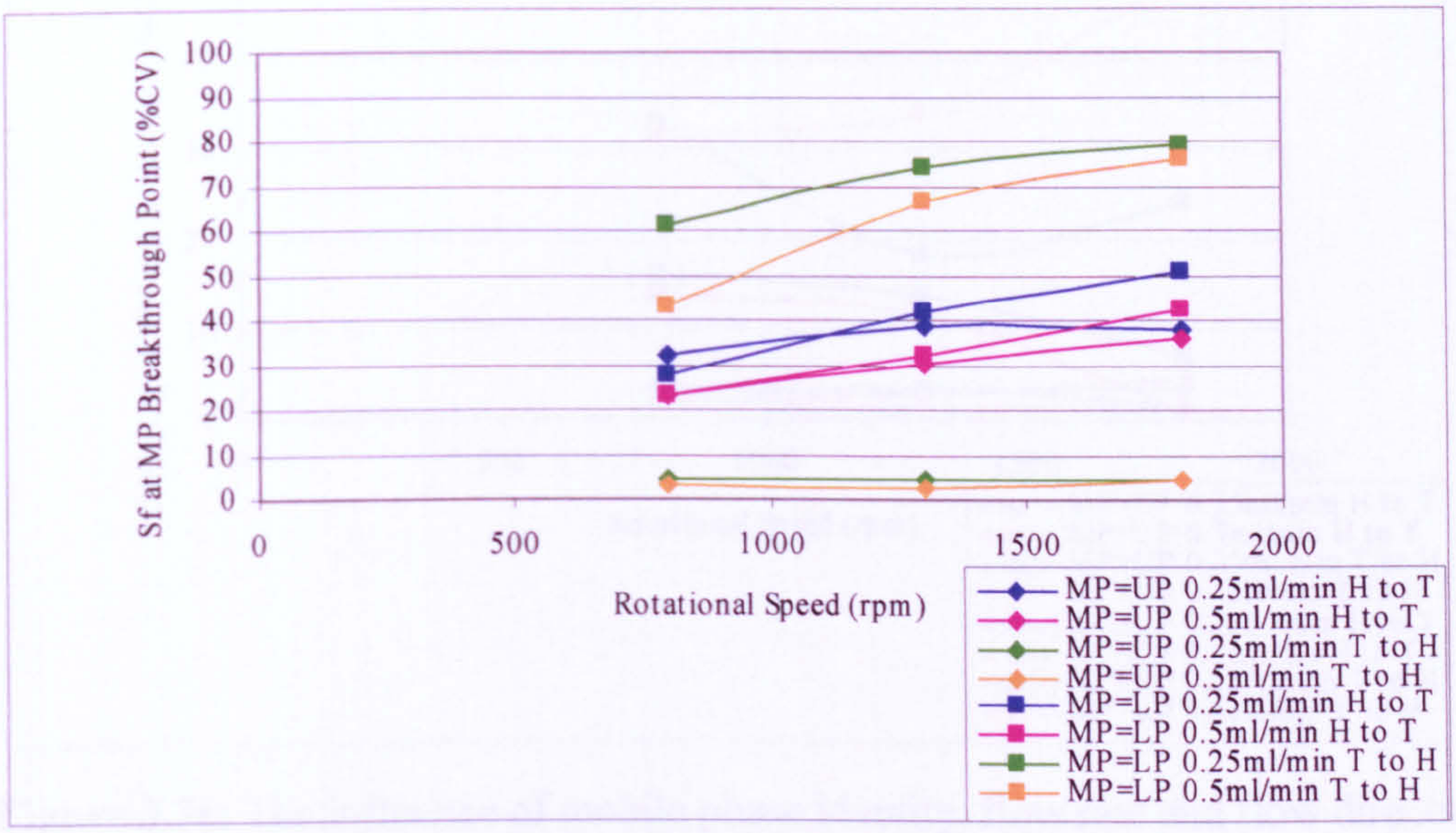

Figure 3.3a: The influence of mobile phase identity, flow rate and flow direction on the stationary phase retention at the mobile phase breakthrough point relative to rotational speed. Column dimensions: 1.6 mm bore, 5.3 m long with a 10.8 ml capacity, fitted to the MILLI #1 CCC centrifuge and rotated in a clockwise direction ("Head" at centre; "Tail" at periphery). Solvent system: 12.5% w/w PEG-1000: 12.5% w/w K_2HPO_4 ATPS.

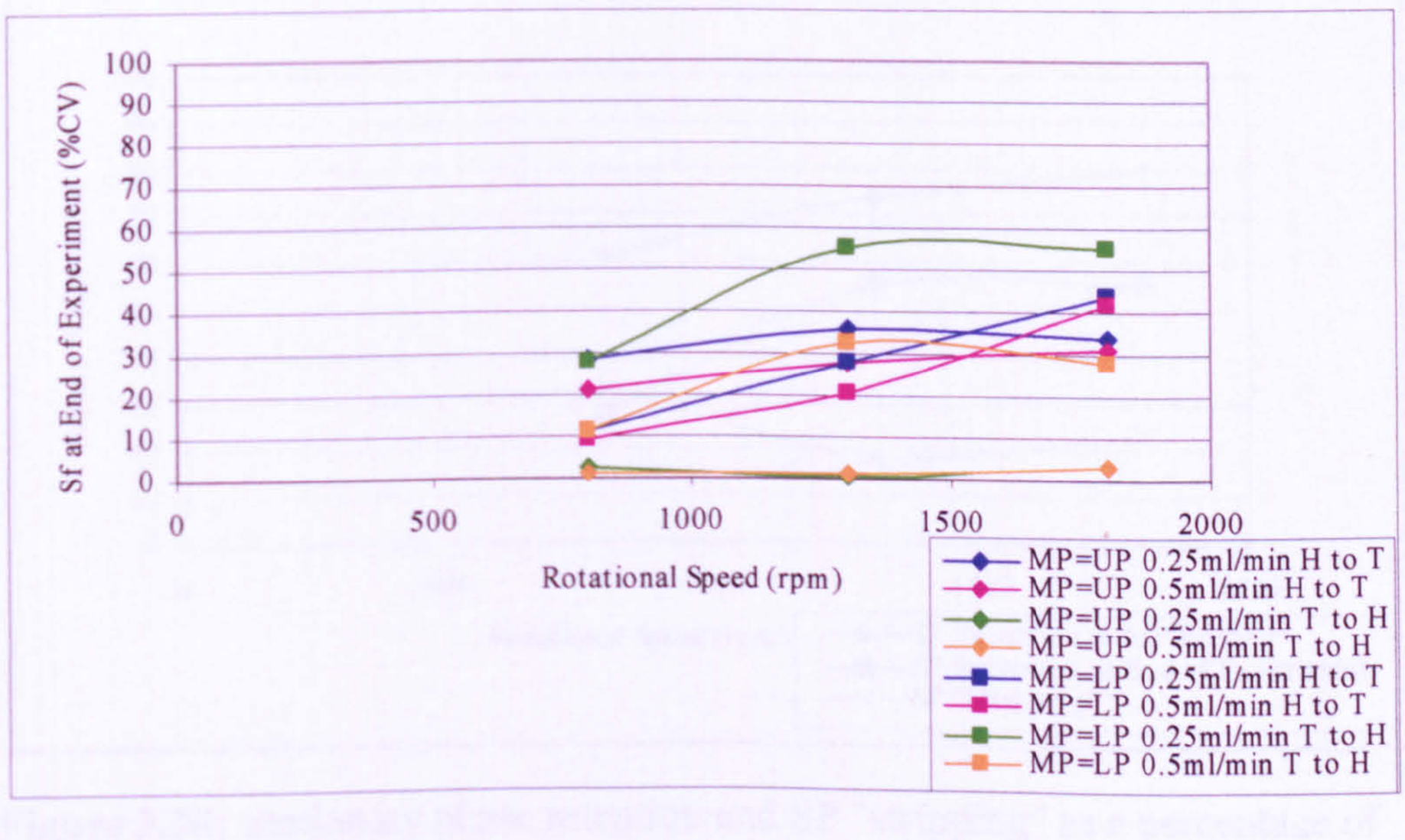

Figure 3.3b: The influence of mobile phase identity, flow rate and flow direction on the stationary phase retention at the end of the experiment relative to rotational speed. Column dimensions: 1.6 mm bore, 5.3 m long with a 10.8 ml capacity, fitted to the MILLI #1 CCC centrifuge and rotated in a clockwise direction ("Head" at centre; "Tail" at periphery). Solvent system: 12.5% w/w PEG-1000: 12.5% w/w K_2HPO_4 ATPS.

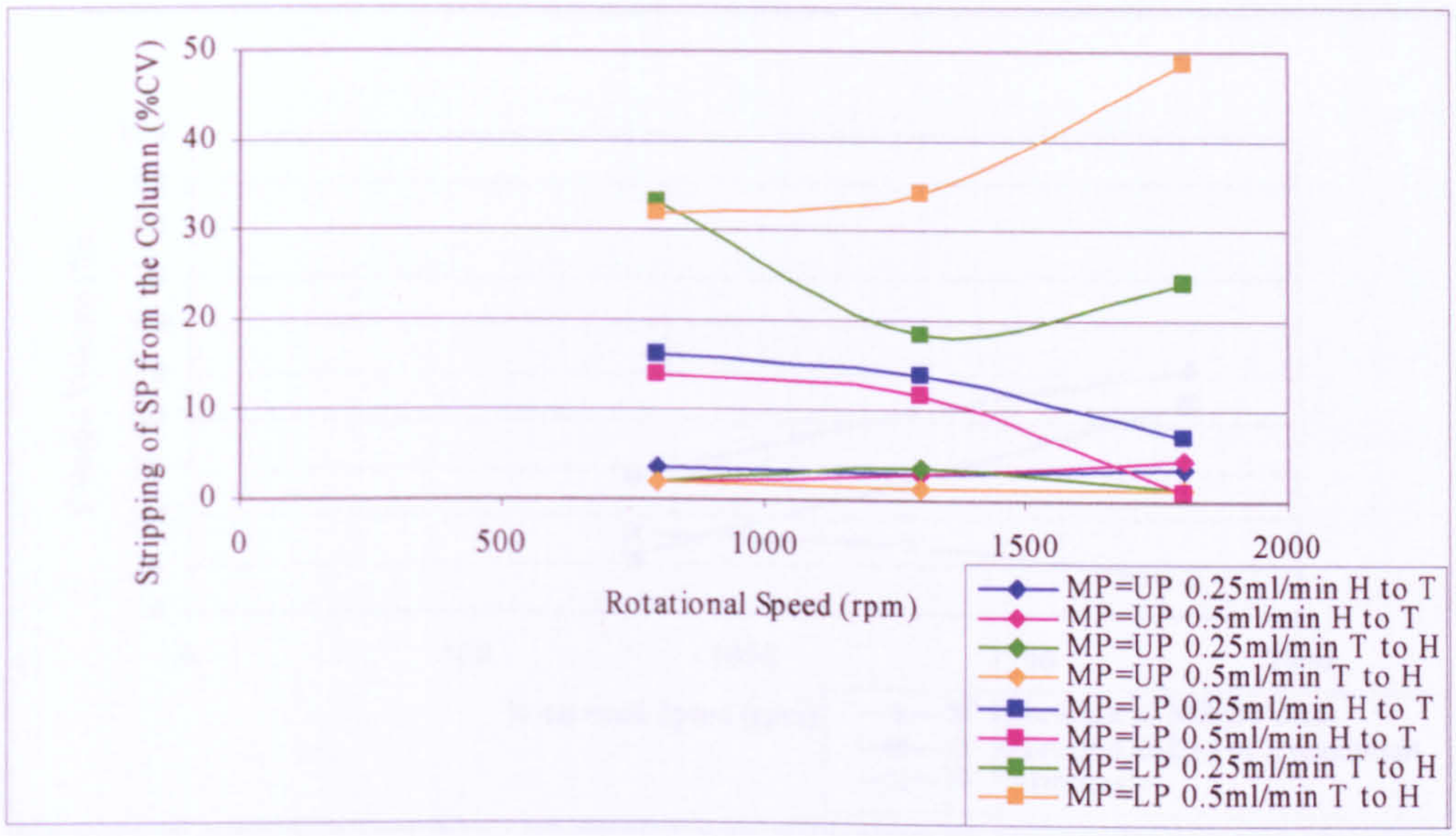

Figure 3.3c: The influence of mobile phase identity, flow rate and flow direction on the loss of stationary phase between the MP breakthrough point and the end of the experiment (SP "stripping") relative to rotational speed. Column dimensions: 1.6 mm bore, 5.3 m long with a 10.8 ml capacity, fitted to the MILLI #1 CCC centrifuge and rotated in a clockwise direction ("Head" at centre; "Tail" at periphery). Solvent system: 12.5% w/w PEG-1000: 12.5% w/w K_2HPO_4 ATPS.

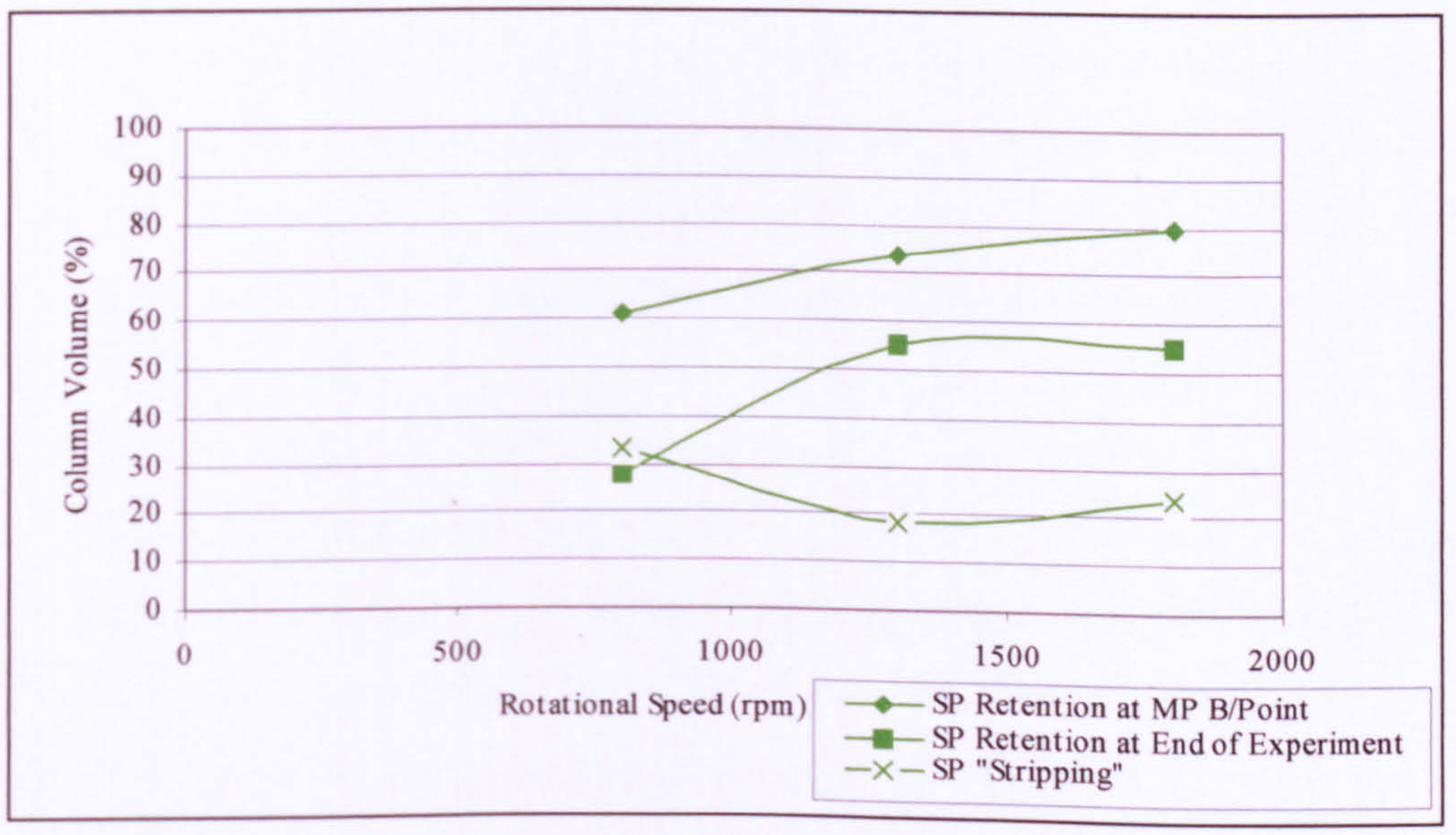

Figure 3.3d: Stationary phase retention and SP "stripping" as a percentage of column volume for the CCC experimental conditions that yielded the highest stationary phase retention values but also the highest SP "stripping" values. The experimental conditions were: MP = LP; direction of MP flow = "Tail" to "Head"; MP flow rate = 0.25 $mlmin^{-1}$.

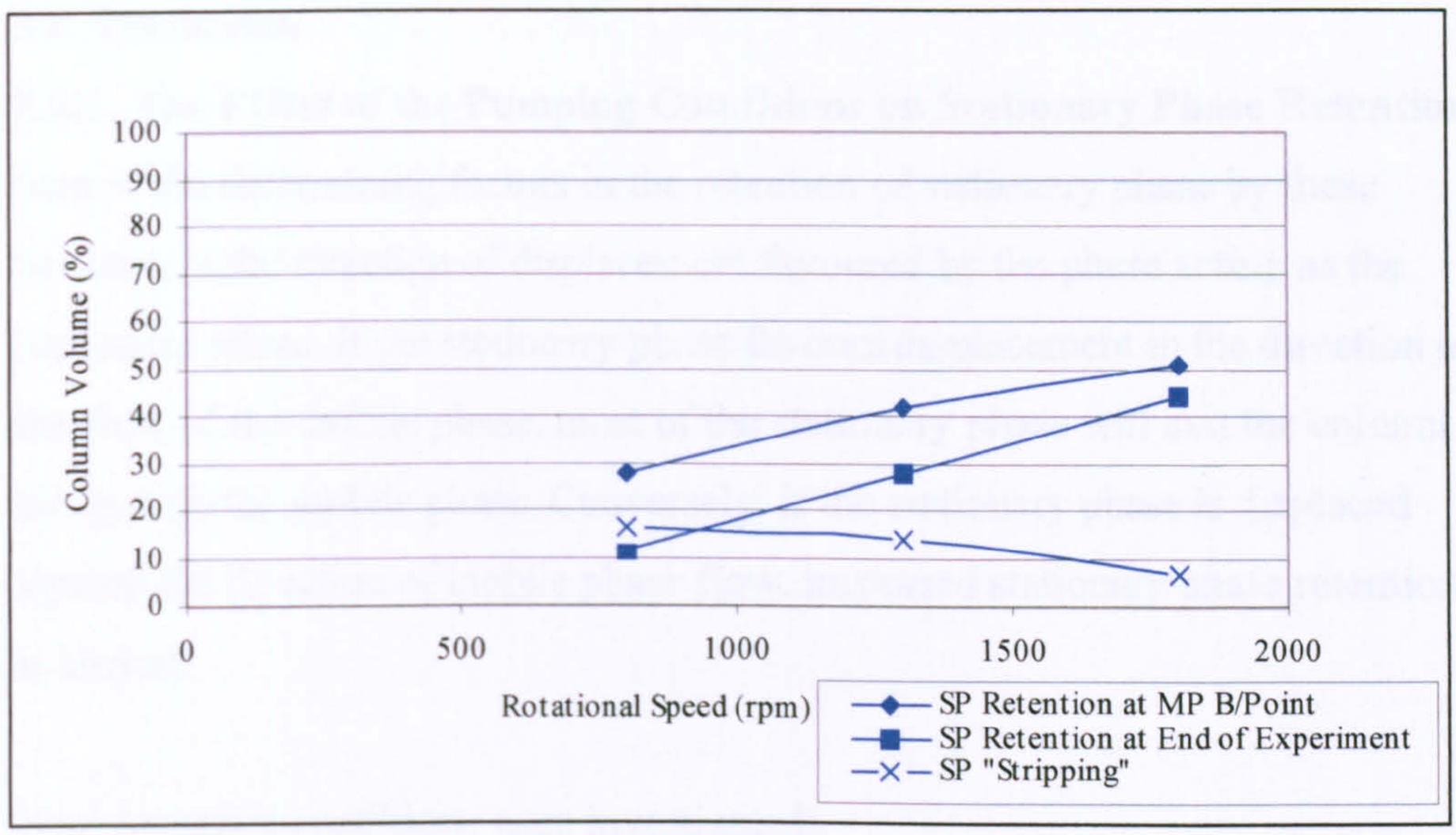

Figure 3.3e: Stationary phase retention and SP "stripping" as a percentage of column volume for the CCC experimental conditions that yielded the most stable stationary phase retention values, and were subsequently used in the lysozyme/myoglobin separation studies using CCC. The experimental conditions were: MP = LP; direction of MP flow = "Head" to "Tail"; MP flow rate = 0.25 $mlmin^{-1}$.

3.4. Discussion

3.4.1. The Effect of the Pumping Conditions on Stationary Phase Retention

One of the determining factors in the retention of stationary phase by these columns is the direction of displacement favoured by the phase acting as the stationary phase. If the stationary phase favours displacement in the direction of the flow of the mobile phase, most of the stationary phase will exit the column along with the mobile phase. Conversely, if the stationary phase is displaced against the direction of mobile phase flow, increased stationary phase retention is achieved.

Four pumping conditions were investigated:

- UP as the MP, pumped "Head" to "Tail"
- UP as the MP, pumped "Tail" to "Head"
- LP as the MP, pumped "Head" to "Tail"
- LP as the MP, pumped "Tail" to "Head"

The results in Table 3.3a, Figure 3.3a and Figure 3.3b show that the highest stationary phase retention at the mobile phase breakthrough point and at the end of the experiment occurs when the lower phase is used as the mobile phase and is pumped in the "Tail" to "Head" direction. This high stationary phase retention occurs because the upper (less dense) phase, acting as the stationary phase, tends to favour moving to the "Tail" of the column.

Therefore, for this phase system, the stationary phase retention data indicates that the lower phase moves to the "Head" and the upper phase moves to the "Tail". However, the data in Table 3.3a and Figure 3.3c show that the conditions that produce the highest stationary phase retention values also yield the highest amount of stationary phase "stripping" during the experiment. This indicates that these conditions, although favourable in absolute terms of retention, are highly unstable when considering how the retention changes during the experiment..

In summary, when the lower phase acts as the mobile phase:

- Pumping the mobile phase in the "Tail" → "Head" direction produces a high initial *Sf*, but a low final *Sf*, indicating that there has been a high level of stationary phase "stripping", and that the hydrodynamic equilibrium created is unstable (Figure 3.3d).
- Pumping the mobile phase in the "Head" → "Tail" direction produces a moderate initial *Sf* and a low final *Sf*, indicating that there has been a low level of stationary phase "stripping", and that the hydrodynamic equilibrium created is reasonably stable (Figure 3.3e).

The previous study by Sutherland and others on a Brunel/DE J – type CCC centrifuge (Sutherland *et al*, 2000) found that the lower phase always moves to the "Tail"; these results with an aqueous two – phase system show the opposite is found in practice. However, these results agree with the prediction made based on Ito's findings (Ito, 1992) which state that for hydrophilic phase systems the more dense phase moves to the "Head". One explanation for these different findings is that Sutherland *et al* used wider – bore tubing than that used by Ito in his study; it is known that in small bore tubing the viscous effects of the phases are more dominant than is found in wider – bore tubing. Hence the findings by Ito are likely to be influenced by the effects of phase viscosity, rather than the effects of the Archimedean Screw Force, which produces wave – like movement of the stationary phase towards one end of the column.

The results for stationary phase retention when the upper phase is the mobile phase show that pumping the mobile phase in the "Head" to "Tail" direction produces greater stationary phase retention than pumping in the "Tail" to "Head" direction. This indicates that the lower phase favours moving to the "Head" end of the column, which correlates with the behaviour of the phases when the lower phase is used as the mobile phase.

The higher stationary phase retention values obtained when the upper phase (rather than the lower phase) acts as the stationary phase could be a phenomenon of the relative viscosities of the phases; it is possible that the more viscose upper phase "sticks" to the internal walls of the column whilst the mobile lower phase flows through it.

3.4.2. The Effect of Mobile Phase Flow Rate on Stationary Phase Retention

The results show that, in general, the slower mobile phase flow rate produces the greater stationary phase retention at the mobile phase breakthrough point. This correlates with the prediction made based on earlier studies (Maryutina *et al*, 2003) that the slower the mobile phase flow rate, the greater the stationary phase retention.

The slower mobile phase flow rate also produces, in general, the least stationary phase "stripping" from the column, although the relationship is not quite as definitive.

3.4.3. The Effect of Rotational Speed on Stationary Phase Retention

The results show that, in general, the greater rotational speed produces the greater stationary phase retention at the mobile phase breakthrough point. This correlates with the prediction made based on earlier studies (Maryutina *et al*, 2003) that the higher the rotational speed of the coil, the greater the stationary phase retention. The effect of rotational speed on the extent of stationary phase "stripping" is more ambiguous. When the upper phase is the mobile phase, there is very little "stripping" anyway, and no clear pattern with respect to rotational speed. When the lower phase is the mobile phase, and is being pumped in the "Head" to "Tail" direction, the extent of "stripping" decreases with increased rotational speed. However, when the lower phase is pumped in the "Tail" to "Head" direction, the stationary phase "stripping" is greatest at 1800 rpm when the flow rate is 0.5 $mlmin^{-1}$.

The extent of the loss of stationary phase from the column was measured from the mobile phase breakthrough point until the end of the experiment. It should be noted that the experiments had a fixed time span set by the operator from the start of the mobile phase pump; 80 minutes if the mobile phase flow rate was 0.25 $mlmin^{-1}$ and 40 minutes if the mobile phase flow rate was 0.5 $mlmin^{-1}$. It is likely that stationary phase "stripping" would have continued to occur if the time periods had been extended, possibly until all stationary phase had been lost from the column. The experiments were limited by time for practical reasons, however it should be noted that the systems did not reach completely stable dynamic equilibrium in these experiments.

3.5. Conclusions

The purpose of this series of experiments was to identify a set of experimental parameters that would yield the greatest stationary phase retention and the least stationary phase "stripping" when a 12.5% w/w PEG-1000: 12.5% w/w K_2HPO_4 ATPS was used in a column of bore 1.6 mm, length 5.3 m and capacity 10.8 ml fitted to the MILLI #1 CCC centrifuge.

Unfortunately, no one set of parameters incorporated both criteria; those conditions that produced high stationary phase retention values also produced large losses of stationary phase from the column due to "stripping". It was thought that unstable stationary phase retention would produce poor protein resolution.

It was decided to compromise and use a set of experimental parameters that, whilst not yielding the best stationary phase retention at the mobile phase breakthrough point, did not subsequently cause a large loss of stationary phase from the column. These experimental parameters were as follows:

- Direction of coil rotation: Clockwise ("Head" at centre/"Tail" at periphery)
- Direction of MP flow: "Head" to "Tail"
- Composition of MP: LP of a 12.5% w/w PEG-1000: 12.5% w/w K_2HPO_4 ATPS
- Composition of SP: UP of a 12.5% w/w PEG-1000: 12.5% w/w K_2HPO_4 ATPS
- Rotational speed of coil: 1800 rpm
- MP flow rate: 0.25 $mlmin^{-1}$

These conditions had given a stationary phase retention value at the mobile phase breakthrough point of 50.93% CV, and at the end of the experiment of 43.98% CV, meaning a loss of only 6.94% CV stationary phase due to "stripping".

It was decided that the next stage of the project (the study of the behaviour of lysozyme and myoglobin in the CCC centrifuges) should incorporate observing the effect of different mobile phase flow rates on the resolution of the proteins. The mobile phase flow rates used would be 0.125, 0.25, 0.5 and 1.0 $mlmin^{-1}$ in the 1.6 mm bore column, or the equivalent flow rates in larger bore columns.

Chapter 4 – Separation of the Proteins Lysozyme and Myoglobin using J – Type CCC Centrifuges

4.1. Introduction

The previous chapter explored the behaviour of a 12.5% w/w PEG-1000: 12.5% w/w dipotassium hydrogen phosphate ATPS in a 1.6 mm bore, 5.3 m long, 10.8 ml capacity column fitted to the MILLI #1 J – type CCC centrifuge. Studies of stationary phase retention and rate of loss of stationary phase from this column (stationary phase "stripping") were carried out for a range of experimental parameters, and from these results a set of optimum experimental conditions were proposed for the next stage of the project, namely the separation of the proteins lysozyme and myoglobin.

The distribution ratios of lysozyme and myoglobin in the 12.5% w/w PEG-1000: 12.5% w/w dipotassium hydrogen phosphate ATPS were1.9 and 0.6 respectively. Theoretically, separation would occur if this phase system was used to separate lysozyme and myoglobin in the application of the CCC process.

The experimental work to date had been carried out using a column of bore 1.6 mm. It was thought that this width of column would not allow sufficient mixing of the two phases to produce protein separation, and so a column of bore 2.7 mm was employed. The later experiments in this chapter used a 4.0 mm bore column fitted to a SMART-MIDI centrifuge to test the hypothesis that increasing column bore increased protein resolution.

The increase in the column bore necessitated an adjustment to the mobile phase flow rates used with the larger bore columns. The rate of liquid flow through a column is termed the mean linear velocity of the liquid, and is given by:

$$\text{Mean linear velocity} = \frac{\text{Mobile phase flow rate}}{\text{*C-S area of column tubing}} \qquad \text{[Equation 4.1a]}$$

*C-S = Cross – sectional

This equation was used to adjust the mobile phase flow rates accordingly, so that linear velocity values remained constant between the different columns. Although this allowed a degree of comparison between the different columns, the equation

does not take into account the volume occupied in the column by the stationary phase.

The experiments detailed in this chapter also investigated the effect of increasing the mobile phase flow rate. It was thought that this would also enhance phase mixing within the column, leading to greater protein resolution.

Use of the SMART-MIDI centrifuge necessitated a decrease in the rotational speed of that employed with the MILLI #1 centrifuge. This is because comparison between the two types of column can only be made if the gravitational force exerted on the column contents is the same for both systems (refer to Section 3.2.2).

The work to separate lysozyme and myoglobin using the J – type CCC centrifuges was the first attempt at protein separation using these instruments, and as such these experiments were the basis of much method development in the techniques involved. A number of operational difficulties were encountered during the experiments *e.g.* erratic readings from the UV detector due to a dirty detector cell, system over – pressurisation causing the rupture of a column. This necessitated a series of modifications to the experimental equipment and procedures as the work progressed. Details of any modifications that were made are given at the appropriate points, together with the reasons behind such modifications.

Experiments in this chapter were only repeated if there had been an equipment failure of some sort; *i.e.* results for a particular set of experimental parameters are not available in duplicate or triplicate.

4.2. Materials and Methods

4.2.1. Preparation of the Aqueous Two – Phase System

The phase system used in these experiments was the 12.5% w/w PEG-1000: 12.5% w/w K_2HPO_4 ATPS. Appropriate quantities were prepared as required following the procedure in Section 2.1.1.

4.2.2. Preparation of the Lysozyme and Myoglobin Loading Samples

Lysozyme and myoglobin loading samples were prepared as in Section 2.5.1. The sample loop used in the CCC study had a volume of 2.32 ml (5.0% CV {column volume}). For each experiment, sufficient loading sample was prepared to completely fill the sample loop, and some of the loading sample was reserved for use in the HPLC analysis of the CCC fractions.

4.2.3. Separation of Lysozyme and Myoglobin using the MILLI #1 J – Type CCC Centrifuge

The MILLI #1 CCC centrifuge was originally fitted with the DEM-PRO #1 coil (refer to Table 2.3.1a). An incident involving over – pressurisation of the system during an experiment caused the tubing of this coil to rupture. The damaged coil was replaced by the DEM-PRO #2 coil; both coils provided columns of similar dimensions.

The protocol for the operation of this CCC centrifuge has been described in Section 2.3.7, with the experimental apparatus arranged as shown in Figure 2.3.1a. The dead volume of the system is defined as the volume of the connecting tubing plus half the volume of the sample loop. The length of this tubing was determined using a tape measure, and with the cross – sectional area of the tubing known, the dead volume was calculated to be 3.46 ml.

The fixed experimental parameters were as follows:

- Direction of coil rotation: Clockwise ("Head" at centre/"Tail" at periphery)
- Direction of MP flow: "Head" to "Tail"
- Composition of MP: LP of a 12.5% w/w PEG-1000: 12.5% w/w K_2HPO_4 ATPS

- Composition of SP: UP of a 12.5% w/w PEG-1000: 12.5% w/w K_2HPO_4 ATPS
- Rotational speed of coil: 1800 rpm (approximately)
- System temperature: 30°C ± 1.0°C
- UV detector wavelength: 280 nm
- UV detector cell: Analytical
- Loading sample composition: Mixture of lysozyme at 1.0 $mgml^{-1}$ and myoglobin at 1.0 $mgml^{-1}$, giving a total protein concentration of 2.0 $mgml^{-1}$. For each experiment, sufficient loading sample was prepared to completely fill the sample loop used, and some of the loading sample was reserved for use in the HPLC analysis of the CCC fractions.
- Loading sample solvent: LP of a 12.5% w/w PEG-1000: 12.5% w/w K_2HPO_4 ATPS.
- Capacity of sample loop: 2.32 ml (5.0% of column volume)

The variable experimental parameters are detailed in Table 4.2.3a.

Table 4.2.3a: The variable experimental parameters in the study of lysozyme and myoglobin separation using the MILLI #1 CCC centrifuge.

Coil Name	Column Bore (mm)	Column Length (m)	Column Capacity (ml)	MP Flow Rate ($mlmin^{-1}$)	Comparable MP Flow Rate in 1.6 mm Bore Column ($mlmin^{-1}$)	Fraction Collection Interval (min)	Fraction Volume (ml)
DEM-PRO #1	2.7	8.0	46.3	0.36	0.125	4	1.44
DEM-PRO #2	2.7	7.9	45.1	0.36	0.125	4	1.44
DEM-PRO #1	2.7	8.0	46.3	0.72	0.25	2	1.44
DEM-PRO #1	2.7	8.0	46.3	1.44	0.50	1	1.44
DEM-PRO #1	2.7	8.0	46.3	2.88	1.0	0.5	1.44

The eluent from the column passed through a UV detector, which was set at wavelength 280 nm. The signal from the detector was analysed using Knauer "Eurochrom® for Windows Basic Edition V3.05" software, producing a chromatogram.

Fractions were collected at the stated time intervals in glass vials and subjected to analysis by HPLC.

After the termination of the experiment, the system contents were evacuated with nitrogen gas, and the volume of stationary phase retained in the column during the experiment was calculated.

4.2.4. Separation of Lysozyme and Myoglobin using the SMART-MIDI J – Type CCC Centrifuge

The SMART-MIDI CCC centrifuge was fitted with two coils connected in series, to give a column of bore 4.0 mm, length 34.3 m and capacity 431.0 ml. The protocol for the operation of this CCC centrifuge has been described in Section 2.3.7, with the experimental apparatus arranged as shown in Figure 2.3.1a, however UV detection was omitted due to equipment malfunction. The dead volume of the system was defined as the volume of the connecting tubing plus half the volume of the sample loop. The length of this tubing was determined using a tape measure, and with the cross – sectional area of the tubing known, the dead volume was calculated to be 22.5 ml.

The fixed experimental parameters were as follows:

- Direction of coil rotation: Forward ("Head" at centre/"Tail" at periphery)
- Direction of MP flow: "Head" to "Tail"
- Composition of MP: LP of a 12.5% w/w PEG-1000: 12.5% w/w K_2HPO_4 ATPS
- Composition of SP: UP of a 12.5% w/w PEG-1000: 12.5% w/w K_2HPO_4 ATPS
- Rotational speed of coil: 1100 rpm (approximately)
- System temperature: 30°C ± 2.0°C

- Loading sample composition: Mixture of lysozyme at 1.0 $mgml^{-1}$ and myoglobin at 1.0 $mgml^{-1}$, giving a total protein concentration of 2.0 $mgml^{-1}$. For each experiment, sufficient loading sample was prepared to completely fill the sample loop used, and some of the loading sample was reserved for use in the HPLC analysis of the CCC fractions.
- Loading sample solvent: LP of a 12.5% w/w PEG-1000: 12.5% w/w K_2HPO_4 ATPS (except for the experiment using a MP flow rate of 6.25 $mlmin^{-1}$, which had a loading sample solvent consisting of 50% LP + 50% UP of this phase system).
- Capacity of sample loop: 21.55 ml (5.0% of column volume)

The variable experimental parameters are detailed in Table 4.2.4a.

Table 4.2.4a: The variable experimental parameters in the study of lysozyme and myoglobin separation using the SMART-MIDI CCC centrifuge.

MP Flow Rate ($mlmin^{-1}$)	Loading Sample Solvent	Comparable MP Flow Rate in 1.6 mm Bore Column ($mlmin^{-1}$)	Fraction Collection Interval (min)	Fraction Volume (ml)
6.25	50% UP + 50% LP of a 12.5% w/w PEG-1000: 12.5% w/w K_2HPO_4 ATPS	1.0	1	6.25
25.0	LP of a 12.5% w/w PEG-1000: 12.5% w/w K_2HPO_4 ATPS	4.0	0.5	12.5

The eluent from the column passed through a UV detector, which was set at wavelength 280 nm. The signal from the detector was analysed using Knauer "Eurochrom® for Windows Basic Edition V3.05" software, producing a chromatogram.

Fractions were collected at the stated time intervals in glass vials and subjected to analysis by HPLC.

After the termination of the experiment, the system contents were evacuated with nitrogen gas, and the volume of stationary phase retained in the column during the experiment was calculated.

4.2.5. Stationary Phase Retention

Stationary phase retention (*Sf*) in the column was calculated at two time points for each experiment: at the mobile phase breakthrough point and at the end of the experiment.

The total volume of this system is divided into the volume occupied by the column (where separation took place) and the volume of the tubing that formed the extra coil (dead) volume; this connects the column to the liquid – handling pumps and the detector. The dead volume would have contained stationary phase at the start of the experiment, the volume of which must be deducted from the volume of eluted stationary phase at the mobile phase breakthrough point. The resulting value was used to obtain the stationary phase retention at the mobile phase breakthrough point.

The stationary phase retention was also calculated at the conclusion of the experiment. The centrifuge and the pumps were stopped, and the system contents evacuated with nitrogen gas. The system contents consisted of both mobile and stationary phase. It was assumed that at the end of the experiment the dead volume contained only mobile phase, so it was not necessary to deduct this volume from the volume of stationary phase collected at this point. The stationary phase volume was used to obtain the stationary phase retention at the end of the experiment.

The following calculations were carried out for each experiment. Table 4.2.5a gives the meaning of each notation in the equations.

$$V_{\text{SP FROM COLUMN}} = V_{\text{SP FROM SYSTEM}} - V_{\text{D}} \qquad \text{[Equation 4.2.5a]}$$

$$V_{\text{SP RETAINED COLUMN MP B/P}} = V_{\text{C}} - V_{\text{SP FROM COLUMN}} \qquad \text{[Equation 4.2.5b]}$$

$$Sf_{\text{MP B/P}}\,(\%) = (V_{\text{SP RETAINED COLUMN}}/V_{\text{C}}) \times 100 \qquad \text{[Equation 4.2.5c]}$$

$$Sf_{\text{E/E}}\,(\%) = (V_{\text{SP RETAINED COLUMN E/E}}/V_{\text{C}}) \times 100 \qquad \text{[Equation 4.2.5d]}$$

Table 4.2.5a: Meaning of notations used in equations to calculate stationary phase retention values.

Notation used in Equation	Meaning of Notation
V_C	Column volume of centrifuge
V_D	Dead volume of system
$V_{SP\ FROM\ SYSTEM}$	Volume stationary phase that eluted from the system at the mobile phase breakthrough point
$V_{SP\ FROM\ COLUMN}$	Volume stationary phase displaced from the column at the mobile phase breakthrough point
$V_{SP\ RETAINED\ COLUMN\ MP\ B/P}$	Volume stationary phase retained in the column at the mobile phase breakthrough point
$V_{SP\ RETAINED\ COLUMN\ E/E}$	Volume stationary phase retained in the column at the end of the experiment (equivalent to the volume of stationary phase evacuated with nitrogen gas from the column at the end of the experiment)
$Sf_{MP\ B/P}$ (%)	Percentage stationary phase retention in the column at the mobile phase breakthrough point
$Sf_{E/E}$ (%)	Percentage stationary phase retention in the column at the end of the experiment

4.3. Results

4.3.1. Chromatograms and Graphs from HPLC Analysis

The chromatogram created from the detector signal in each experiment has been annotated to indicate the position of critical time points during the experiment, including the $K = 1$ point. The results from the HPLC analysis of the fractions have been plotted to show how the lysozyme and myoglobin eluted over the time course of the experiment, and have been annotated with the predicted elution times of the proteins. For an explanation of the method used to calculate the $K = 1$ point and the predicted elution times of the proteins, refer to Section 2.6.2.

The chromatogram and HPLC graph for the experiment using the MILLI #1 centrifuge that gave the highest resolution between lysozyme and the myoglobin species are shown in Figures 4.3.1a and 4.3.1b. The chromatograms and HPLC graphs from this and all the other experiments are shown in Appendix 1.

In all the experiments:

- Rotational speed = 1800 rpm
- LP = MP
- Sample volume = 2.32 ml (5.0% CV)
- Pumping of the mobile phase commenced at time zero.
- The recording of data began at 1.5 minutes.
- The mobile phase breakthrough point caused mixing of the two phases in the eluent that appears as the first peak on the chromatogram (the operator also observed at this point drops of mobile phase eluting from the column together with the stationary phase).
- The sample was injected onto the column after the MP breakthrough point at the time indicated on each chromatogram (the pre – equilibration method).
- Fraction collected commenced immediately, and continued until the end of the experiment.

The experiment using the mobile phase flow rate 0.36 $mlmin^{-1}$ was repeated once. This was because the coil inlet/outlet tube of the DEM-PRO #1 coil ruptured during the post – experiment cleaning process (Step Number 11 of Table 2.3.7a). This occurrence necessitated the production of a new coil (called DEM-PRO #2), and the introduction of a pressure gauge and pressure release valve located

upstream of the centrifuge. The experiment was repeated to assess the performance of the new coil, and check for any faults. The data obtained is reported in the tables of results, but is omitted from the graphs, where the data from the DEM-PRO #1 coil is used instead.

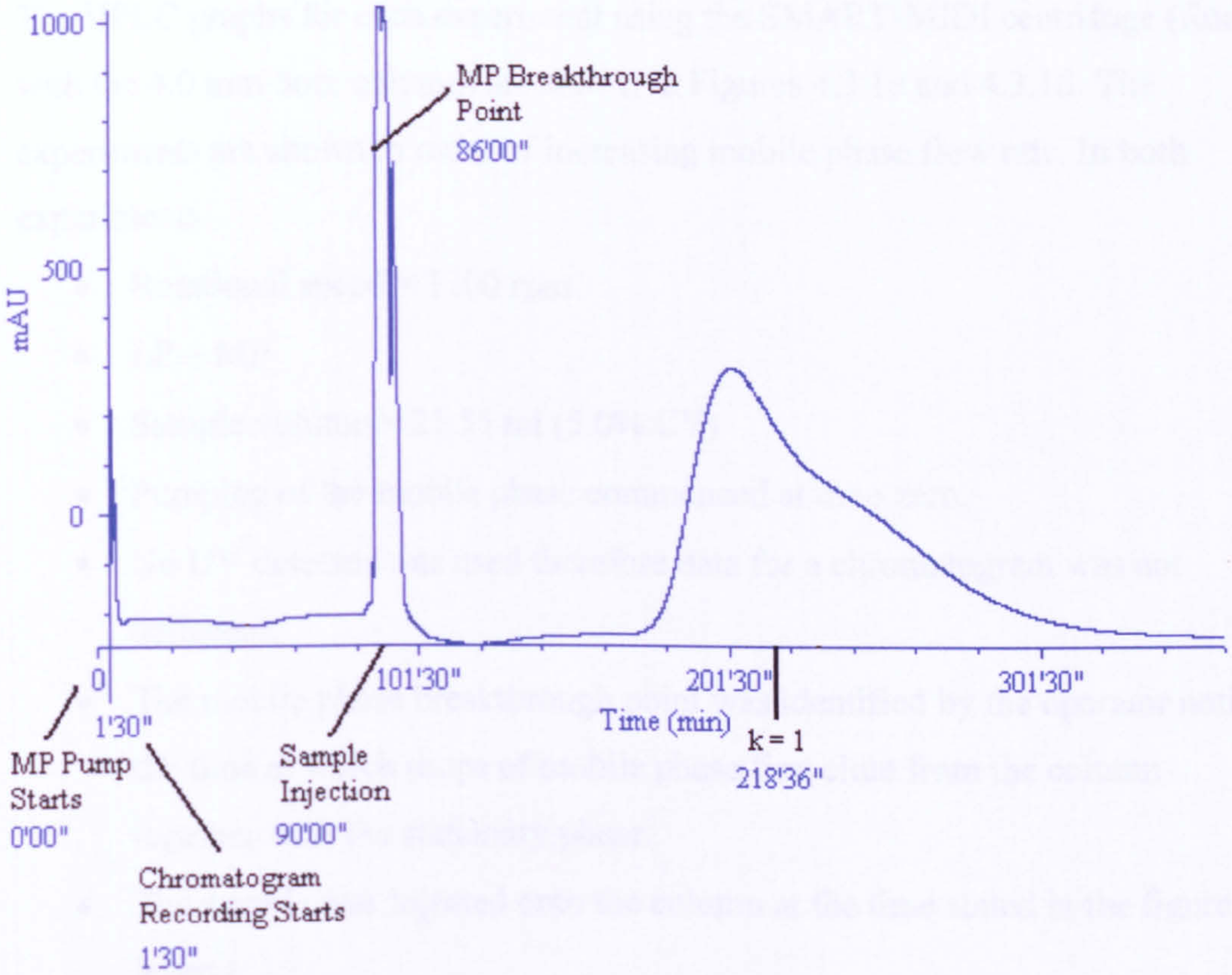

Figure 4.3.1a: Chromatogram from experiment using MP flow rate 0.36 mlmin^{-1} in the DEM-PRO #1 coil with 2.7 mm bore. The k = 1 point has been quoted in units of time, having been converted from retention volume using Equation 2.6.2b. The retention volume was calculated using Equation 2.6.2a.

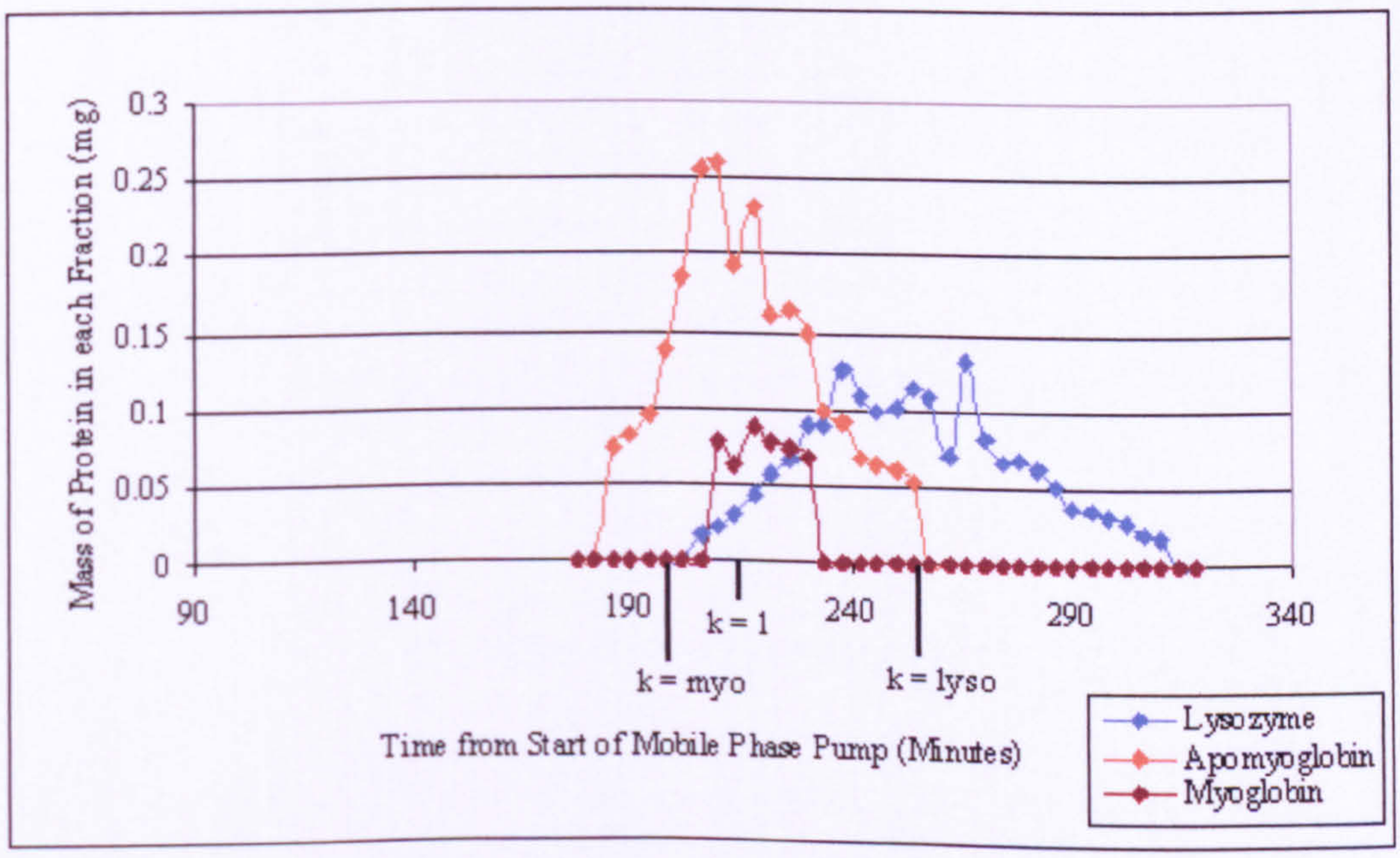

Figure 4.3.1b: Chromatogram created from HPLC analysis of fractions from experiment using MP flow rate 0.36 mlmin^{-1} in the DEM-PRO #1 coil with 2.7 mm bore. The points k = myo and k = lyso are the theoretical retention times of myoglobin and lysozyme respectively, calculated using Equations 2.6.2a and 2.6.2b. The k = 1 point was also calculated using Equations 2.6.2a and 2.6.2b.

The HPLC graphs for each experiment using the SMART-MIDI centrifuge (fitted with the 4.0 mm bore column) are shown in Figures 4.3.1c and 4.3.1d. The experiments are shown in order of increasing mobile phase flow rate. In both experiments:

- Rotational speed = 1100 rpm
- LP = MP
- Sample volume = 21.55 ml (5.0% CV)
- Pumping of the mobile phase commenced at time zero.
- No UV detector was used therefore data for a chromatogram was not collected.
- The mobile phase breakthrough point was identified by the operator noting the time at which drops of mobile phase first elute from the column together with the stationary phase.
- The sample was injected onto the column at the time stated in the figure legend.
- Fraction collected commenced at the time stated in the figure legend, and continued until the end of the experiment.

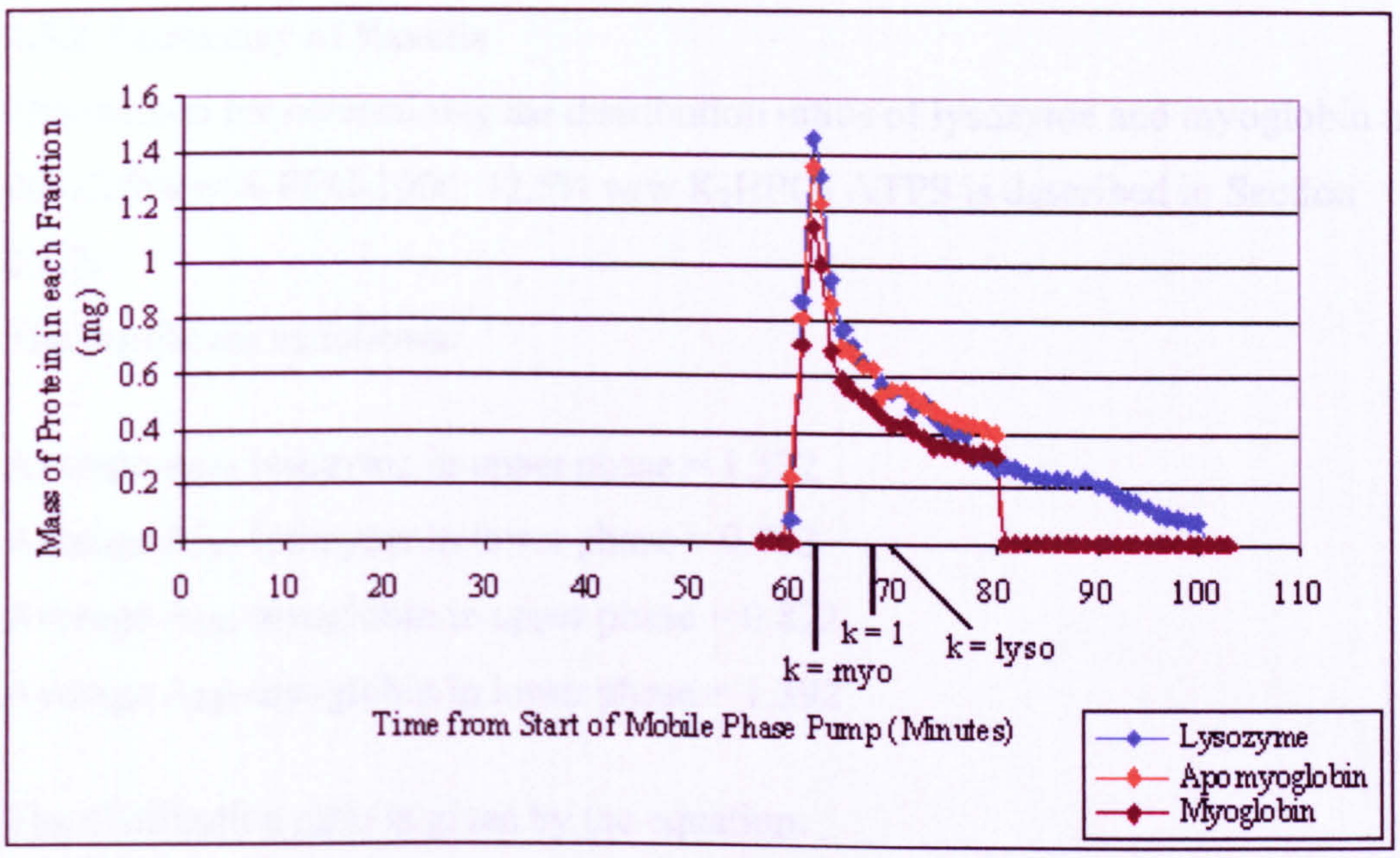

Figure 4.3.1c: Chromatogram created from HPLC analysis of fractions from experiment using MP flow rate 6.25 $mlmin^{-1}$ in the SMART-MIDI coil with 4.0 mm bore. The sample was injected onto the column as soon as the mobile phase pump was started (a sandwich injection). Fraction collection began after 40 minutes; fractions were collected every minute. The points k = myo and k = lyso are the theoretical retention times of myoglobin and lysozyme respectively, calculated using Equations 2.6.2a and 2.6.2b. The k = 1 point was also calculated using Equations 2.6.2a and 2.6.2b.

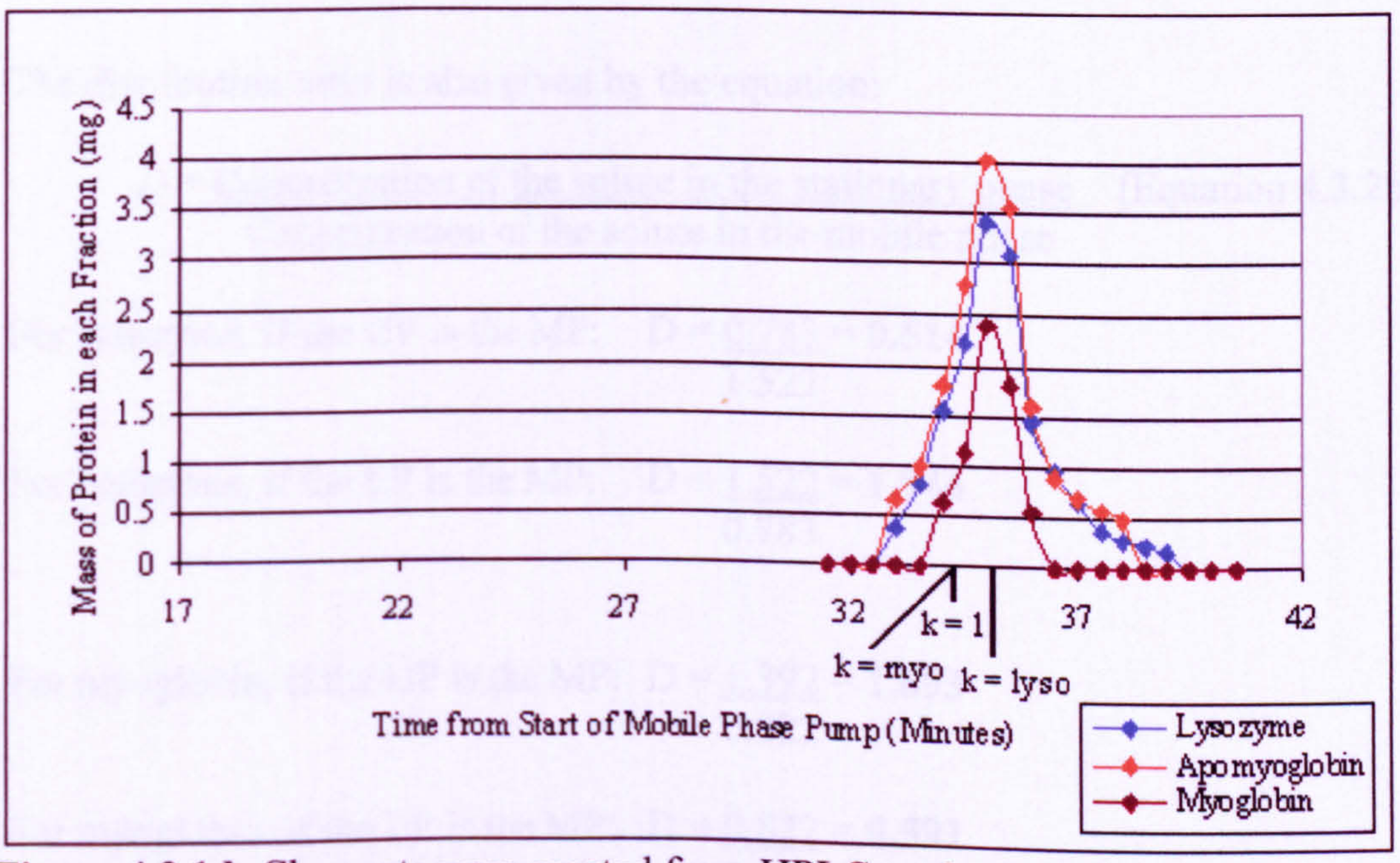

Figure 4.3.1d: Chromatogram created from HPLC analysis of fractions from experiment using MP flow rate 25.0 $mlmin^{-1}$ in the SMART-MIDI coil with 4.0 mm bore. The column was pre – equilibrated before the sample was injected at 17 minutes. Fraction collection began immediately; fractions were collected every 30 seconds. The points k = myo and k = lyso are the theoretical retention times of myoglobin and lysozyme respectively, calculated using Equations 2.6.2a and 2.6.2b. The k = 1 point was also calculated using Equations 2.6.2a and 2.6.2b.

4.3.2. Summary of Results

The method for determining the distribution ratios of lysozyme and myoglobin in the 12.5% w/w PEG-1000: 12.5% w/w K_2HPO_4 ATPS is described in Section 2.5.2.

The results are as follows:

Average A_{280} lysozyme in upper phase = 1.522

Average A_{280} lysozyme in lower phase = 0.783

Average A_{280} myoglobin in upper phase = 0.822

Average A_{280} myoglobin in lower phase = 1.392

The distribution ratio is given by the equation:

$$D = \frac{\text{Concentration of the solute in the upper phase}}{\text{Concentration of the solute in the lower phase}} \quad \text{[Equation 4.3.2a]}$$

For lysozyme: $D = \frac{1.522}{0.783} = \mathbf{1.944\ (1.9)}$

For myoglobin: $D = \frac{0.822}{1.392} = \mathbf{0.591\ (0.6)}$

The distribution ratio is also given by the equation:

$$D = \frac{\text{Concentration of the solute in the stationary phase}}{\text{Concentration of the solute in the mobile phase}} \quad \text{[Equation 4.3.2b]}$$

For lysozyme, if the UP is the MP: $D = \frac{0.783}{1.522} = \mathbf{0.514}$

For lysozyme, if the LP is the MP: $D = \frac{1.522}{0.783} = \mathbf{1.944}$

For myoglobin, if the UP is the MP: $D = \frac{1.392}{0.822} = \mathbf{1.693}$

For myoglobin, if the LP is the MP: $D = \frac{0.822}{1.392} = \mathbf{0.591}$

Table 4.3.2a summarises the values obtained for stationary phase retention, predicted and observed protein elution times, percentage protein recovery and protein resolution for the columns used in this study. Note that the table is extended over two pages, with the footnotes located on the second page.

Table 4.3.2a: Summary of the values obtained for stationary phase retention, predicted and observed protein elution times, percentage protein recovery and protein resolution for the columns used in this study. Fixed parameters in all experiments were as follows: Direction of coil rotation = Clockwise/Forward ("Head" at centre and "Tail" at Periphery); Direction of MP flow = "Head" to "Tail"; MP = LP & SP = UP of a 12.5% w/w PEG-1000: 12.5% w/w K_2HPO_4 ATPS.

Column Bore (mm)	MP Flow Rate ($mlmin^{-1}$)	Rot. Speed (rpm)	$K=1$ (min)	Predicted Retention Time Myo/Apo (min)	Observed Retention Time Myo/Apo (min)	Predicted Retention Time Lyso (min)	Observed Retention Time Lyso (min)	$Sf_{MP\ B/P}$ (%)	$Sf_{E/E}$ (%)	Resolution Apo/Lyso	Resolution Myo/Lyso
2.7 #1	0.36	1800	128	107	122	166	162	42.8	32.4	0.48	0.42
2.7 #2	0.36	1800	125	102	116	163	146	45.7	33.3	0.28	0.29
2.7	0.72	1800	64	56	64	71	71	32.6	11.9	0.23	0.32
2.7	1.44	1800	32	29	35	36	37	25.5	13.0	0.21	0.25
2.7	2.88	1800	16	15	18	17	19	16.8	5.4	0.13	0.22
4.0	6.25	1100	69	63	62	70	62	21.7	2.3	Negligible	Negligible
4.0	25.0	1100	17	17	18	18	18	7.8	N/C	Negligible	Negligible

Table 4.3.2a: Continued

Column Bore (mm)	MP Flow Rate ($mlmin^{-1}$)	Rotational Speed (rpm)	Recovery Apomyoglobin (%)	Recovery Myoglobin (%)	Recovery Lysozyme (%)
2.7 #1	0.36	1800	193	0	132
2.7 #2	0.36	1800	113	0	115
2.7	0.72	1800	128	64	131
2.7	1.44	1800	160	122	169
2.7	2.88	1800	167	355	120
4.0	6.25	1100	55	46	109
4.0	25.0	1100	96	41	93

***K* = 1 point:** the time interval between sample injection and protein elution if the proteins were distributed equally between the two phases in the column.
Predicted & Observed Retention Times: the time interval between sample injection and protein elution, using the distribution ratios of the proteins. Predicted and observed elution times are calculated or reported with the sample injection time taken as time zero.
Lyso: Lysozyme
Apo: Apomyoglobin
Myo: Myoglobin
Sf $_{MP\ B/P}$ **(%):** Percentage stationary phase retention in the column at the mobile phase breakthrough point.
Sf $_{E/E}$ **(%):** Percentage stationary phase retention in the column at the end of the experiment.
The difference in the stationary phase retention value at the end of the experiment from the stationary phase retention value at the mobile phase breakthrough point gave an indication of how much stationary phase was lost to "stripping" between the mobile phase breakthrough point and the end of the experiment.
2.7 #1: the experiment used the 2.7 mm bore DEM-PRO #1 coil.
2.7 #2: the experiment used the 2.7 mm bore DEM-PRO #2 coil.
N/C: Not collected; the column was evacuated with water rather than nitrogen gas.
Negligible: the shape of the peaks on these HPLC graphs made it impossible to calculate the protein resolution in these experiments.

4.3.3. Analysis of Stationary Phase Retention and Protein Resolution Values

The data from the experiments using the 2.7 mm bore column (as reported in Table 4.3.2a) is presented graphically in Figures 4.3.3a to 4.3.3d. The data for the mobile phase flow rate of 0.36 mlmin^{-1} was taken from the experiment using the DEM-PRO #1 coil, rather than the DEM-PRO #2 coil.

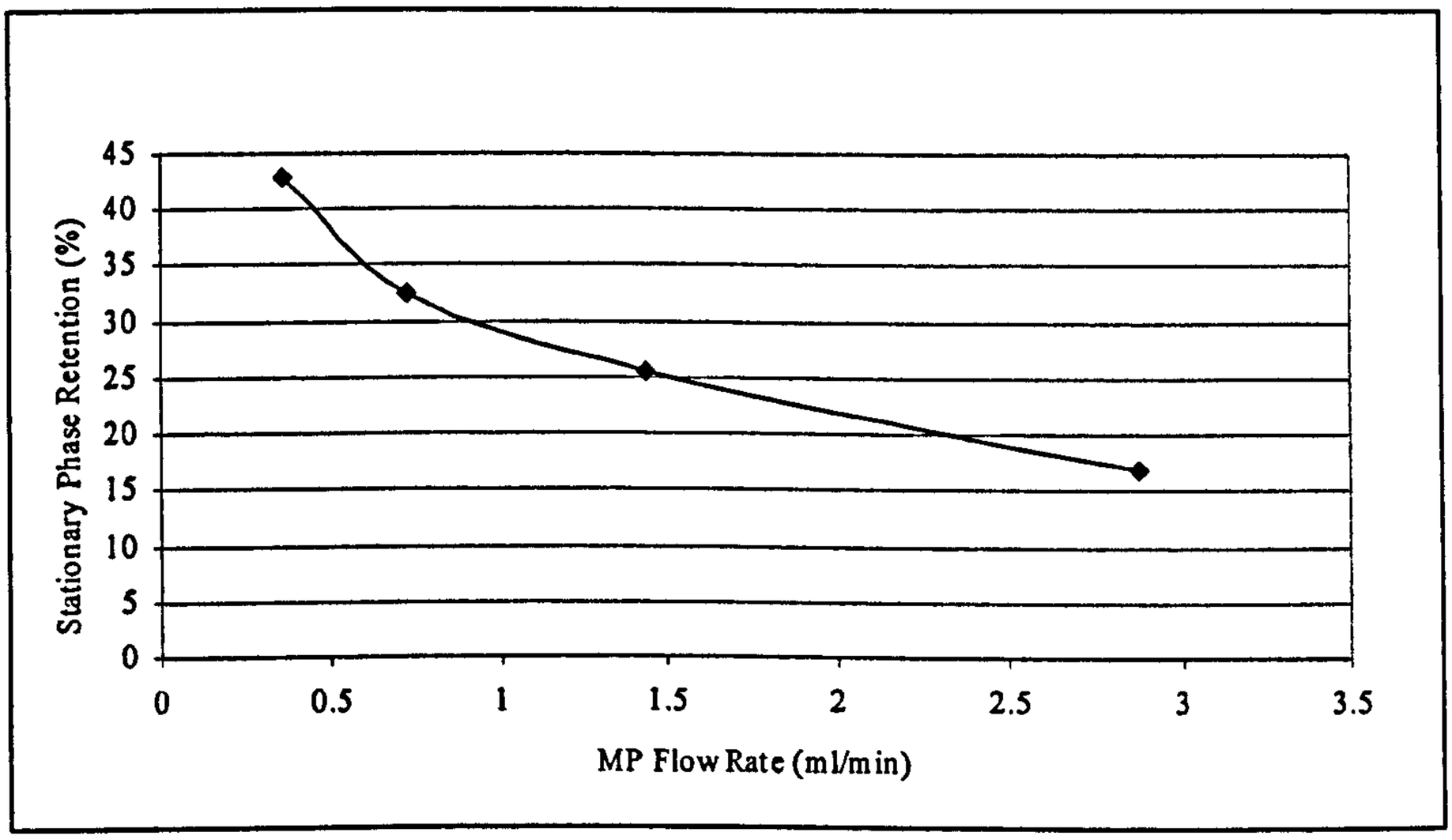

Figure 4.3.3a: Graph of stationary phase retention at the mobile phase breakthrough point at increasing mobile phase flow rates in the experiments using the 2.7 mm bore column for the separation of lysozyme and myoglobin.

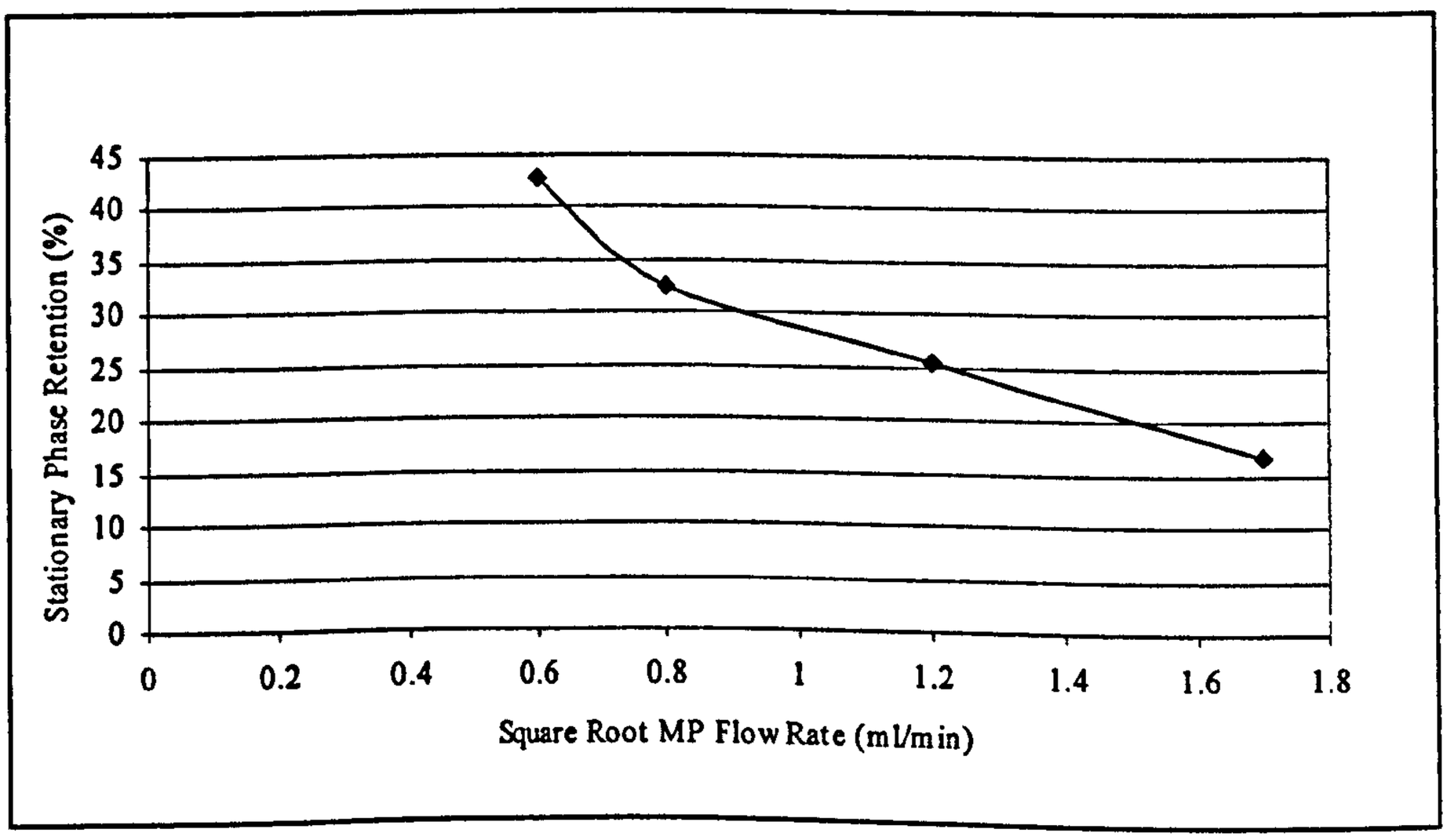

Figure 4.3.3b: Graph of stationary phase retention at the mobile phase breakthrough point against the square root of the mobile phase flow rates (Du plot) in the experiments using the 2.7 mm bore column for the separation of lysozyme and myoglobin.

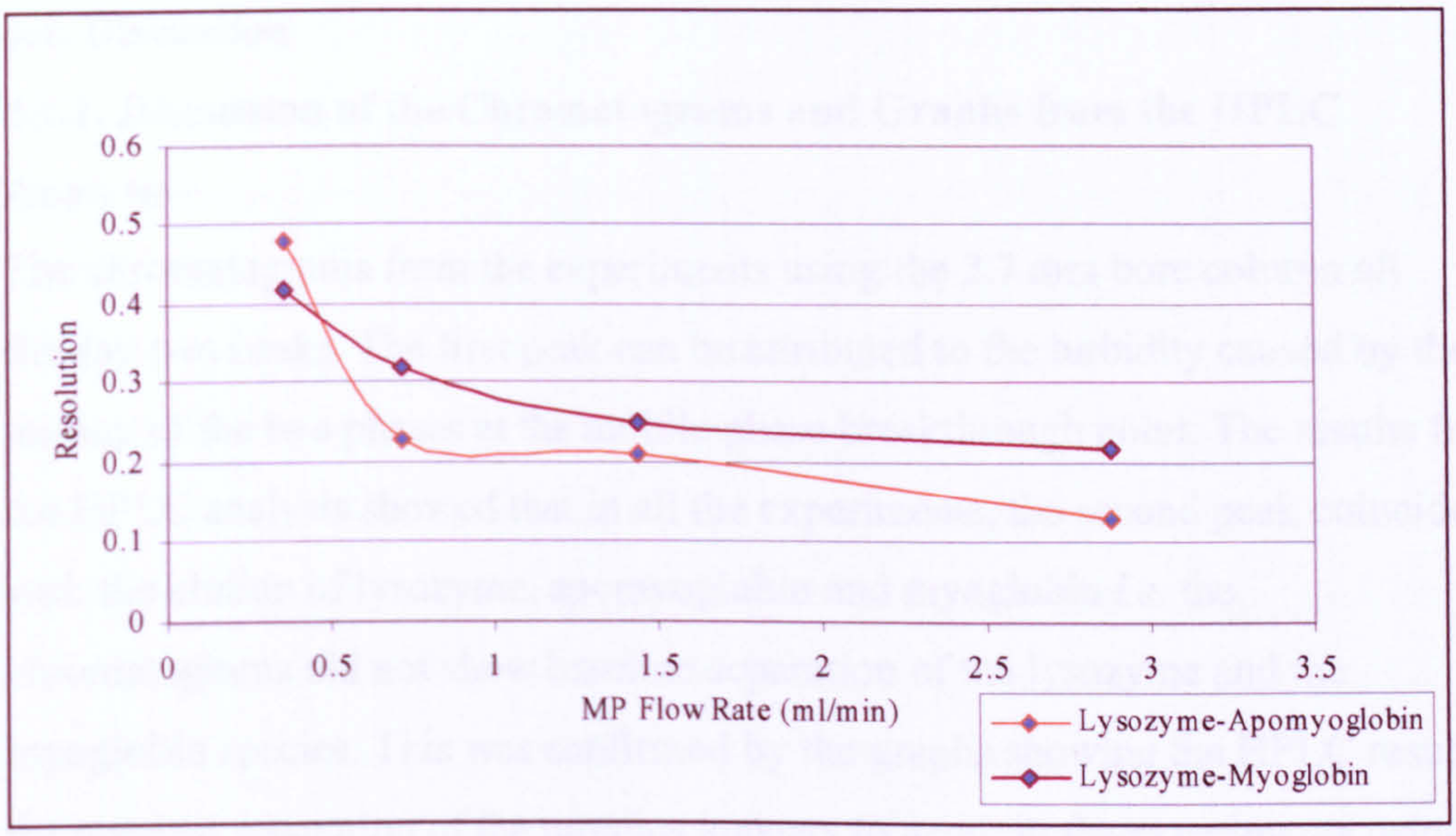

Figure 4.3.3c: Graph of protein resolution at increasing mobile phase flow rates in the experiments using the 2.7 mm bore column for the separation of lysozyme and myoglobin.

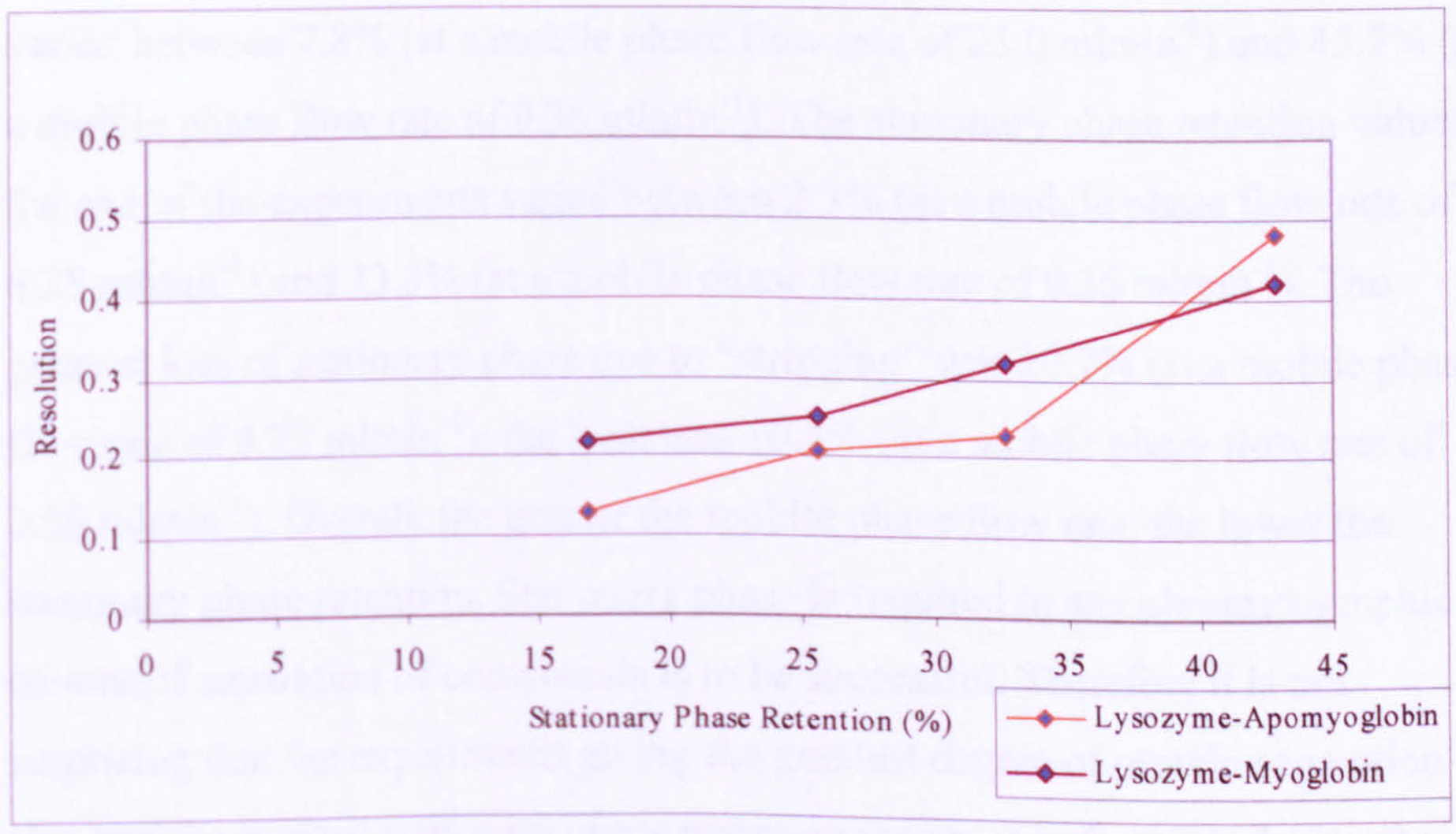

Figure 4.3.3d: Protein resolution at the stationary phase retention values obtained in the experiments using the 2.7 mm bore column for the separation of lysozyme and myoglobin.

4.4. Discussion

4.4.1. Discussion of the Chromatograms and Graphs from the HPLC Analysis

The chromatograms from the experiments using the 2.7 mm bore column all display two peaks. The first peak can be attributed to the turbidity caused by the mixing of the two phases at the mobile phase breakthrough point. The results from the HPLC analysis showed that in all the experiments, the second peak coincided with the elution of lysozyme, apomyoglobin and myoglobin *i.e.* the chromatograms did not show baseline separation of the lysozyme and the myoglobin species. This was confirmed by the graphs showing the HPLC results; the greatest separation of the proteins appears to occur in the experiments using a mobile phase flow rate of 0.36 $mlmin^{-1}$, which was the lowest flow rate used in these experiments.

4.4.2. Discussion of the Stationary Phase Retention and Protein Resolution Values

The stationary phase retention values at the mobile phase breakthrough point varied between 7.8% (at a mobile phase flow rate of 25.0 $mlmin^{-1}$) and 45.7% (at a mobile phase flow rate of 0.36 $mlmin^{-1}$). The stationary phase retention values at the end of the experiments varied between 2.3% (at a mobile phase flow rate of 6.25 $mlmin^{-1}$) and 33.3% (at a mobile phase flow rate of 0.36 $mlmin^{-1}$). The greatest loss of stationary phase due to "stripping" was 20.7% (at a mobile phase flow rate of 0.72 $mlmin^{-1}$); the least was 10.4% (at a mobile phase flow rate of 0.36 $mlmin^{-1}$). Overall, the greater the mobile phase flow rate, the lower the stationary phase retention. Stationary phase is required in any chromatographic column if separation of compounds is to be successful. Therefore it is not surprising that the experiments giving the greatest degree of protein separation also had the highest stationary phase retention values at both points during the experiment.

4.4.3. Discussion of the Protein Recovery Values

The percentage recovery of lysozyme, apomyoglobin and myoglobin in each experiment can be seen in Table 4.3.2a. In many cases, the percentage recovery of a protein exceeds 100%. This can be explained by considering how the HPLC

detector calculated the concentration of protein present in very small amounts in the fractions from the CCC experiment.

The detectors typically used with HPLC analysers will have an upper and lower limit of sensitivity. The lower limit occurs when the compound of interest is present at a certain (low) concentration. The detector will estimate what response should be reported; this will often be higher than the correct response for the quantity of compound actually present in the sample. Therefore, the HPLC should be used with caution when measuring very small quantities of a compound, and "detection limits" should be established. Detection limits are concentrations of a particular compound above and below which the detector response can no longer be taken as reliable.

If a sample has too low a concentration of the compound of interest, the sample can be concentrated down and the concentrate analysed instead.

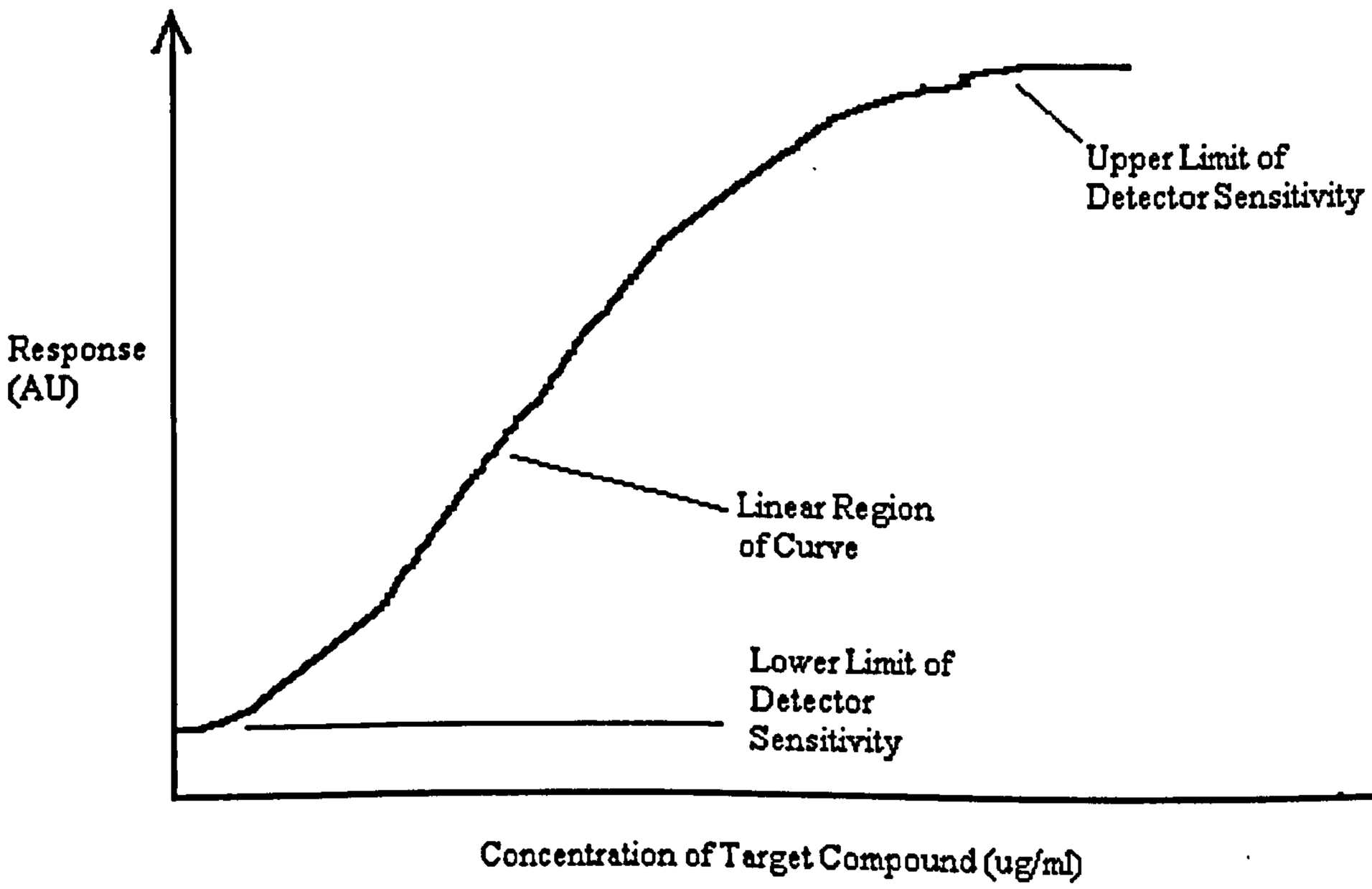

Figure 4.4.3a: Illustration of the location of detection limits on a graph of the concentration of a target compound against the response generated by the detector used to analyse the concentration of target compound in samples.

An Eppendorf "5301 Concentrator" (Eppendorf UK Limited, Histon, Cambridge, UK) was used in an attempt to concentrate the proteins present in the fractions from the CCC experiment. It was difficult to control the amount of liquid being

lost by each fraction in the concentrator, and the proteins had a tendency to precipitate. This method was deemed unsuccessful, and it was decided to proceed with analysis of the unadulterated fractions by HPLC. It was considered important to obtain a complete picture of how the proteins eluted from the CCC centrifuge, despite the knowledge that the very small concentrations of protein in each fraction would potentially lead to detection errors as explained above.

In addition, it is possible that the percentage recovery values for apomyoglobin and myoglobin in each experiment are affected by the particular structure of myoglobin. Myoglobin consists of a polypeptide chain bound to a haem group. Apomyoglobin is myoglobin in which the haem group has become detached. In six of the seven experiments detailed in Table 4.3.2a, the percentage recovery of myoglobin is less than that of apomyoglobin in the same experiment. It is possible that the CCC process has caused degradation of the myoglobin to apomyoglobin in these experiments; this would account for the difference in the percentage recovery values between the two types of myoglobin.

In those experiments where the percentage recovery is less than 100%, it is possible that the proteins have adhered to the internal surfaces of the system. If this was suspected, the system was cleaned with a 0.5 M sodium hydroxide solution, and rinsed several times with distilled water before further use.

4.4.4. Discussion on the Protein Resolution Values

The greatest separation of lysozyme and the myoglobin species was achieved in the experiments using a mobile phase flow rate of 0.36 $mlmin^{-1}$; the least separation occurred in the experiment with a mobile phase flow rate of 25.0 $mlmin^{-1}$. It would appear that in these experiments, the slower the mobile phase flow rate, the greater the protein resolution. The resolution values achieved were less than one – third of those indicating complete or baseline separation; however a stationary phase retention of 45.7% (at a mobile phase flow rate of 0.36 $mlmin^{-1}$) would most probably be insufficient to obtain complete separation, even if the proteins had exhibited their predicted retention times.

4.5. Conclusions

It was found that optimum conditions for separation of lysozyme and myoglobin using a 12.5 % w/w PEG-1000: 12.5% dipotassium hydrogen phosphate ATPS and a J – type CCC centrifuge were: 2.7 mm bore column fitted to the MILLI #1 centrifuge; rotational speed 1800 rpm; mobile phase flow rate 0.36 $mlmin^{-1}$; loading sample volume 2.32 ml (5.0% of the column volume) loaded onto a pre – equilibrated column.

The mobile phase flow rate was a definitive factor in the magnitude of protein separation, whereas increasing the bore size of the column appeared to have no positive effect on resolution. However, it was of concern that the mobile phase flow rate of 0.36 $mlmin^{-1}$ in a 2.7 mm bore column would be too slow to provide a viable commercial separation procedure.

Therefore, it can be concluded that under these experimental conditions using this design of column on the J – type CCC centrifuge, the complete separation of lysozyme and myoglobin is not achievable.

It was thought that the problems encountered when using the J – type CCC centrifuge for protein resolution (the incomplete partition of proteins between the phases and the poor stationary phase retention) may be overcome by using a centrifuge that operated on the principles of centrifugal partition chromatography; this work is addressed in the next chapter.

Chapter 5 – Separation of the Proteins Lysozyme and Myoglobin using a CPC Centrifuge

5.1. Introduction

The separation of lysozyme and myoglobin using the Brunel/DE J – type CCC centrifuges was only partially successful (refer to Chapter 4). The incomplete separation of these proteins was thought to be caused largely by the poor mixing of the two phases within these columns, rather than inadequate stationary phase retention. This was because the proteins eluted closer to the $K = 1$ point than at their predicted elution points, and the volume of stationary phase retained in the columns was sufficient to enable separation to take place.

The model system used for the J – type centrifuge experiments was applied to the CPC centrifuge. It was considered that the more vigorous cascade mixing typical of the CPC process might overcome the problem with mass transfer of the proteins. Therefore, retaining the same model system allowed a direct comparison to be made between the performance of the J – type centrifuge and the CPC centrifuge.

The design and operation of the CPC centrifuge and ancillary equipment has been described previously in Section 2.4. In this chapter, the influence of various experimental parameters, namely mobile phase flow rate, rotational speed, operational mode (ascending or descending), injection method, and loading sample volume on the resolution of lysozyme and myoglobin in the CPC are described. Once the optimal experimental conditions had been determined, the aim was to perform the same experiment on the pilot scale CPC centrifuge, and compare the performance of the two instruments.

Experiments in this chapter were not repeated. Replicates were not undertaken because the aim of the experiments was to indentify *trends* in the operating parameters, rather than obtain absolute values for each parameter. That these separations were reasonably robust can be judged by the observation that the optimal operating conditions identified on the 1 litre centrifuge and used in the scale – up experiments on the 12.5 litre pilot scale centrifuge produced protein resolution as predicted from the smaller scale study.

5.2. Materials and Methods

5.2.1. Preparation of the Aqueous Two – Phase System

The phase system used in these experiments was the 12.5% w/w PEG-1000: 12.5% w/w K_2HPO_4 ATPS. 4000 g quantities were prepared as required following the procedure in Section 2.2.1.

5.2.2. Preparation of the Lysozyme and Myoglobin Loading Samples

Lysozyme and myoglobin loading samples were prepared as in Section 2.5.1. The sample loop volumes used in the CPC study were: 8.0 ml (1.86% CV {column volume}); 21.5 ml (5.0% CV); 43.0 ml (10.0% CV); 86.0 ml (20.0% CV). For each experiment, sufficient loading sample was prepared to completely fill the sample loop used, and some of the loading sample was reserved for use in the HPLC analysis of the CPC fractions.

5.2.3. Separation of Lysozyme and Myoglobin using the CPC Centrifuge

The protocol for the operation of the CPC centrifuge has been described in Section 2.4.5.

The column used was rotor number 1, total capacity 500 ml, of which 429 ml was the total cell volume and 71 ml was the total volume of the interconnecting ducts. The external dead volume was 1 ml, which was taken to be negligible.

The mobile phase flow rate used was either 5.0 $mlmin^{-1}$ or 10.0 $mlmin^{-1}$, and the rotational speed of the centrifuge was 1000 rpm, 2000 rpm or 3000 rpm. The centrifuge was used in either descending mode (with lower phase as the mobile phase), or in ascending mode (with upper phase as the mobile phase).

The eluent from the column passed through the UV detector, which was set at wavelength 280 nm. The signal produced was analysed using Windows "Excel" software, producing a chromatogram that was later annotated to indicate the position of critical time points during the experiment.

Fractions were collected every minute in graduated 15 ml centrifuge tubes to allow accurate calculation of stationary phase retention and rate of loss of stationary phase from the column (stationary phase "stripping").

5.2.4. Stationary Phase Retention

Stationary phase retention (*Sf*) in the column was calculated at three time points for each experiment: at the mobile phase breakthrough point, at the equilibrium point, and at the end of the experiment.

The total volume of the column was divided into the volume occupied by the cells (the active part of the column where separation takes place) and the ducts that connect the cells (it is assumed that the ducts are full of mobile phase during each experiment, and were inactive as far as the separation process was concerned). The ducts would have contained stationary phase at the start of the experiment, the volume of which must be deducted from the volume of eluted stationary phase at the mobile phase breakthrough point. The total cell volume is known and therefore the volume of stationary phase retained in the cells at a particular time point can be calculated. This value is used to give the stationary phase retention at that time point as a percentage of the total "active" volume of the column.

The following calculations were carried out for each experiment. Table 5.2.4a gives the meaning of each notation in the equations.

$$V_{\text{SP FROM CELLS AT MP B/P}} = V_{\text{SP FROM SYSTEM AT MP B/P}} - V_{\text{D}} \quad \text{[Equation 5.2.4a]}$$

$$V_{\text{SP RETAINED IN CELLS AT MP B/P}} = V_{\text{C}} - V_{\text{SP FROM CELLS AT MP B/P}} \quad \text{[Equation 5.2.4b]}$$

$$Sf_{\text{MP B/P}}\,(\%) = (V_{\text{SP RETAINED IN CELLS AT MP B/P}}/V_{\text{C}}) \times 100 \quad \text{[Equation 5.2.4c]}$$

$$V_{\text{SP FROM CELLS AT E/P}} = V_{\text{SP FROM SYSTEM AT E/P}} - V_{\text{D}} \quad \text{[Equation 5.2.4d]}$$

$$V_{\text{SP RETAINED IN CELLS AT E/P}} = V_{\text{C}} - V_{\text{SP FROM CELLS AT E/P}} \quad \text{[Equation 5.2.4e]}$$

$$Sf_{\text{E/P}}\,(\%) = (V_{\text{SP RETAINED IN CELLS AT E/P}}/V_{\text{C}}) \times 100 \quad \text{[Equation 5.2.4f]}$$

$$V_{\text{SP FROM CELLS AT E/E}} = V_{\text{SP FROM SYSTEM AT E/E}} - V_{\text{D}} \quad \text{[Equation 5.2.4g]}$$

$$V_{\text{SP RETAINED IN CELLS AT E/E}} = V_{\text{C}} - V_{\text{SP FROM CELLS AT E/E}} \quad \text{[Equation 5.2.4h]}$$

$$Sf_{\text{E/E}}\,(\%) = (V_{\text{SP RETAINED IN CELLS AT E/E}}/V_{\text{C}}) \times 100 \quad \text{[Equation 5.2.4i]}$$

Table 5.2.4a: Meaning of notations used in equations to calculate stationary phase retention values.

Notation used in Equation	Meaning of Notation
V_C	Total volume of cells
V_D	Total volume of the interconnecting ducts ≡ Dead volume of system
$V_{SP\ FROM\ CELLS\ AT\ MP\ B/P}$	Volume stationary phase displaced from the cells at the mobile phase breakthrough point
$V_{SP\ FROM\ SYSTEM\ AT\ MP\ B/P}$	Volume stationary phase that eluted from the whole system at the mobile phase breakthrough point
$V_{SP\ RETAINED\ IN\ CELLS\ AT\ MP\ B/P}$	Volume stationary phase retained in the cells at the mobile phase breakthrough point
$Sf_{MP\ B/P}$ (%)	Percentage stationary phase retention in the cells at the mobile phase breakthrough point
$V_{SP\ FROM\ CELLS\ AT\ E/P}$	Volume stationary phase displaced from the cells at the equilibrium point
$V_{SP\ FROM\ SYSTEM\ AT\ E/P}$	Volume stationary phase that eluted from the whole system at the equilibrium point
$V_{SP\ RETAINED\ IN\ CELLS\ AT\ E/P}$	Volume stationary phase retained in the cells at the equilibrium point
$Sf_{E/P}$ (%)	Percentage stationary phase retention in the column at the equilibrium point
$V_{SP\ FROM\ CELLS\ AT\ E/E}$	Total volume stationary phase displaced from the cells at the end of the experiment
$V_{SP\ FROM\ SYSTEM\ AT\ E/E}$	Volume stationary phase that eluted from the whole system at the end of the experiment
$V_{SP\ RETAINED\ IN\ CELLS\ AT\ E/E}$	Volume stationary phase retained in the cells at the end of the experiment
$Sf_{E/E}$ (%)	Percentage stationary phase retention in the cells at the end of the experiment

5.3. Results

5.3.1. Chromatograms and Graphs from HPLC Analysis

The chromatogram created from the detector signal in each experiment has been annotated to indicate the position of critical time points during the experiment. The results from the HPLC analysis of the fractions have been plotted to show how the lysozyme and myoglobin eluted over the time course of the experiment, and have been annotated with the predicted elution times of the proteins.

The on – line and HPLC chromatograms from the experiment which gave the highest resolution between lysozyme and the myoglobin species are shown in Figures 5.3.1a and 5.3.1b. The on – line and HPLC chromatograms from this and all the other experiments are shown in Appendix 2.

In this experiment:

- The mobile phase flow rate was 5.0 $mlmin^{-1}$.
- The recording of data commenced at time zero.
- The mobile phase breakthrough point caused mixing of the two phases in the eluent that appears as a peak on the chromatogram (the operator also observed at this point drops of mobile phase eluting from the column together with the stationary phase).
- Fraction collected commenced simultaneously with sample injection, and continued until the end of the experiment.

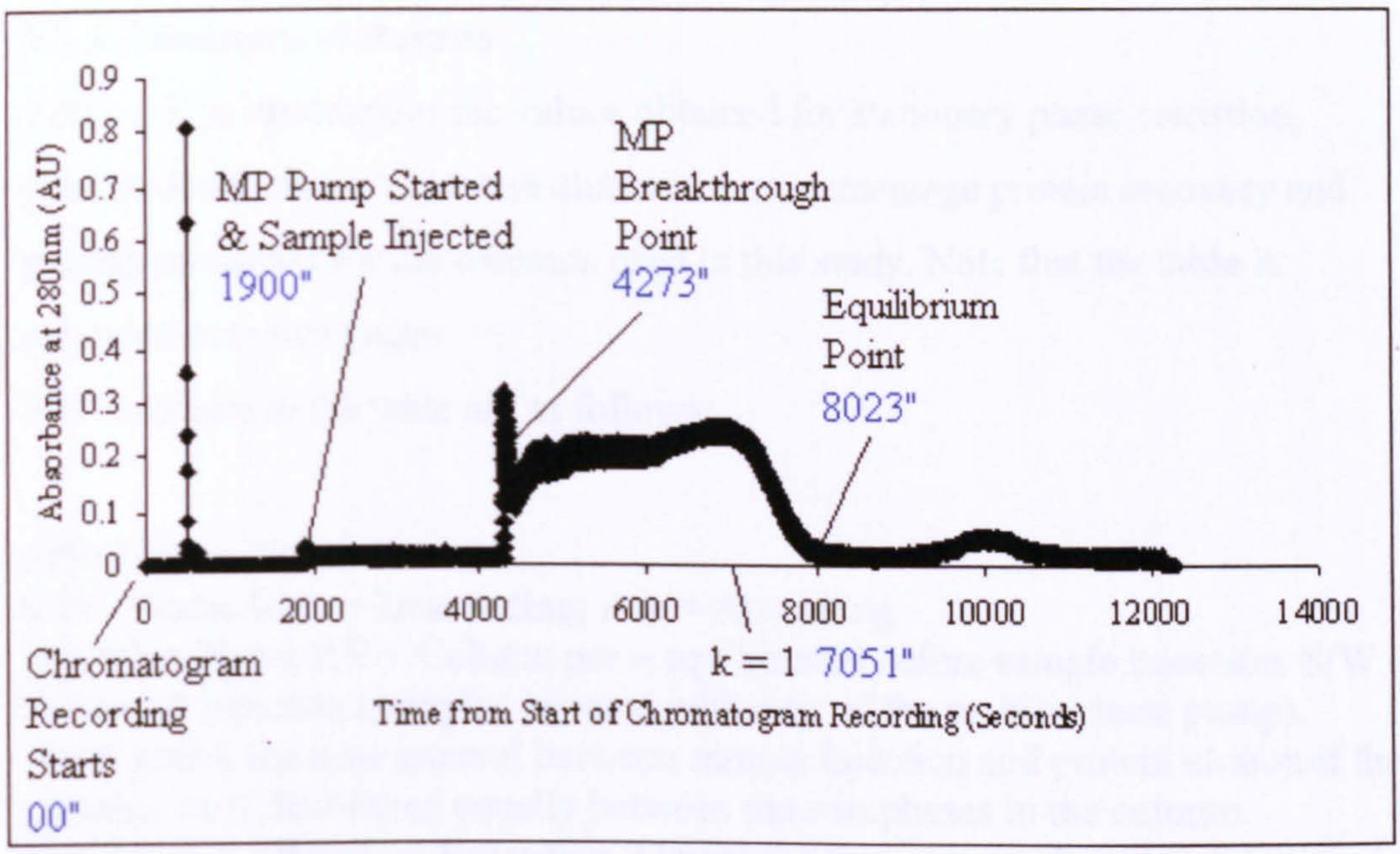

Figure 5.3.1a: Chromatogram from the experiment to determine the influence of decreasing the MP flow rate to 5.0 $mlmin^{-1}$. The experimental parameters were: rotational speed 2000 rpm; LP was the MP (descending mode); sandwich injection; sample volume was 8.0 ml (1.86% CV). The MP flow rate was 5.0 $mlmin^{-1}$.

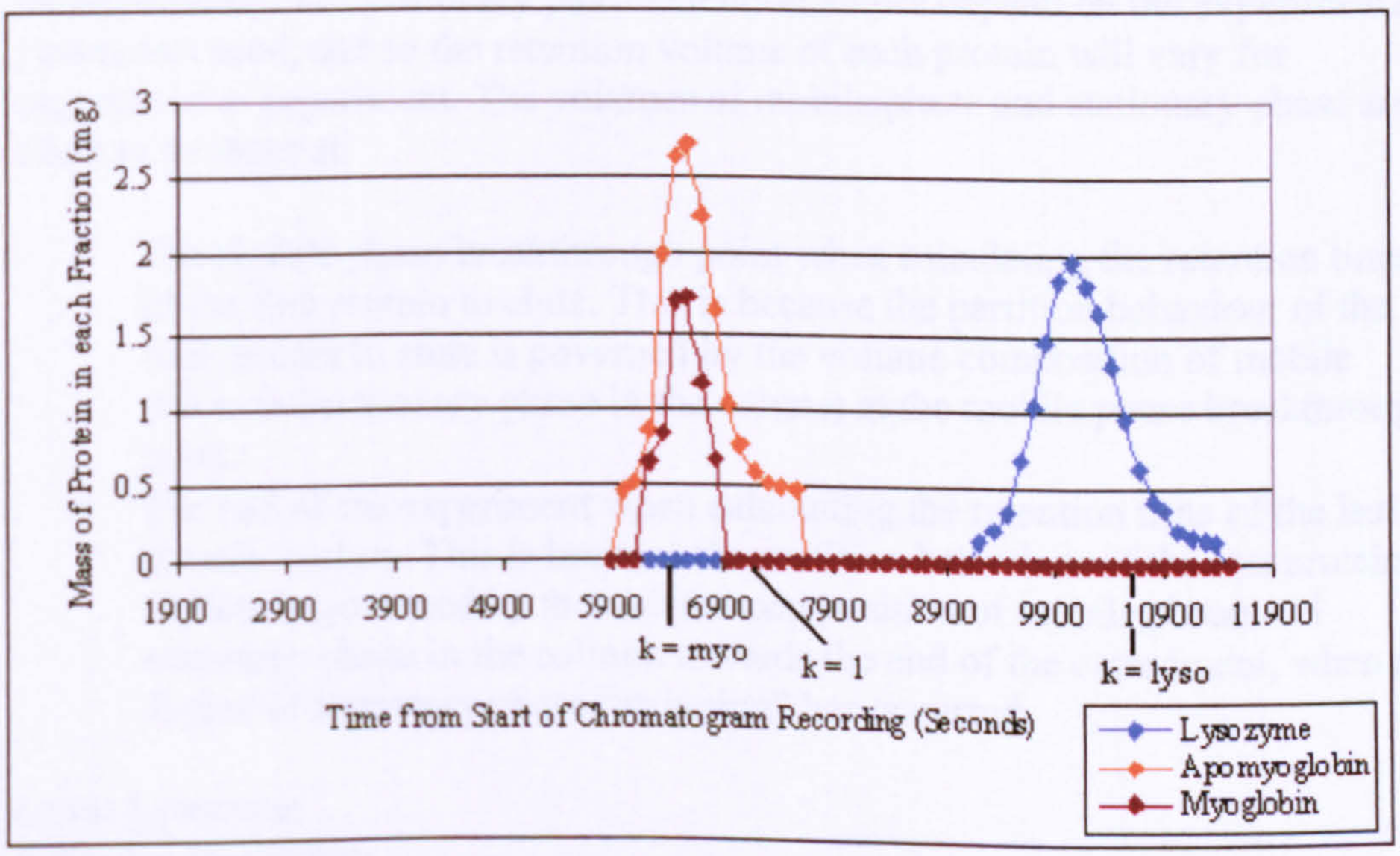

Figure 5.3.1b: Chromatogram created from HPLC analysis of fractions from the experiment to determine the influence of decreasing the MP flow rate to 5.0 $mlmin^{-1}$. The experimental parameters were: rotational speed 2000 rpm; LP was the MP (descending mode); sandwich injection; sample volume was 8.0 ml (1.86% CV). The MP flow rate was 5.0 $mlmin^{-1}$.

5.3.2. Summary of Results

Table 5.3.2a summarises the values obtained for stationary phase retention, predicted and observed protein elution times, percentage protein recovery and protein resolution for the columns used in this study. Note that the table is extended over two pages.

The footnotes to the table are as follows:

MP: Mobile Phase
CPC Mode: Desc = Descending; Asc = Ascending
Injection Type: P/E = Column pre – equilibrated before sample injection. S/W = Sandwich injection (samples injected with start of the mobile phase pump).
***K* = 1 point:** the time interval between sample injection and protein elution if the proteins were distributed equally between the two phases in the column.
Predicted & Observed Retention Times: the time interval between sample injection and the peak of protein elution, using the distribution ratios of the proteins.
Predicted and observed retention times are calculated or reported with the sample injection time taken as time zero.
The predicted retention time of each protein is first calculated as the predicted retention volume. This depends on what volume of stationary phase has been retained in the column as the proteins enter it, and what this value is at the end of the experiment. The stationary phase retention values depend on the experimental parameters used, and so the retention volume of each protein will vary for experiment to experiment. The volumes of mobile phase and stationary phase are taken to be those at:

- The mobile phase breakthrough point when calculating the retention time of the first protein to elute. This is because the partition behaviour of the first protein to elute is governed by the volume composition of mobile phase and stationary phase in the column at the mobile phase breakthrough point.
- The end of the experiment when calculating the retention time of the last protein to elute. This is because the partition behaviour of the last protein to elute is governed by the volume composition of mobile phase and stationary phase in the column towards the end of the experiment, when a degree of stationary phase "stripping" has occurred.

Lyso: Lysozyme
Apo: Apomyoglobin
Myo: Myoglobin
$Sf_{MP\ B/P}$ **(%):** Percentage stationary phase retention in the column cells at the mobile phase breakthrough point.
$Sf_{E/P}$ **(%):** Percentage stationary phase retention in the column cells at the equilibrium point.
$Sf_{E/E}$ **(%):** Percentage stationary phase retention in the column cells at the end of the experiment.

The difference in the stationary phase retention value at the end of the experiment from the stationary phase retention value at the mobile phase breakthrough point gave an indication of how much stationary phase was lost to "stripping" between the mobile phase breakthrough point and the end of the experiment.
N/C: Data not collected.
Recovery (of Proteins) (%): Data shown is from HPLC results that include those fractions where the value for the mass of each protein is above or below the detector limit.

Table 5.3.2a: Summary of the values obtained for stationary phase retention, predicted and observed protein elution times, percentage protein recovery and protein resolution from the CPC study. Fixed parameters in all experiments were as follows: Phase system 12.5% w/w PEG-1000: 12.5% w/w K_2HPO_4 ATPS.

MP & CPC Mode	MP Flow Rate ($mlmin^{-1}$)	Rotational Speed (rpm)	Injection Type & Loading Sample Volume (ml) (%CV)	$K = 1$ (sec)	Predicted Retention Time Myo/Apo (sec)	Observed Retention Time Myo/Apo (sec)	Predicted Retention Time Lyso (sec)	Observed Retention Time Lyso (sec)	$Sf_{MP\ B/P}$ (%)	$Sf_{E/P}$ (%)	$Sf_{E/E}$ (%)
LP Desc	5	2000	P/E 8.0 ml 1.86%	5148	4561	4570	8076	7150	69.9	44.8	N/C
UP Asc	10	2000	S/W 8.0 ml 1.86%	2574	3584	3540	2481	2760	40.3	33.8	32.4
UP Asc	10	2000	S/W 8.0 ml 1.86%	2574	3328	3240	2685	2880	24.5	18.6	18.2
LP Desc	10	2000	S/W 8.0 ml 1.86%	2574	2371	2460	4415	3600	61.1	N/C	N/C
LP Desc	5	2000	S/W 8.0 ml 1.86%	5148	4493	4680	8729	8160	73.2	N/C	58.9
LP Desc	10	1000	S/W 8.0 ml 1.86%	2574	2549	2760	3271	3240	43.8	14.7	11.7
LP Desc	10	3000	S/W 8.0 ml 1.86%	2574	2513	2460	3746	3180	47.3	35.2	32.2
LP Desc	10	2000	S/W 21.5 ml 5.0%	2574	2455	2640	3303	3360	52.9	15.2	13.1
LP Desc	10	2000	S/W 43.0 ml 10.0%	2574	2410	2520	3524	3480	57.3	25.9	22.6
LP Desc	10	2000	S/W 86.0 ml 20.0%	2574	2470	3180	3114	3240	51.5	4.9	4.9

Table 5.3.2a: Continued

MP & CPC Mode	MP Flow Rate ($mlmin^{-1}$)	Rotational Speed (rpm)	Injection Type & Loading Sample Volume (ml) (%CV)	Resolution Apo/Lyso	Resolution Myo/Lyso	Recovery Apomyoglobin (%)	Recovery Myoglobin (%)	Recovery Lysozyme (%)
LP Desc	5	2000	P/E 8.0 ml 1.86%	1.83	1.98	108	101	131
UP Asc	10	2000	S/W 8.0 ml 1.86%	1.21	1.20	138	123	81
UP Asc	10	2000	S/W 8.0 ml 1.86%	0.63	0.70	117	43	137
LP Desc	10	2000	S/W 8.0 ml 1.86%	1.95	1.88	115	163	109
LP Desc	5	2000	S/W 8.0 ml 1.86%	2.90	3.25	149	60	62
LP Desc	10	1000	S/W 8.0 ml 1.86%	0.72	0.79	148	101	110
LP Desc	10	3000	S/W 8.0 ml 1.86%	1.49	1.61	160	126	124
LP Desc	10	2000	S/W 21.5 ml 5.0%	1.13	1.23	132	108	95
LP Desc	10	2000	S/W 43.0 ml 10.0%	1.21	1.29	90	67	102
LP Desc	10	2000	S/W 86.0 ml 20.0%	0.08	0.09	195	89	342

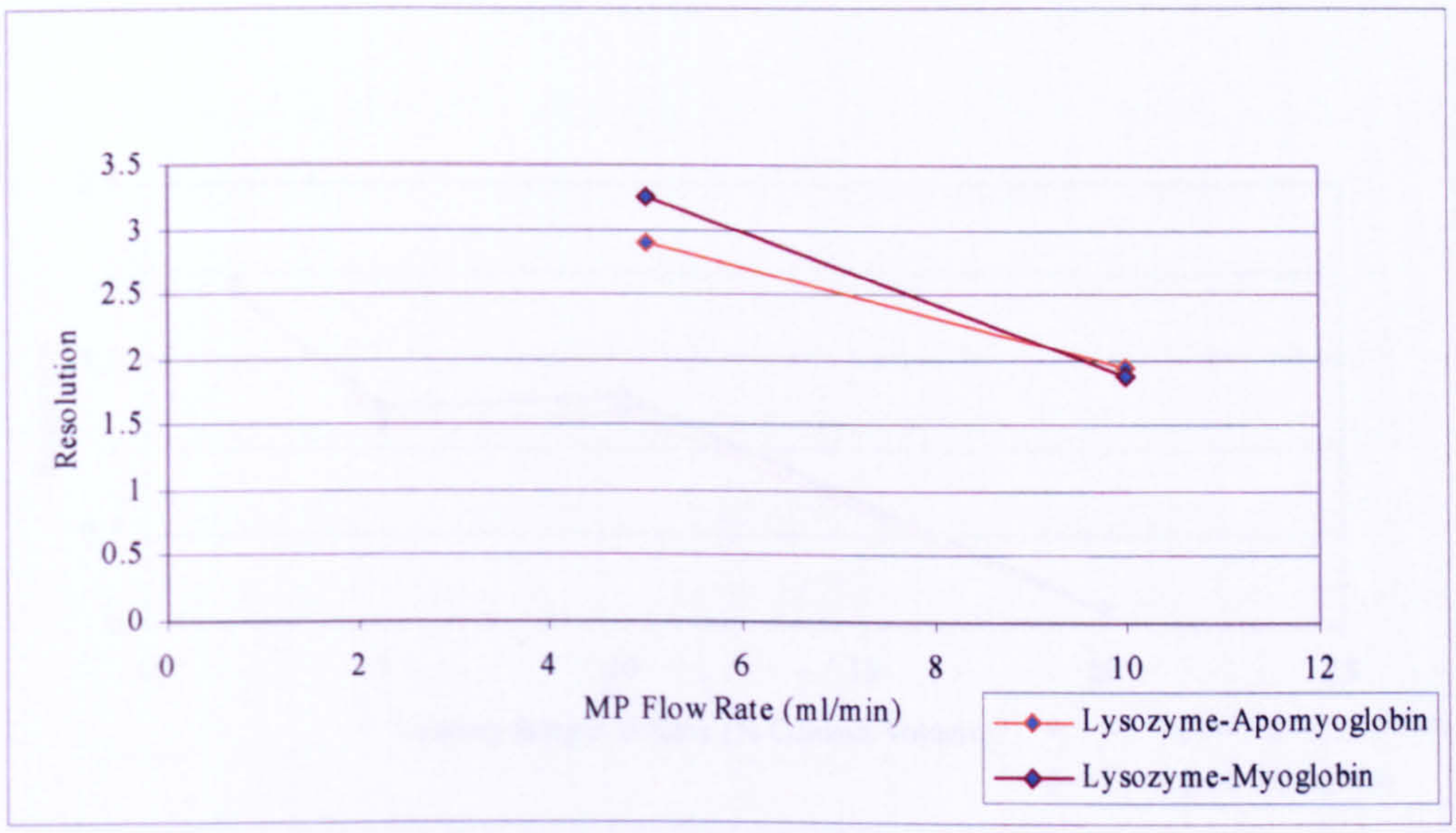

Figure 5.3.2a: Graph of protein resolution at increasing mobile phase flow rates in the 500 ml column of the CPC centrifuge. The experimental parameters were: rotational speed 2000 rpm; LP was the MP (descending mode); sandwich injection; loading sample volume was 8.0 ml (1.86% CV).

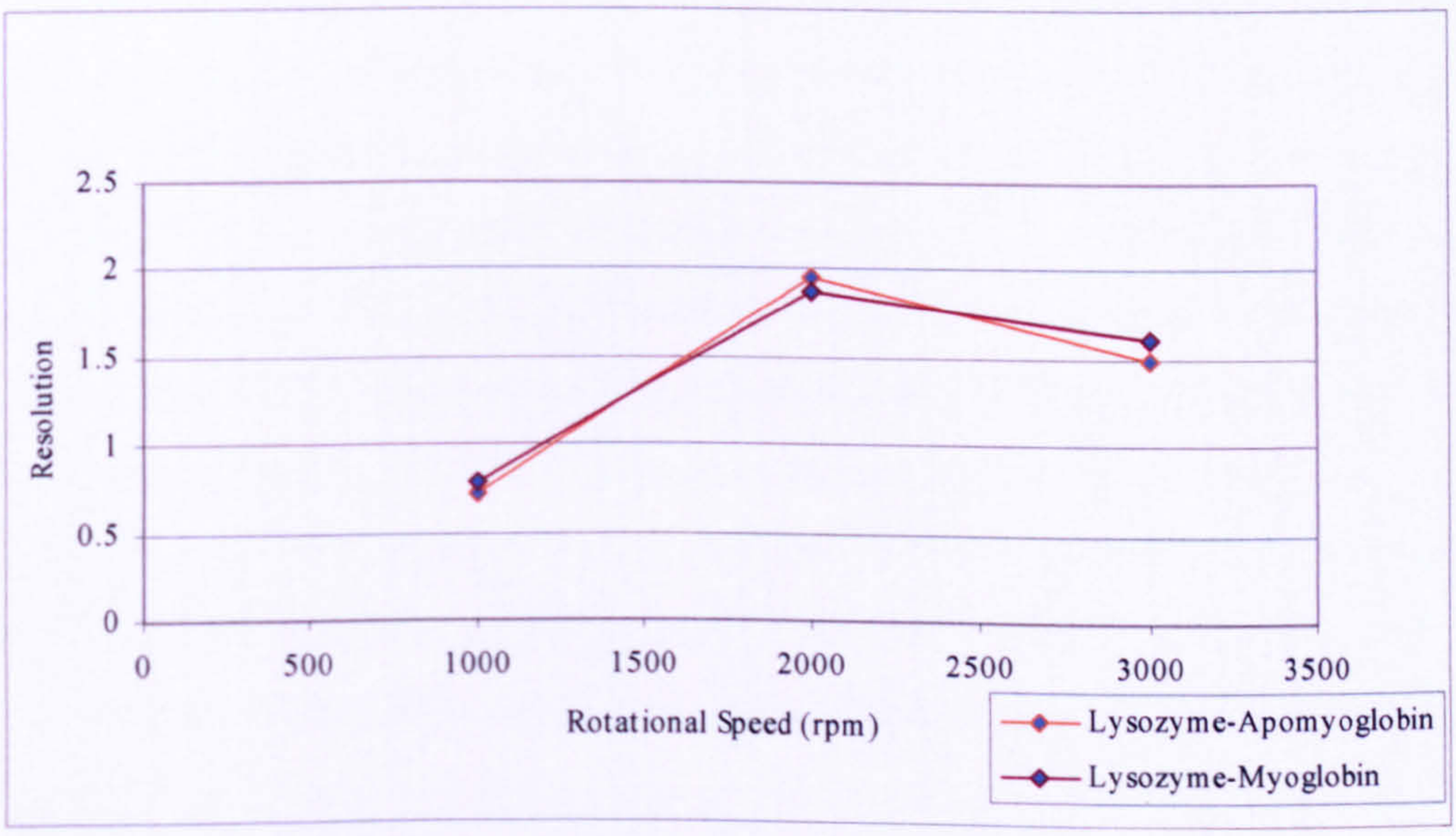

Figure 5.3.2b: Graph of protein resolution at increasing rotational speed in the 500 ml column of the CPC centrifuge. The experimental parameters were: MP flow rate 10.0 mlmin^{-1}; LP was the MP (descending mode); sandwich injection; loading sample volume was 8.0 ml (1.86% CV).

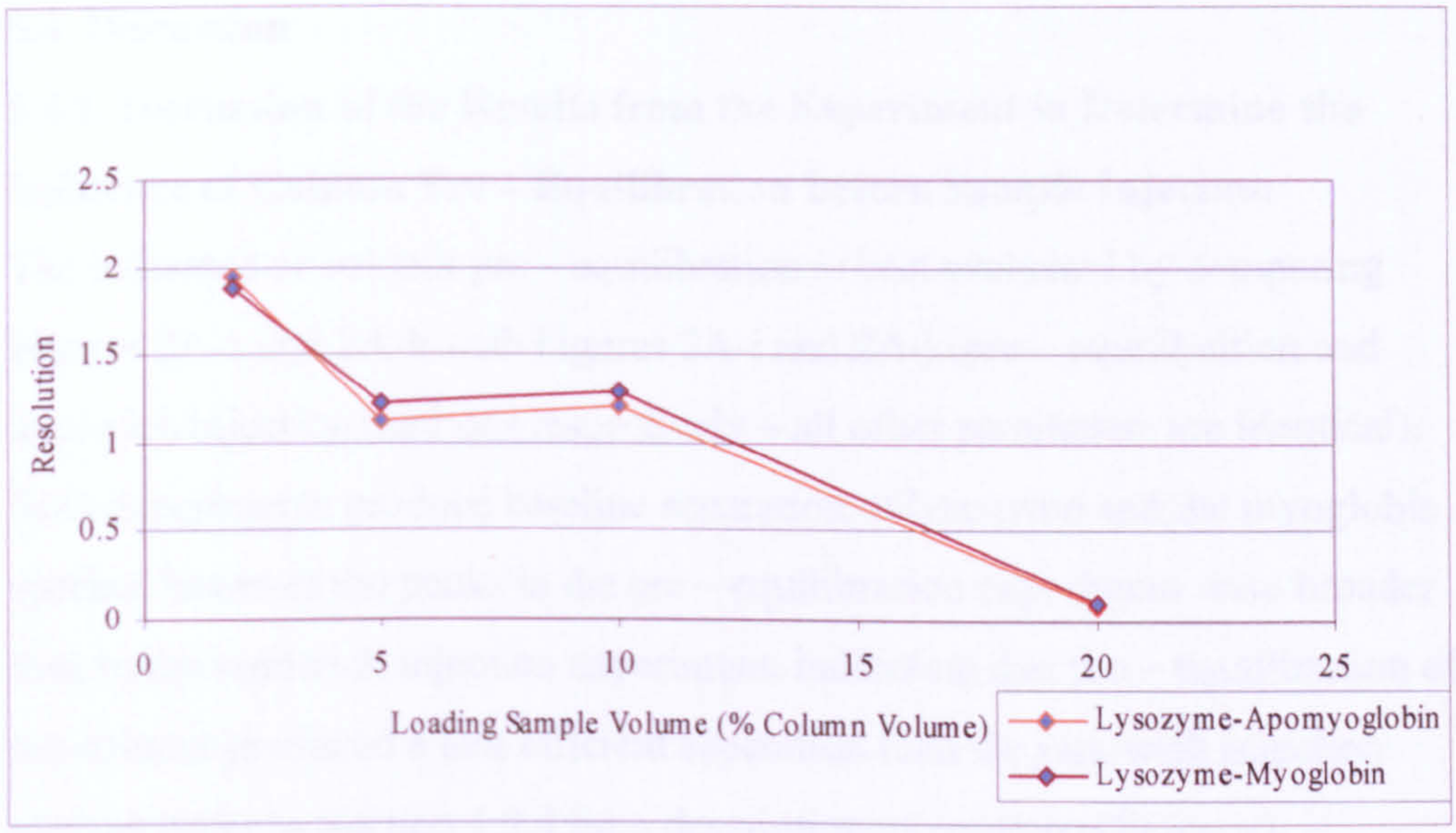

Figure 5.3.2c: Graph of protein resolution at increasing loading sample volumes in the 500 ml column of the CPC centrifuge. The experimental parameters were: MP flow rate 10.0 $mlmin^{-1}$; rotational speed 2000 rpm; LP was the MP (descending mode); sandwich injection.

5.4. Discussion

5.4.1. Discussion of the Results from the Experiment to Determine the Influence of Column Pre – Equilibration before Sample Injection

The influence of column pre – equilibration is best evaluated by comparing Figures 2A-a and 2A-b with Figures 2A-i and 2A-j (pre – equilibration and sandwich injection methods respectively – all other parameters are identical). Both experiments produce baseline separation of lysozyme and the myoglobin species, however the peaks in the pre – equilibration experiment were broader than in the sandwich injection experiment, indicating that pre – equilibration of the column produced a less efficient separation than the sandwich injection method (refer to Section 1.2.4 for a description of column efficiency). Furthermore, Table 5.3.2a shows that resolution of lysozyme/apomyoglobin and lysozyme/myoglobin is much greater in the sandwich injection method. It is likely that the sandwich injection method is more efficient and produces better resolution because protein separation occurs when there is a reasonable volume of stationary phase in the column. Allowing the column to equilibrate and then injecting the sample means that there has been considerable loss of stationary phase and so the protein separation occurs in a column with a depleted volume of stationary phase. Therefore, the sandwich injection method gives better protein separation than the column pre – equilibration method. It has the additional advantage of decreasing the time taken in performing the experiment (the sandwich injection experiment took 3 hours 12 minutes to complete, as opposed to 4 hours 22 minutes for the pre – equilibration experiment). In the sandwich injection method experiment, the sample is already separating as the column is undergoing the equilibration process, so the experiment takes less time than if the pre – equilibration method is used.

5.4.2. Discussion of the Results from the Experiments to Determine the Influence of the Centrifuge Operation Mode

The centrifuge can be operated either in ascending mode (with the upper phase as the mobile phase) or in descending mode (with the lower phase as the mobile phase).

The experiment in ascending mode was performed in duplicate (Figures 2A-c to 2A-f). The experiment shown in Figures 2A-c and 2A-d had the largest stationary

phase retention values of the two, and also the greatest resolution values between the proteins; these factors are connected because a reasonable quantity of stationary phase in the column is necessary to allow protein separation to take place. The second experiment (Figures 2A-e and 2A-f) had resolution values almost half of the first experiment, almost certainly due to the lower stationary phase retention in this experiment. The variation in the results from these two experiments indicates that this operation mode is quite unstable. This may in part be due to this centrifuge lacking any mechanism of temperature control. The composition of aqueous two – phase systems, and hence their interfacial tension values, is temperature – dependent. The phase system used in these experiments is very close to the critical point in the phase diagram, and so only a small temperature increase is required to cause a decrease in interfacial tension. This will lead to more emulsification of the phases in the column, resulting in lower stationary phase retention, increased stationary phase "stripping", and lower protein resolution.

The one comparable experiment that was conducted in descending mode (Figures 2A-g and 2A-h) produced larger stationary phase retention and resolution than those conducted in ascending mode. Descending mode uses the upper phase as the stationary phase. The highly – viscous nature of this phase allows it to be retained within the column much more readily than the less viscous lower phase. Therefore, for protein separation, descending mode is the preferred operating mode of the CPC centrifuge.

5.4.3. Discussion of the Results from the Experiment to Determine the Influence of Decreasing the Mobile Phase Flow Rate

All experiments were conducted at a mobile phase flow rate of 10.0 $mlmin^{-1}$, except for those shown Figures 2A-a & 2A-b and Figures 2A-i & 2A-j, which were conducted at a flow rate of 5.0 $mlmin^{-1}$. The column was pre – equilibrated in the first of these experiments, and there is no comparable experiment at the faster flow rate. Comparing the results of the experiment shown Figures 2A-i and 2A-j with those of the experiment shown in Figures 2A-g and 2A-h (which has identical experimental parameters except for a flow rate of 10.0 $mlmin^{-1}$), the slower flow rate produces the larger stationary phase retention and better protein resolution values. Therefore, it can be concluded that the slower the mobile phase

flow rate, the better the separation of the proteins. The experiment conducted at a flow rate of 10.0 $mlmin^{-1}$ produced an entirely satisfactory protein separation. A slower flow rate increases the time taken for the separation to occur; therefore a flow rate of 10.0 $mlmin^{-1}$ is deemed satisfactory both in terms of protein resolution and time efficiency.

5.4.4. Discussion of the Results from the Experiments to Determine the Influence of Centrifuge Rotational Speed

The experiments were conducted at three different rotational speeds: 1000 rpm (Figures 2A-k and 2A-l); 2000 rpm (Figures 2A-g and 2A-h); and 3000 rpm (Figures 2A-m and 2A-n). A rotational speed of 2000 rpm produced the greatest stationary phase retention and the greatest protein resolution; 3000 rpm also produced a baseline separation. The experiment at 1000 rpm produced an incomplete separation.

Therefore, 2000 rpm appears to be the optimum rotational speed for protein separation.

The effect of mobile phase flow rate and centrifuge rotational speed have been observed experimentally for aqueous – organic phase systems in CPC centrifuges (Foucault *et al*, 1992a; Foucault *et al*, 1992b). For a given phase system, droplet velocity is dictated by droplet size (refer to Section 1.3.6). If rotational speed and mobile phase flow rate are both increased, droplet size decreases but droplet number increases. This increases the interfacial area between the two phases in the centrifuge, leading to higher column efficiency and separation of components. However, an increase in droplet number created by increasing the mobile phase flow rate decreases the volume in the column available for stationary phase. Reduced stationary phase leads to lower column efficiency and separation of components. These statements imply that with aqueous – organic phase systems in CPC, optimum component separation is achieved by moderating both the mobile phase flow rate and the rotational speed of the centrifuge.

In this study using an aqueous two – phase system, it appears that this approach of using a moderate rotational speed and mobile phase flow rate to gain optimum protein resolution also applies. A rotational speed of 2000 rpm (the middle value of the range tested) gives the best resolution. Of the two mobile phase flow rates

examined, the lower rate of 5.0 $mlmin^{-1}$ gives the best protein resolution, but is found to be too time – consuming. These results lead to the conclusion that the observations by Foucault *et al* on the behaviour of aqueous – organic phase systems in CPC centrifuges can be applied tentatively to aqueous two – phase systems. A more extensive study *e.g.* experiments performed in triplicate; more rotational speeds such as 500 rpm, 1500 rpm, 2500 rpm, 3500 rpm, 4000 rpm; more mobile phase flow rates such as 2.5 $mlmin^{-1}$, 7.5 $mlmin^{-1}$, 12.5 $mlmin^{-1}$, 15.0 $mlmin^{-1}$ would explore this hypothesis further.

5.4.5. Discussion of the Results from the Experiments to Determine the Influence of Loading Sample Volume

The concentration of lysozyme and myoglobin in the loading sample used in this study was limited to 2.2 $mgml^{-1}$ lysozyme and 2.2 $mgml^{-1}$ myoglobin (± 0.2 $mgml^{-1}$ each protein). It was found that these proteins precipitated when concentrations were increased above this level. Examination of the effect of increasing the mass of protein loaded onto the column had to therefore be conducted by varying the volume of the loading samples used in these experiments.

There were four different volumes of loading sample used: 8.0 ml (1.86% CV); 21.5 ml (5.0% CV); 43.0 ml (10.0% CV); and 86.0 ml (20.0% CV). The effect of increasing the volume of the loading sample was examined in the experiments shown in Figures 2A-g & 2A-h, 2A-o & 2A-p, 2A-q & 2A-r, and 2A-s & 2A-t respectively. The largest loading sample volume (86.0 ml or 20.0% CV) produced no protein separation; overloading the column in this way caused severe loss of stationary phase during the experiment, possibly because the large volume of protein solution had caused the emulsification of the two phases in the column. The experiments using loading samples of 21.5 ml (5.0% CV) and 43.0 ml (10.0% CV) were very similar to one another in that they produced almost complete protein separation. The experiment using the 8.0 ml (1.86% CV) loading sample produced the best separation of the four experiments; however use of this relatively small sample volume was deemed impractical and cost – inefficient when considering the scale – up and industrial application of this methodology. The separation achieved in the experiment where a 43.0 ml (10.0% CV) loading

sample had been used was considered acceptable and this volume of loading sample was recommended for future applications.

5.4.6. Discussion of the Protein Recovery Values

The percentage recovery of lysozyme, apomyoglobin and myoglobin in each experiment can be seen in Table 5.3.2a. In many cases, the percentage recovery of a protein exceeds 100%. This can be explained by considering how the HPLC detector calculated the concentration of protein present in very small amounts in the fractions from the CCC experiment, and was discussed in Section 4.4.3.

5.5. Conclusions

The optimum conditions for separation of lysozyme and myoglobin using a 12.5 % w/w PEG-1000: 12.5% K_2HPO_4 ATPS in the 500 ml column of the Armen CPC centrifuge were: rotational speed 2000 rpm; mobile phase flow rate 10.0 $mlmin^{-1}$; operated in descending mode (lower phase as mobile phase); loading sample volume 43.0 ml (10.0% CV) loaded by the sandwich injection method. These experimental parameters were employed in scale – up experiments, where the 500 ml capacity centrifuge was replaced by a 12.5 litre – capacity instrument (refer to Appendix 3).

The CPC centrifuge provided, in general, greater resolution of the proteins than the J – type centrifuge, and for this reason was chosen as the centrifuge to use in the next stage of the study – the purification of a target protein (phosphomannose isomerase) from a fermentation supernatant.

Chapter 6 – Purification of Phosphomannose Isomerase using a CPC Centrifuge

6.1. Introduction

Following the successful separation of a lysozyme and myoglobin mixture using CPC, the next objective was to use the same centrifuge to perform a purification of the enzyme phosphomannose isomerase (PMI) from an *E. coli* fermentation supernatant supplied by the industrial partner in this project, Syngenta Limited.

PMI is a 50 kDa metalloprotein involved in the metabolism of mannose in both prokaryotes and eukaryotes. Mannose and its derivatives are common constituents of plant and animal cells, and are key components in carbohydrate metabolism. Mannose is phosphorylated by hexokinase to mannose-6-phosphate. PMI then catalyses the reversible interconversion of mannose-6-phosphate and fructose-6-phosphate (Privalle *et al*, 2000). Fructose-6-phosphate is an intermediate of glycolysis, ultimately producing energy for the organism.

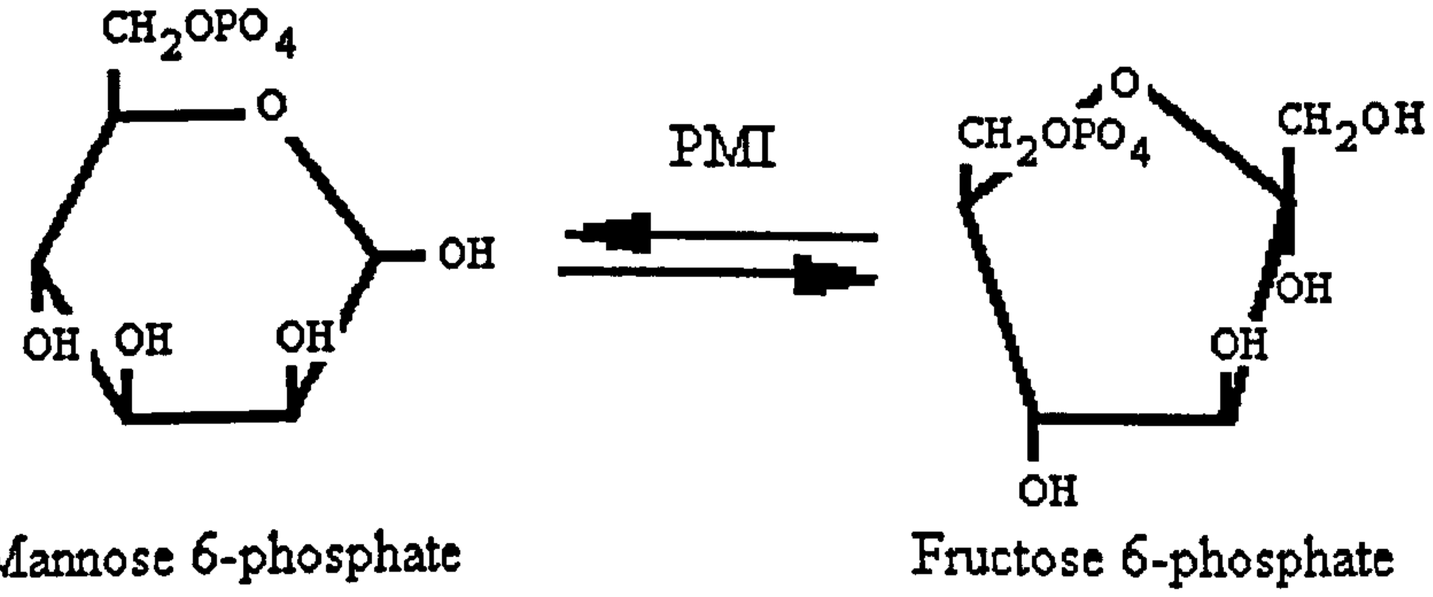

Figure 6.1a: Reaction catalysed by PMI (adapted from Privalle *et al*, 2000).

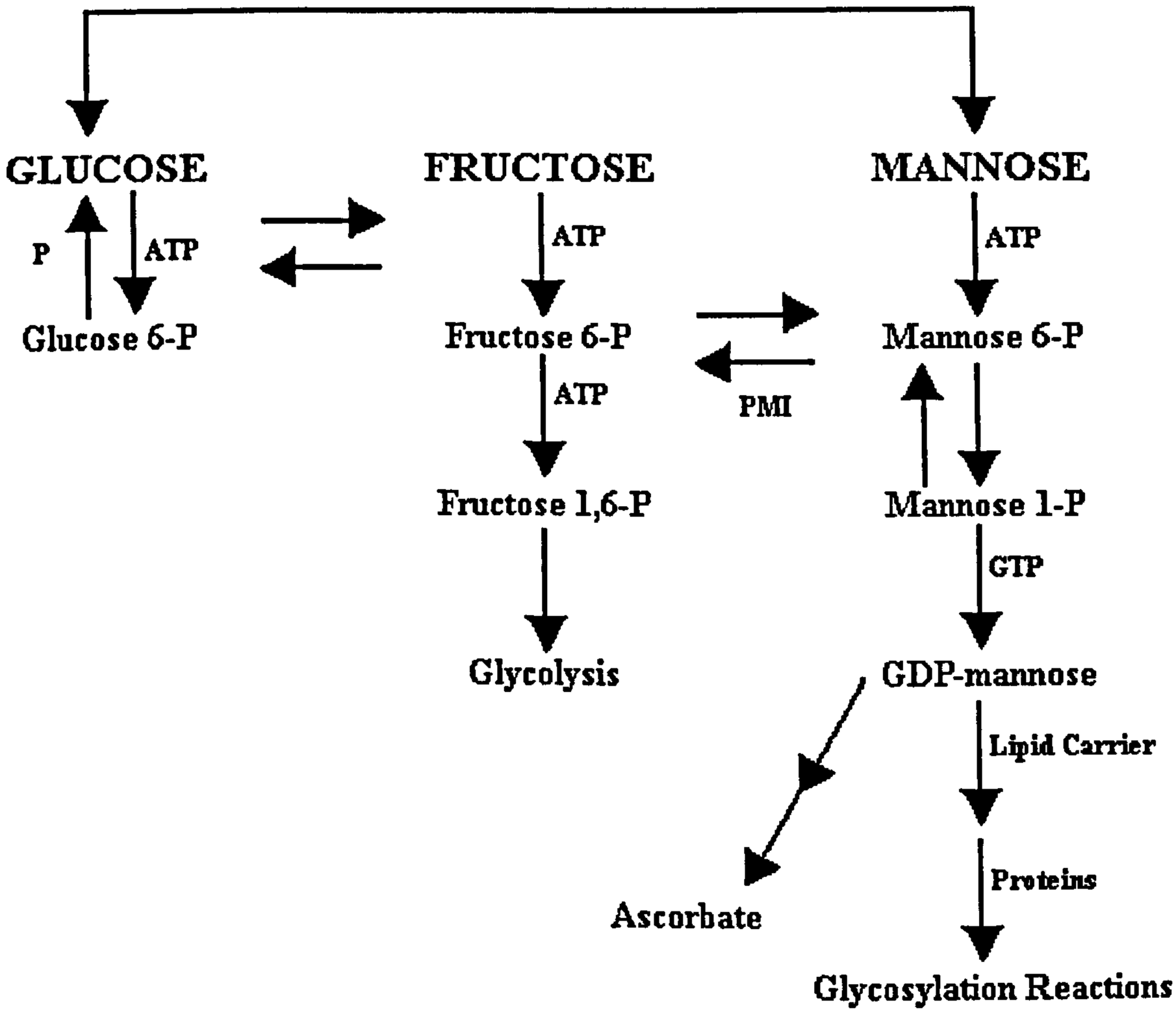

Figure 6.1b: Basic intermediary metabolism involving mannose in non – leguminous plant cells (adapted from Privalle *et al*, 2000).

PMI is of interest to Syngenta, who have used its gene as a plant transformation selectable marker. The PMI gene is inserted into a cassette along with a gene of interest, and the cassette is then inserted into the genome of the target plant cells. Plants without the inserted cassette exhibit poor growth, as they cannot metabolise mannose-6-phosphate. Syngenta have employed this method in the transformation of crop species (Attenborough, 2006).

Syngenta have devised an efficient expression system for PMI using *E. coli*. Large quantities of the enzyme can be rapidly produced, making it an ideal candidate protein for this project.

An assay to measure the activity of this enzyme has also been devised by Syngenta, and is used in this study. It is based on the reversible reduction of the nicotinamide adenine dinucleotide coenzymes NAD^+ or $NADP^+$ to NADH or NADPH. The reduced forms of the coenzymes can be detected at 340 nm, where the oxidised forms have negligible absorbance at this wavelength. The assay for

PMI is a coupled enzyme assay, where a product of the test enzyme (PMI) is used as a substrate for a second enzyme reaction which involves the reduction of $NADP^+$ to NADPH:

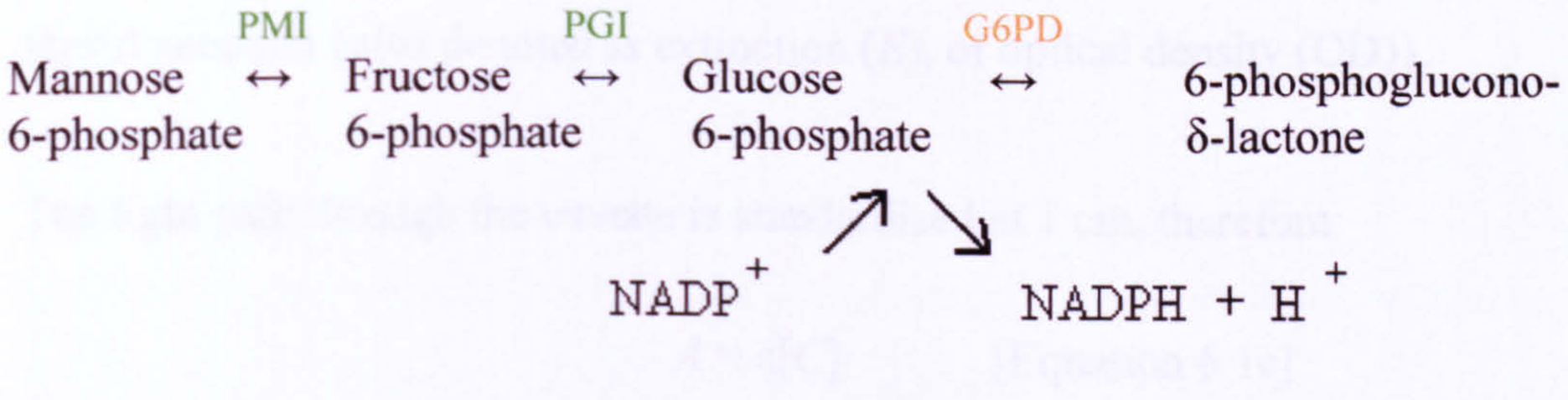

Part of the Glycolytic Pathway
Part of the Pentose Phosphate Pathway
PMI = Phosphomannose isomerase
PGI = Phosphoglucose isomerase
G6PD = Glucose-6-phosphate dehydrogenase

Figure 6.1c: Steps in the coupled enzyme assay for PMI, illustrating the interaction of the glycolytic and pentose phosphate pathways.

In coupled enzyme assays, not only must all the substrates be present in excess, but the second enzyme (in the indicator reaction) must also be in excess. Note that it is enzyme *activity* that is measured, not enzyme quantity. Inactive enzyme may be present in the sample which will not be detected by this assay, but could be quantified by methods that detect total protein *e.g.* the Bradford assay.

This assay is classified as a continuous or kinetic assay. The change in substrate or product is monitored as a function of time, to provide a progress curve for the reaction. These curves start off in a near – linear manner, decreasing in slope as the reaction proceeds and substrate is consumed. The initial velocity of the reaction can be obtained by drawing a tangent to the curve at zero time and measuring its slope.

PMI concentration is calculated using the Beer Lambert Law, which states that:

$$\log_{10}(I_0/I) = \varepsilon l[C] \qquad \text{[Equation 6.1a]}$$

I_0 Intensity of the incident light
I Intensity of the emergent light
ε Absorption coefficient or Absorptivity (a constant for the absorbing substance at that wavelength)
$[C]$ Solute concentration ($molL^{-1}$ or gL^{-1})
l Light path through the absorbing solution (cm)

Equation 6.1a can be re – written as:

$$A = \varepsilon l[C] \qquad \text{[Equation 6.1b]}$$

Note: the spectrophotometer gives a direct measurement of $\log_{10}(I_0/I)$, called the absorbance (A) {also denoted as extinction (E), or optical density (OD)}.

The light path through the cuvette is standardised at 1 cm, therefore:

$$A = \varepsilon[C] \qquad \text{[Equation 6.1c]}$$

$$[C] = \frac{A}{\varepsilon} \qquad \text{[Equation 6.1d]}$$

In the protocol for this assay, the presence of the PMI enzyme is measured in terms of activity. 1 unit (U) of activity is defined as the number of μmoles of NADP reduced per minute. Concentration of enzyme activity is given by:

$$\text{Conc}^{n}\ \text{Activity} = \frac{[\text{Change in abs/min}] \times [1000\ \mu\text{l/Vol}\ (\mu\text{l})\ \text{sample in cuvette}]}{\text{Absorption coefficient for PMI}}$$

or

$$\text{Uml}^{-1} = \frac{[\Delta A/\text{min}] \times [1000\mu\text{l/Vol}\ (\mu\text{l})\ \text{sample in cuvette}]}{6.2} \qquad \text{[Equation 6.1e]}$$

The absorption coefficient for PMI is 6.2, as given in the Syngenta protocol for this assay. The protocol is an in – house document, and is not available in the public arena.

Analysis of the activity of PMI in each phase of the two – phase system provides a distribution ratio for the active enzyme that is essential when devising a protocol for separation by CPC.

The assay was also to be used in determining the activity of the enzyme in fractions collected during the separation process. These enzyme activity values can be used to calculate the specific activity in each fraction. Specific activity is a measure of how much of the protein present in a fraction is active enzyme, and is given by:

$$\text{Specific activity} = \frac{\text{Enzyme activity in fraction (Uml}^{-1})}{\text{Conc}^{n}\ \text{total protein in fraction (mgml}^{-1})} \qquad \text{[Equation 6.1f]}$$

The total protein present in the fraction is likely to be a mixture of active and inactive PMI, plus other proteins and enzymes. Calculating active PMI as a fraction of all protein present in the fractions allows the effectiveness and suitability of the CPC separation process for the purification of active enzymes to be assessed.

The cell paste supplied as the raw material for the CPC experimental work was produced by Syngenta using fermentation of recombinant *E. coli* (as detailed in Section 6.2.1). Syngenta currently produce purified PMI from this cell paste by thawing the frozen cell paste in buffer and passing it through a cell disruptor. After clarification by centrifugation the extract is taken to a concentration of 0.2% protamine sulphate and centrifuged. The supernatant is loaded onto a Q Sepharose column and the protein eluted with a 0-250 mM sodium chloride gradient. Fractions containing PMI are pooled, concentrated and further purified on a Superdex 200 column in a 50 mM ammonium bicarbonate buffer. PMI concentration in the pooled fractions is estimated by densitometry and the sample aliquoted into vials. The samples are then lyophilised for storage at –18°C. The purity of the PMI from this preparation is estimated to be 98.5%. Percentage recovery data is not available.

The aim of this study is to investigate the feasibility of replacing the two solid – liquid chromatography stages with purification using CPC. Successful purification using the 500 ml CPC centrifuge would indicate that large – scale purification of PMI (using the 12.5 litre centrifuge) is possible.

6.2. Materials and Methods

6.2.1. Preparation of the Fermentation Cell Paste

The following fermentation stage in the production of recombinant PMI was carried out by Syngenta employees, and the cell paste produced was supplied for use in this study.

In brief, *E. coli* cells containing the PMI gene were grown in Luria Bertani (LB) medium overnight at 37°C. A fermenter was prepared with 20 litres low – cellulose medium (LCM), supplemented with 200 $\mu g ml^{-1}$ Ampicillin (Sigma). Innoculation of the batch culture was with 1 litre of the LB medium containing the *E. coli* cells, and the fermentation temperature was 37°C. PMI production was induced by the addition of 0.5 mM isopropyl β-D-1-thiogalactopyranoside (IPTG) (Sigma) at 28°C. The cells were harvested by continuous centrifugation, and the cell paste stored at –80°C.

Specific details of the PMI expression vector used in this process is proprietary information held by Syngenta, and as such was unavailable.

6.2.2. Preparation of the Fermentation Supernatant

The fermentation stage produced PMI as an intracellular protein, and the resulting cell paste consisted of intact *E. coli* cells. These cells were ruptured to release the PMI into a solution that was used in the next stage of the purification process. Preparation of the fermentation supernatant was done in collaboration with Sheila Attenborough, Technical Specialist at the Syngenta laboratories (Bracknell, UK), and was carried out as follows: 1.0 M Trishydroxymethylaminomethane (Tris) solution was prepared from TRIZMA® base (Sigma) and ultrapure water (purity 18.2 $M\Omega cm^{-1}$). The pH was adjusted to 7.0 using concentrated hydrochloric acid (pH 14.1 M). This solution was then diluted to produce a 50 mM Tris buffer solution. Approximately 10 g cell paste was removed from –80°C storage and homogenised using a pestle and mortar with 50 ml of the 50 mM Tris buffer solution. The resulting cell "slurry" was passed through a cell disruptor (Constant Systems, Daventry, Northamptonshire, UK) at a pressure of 35 000 psi. The preparation was centrifuged at 50 000 G for 30 minutes at 4°C using a Sorvall "RC5C Plus" centrifuge fitted with a SS-34 rotor (Thermo Scientific, Basingstoke, Hampshire, UK). The supernatant (approximate volume 70 ml) was stored at –80°C as 10 ml aliquots.

6.2.3. Determination of the Distribution Ratio of PMI in the Aqueous Two – Phase System

The separation of lysozyme and myoglobin with the CPC centrifuge used the 12.5% w/w PEG-1000: 12.5% w/w K_2HPO_4 aqueous two – phase system. The same phase system was now used to perform a purification of PMI from the fermentation supernatant. This part of the study was concerned not with establishing the optimum phase system for PMI, but rather to use PMI to explore how a protein from a fermentation preparation behaved in the CPC separation process.

Designing the CPC stage of the purification process required knowledge of the distribution ratio of PMI in this phase system. This was determined by adding pure PMI to the phase system and measuring the enzyme activity in the upper and lower phases. The assay used is detailed in Section 6.1. A 100 g quantity of the phase system was prepared (as in Section 2.2.1), mixed thoroughly and a 1.0 ml aliquot transferred to a microcentrifuge tube. 10 µl of purified PMI solution (purified by Syngenta using their existing method and with concentration 0.5 $mgml^{-1}$) was added to the 1.0 ml phase system, and mixed by inversion. A 25 µl aliquot of the mixture was removed and stored on ice. The phase system in the microcentrifuge tube was allowed to separate into upper and lower phases, 25 µl aliquots taken from each phase and stored on ice.

The PMI assay mix was prepared as follows: 735.0 µl 50 mM Tris buffer solution at pH 7.0 (as made in Section 6.2.2); 100.0 µl 16 mM mannose-6-phosphate solution (Sigma); 100.0 µl 8mM NADP solution (Sigma);

20.0 µl 100 Uml^{-1} phosphoglucose isomerase solution (Sigma);

20.0 µl 100 Uml^{-1} glucose-6-phosphate dehydrogenase solution (Sigma).

The assay mix was transferred to a semi – micro quartz cuvette and the absorbance at wavelength 340 nm recorded over 80 seconds in a Hitachi U-2010 spectrophotometer (path length 10 mm) equipped with Hitachi "UV Solutions 1.1" software until a stable baseline reading was produced. The 25 µl sample from the mixed phases was added to the cuvette, and the enzymatic reaction followed by monitoring changes in the absorbance at wavelength 340 nm recorded over a 120 second time period.

This procedure was repeated for both upper phase and lower phase samples, using fresh PMI assay mix on each occasion.

The data for each sample was displayed graphically (absorbance at wavelength 340 nm against time in minutes), and the gradient of the line calculated by the software. The gradient of each graph gave the rate of change of absorbance at 340nm, which is directly related to the activity of PMI present in the sample. The data was used to determine a distribution ratio of PMI in this phase system.

6.2.4. Studying the Effect of PMI Supernatant Concentration on Phase Separation

This part of the study aimed to establish the maximum concentration of PMI supernatant that could be used to make the 12.5% w/w PEG-1000: 12.5% w/w K_2HPO_4 phase system without affecting the rate of phase separation.

The supernatant prepared in Section 6.2.2 was defrosted and serially diluted with distilled water (purity 1.0 $M\Omega cm^{-1}$) to create 10 ml solutions of the following dilutions: 0.1%, 1.0% and 10.0%. Separate 10 g phase systems were created by combining 1.25 g PEG-1000, 1.25 g dipotassium hydrogen phosphate and 7.5 g of the diluted supernatant solution (plus a phase system made with distilled water to act as a control) in graduated 10 ml measuring cylinders equipped with stoppers.

The contents of each cylinder were mixed by inversion, and the positions of the interfaces (refer to Figure 6.2.4a) noted at 10 second intervals, using the graduations on the measuring cylinders as a guide.

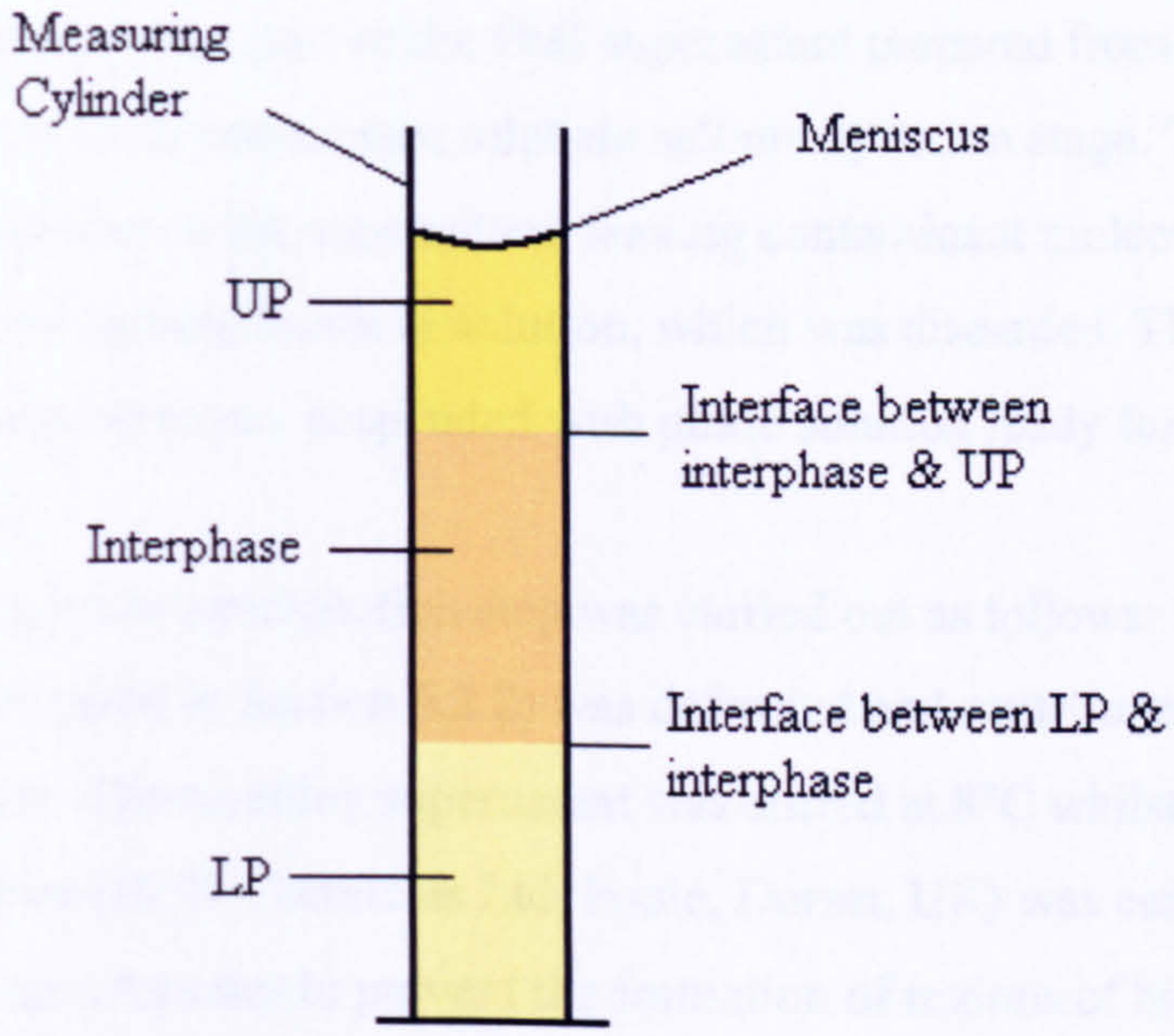

Figure 6.2.4a: Diagram illustrating the location of the different phases and interfaces during the early stages of the separation of a 12.5% w/w PEG-1000: 12.5% w/w K_2HPO_4 ATPS made with dilutions of the PMI fermentation supernatant.

This process was performed in triplicate for each solution, and the position of each interface within the measuring cylinder plotted against time (refer to Figures 6.3.2a, 6.3.2b, 6.3.2c and 6.3.2d). The measurements were stopped for each experiment at the time shown in Figures 6.3.2a, 6.3.2b and 6.3.2c (pure water, 0.1% and 1.0% supernatant solutions respectively). Measurements for the experiment using the 10.0% supernatant solution (Figure 6.3.2d) were stopped after 30 minutes; there was no further change in the position of the interfaces in this phase system after 660 seconds or 11 minutes.

6.2.5. Preparation of the CPC Loading Sample: Partial Purification using Ammonium Sulphate Precipitation

The results from the study of the effect of PMI supernatant concentration on phase separation showed that the PMI fermentation supernatant diluted 10 – fold with water would create an emulsion when used with the 12.5% w/w PEG-1000: 12.5% w/w K_2HPO_4 ATPS, thus prohibiting phase separation. However, using a more dilute supernatant was not practical when attempting to transfer the experiment to the CPC centrifuge stage. It was thought that the factors causing the emulsification were most likely to be contaminant proteins that could be removed

by another purification step, and so the PMI supernatant prepared from the cell paste was subjected to an ammonium sulphate salt precipitation stage. This precipitated the proteins in the supernatant, leaving contaminant molecules such as nucleic acids and carbohydrates in solution, which was discarded. The precipitated proteins were re – suspended with phase solution ready for the CPC purification stage.

The ammonium sulphate precipitation step was carried out as follows: 50 ml PMI supernatant (as prepared in Section 6.2.2) was defrosted and centrifuged at 6000 rpm for 10 minutes. The resulting supernatant was stirred at 8°C whilst 16.25 g ammonium sulphate (BDH Chemicals Ltd, Poole, Dorset, UK) was cautiously added. Caution was necessary to prevent the formation of regions of high – salt concentration within the solution, which could potentially denature the enzyme. The mixture was stirred for 65 minutes at 8°C, then centrifuged at 10 000 rpm for 20 minutes. The supernatant was discarded, and the pellet re – suspended in 40.0 ml upper phase of a 12.5% w/w PEG-1000: 12.5% w/w K_2HPO_4 ATPS by stirring overnight at 8°C.

6.2.6. Determination of the Protein Concentration in the CPC Loading Sample

The PMI suspension produced from the ammonium sulphate precipitation stage (Section 6.2.5) contained both the PMI enzyme and contaminant proteins. It was necessary to know the total protein concentration of the suspension, so that (if necessary) a dilution could be made before the CPC stage was undertaken. Knowledge of the total protein concentration of the suspension would also ensure that the CPC loading sample would have approximately the same protein concentration as that used in the lysozyme/myoglobin separation experiments, thus facilitating comparison between the two studies.

Protein concentration was determined according to the Bradford method (Bradford, 1976). A standard curve was created using the following solutions of BSA (Sigma) dissolved in the upper phase of a 12.5% w/w PEG-1000: 12.5% w/w K_2HPO_4 ATPS: 0.25 $mgml^{-1}$; 0.5 $mgml^{-1}$; 0.75 $mgml^{-1}$; 1.0 $mgml^{-1}$; 1.5 $mgml^{-1}$.

0.1 ml of each solution (plus 0.1 ml upper phase acting as a blank) was added to 3.0 ml Bradford reagent (Sigma) and incubated at room temperature for 20

minutes. The absorbance at 595 nm was obtained using a Hitachi U-1800 spectrophotometer, and the data presented graphically.

The PMI suspension (as prepared in Section 6.2.5) was diluted 1:10 with upper phase and analysed by the Bradford method (above) to give the total protein concentration of the PMI solution.

6.2.7. Purification of PMI using the CPC Centrifuge

The CPC centrifuge was used to purify the PMI from any remaining contaminant proteins present in the preparation from the ammonium sulphate precipitation stage.

The distribution ratio calculated earlier (refer to Sections 6.2.3 and 6.3.1) indicated that PMI favoured the upper phase of the phase system in an approximate ratio of 10:1. Therefore, the upper phase was used as the mobile phase for this experiment, ensuring that the majority of the PMI would elute from the column with the mobile phase.

The partially – purified PMI suspension had a total protein concentration of $\approx$13 $mgml^{-1}$. The CPC experiments with lysozyme and myoglobin used loading samples of total protein concentration $\approx$ 4.5 $mgml^{-1}$. In order to create a loading sample of comparable total protein concentration, and to prevent overloading the column with protein, the PMI suspension was diluted 1:3 with upper phase.

The protocol for the operation of the CPC centrifuge has been described in Section 2.4.5. The operational parameters used were:

- Direction of MP flow: Ascending
- MP flow rate: 10.0 $mlmin^{-1}$
- Phase system: 12.5% w/w PEG-1000: 12.5% w/w K_2HPO_4 ATPS equilibrated and separated at 30°C
- Composition of MP: upper phase of this phase system
- Composition of SP: lower of this phase system
- Rotational speed of column: 2000 rpm
- Back pressure regulator: Not fitted

- Method of loading sample: Sample was diluted as above and 50 ml drawn up into a syringe. Syringe was inverted to mix the contents before the sample loop was filled via the injection port
- Concentration of total protein in loading sample (approximate): 4.5 $mgml^{-1}$
- Sample loop capacity: 43.0 ml (10.0% of column volume)
- Mass of protein loaded (approximate): 193.5 mg
- Chromatogram recording started: 0' 00"
- MP pump started: 18' 10"
- Sample injection made: 18' 10" (Sandwich Injection)
- Start of collection of first fraction: 18' 10"
- Time interval of fraction collection: 1' 00"
- Experiment stopped: 118' 10"

Fractions were collected every minute in graduated 15 ml centrifuge tubes to allow accurate calculation of stationary phase retention and rate of stationary phase "stripping". Fractions were then pooled in pairs to reduce the number of samples destined for further analysis; *i.e.* fractions 1 and 2 were combined to give "fraction 2", fractions 3 and 4 were combined to give "fraction 4", and so on. The flow chart below illustrates the stages used in analysing the CPC fractions. The PMI assay was carried out on fractions 34/35 to 58/59 inclusive; these were collected as the first and second peaks appeared on the chromatogram (Figures 6.3.4a and 6.3.4b). PMI has a distribution ratio of approximately 10:1 in this phase system, and it was therefore predicted that it would be one of the first proteins to elute from the column, and that these fractions were most likely to contain PMI. Fractions 66/67 were collected towards the end of the experiment, when the chromatogram reading was returning to baseline. They were assayed to confirm that all the PMI had eluted by the later stages of the CPC run.
The Bradford assay was carried out on fractions 34/35 to 76/77 inclusive; these were collected over the time period when all three peaks appeared on the chromatogram. These peaks indicate the likely presence of protein.
The specific activity was calculated in fractions 34/35 to 58/59 inclusive and fraction 66/67.

Fractions 34/35 to 62/63 inclusive were subjected to sodium dodecyl sulphate polyacrylamide gel electrophoresis (SDS-PAGE) to further analyse the protein content of the fractions, and densitometry of the gels quantified this protein content.

The CPC loading sample was analysed alongside the fractions, to allow comparison of the PMI supernatant both before and after the CPC process.

Measurement of PMI Activity (using the PMI Assay)

↓

Measurement of Total Protein (using the Bradford Assay)

↓

Calculating the Specific Activity (using PMI Activity and Total Protein data)

↓

SDS-PAGE and Densitometry

6.2.8. Analysis of Fractions: Measurement of PMI Activity

The PMI assay detailed in Section 6.1 was used to calculate the concentration of active PMI (in Uml^{-1}) present in selected fractions from the CPC stage.

A standard curve was created to determine the concentration range over which the PMI assay exhibits linear behaviour; this information was then used to dilute the CPC fractions (if necessary) to bring the concentration of active PMI in each to within this linear range.

The standard curve was created as follows: purified PMI (Syngenta) was dissolved in 50 mM Tris buffer, pH 7.0 (as made in Section 6.2.2) to create the following standard solutions: 0.005 $mgml^{-1}$; 0.05 $mgml^{-1}$; 0.1 $mgml^{-1}$; 0.25 $mgml^{-1}$; 0.5 $mgml^{-1}$.

The PMI assay mix was prepared as follows: 750.0 µl 50 mM Tris buffer solution at pH 7.0; 100.0 µl 16 mM mannose-6-phosphate solution (Sigma); 100.0 µl 8mM NADP solution (Sigma); 20.0 µl 100 Uml^{-1} phosphoglucose isomerase solution (Sigma); 20.0 µl 100 Uml^{-1} glucose-6-phosphate dehydrogenase solution (Sigma). The assay mix was transferred to a semi – micro quartz cuvette, 10.0 µl of the 0.005 $mgml^{-1}$ standard solution added, and changes in the absorbance at wavelength 340 nm recorded over 120 seconds in a Hitachi U-1800 spectrophotometer (path length 10 mm) equipped with Hitachi "UV Solutions

2.0" software. The procedure was repeated for the remaining standard solutions, with the data for each sample being displayed graphically. This information was used to construct the standard curve graph.

The procedure was repeated with the selected CPC fractions and loading sample replacing the standard solutions. Fractions estimated to contain high concentrations of PMI were diluted either 1:40 or 1:100 to bring the response of the spectrophotometer to within the linear range on the standard curve. The CPC loading sample was diluted 1:200 for the same reason. Those fractions estimated to have low concentrations of PMI were not diluted.

6.2.9. Analysis of Fractions: Measurement of Total Protein Concentration

Protein concentration was determined according to the Bradford method (Bradford, 1976), and the standard curve prepared as in Section 6.2.6.

The fractions were diluted as necessary with upper phase to bring the absorbance readings to within the linear range on the standard curve, and analysed as in Section 6.2.6, to give the concentration of total protein in each fraction.

6.2.10. Analysis of Fractions: Trichloroacetic acid precipitation, SDS-PAGE and Gel Staining

Trichloroacetic acid precipitation was carried out on fractions 34/35 to 62/63 (plus the loading sample) to remove any polyethylene glycol (PEG) present before analysis by SDS-PAGE.

Each fraction consisted mainly of upper (mobile) phase and a small volume of lower (stationary) phase (as a result of stationary phase "stripping" from the column during the CPC separation process). The proteins in each fraction had partitioned between these two phases according to their individual distribution ratios.

To obtain an aliquot that contained proportionate amounts of each protein as they were present in the fraction overall, each fraction was mixed by inversion and an aliquot of appropriate volume transferred to a microcentrifuge tube. The volume of the aliquot depended on the estimated concentration of protein present in the fraction; approximately 50 µg per aliquot was required for successful analysis by SDS-PAGE.

The volume of each aliquot was increased to 500 µl with 50 mM Tris buffer, pH 7.0, then 500 µl ultrapure water (purity = 18.2 $M\Omega cm^{-1}$) added to produce a total volume of 1.0 ml.

250 µl 8.75 M trichloroacetic acid (Sigma) solution was added to each 1.0 ml aliquot, and the samples incubated at 4°C for 10 minutes.

The samples were centrifuged at 13 000 rpm for 5 minutes in a "Heraeus Biofuge Pico" microcentrifuge (Thermo Scientific, Basingstoke, UK) and the supernatant removed. Each pellet was washed twice with 1.0 ml ice – cold acetone (Fisher Scientific UK Ltd, Loughborough, Leicestershire, UK) and left overnight at room temperature to dry.

1x Laemmlli buffer solution, pH 7.0 was prepared as follows (all reagents from Sigma): 0.0625 M Tris buffer; 2.0% sodium dodecyl sulphate (SDS); 5.0% glycerol; 0.01% bromophenol blue; 0.2% β-mercaptoethanol.

100 µl of the buffer solution was added to each sample prepared by trichloroacetic acid precipitation and the samples boiled in a water bath for six minutes.

Electrophoresis was carried out using a "Mini-Protean 2" gel electrophoresis system (Bio-Rad, Hemel Hempstead, Hertfordshire, UK), Tris-glycine SDS running buffer (Invitrogen, Paisley, UK), and 10 – well 10% Tris-HCl electrophoresis gels (Bio-Rad). Each gel was loaded with the following: 5.0 µl "High-Range Rainbow" molecular weight marker (GE Healthcare UK Ltd, Chalfont St Giles, Buckinghamshire, UK); 35.0 µl pure PMI solution, concentration 5.0 $mgml^{-1}$ (Syngenta); 35.0 µl each sample (prepared as above).

The system was connected to a "POWER PAC 300" power pack (Bio-Rad), and electrophoresis carried out at 80 Volts over 90 minutes to ensure efficient resolution of proteins.

On completion of electrophoresis, the gels were washed in ultrapure water three times, stained with "SimplyBlue™ SafeStain" (Invitrogen) for two hours, and de – stained in ultrapure water overnight.

6.2.11. Analysis of Fractions: Gel Imaging and Densitometry

Images of the gels were taken in the Division of Biosciences laboratories, Brunel University using a UMAX flatbed scanner (Milton Keynes, Buckinghamshire, UK) and "Vista Scan Version 3.7.5" software (LaserSoft Imaging AG, Kiel, Germany). The images were analysed using densitometry by Sheila

Attenborough, Technical Specialist (Syngenta, Bracknell, UK). "Scanner Control" software (Molecular Devices Ltd, Wokingham, Berkshire, UK) was used for the scanning process, and "ImageQuant 5.0" (Molecular Devices) for the quantification process.

6.3. Results

6.3.1. Determination of the Distribution Ratio of PMI in the Aqueous Two – Phase System

The PMI distribution ratio in the phase system was determined by measuring the concentration of enzyme activity in the upper and lower phases.

The concentration of PMI activity in each phase is the number of μmoles of NADP reduced per minute, and is given by:

$$\text{Activity} = \frac{[\text{Change in absorbance/min}] \times [1000\ \mu\text{l/Vol test sol}^{n}\ \text{in cuvette (in } \mu\text{l)}]}{\text{Absorption coefficient for PMI}}$$

[Equation 6.3.1a]

Activity = Concentration of PMI activity measured in Uml^{-1}
Absorption coefficient for PMI = 6.2

$$\text{For the upper phase, activity} = \frac{[0.06899] \times [1000/25]}{6.2} = 0.44510\ \text{Uml}^{-1}$$

$$\text{For the lower phase, activity} = \frac{[0.006788] \times [1000/25]}{6.2} = 0.04379\ \text{Uml}^{-1}$$

$$\text{The ratio of PMI activity upper phase: lower phase} = \frac{0.44510}{0.04379} = 10.16$$

Therefore, the distribution ratio for PMI (UP/LP) ≈ **10:1.**

This indicates that the PMI favours the upper phase of this phase system over the lower phase by a factor of ten.

When using aqueous two – phase systems to separate or purify proteins, it is important to determine if the phase system will cause the protein to precipitate, as this will adversely affect the efficiency of the process. Insoluble material present in an ATPS will precipitate at the interface between the two phases, rather than collecting in one of the phases. If the insoluble material is an enzyme (*e.g.* PMI) the extent of precipitation can be quantified using the appropriate assay. This is done by measuring the enzyme activity in the upper phase, lower phase, and in the phases when they are mixed together.

The sum of the activities in the upper and lower phases should be equal to the activity in the mixed phases. If it is less than the activity in the mixed phases, it

indicates that some active enzyme has precipitated at the interface during phase separation.

PMI activity UP + PMI activity LP = 0.44510 + 0.04379 = 0.49 Uml^{-1} .
This value of PMI activity is for 1.0 ml upper phase plus 1.0 ml lower phase.
Therefore, for 1.0 ml of these combined phases, activity = $\frac{0.49}{2}$ = **0.25 Uml^{-1}**

PMI activity in 1.0 ml of the mixed phases = $\frac{[0.03711] \times [1000/25]}{6.2}$ = **0.24 Uml^{-1}**

The sum of the PMI activity in the upper and lower phases is approximately the same as the PMI activity in the mixed phases. Therefore it can be concluded that the enzyme did not precipitate at the interface between the two phases when it was added to this phase system. Importantly, there appears to be no loss of activity after the enzyme has been subjected to the mixing and separating processes in the phase system.

6.3.2. Studying the Effect of PMI Supernatant Concentration on Phase Separation

Four separate 10 g quantities of the 12.5% w/w PEG-1000: 12.5% w/w K_2HPO_4 phase system were created using dilutions of the PMI fermentation supernatant and the separation times of each evaluated by measuring the positions of the interfaces when the phase system was allowed to undergo separation in a 10 ml measuring cylinder (refer to Section 6.2.4). Figures 6.3.2a, 6.3.2b, 6.3.2c and 6.3.2d show the positions of the interfaces for each phase system over time. Complete phase separation is judged to have occurred when the two lines on each graph (representing the position of the interface between the upper phase and interphase, and between the lower phase and the interphase) merge together.

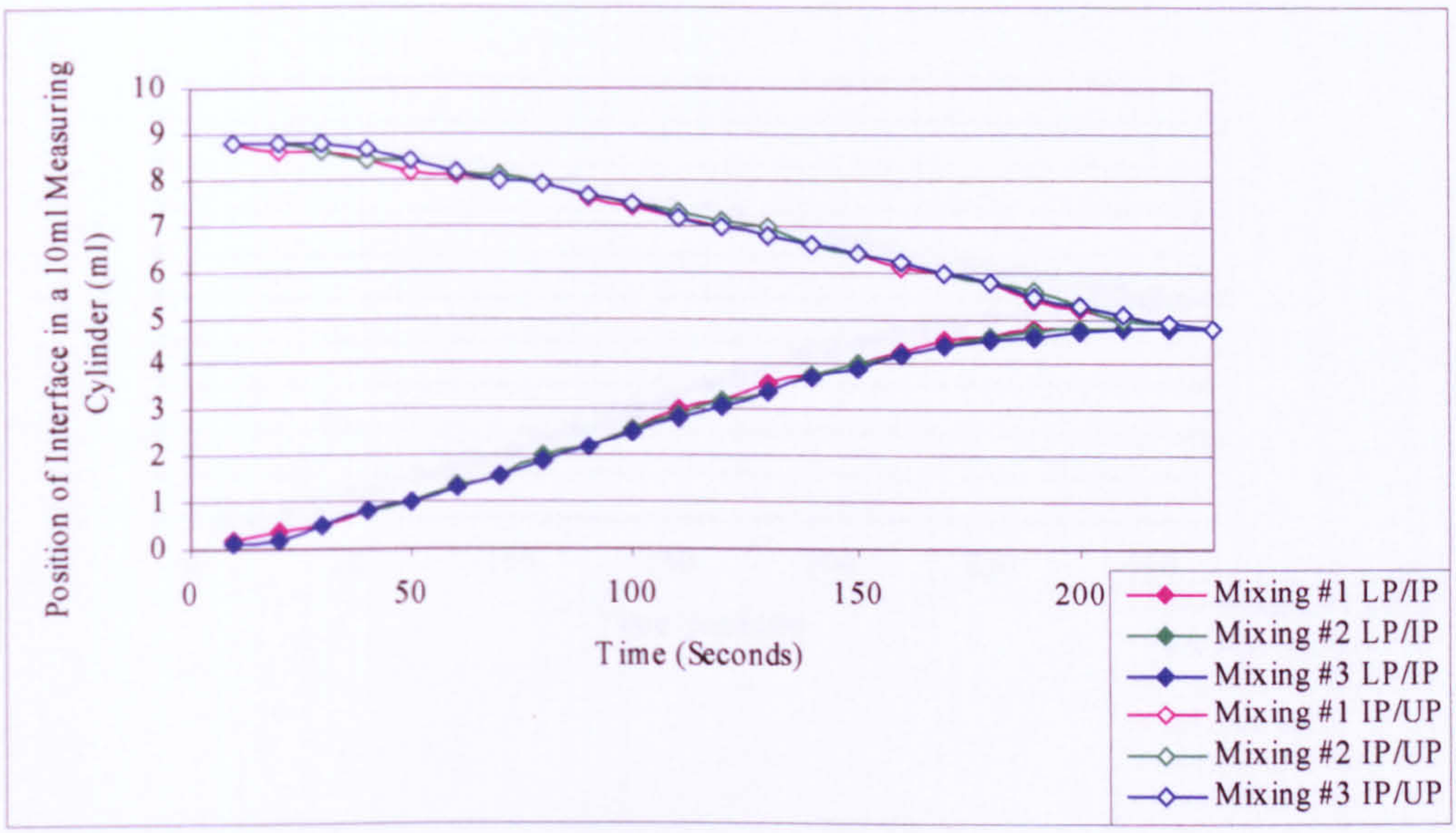

Figure 6.3.2a: Position of the interfaces between the lower phase and the interphase, and between the upper phase and the interphase of a 10 g 12.5% w/w PEG-1000: 12.5% w/w K_2HPO_4 ATPS created using distilled water. The phase system was shaken in a stopped 10 ml graduated measuring cylinder and allowed to phase separate over time.

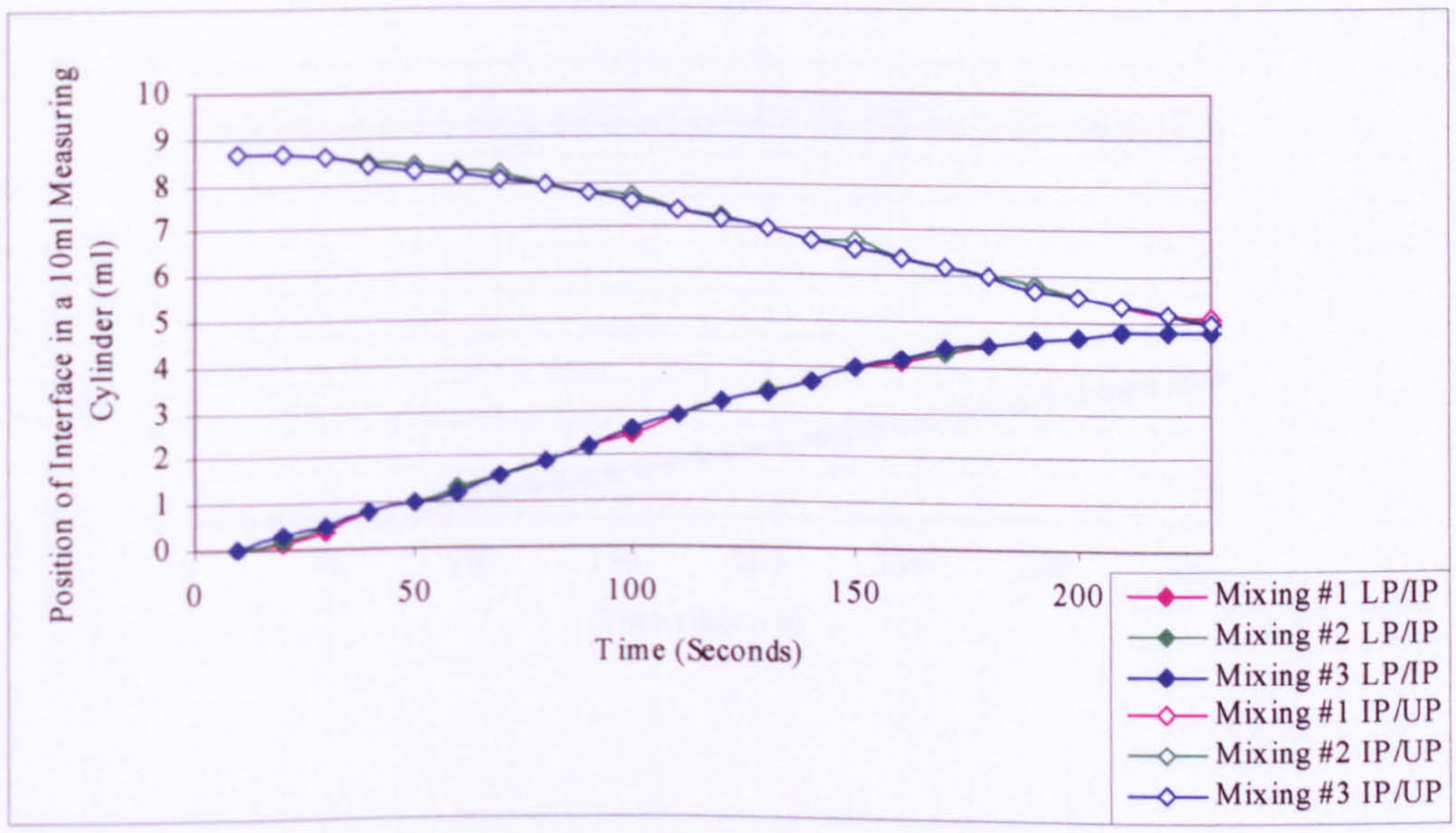

Figure 6.3.2b: Position of the interfaces between the lower phase and the interphase, and between the upper phase and the interphase of a 10 g 12.5% w/w PEG-1000: 12.5% w/w K_2HPO_4 ATPS created using a 0.1% dilution of a PMI fermentation supernatant. The phase system was shaken in a stopped 10 ml graduated measuring cylinder and allowed to phase separate over time.

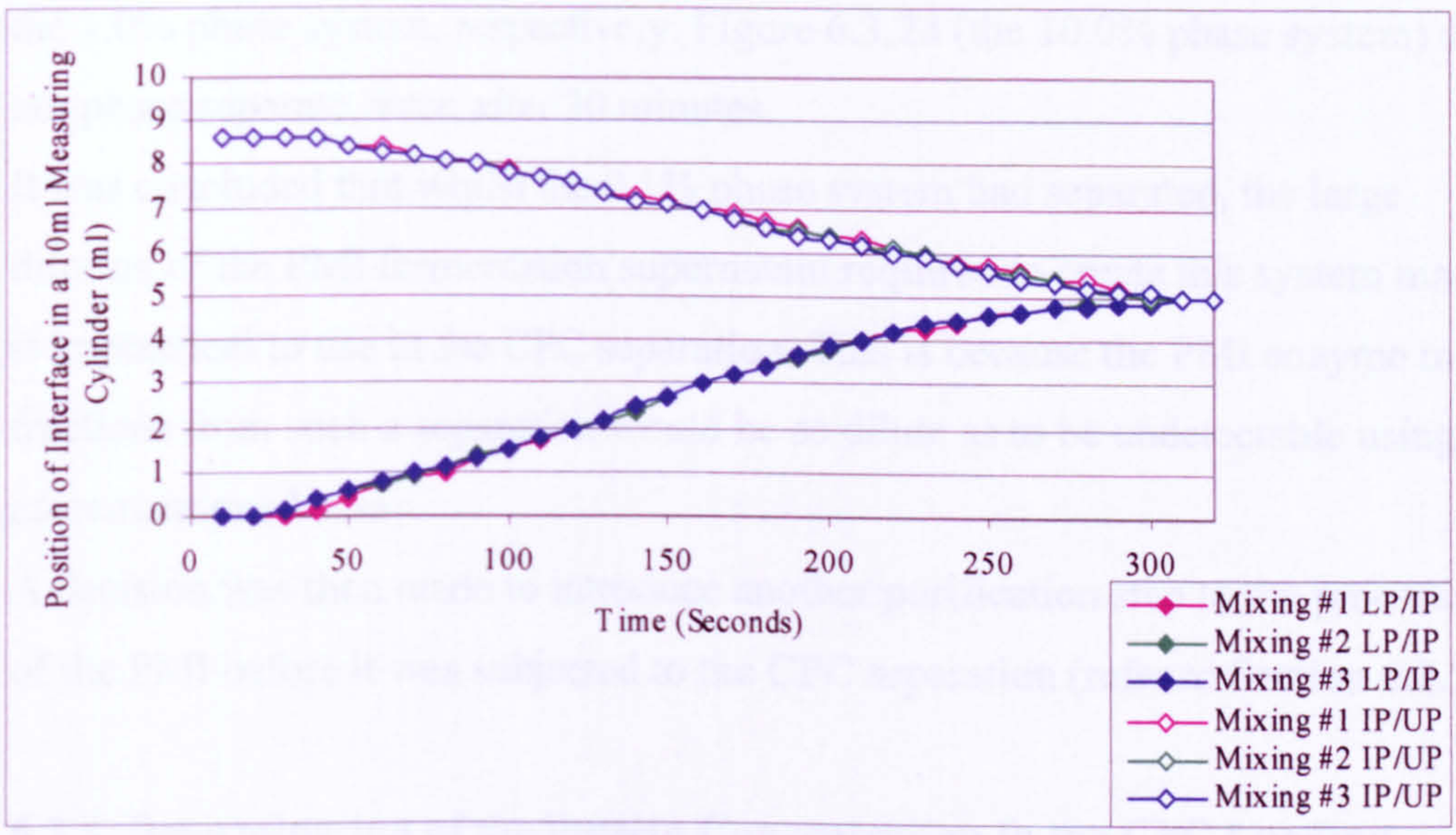

Figure 6.3.2c: Position of the interfaces between the lower phase and the interphase, and between the upper phase and the interphase of a 10 g 12.5% w/w PEG-1000: 12.5% w/w K_2HPO_4 ATPS created using a 1.0% dilution of a PMI fermentation supernatant. The phase system was shaken in a stopped 10 ml graduated measuring cylinder and allowed to phase separate over time.

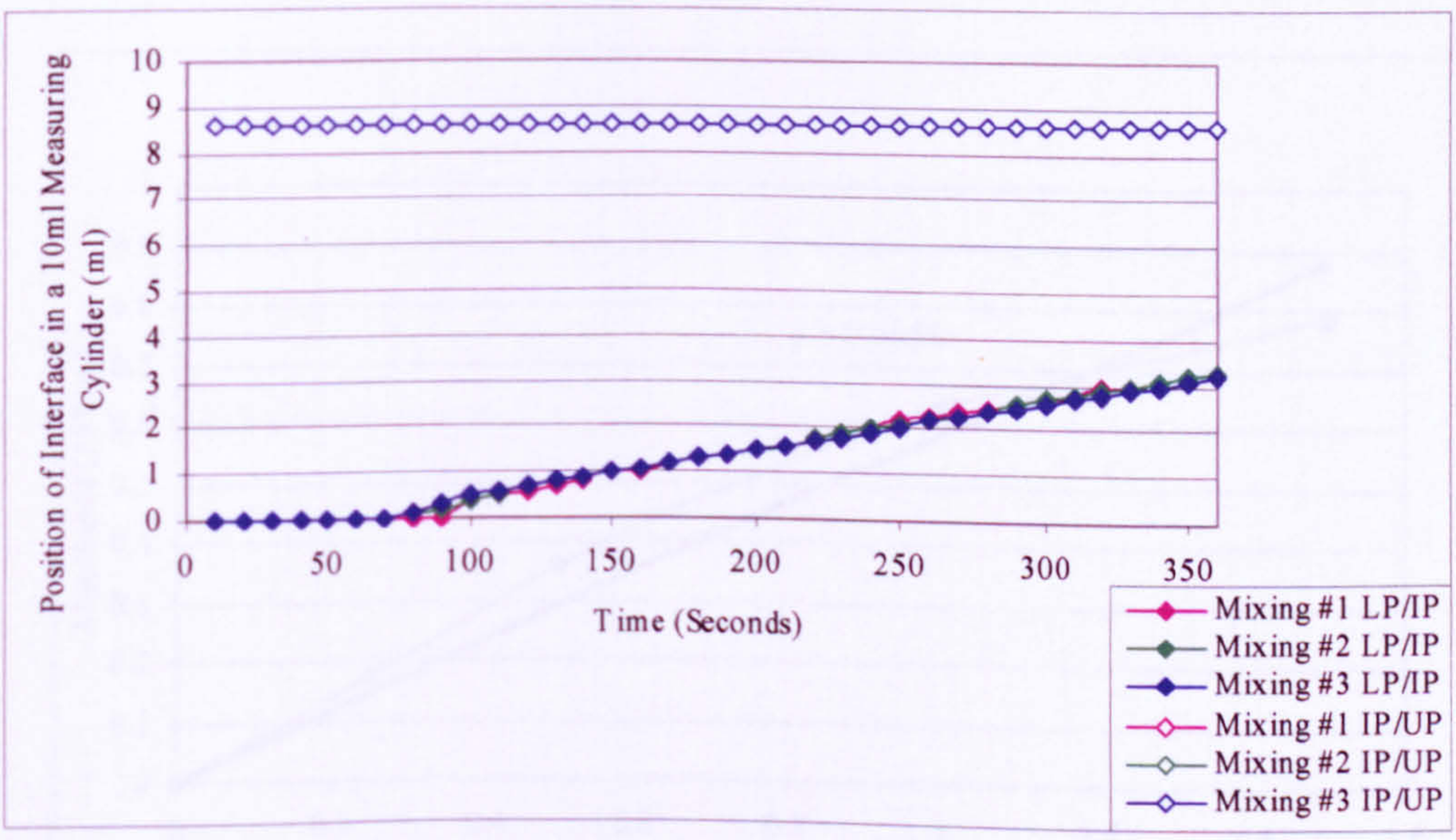

Figure 6.3.2d: Position of the interfaces between the lower phase and the interphase, and between the upper phase and the interphase of a 10 g 12.5% w/w PEG-1000: 12.5% w/w K_2HPO_4 ATPS created using a 10.0% dilution of a PMI fermentation supernatant. The phase system was shaken in a stopped 10 ml graduated measuring cylinder and allowed to phase separate over time.

The results in Figures 6.3.2b and 6.3.2c show that complete phase separation had occurred after 230 seconds for the 0.1% phase system and after 320 seconds for the 1.0% phase system, respectively. Figure 6.3.2d (the 10.0% phase system) did not phase separate, even after 30 minutes.

It was concluded that whilst the 0.1% phase system had separated, the large dilution of the PMI fermentation supernatant required to create this system made it impractical to use in the CPC separation. This is because the PMI enzyme in the fractions from such a separation would be so dilute as to be undetectable using the aforementioned assay.

A decision was then made to introduce another purification step to the processing of the PMI before it was subjected to the CPC separation (refer to Section 6.2.5).

6.3.3. Determination of the Protein Concentration in the CPC Loading Sample using the Bradford Assay

A standard curve was created from the change in absorbance at wavelength 595 nm for each standard solution of BSA; the concentrations used were between 0.25 $mgml^{-1}$ and 1.5 $mgml^{-1}$ (Figure 6.3.3a).

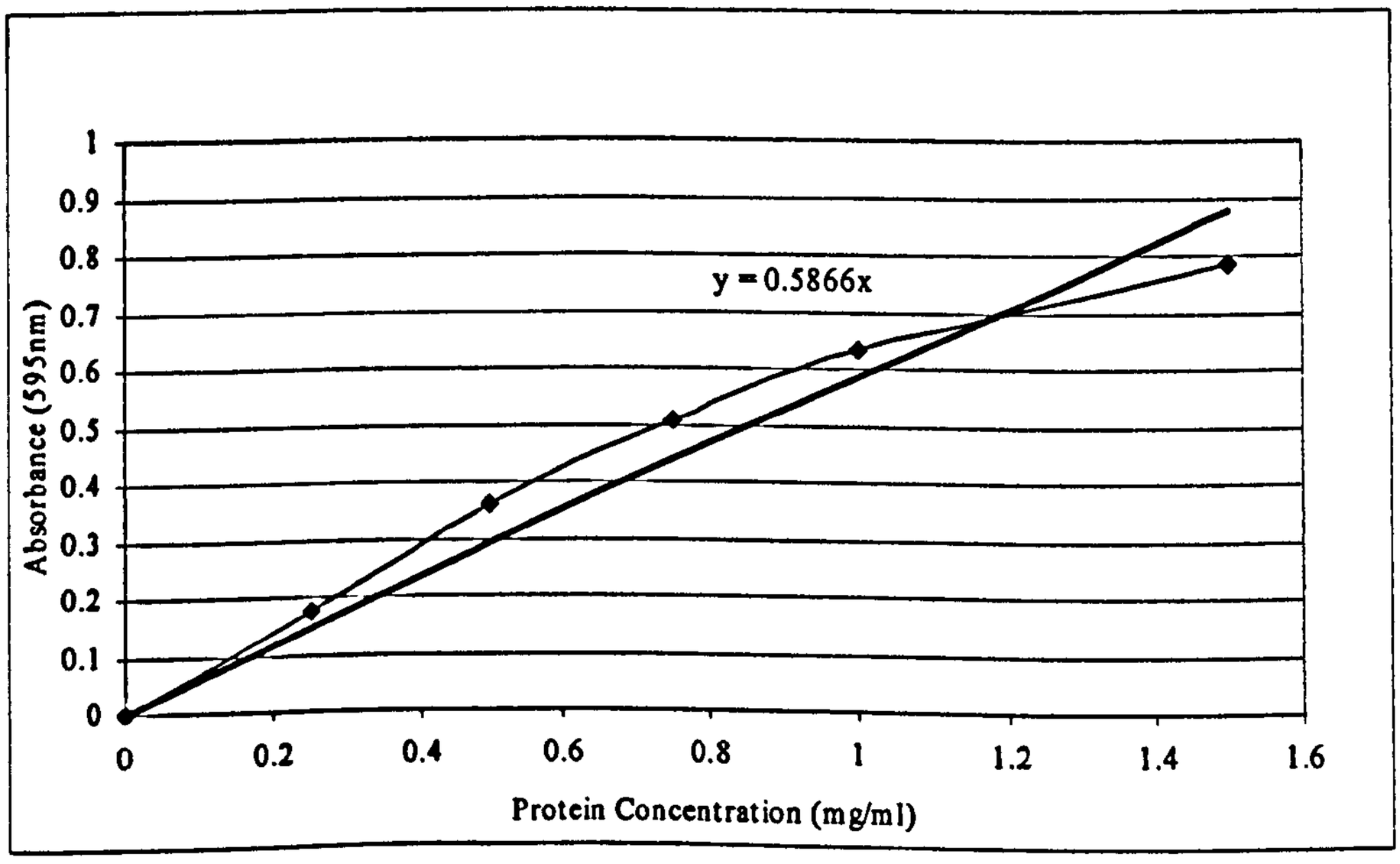

Figure 6.3.3a: Graph of absorbance at 595 nm against concentration of protein ($mgml^{-1}$) for BSA standard solutions made with the upper phase of a 12.5% w/w PEG-1000: 12.5% w/w K_2HPO_4 ATPS.

The absorbance at 595 nm of the CPC loading sample prepared in Section 6.2.5 and diluted 1:10 was measured and found to be 0.769 AU.

The equation of the straight line from the standard curve (Figure 6.3.3a) was used to calculate the protein concentration in the loading sample as follows:

Abs of solution at 595 nm = (Line gradient × Protein conc^{n}) + Intercept

[Equation 6.3.3a]

$$y = (0.5866 \times x) + 0$$

$$0.769 = 0.5866 \times x$$

$$x = 1.31 \text{ mgml}^{-1}$$

The concentration of protein in the 1:10 dilution is 1.31 mgml^{-1}

Therefore, the concentration of protein in the loading sample = 1.31 × 10

= 13.10 mgml^{-1}

The CPC experiments to separate lysozyme and myoglobin used loading samples of total protein concentration ≈ 4.5 mgml^{-1}. It was considered important to be able to compare the CPC centrifuge performance in the lysozyme and myoglobin separation with that from the PMI purification. For this reason, the PMI suspension was diluted 1:3 with upper phase before being loaded onto the CPC column.

6.3.4. Purification of PMI using the CPC Centrifuge

The eluent from the column passed through the UV detector, which had been set at wavelength 280 nm. The signal from the detector was sent to and interpreted by the Picolog software to produce the chromatogram seen in Figure 6.3.4a.

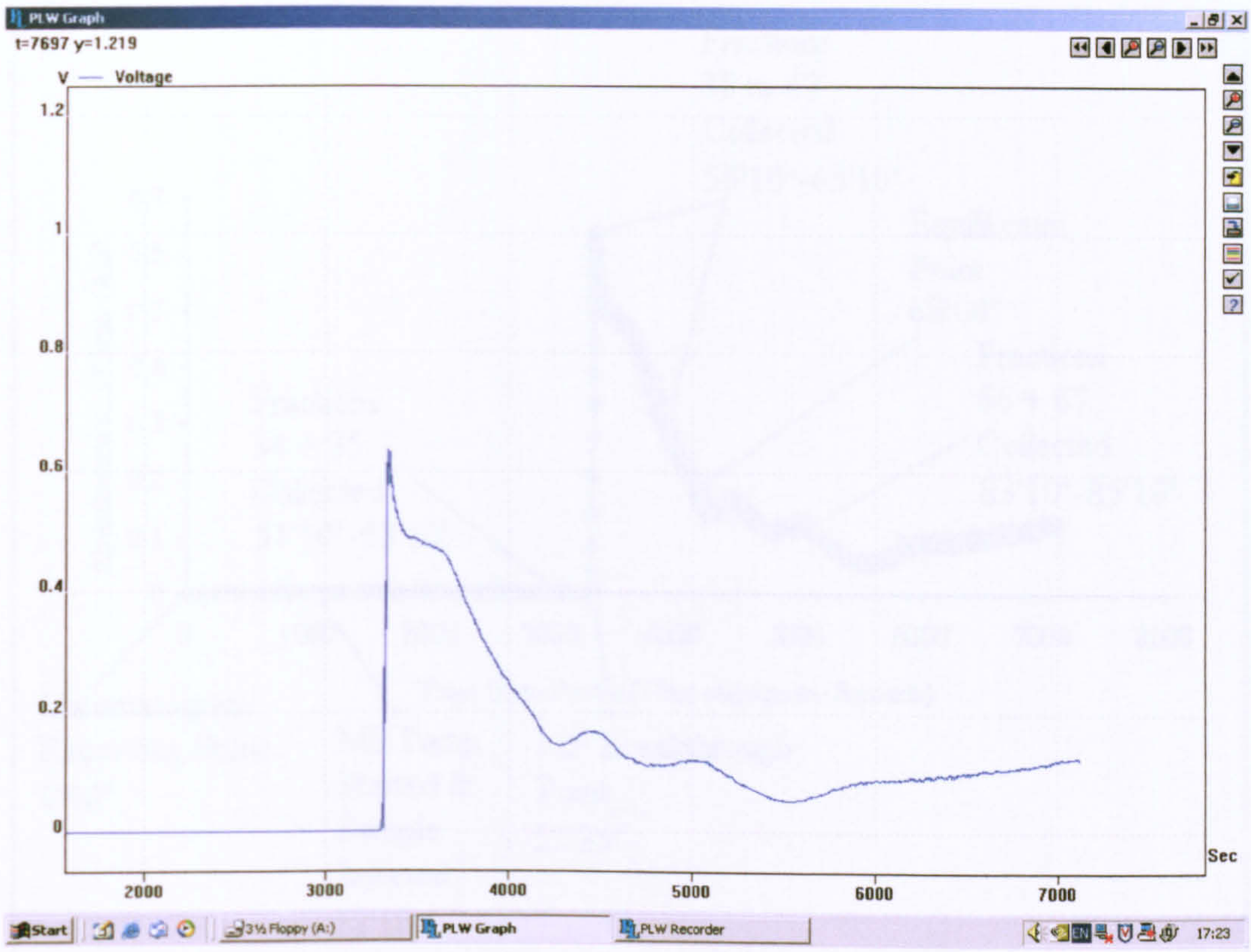

Figure 6.3.4a: Screen capture of the chromatogram produced by the Picolog software from the purification of PMI using the CPC centrifuge.

Experimental timings were recorded as follows (taking the start of chromatogram recording as 0' 00"):

- MP breakthrough point: 55' 25" ≡ 3325"
- Volume of SP collected at MP breakthrough point: 349 ml
- Equilibrium point: 68' 00" ≡ 4080"
- Volume of SP collected at equilibrium point: 373 ml

The data from the UV detector was further analysed using Windows "Excel" software, reproducing the chromatogram that was then annotated to indicate the position of critical time points during the experiment (Figure 6.3.4b).

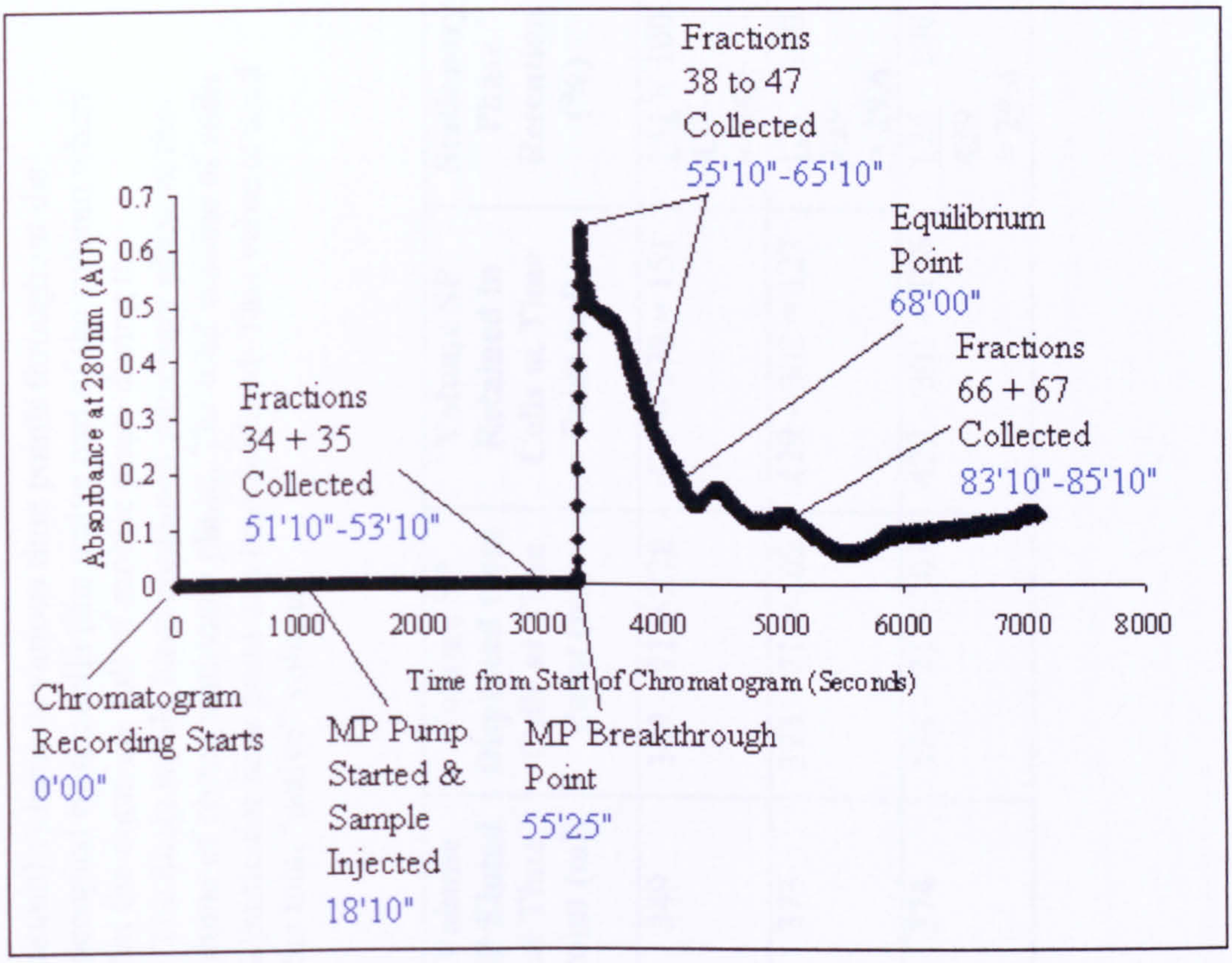

Figure 6.3.4b: Chromatogram created from data recorded during the purification of PMI using the CPC centrifuge. The figures in blue type are the timings of important events that occurred during the experiment.

The stationary phase retention was calculated from the volume of stationary phase that had eluted from the column at a certain time points during the experiment (Table 6.3.4a).

Table 6.3.4a: Stationary phase retention as a percentage of total cell (or column) volume at various time points throughout the experiment. The total volume of the centrifuge is divided into the volume occupied by the cells (the active part of the column where separation takes place) and the ducts that connect the cells (it is assumed that the ducts are full of mobile phase during the experiment, and are inactive as far as the separation process is concerned). The ducts would have contained stationary phase at the start of the experiment, the volume of which must be deducted from the volume of eluted stationary phase. The total volume of cells is known, therefore the volume of stationary phase retained in the cells at a particular time point can be calculated. This value is used to give the stationary phase retention at that time point as a percentage of the total "active" volume.

Time Point	Total Volume of CPC Centrifuge (ml)	Total Volume Cells in CPC Centrifuge (ml)	Total Volume Ducts in CPC Centrifuge (ml)	Volume SP Eluted at Time Point (ml)	Volume SP Displaced from Cells at Time Point (ml)	Volume SP Retained in Cells at Time Point (ml)	Stationary Phase Retention (%)
MP breakthrough point	500	429	71	349	349 – 71 = 278	429 – 278 = 151	$\frac{151}{429} \times 100$ = **35.2**
Equilibrium point	500	429	71	373	373 – 71 = 302	429 – 302 = 127	$\frac{127}{429} \times 100$ = **29.6**
End of experiment	500	429	71	374	374 – 71 = 303	429 – 303 = 126	$\frac{126}{429} \times 100$ = **29.4**

6.3.5. Analysis of Fractions: Measurement of PMI Activity

A standard curve was created from the change in absorbance at wavelength 340 nm per minute for each standard solution of PMI; concentrations used were between 0.0005 $mgml^{-1}$ and 0.5 $mgml^{-1}$ (Figure 6.3.5a).

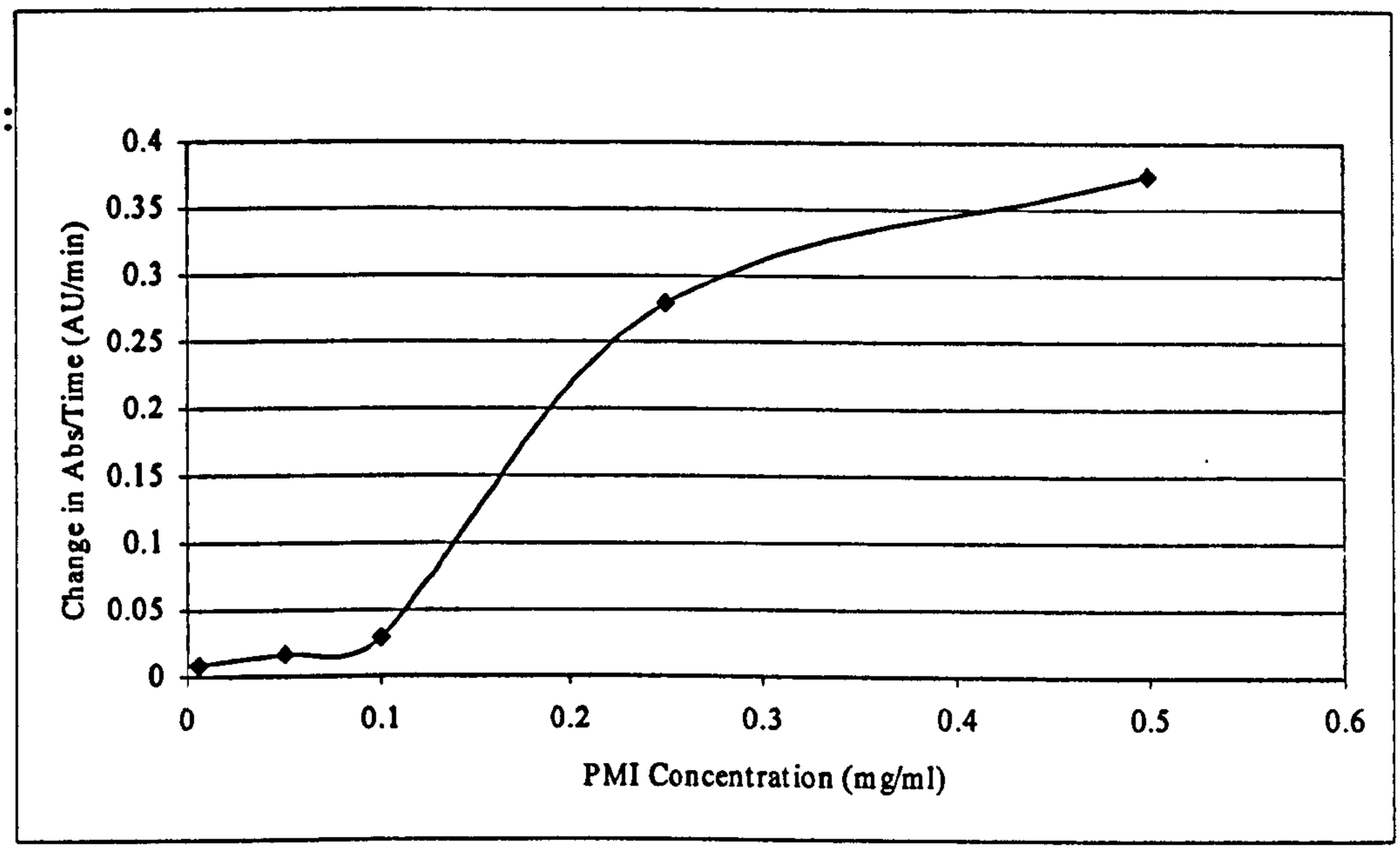

Figure 6.3.5a: Change of absorbance at 340 nm over time ($AUmin^{-1}$) for PMI standard solutions of concentrations 0.005 $mgml^{-1}$ to 0.5 $mgml^{-1}$.

It can be concluded from Figure 6.3.5a that the linear range of the standard curve was between the PMI concentrations of 0.1 $mgml^{-1}$ (0.02861 $AUmin^{-1}$) and 0.25 $mgml^{-1}$ (0.279 $AUmin^{-1}$).

This information was used to determine which fractions had an active PMI concentration that was outside the linear range, and the PMI activity was calculated for each fraction:

$$\text{PMI activity in } Uml^{-1} = \frac{[\text{Change in } A_{340}/\text{min}] \times [1000\ \mu l/\text{Cuvette sample in } \mu l]}{\text{Absorption coefficient for PMI}}$$

[Equation 6.3.5a]

Cuvette sample volume = 1000 µl
Absorption coefficient for PMI = 6.2

The results are shown in Table 6.3.5a.

Table 6.3.5a: Concentration of PMI activity present in selected fractions and the loading sample from the CPC stage of PMI purification. Those fractions marked with an * had a PMI activity level below the linear range on the standard curve. No fractions had a PMI activity level above the linear range on the standard curve. N/A = Not applicable

Fraction or Loading Sample Name	Change in A_{340} over Time ($AUmin^{-1}$)	PMI Activity (Uml^{-1})	Dilution	PMI Activity – Corrected for Dilution (Uml^{-1})	Fraction or Loading Sample Volume (ml)	PMI Activity (Units)
Blank	0	0	N/A	0	N/A	0
34 + 35 (34)*	0.0003126	0.000050419	Neat	0.00	19.0	0
36 + 37 (36)*	0.002395	0.00038629	Neat	0.00	18.9	0
38 + 39 (38)	0.2423	0.039080645	1 in 100	3.91	18.6	72.73
40 + 41 (40)	0.1976	0.031870968	1 in 100	3.19	18.8	59.97
42 + 43 (42)	0.2221	0.035822581	1 in 100	3.58	18.2	65.16
44 + 45 (44)	0.1156	0.018645161	1 in 100	1.86	18.4	34.22
46 + 47 (46)	0.09429	0.015208065	1 in 40	0.61	18.4	11.22
48 + 49 (48)*	0.02627	0.004237097	1 in 40	0.17	18.3	3.11
50 + 51 (50)	0.1065	0.017177419	Neat	0.02	18.6	0.37
52 + 53 (52)	0.03586	0.005783871	Neat	0.01	18.5	0.19
54 + 55 (54)*	0.01429	0.002304839	Neat	0.00	18.5	0
56 + 57 (56)*	0.007027	0.001133387	Neat	0.00	18.75	0
58 + 59 (58)*	0.00402	0.000648387	Neat	0.00	18.6	0
Total				**13.35**		**246.97**
66 + 67 (66)*	0.001725	0.000278226	Neat	0.00		0
Loading Sample	0.2111	0.034048387	1 in 200	**6.81**	43.0	**292.83**

From the data in Table 6.3.5a:

$$\text{Percentage recovery active PMI} = \frac{\text{Total PMI Activity in Fractions}}{\text{PMI Activity in Loading Sample}} \times 100$$

$$= \frac{246.97}{292.83} \times 100$$

$$= \mathbf{84\%}$$

6.3.6. Analysis of Fractions: Measurement of Total Protein Concentration

A standard curve was created from the change in absorbance at wavelength 595 nm for each standard solution of BSA; concentrations used were between 0.25 $mgml^{-1}$ and 1.5 $mgml^{-1}$ (Figure 6.3.6a).

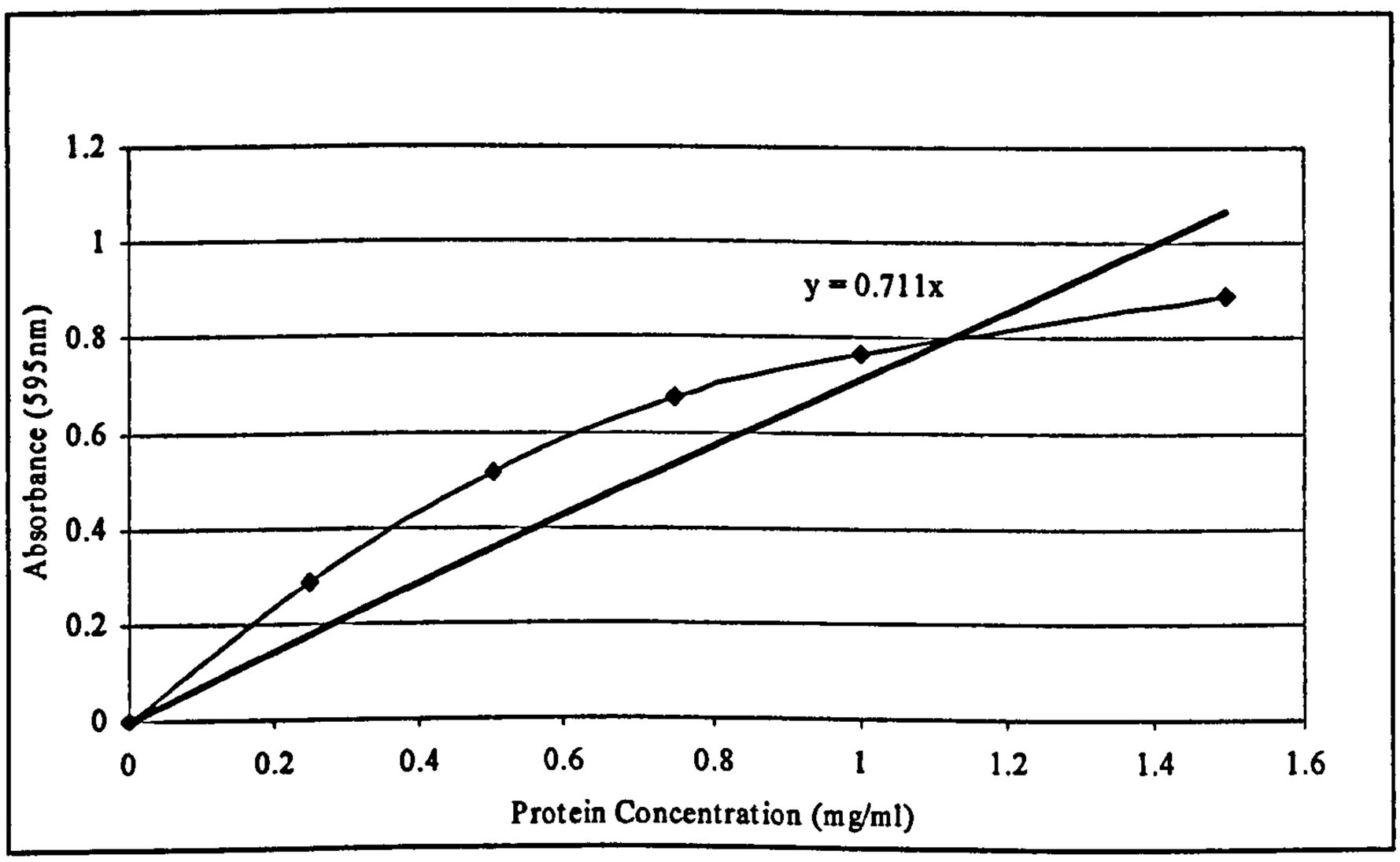

Figure 6.3.6a: Graph of absorbance at 595 nm against concentration of protein ($mgml^{-1}$) for BSA standard solutions made with the upper phase of a 12.5% w/w PEG-1000: 12.5% w/w K_2HPO_4 ATPS.

The equation of the straight line in this graph was $y = 0.711 \times x$. This equation was used to calculate the total protein concentration in each fraction, and if the fraction had been diluted, a calculation made to give the total protein concentration in the undiluted fraction. This figure was then multiplied by the volume of the fraction, to give the mass of total protein in each fraction (Table 6.3.6a).

Table 6.3.6a: Details of total protein present in the fractions and the loading sample from the CPC stage of PMI purification. N/A = not applicable. L/S = loading sample.

Fraction or Loading Sample Name	Conc^{n} Total Protein (mgml^{-1})	Dilution	Conc^{n} Total Protein – Corrected for Dilution (mgml^{-1})	Fraction or Sample Volume (ml)	Mass Total Protein (mg)
Blank	0	N/A	0	N/A	0
34 + 35 (34)	0.00141	Neat	0.00141	19.0	0
36 + 37 (36)	0	Neat	0	18.9	0
38 + 39 (38)	0.39944	1 in 10	3.99437	18.6	74
40 + 41 (40)	0.34599	1 in 10	3.45992	18.8	65
42 + 43 (42)	0.30380	1 in 10	3.03797	18.2	55
44 + 45 (44)	0.20816	1 in 10	2.08158	18.4	38
46 + 47 (46)	0.07032	1 in 10	0.70323	18.4	13
48 + 49 (48)	0.09001	1 in 10	0.90014	18.3	16
50 + 51 (50)	0.13924	Neat	0.13924	18.6	3
52 + 53 (52)	0.09986	Neat	0.09986	18.5	2
54 + 55 (54)	0.09142	Neat	0.09142	18.5	2
56 + 57 (56)	0.07173	Neat	0.07173	18.75	1
58 + 59 (58)	0.06892	Neat	0.06892	18.6	1
60 + 61 (60)	0.04923	Neat	0.04923	18.7	1
62 + 63 (62)	0.02813	Neat	0.02813	18.5	1
64 + 65 (64)	0.03797	Neat	0.03797	18.5	1
66 + 67 (66)	0.02672	Neat	0.02672	18.5	0
68 + 69 (68)	0.02532	Neat	0.02532	18.5	0
70 + 71 (70)	0.02532	Neat	0.02532	18.4	0
72 + 73 (72)	0.02532	Neat	0.02532	18.4	0
74 + 75 (74)	0.01828	Neat	0.01828	18.8	0
76 + 77 (76)	0.01828	Neat	0.01828	19.0	0
Total					**273**
L/S	0.53446	1 in 10	5.34459	43.0	230

$$\text{Percentage recovery total protein} = \frac{\text{Mass Total Protein in Fractions}}{\text{Mass Total Protein in Loading Sample}} \times 100$$

[Equation 6.3.6a]

$$= \frac{273}{230} \times 100$$

$$= \mathbf{119\%}$$

This result indicates that there was complete recovery of protein from the CPC centrifuge.

6.3.7. Analysis of Fractions: Calculation of Specific Activity

The specific activity of PMI in each fraction was calculated from the values for PMI activity and total protein concentration using the equation:

$$\text{Specific activity} = \frac{\text{PMI activity in fraction (Uml}^{-1}\text{)}}{\text{Conc}^{n}\text{ total protein in fraction (mgml}^{-1}\text{)}}$$

[Equation 6.3.7a]

This gave an indication of how much of the protein in each fraction was active PMI, and therefore a measure of the purity of PMI in that fraction. These results are shown in Table 6.3.7a.

Table 6.3.7a: Specific activity in selected fractions and the loading sample from the CPC stage of PMI purification.

Fraction or Loading Sample Name	PMI Activity – Corrected for Dilution (Uml^{-1})	$Conc^{n}$ Total Protein – Corrected for Dilution ($mgml^{-1}$)	Specific Activity (Umg^{-1})	Purification Factor*
Blank	0	0	0	0
34 + 35 (34)	0.00005	0.00141	0.04	0.03
36 + 37 (36)	0.00039	0	0	0
38 + 39 (38)	3.90806	3.99437	0.98	0.77
40 + 41 (40)	3.18710	3.45992	0.92	0.72
42 + 43 (42)	3.58226	3.03797	1.18	0.93
44 + 45 (44)	1.86452	2.08158	0.90	0.71
46 + 47 (46)	0.60832	0.70323	0.87	0.69
48 + 49 (48)	0.16948	0.90014	0.19	0.15
50 + 51 (50)	0.01718	0.13924	0.12	0.09
52 + 53 (52)	0.00578	0.09986	0.06	0.05
54 + 55 (54)	0.00230	0.09142	0.03	0.02
56 + 57 (56)	0.00113	0.07173	0.02	0.02
58 + 59 (58)	0.00065	0.06892	0.01	0.01
66 + 67 (66)	0.00028	0.02672	0.01	0.01
Loading Sample	6.80968	5.34459	**1.27**	N/A

$$\text{* Purification Factor} = \frac{\text{Specific Activity in Fraction}}{\text{Specific Activity in Loading Sample}}$$

[Equation 6.3.7b]

The results in Table 6.3.7a show that the majority of the active PMI enzyme is in fractions 38 to 47.

The PMI activity and concentration of total protein in the selected fractions were plotted (Figure 6.3.7a), giving the elution profile of the PMI and total protein from the CPC loading sample. This graph also indicates how the concentration of active PMI relates to the concentration of total protein during the elution process. The active PMI elutes at approximately the same time as the contaminant proteins from the loading sample (co – elution), and therefore there appear to be little separation of the PMI from these other proteins.

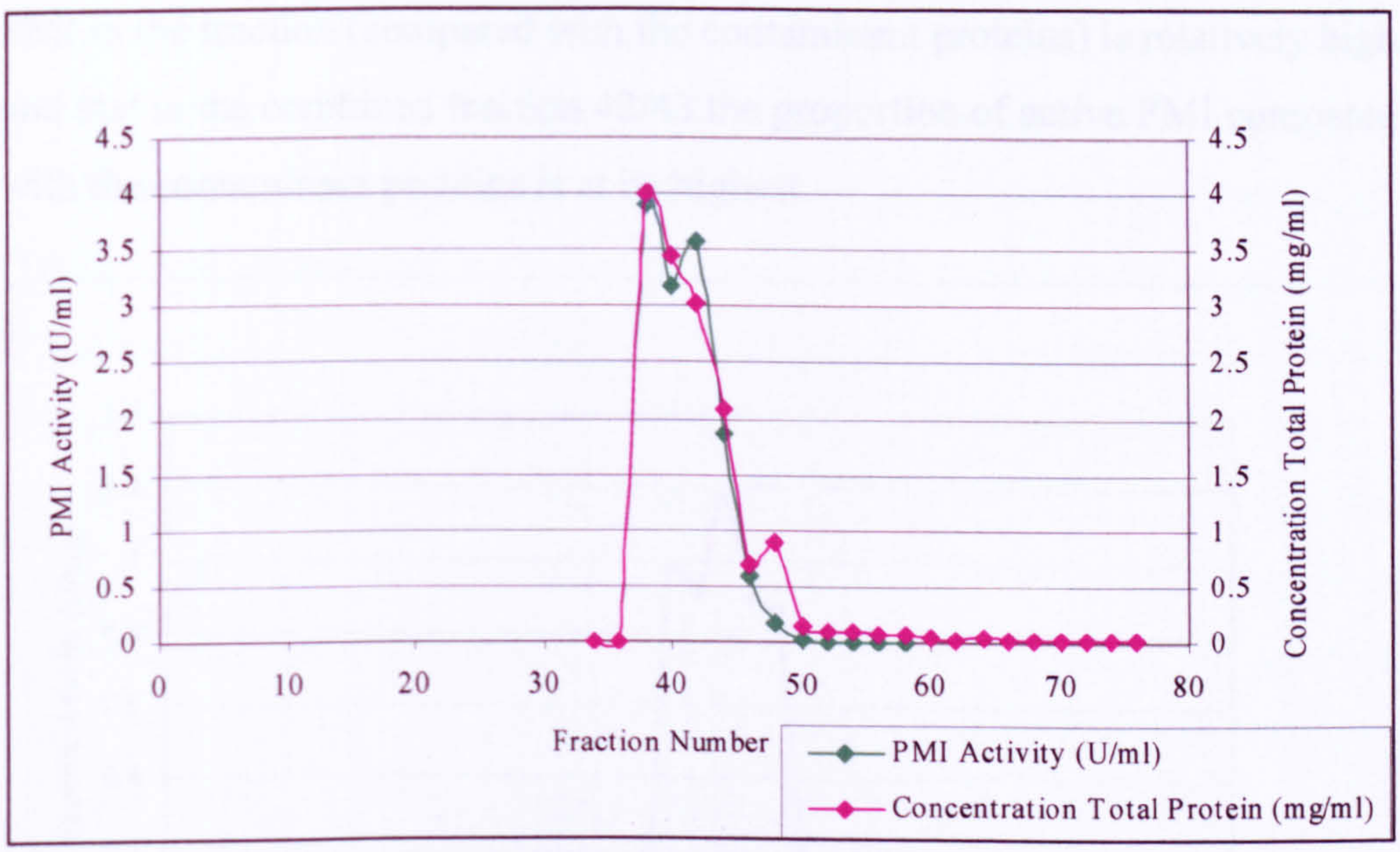

Figure 6.3.7a: PMI activity and concentration of total protein in selected fractions from the CPC stage of PMI purification.

The fraction containing both the highest PMI activity (~4.0 Uml^{-1}) and concentration total protein (~4.0 $mgml^{-1}$) was fraction 38/39.

If the elution profile in Figure 6.3.7a is compared with the chromatogram from the experiment (Figure 6.3.4b), it can be seen that fraction 38/39 was collected just as the mobile phase breakthrough point occurred. A large proportion of the first and largest peak on the chromatogram relates to the elution of fractions 40/41, 42/43, 44/45 and 46/47. The second and third peaks on the chromatogram do not appear to relate to the elution profile of the proteins as shown in Figure 6.3.7a. It is possible that these smaller peaks were caused by the simultaneous elution of stationary phase with the mobile phase (stationary phase "stripping"), producing a turbidity in the eluent that was detected by the UV detector. The presence of suspected artefact peaks on a chromatogram illustrates the importance of

collecting the eluent as fractions for analysis using other methods, rather than relying solely on the information obtained from an on – line UV detector.

The data can also be plotted as the specific activity in the selected fractions (Figure 6.3.7b) to show how the proportion of active PMI compared with total protein changed during the elution process. This graph indicates that there are five fractions: 38/39, 40/41, 42/43, 44/45 and 46/47 where the proportion of active PMI in the fraction (compared with the contaminant proteins) is relatively high, and that in the combined fraction 42/43 the proportion of active PMI compared with the contaminant proteins is at its highest.

Figure 6.3.7b: Specific activity in selected fractions from the CPC stage of PMI purification.

6.3.8. Analysis of Fractions: Gel Imaging and Densitometry

The image obtained from scanning the SDS-PAGE gels is shown in Figure 6.3.8a.

A large dark band at 50 kDa in the pure PMI control lane indicates the position of the pure PMI; however it is interesting to note that this lane also contains four lighter bands, indicating at least four other proteins of differing molecular weights were present in the purified PMI sample supplied by Syngenta.

No bands are visible in lanes 34/35 and 36/37, indicating that these fractions did not contain detectable quantities of protein. Lanes 38/39, 40/41 and 42/43 each have a large dark band at the 50 kDa position, implying that these fractions have

relatively large quantities of PMI. The presence of ten to twelve other bands of varying intensities in each of these lanes indicates that these three fractions also contain several contaminant proteins, although they are present in smaller quantities than the PMI. Lanes 44/45 and 46/47 both contain a light band at the 50 kDa position, whilst the lane for fractions 48/49 has a barely visible band in the same position. Lanes 50/51 to 61/62 each contain four or five bands of varying intensities, one of which appears to be at the 50 kDa position, but these are barely visible. The presence of other, darker bands in each lane indicates that these fractions contain four or five contaminant proteins in greater quantities than PMI. The lane containing the loading sample does not have any visible bands. The likely cause of this was that the loading sample was too dilute for the proteins it contained to be visible on the gel. The loading sample was reanalysed, following the method detailed in Section 6.2.10, but omitting the trichloroacetic acid precipitation stage. The TCA precipitation stage was not required, as the pellet was re – suspended in buffer, not upper phase, and so there was no PEG present in the sample. Some of the pellet from the initial ammonium sulphate precipitation stage was re – suspended in 50 mM Tris buffer, and four volumes (estimated to contain 5, 10, 15 and 20 μg) total protein were subjected to SDS-PAGE. The result can be seen in Figure 6.3.8c.

Densitometry analysis was carried out on the gels as in Section 6.2.11, and the results reported in Table 6.3.8b.

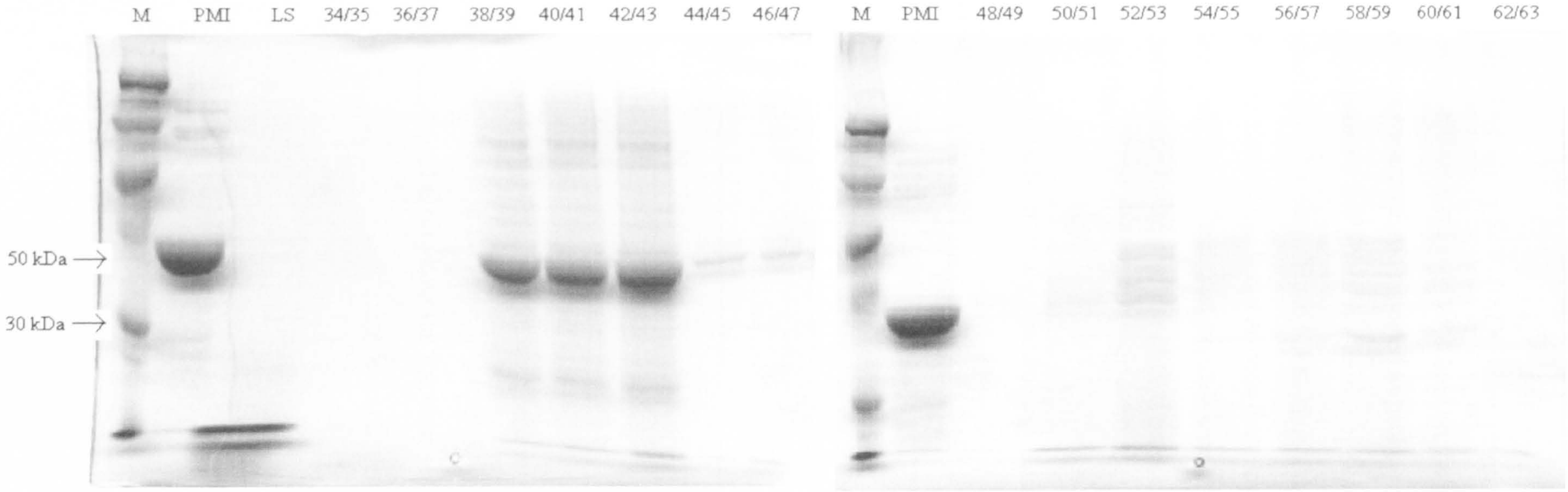

Figure 6.3.8a: Image of SDS-PAGE gel loaded with fractions 34/35 to 62/63 from the CPC stage of PMI purification. M = Molecular size marker. PMI = Pure PMI solution (Syngenta); concentration = 5.0 $mgml^{-1}$. LS = CPC loading sample.

The results obtained by SDS-PAGE were quantified using densitometry. The densitometry software scanned each lane on the gel. The intensity of bands in each lane was measured and reported as peaks on a graph. The area under each peak was calculated and given as a percentage of the total area under all peaks corresponding to that lane. Table 6.3.8a shows the data from the densitometry analysis of fraction 40/41; it can be seen that band/peak number 6 had the greatest percentage peak area. Band/peak number 6 was at the 50 kDa position on the gel, which corresponds to the position of PMI on the gel. Therefore, it can be concluded that the PMI in fraction 40/41 had a purity of 85.7%.

Table 6.3.8a: Results from the densitometry analysis of fraction 40/41.

Band/Peak Number	Peak Area	Peak Area (%)
1	582.7	4.7
2	242.6	1.9
3	9.5	0.1
4	142.4	1.1
5	28.3	0.2
6	10681.0	85.7
7	37.9	0.3
8	358.8	2.9
9	236.5	1.9
10	150.3	1.2
Total	**12470.0**	**100.0**

The peak area for the PMI band in each lane was plotted as a percentage of the total area of all bands in that lane (Figure 6.3.8b). This gives an indication of how PMI was distributed throughout the fractions collected during the experiment.

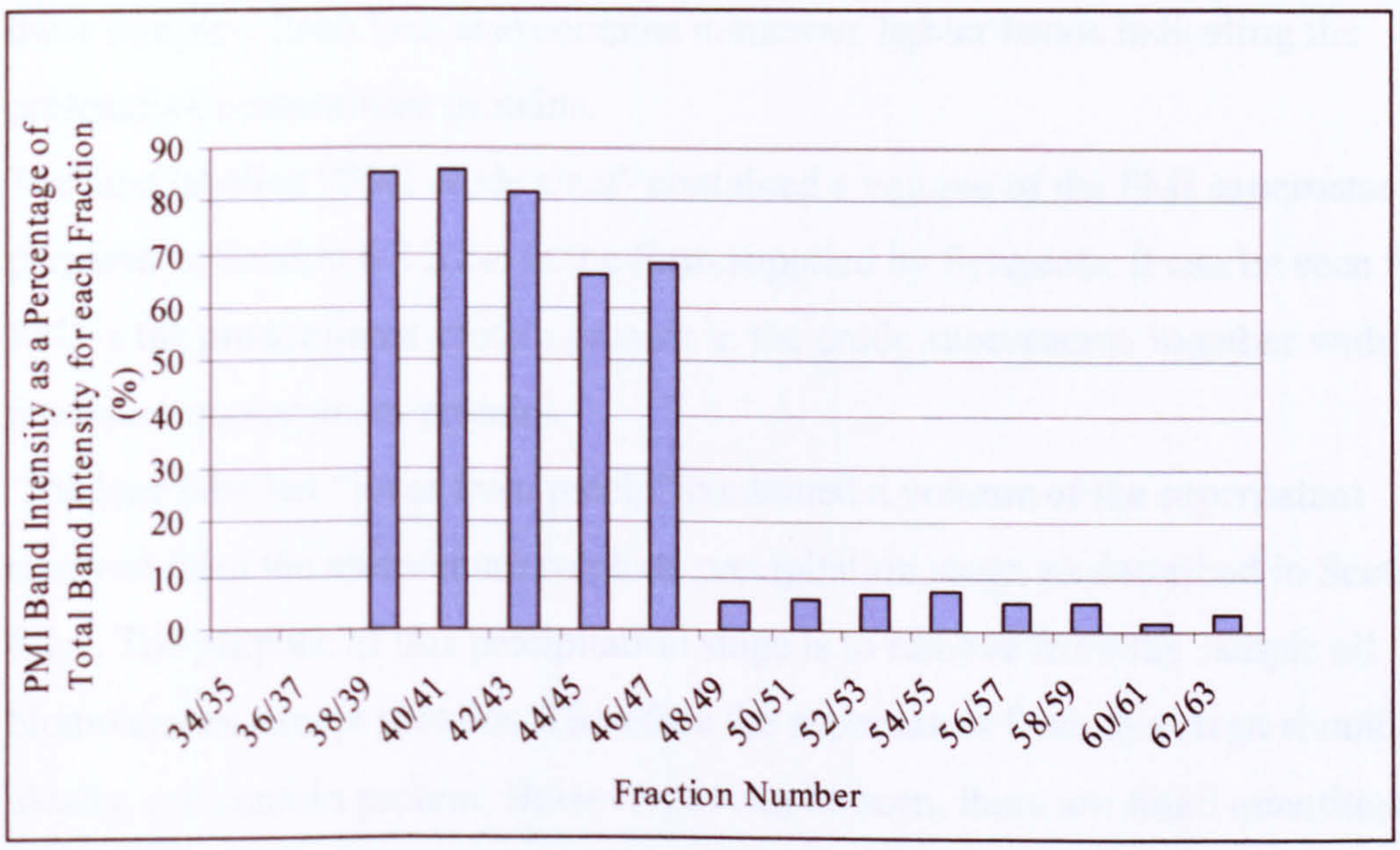

Figure 6.3.8b: PMI band intensity as a percentage of the total band intensity for each CPC fraction subjected to SDS-PAGE and densitometry analysis.

The lane corresponding to the CPC loading sample in the previous gel (Figure 6.3.8a) did not contain any bands; the likely cause was that the loading sample was too dilute for the proteins it contained to be visible on the gel. As previously stated, the loading sample was reanalysed by SDS-PAGE, and the image obtained from scanning these gels is shown in Figure 6.3.8c. A large dark band at 50 kDa in the pure PMI control lane indicates the position of the pure PMI; however it is interesting to note that this lane also contains a number of lighter bands, indicating the presence of other proteins of differing molecular weights in the purified PMI sample supplied by Syngenta.

The lane labelled "5 μg" contained a volume of the CPC loading sample sufficient to give an estimated 5 μg total protein in that lane. It can be seen that the darkest band in the lane is present at the 50 kDa position, indicating that the predominant protein present in this sample was PMI. The lane also contains numerous lighter bands, indicating the presence of contaminant proteins that are present in smaller quantities than the PMI protein.

The lanes labelled "10 μg", "15 μg" and "20 μg" contained volumes of the CPC loading sample sufficient to give an estimated 10, 15 and 20 μg total protein in those lanes, respectively. Like the "5 μg" lane, the darkest band in each lane is present at the 50 kDa position, indicating that PMI was the predominant protein in

these samples. Each lane also contains numerous lighter bands indicating the presence of contaminant proteins.

The lane labelled "PMI crude s/nat" contained a volume of the PMI supernatant as prepared in Section 6.2.2 *i.e.* in the form supplied by Syngenta. It can be seen that PMI is the predominant protein present in the crude supernatant, together with numerous contaminant proteins.

The lane labelled "S/nat from precip" contained a volume of the supernatant reserved from the ammonium sulphate precipitation stage, as described in Section 6.2.5. The purpose of this precipitation stage is to remove from the sample all biomolecules except proteins. Therefore the supernatant from this stage should, ideally, not contain protein. However, as can be seen, there are small quantities of some proteins present in the supernatant. It is interesting to note that the band at the 50 kDa position is not the darkest band in this lane. This indicates that although the ammonium sulphate precipitation did cause some loss of PMI, there was a proportionally greater loss of a contaminant protein from the sample *i.e.* the ammonium sulphate precipitation partly purified the crude supernatant by removing an unwanted contaminant protein. This result is shown numerically in Table 6.3.8b, indicated by an asterisk (*).

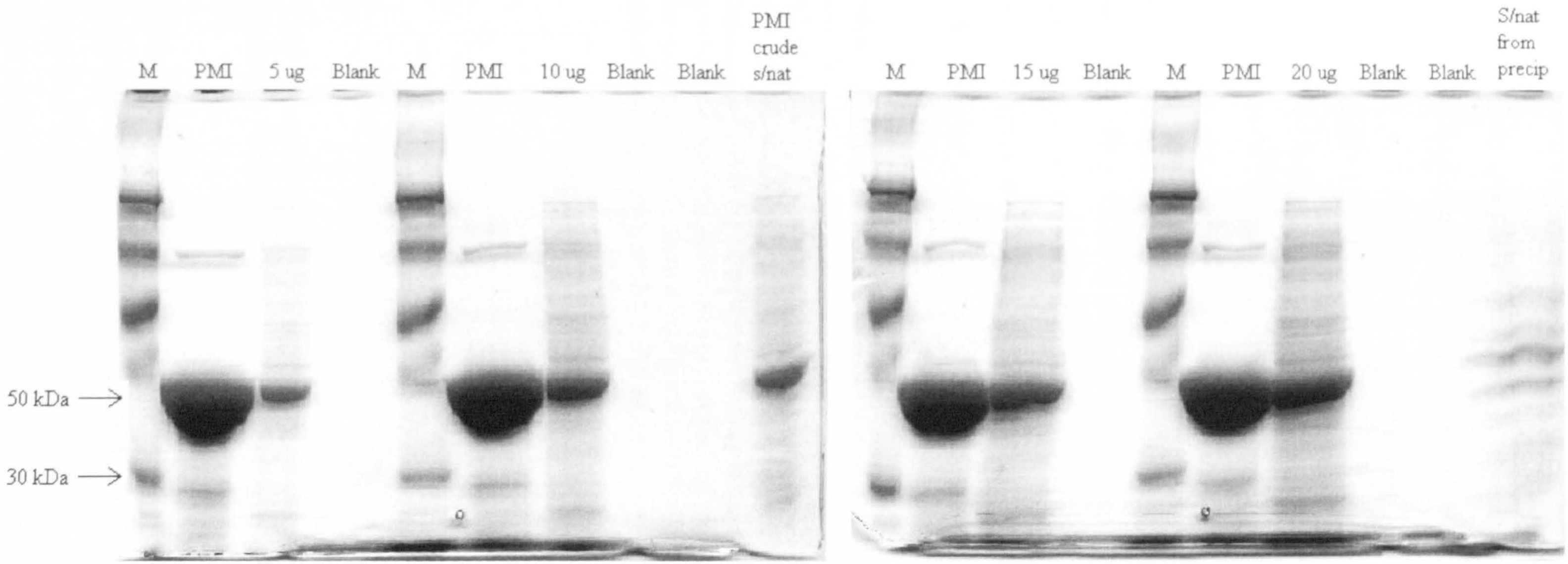

Figure 6.3.8c: Image of SDS-PAGE gels loaded with increasing volumes of the CPC loading sample. The CPC loading samples contained approximately 5 µg, 10 µg, 15 µg and 20 µg total protein. PMI crude s/nat = the PMI supernatant as prepared in Section 6.2.2. S/nat from precip = the supernatant retained from the ammonium sulphate precipitation stage (Section 6.2.5).
M = Molecular size marker. PMI = Pure PMI solution (Syngenta); concentration = 5.0 $mgml^{-1}$. Blank = Lane not used.

The gel shown in Figure 6.3.8c was also subjected to quantitative densitometry analysis. It was the intention to analyse all the lanes on the gel, unfortunately the software used was not able to produce a result for the lanes containing pure PMI solution (labelled "PMI" on the gel), nor the lane containing the CPC loading sample of approximately 15 µg total protein. It is postulated that the large band present at the 50 kDa position in each of these lanes disrupted the analysis by the software.

The peak area of the band located at the 50 kDa position in each relevant lane is shown in Table 6.3.8b. The peak area is reported as a percentage of the total area under all peaks in that lane. The number of bands detected by the software in each lane is also shown; this gives an indication of the number of other (contaminant) proteins present in the sample.

Table 6.3.8b: Results from the densitometry analysis of the CPC loading sample from the CPC stage of PMI purification using SDS-PAGE. Samples 5 µg, 10 µg and 20 µg refer to increasing volumes of the CPC loading sample analysed by SDS-PAGE, so that the samples were estimated to contain 5, 10 and 20 µg total protein respectively. The peak area is the peak area of the band at the 50 kDa position in each lane, given as a percentage of the total peak areas in that lane. The number of bands in that lane gives an indication of the number of contaminant proteins present in that sample.

Sample	Peak Area (%)	Number of Bands Detected in Lane
5 µg	74.0	38
10 µg	64.7	37
20 µg	64.8	23
PMI crude s/nat	53.7	29
S/nat from precip	27.4*	14

* This was the second – highest percentage peak area value for this lane; the highest was 43.8% for a protein with a slightly greater molecular weight than PMI.

The results in Table 6.3.8b show that there is an increase in the percentage peak area of PMI in the loading sample(s) when compared with the percentage peak area of PMI in the PMI crude supernatant sample. It can therefore be concluded that the ammonium sulphate precipitation stage did partially purify the PMI by between 11.0% and 20.3%.

The discrepancy in the number of bands (and therefore number of proteins) in the 5, 10 and 20 μg CPC samples can be explained by band merging; in the 20 μg sample, the larger quantities of protein means that the bands in that lane start to merge together, thus decreasing the number of visible bands. This leads to a decreased number of proteins being detected, despite still being present in the sample.

The effectiveness of the CPC stage in the purification of PMI can be assessed by comparing the percentage peak area of the PMI in the CPC fractions when subjected to SDS-PAGE with that of the CPC loading sample. Table 6.3.8a shows that the PMI in fraction 40/41 (the fraction with the greatest purity of PMI) had a percentage peak area of 85.7%. Table 6.3.8b shows that the PMI in the CPC loading sample had a percentage peak area of between 64.7% and 74.0%. This means that the purification of the PMI achieved by the CPC stage was between approximately 11.7% and 21.0%.

6.4. Conclusions

The recovery of active PMI enzyme from the CPC process was a reasonable 84%, and the recovery of total protein was 119%. This last figure shows that proteins did not adhere to the internal surfaces of the CPC centrifuge.

It can be concluded from the SDS-PAGE of the fractions (Figure 6.3.8a) that the majority of the PMI protein has eluted in three fractions collected soon after the mobile phase breakthrough point; this was as expected, given that the Distribution Ratio for PMI in this phase system had a value of 10. Very small quantities of PMI, together with various contaminant proteins, eluted over the following 18 minutes of the experiment. This indicates that there has been some purification of the PMI protein away from the contaminant proteins. However, the three PMI fractions also contain some contaminant proteins. This conclusion is strengthened by the results from the densitometry of these gels (Figure 6.3.8b).

It can be concluded from the SDS-PAGE of the loading sample (Figure 6.3.8c) that the ammonium sulphate precipitation step did itself partially purify the PMI. It can also be concluded from comparing the SDS-PAGE gel densitometry data of the fractions and the CPC loading sample that CPC was successful to a degree in the purification of PMI from its fermentation supernatant.

However, the current methods used by Syngenta produce PMI with a purity of 98.5%; the CPC stage, whilst replacing the two solid – liquid stages of chromatography used by Syngenta with one liquid – liquid chromatography stage produced PMI with a maximum purity of only 85.7%.

It may be possible to enhance this figure by selecting a different ATPS that provides better separation of the PMI away from the contaminant proteins.

Analysis of fractions by SDS-PAGE and densitometry has limitations. For example, the method distinguishes proteins only according to their molecular size or weight, and co – migrating proteins are not distinguished from one another *i.e.* a band on the gel may contain more than one protein of the same, or very similar, molecular weight. One way of determining the number of different proteins in a sample would be to employ a technique such as isoelectric focusing, which separates proteins on the basis of size *and* charge. The purpose of this project was to purify one target protein (PMI) from a complex mixture of proteins. It was not deemed necessary to determine the identity of the contaminant proteins, and so

methods such as isoelectric focusing were not employed. It is of course possible that the band at the 50 kDa position contains proteins other than PMI. The specific activity values for fractions where PMI has concentrated indicate that this may be the case.

Chapter 7 – Summary, Discussion and Further Research

7.1. Stationary Phase Retention Studies on J – Type CCC Centrifuges (Chapter 3)

Chapter 3 focussed on the behaviour of a 12.5% w/w PEG-1000: 12.5% K_2HPO_4 aqueous two – phase system in a J – type CCC centrifuge, with the aim of identifying the operational parameters that would yield the greatest stationary phase retention values. This phase system was specifically selected as one which had been extensively studied in other CCC centrifuges; its use here would allow comparisons to be drawn on the performance of different centrifuges. Good stationary phase retention in the column is a requirement for successful chromatographic separations, and previous work in the liquid – liquid chromatography field shows that stationary phase retention varies considerably from system to system. The stationary phase retention in a 1.6 mm bore column fitted to the "MILLI #1" J – type centrifuge was measured at intervals throughout each experiment, thus giving an indication of the stability of the stationary phase within the column over time. The results showed that the conditions giving the highest overall stationary phase retention also caused the largest loss of stationary phase during the experiment, indicating unstable conditions within the column. A set of conditions was identified that gave minimal loss of stationary phase during the experiment, plus moderate overall stationary phase retention; these conditions were selected to take forward into the work to separate a mixture of the proteins lysozyme and myoglobin.

The stationary phase retention of this model aqueous two – phase system was markedly lower than the retention of aqueous – organic phase systems that have previously been studied in these centrifuges. This may be attributed to its lower interfacial tension, its smaller density difference between the two phases, and the greater viscosity of the phases. In particular, the higher viscosity of the PEG – rich phase, coupled with the relatively small bore tubing of the 1.6 mm column may also have influenced the results.

A further investigation to test these hypotheses could examine the stationary phase retention of a number of different aqueous two – phase systems in this centrifuge, using columns of different bore sizes. These different phase systems could be made from PEG of different molecular weights (*e.g.* PEG-600; PEG-

3000; PEG-6000). Such phase systems would have different physicochemical properties from the model system that was used in this study, and such further work would have the potential to identify a phase system that exhibits more favourable stationary phase retention behaviour in the J – type CCC centrifuges.

7.2. Separation of the Proteins Lysozyme and Myoglobin using J – Type CCC Centrifuges (Chapter 4)

The optimal experimental parameters for the operation of a J – type centrifuge that were identified in Chapter 3 were used in this part of the study to separate a mixture of the proteins lysozyme and myoglobin. The distribution ratios of these proteins in this phase system were measured and found to be sufficiently different from each other to allow (in theory) full separation to occur in the CCC process. Columns of bore 2.7 mm and 4.0 mm were used, as it was proposed that increasing column bore would facilitate the mixing and settling process required for good protein resolution.

The variable parameter in these experiments was mobile phase flow rate, which was adjusted to allow for the increase in column bore; all other parameters remained constant between experiments.

It was found that reducing the mobile phase flow rate increased both stationary phase retention and protein resolution; increasing column bore did not increase protein resolution. However, complete separation of the two proteins was not achieved. The proteins tended to elute closer to the $K = 1$ point than their predicted elution points; this indicates insufficient mixing of the proteins in the column. It was considered that the wave – like behaviour of the two phases in the column, as visualised in the work on the spiral coil (Guan *et al*, 2007), was insufficient for the proteins to achieve their theoretical partition coefficients within the column. This factor, combined with the poor stationary phase retention, gave rise to poor protein resolution.

Increasing the mobile phase flow rate did not appear to change the nature of the mixing process within the column. It was considered that increasing the gravitational force on the column (by increasing the rotational speed) might enhance the mixing process, but higher rotational speeds could only be achieved using a specially – designed coil. However, it was decided at this point to put the study of the J – type centrifuges aside in favour of concentrating on a different

type of CCC, namely centrifugal partition chromatography, in which the mixing process was considered to be more effective than that exhibited in the J – type centrifuges.

7.3. Separation of the Proteins Lysozyme and Myoglobin using a CPC Centrifuge (Chapter 5)

The study of the behaviour of lysozyme and myoglobin in two J –type CCC centrifuges showed that this type of centrifuge was unable to resolve a mixture of these proteins. It was thought that the main reason for this was the wave – like interaction of the two phases in the column provided insufficient mixing for protein separation. Another contributory factor was the unstable conditions in the columns led to poor stationary phase retention.

It was considered that these problems could be overcome by using a CPC centrifuge, in which the mobile phase cascades through the stationary phase. This would afford a greater degree of phase mixing than the J – type centrifuge.

The model ATPS used in the stationary phase retention studies and in the J – type centrifuge studies was then employed in a 500 ml capacity column of a CPC centrifuge. The effect of variable parameters such as rotational speed, mobile phase flow rate, type of mobile phase, and loading sample volume were explored, and a set of optimal conditions for protein separation was identified. Baseline separation of the proteins was achieved, with the elution times being as predicted from the theoretical partition coefficients. This was in contrast to the elution of the proteins from the J – type centrifuge, where protein elution was non – theoretical. The optimal conditions for protein separation on the 500 ml CPC centrifuge were applied to a scale – up experiment which also yielded complete protein separation. Overall, the resolution of lysozyme and myoglobin in the CPC centrifuge was superior to that in the J – type centrifuge.

A number of observations can be made on the study of lysozyme and myoglobin in the selected model ATPS when applied to both the J – type and CPC centrifuges.

The first is that lysozyme and myoglobin showed limited solubility in the model phase system. If the concentration of protein exceeded 2.5 $mgml^{-1}$, protein precipitation occurred. This contrasted with previous studies (Ito *et al*, 2003)

where protein concentrations of 20 $mgml^{-1}$ were reported. Such high concentrations, with the possibility of un-dissolved protein, were not used because of concerns this might block the centrifuges and/or ancillary tubing. Ito *et al* used sonication to create high protein concentrations; sonication was not employed because it can cause the denaturation of proteins. However, it is important to find phase systems that can dissolve proteins at higher concentrations, as industry now requires high throughput purification techniques, and so greater protein concentrations in loading samples would almost certainly be a requirement in satisfying this demand.

The wave – like mixing behaviour of the aqueous two – phase system in the J – type centrifuges proved insufficient to allow full separation of the proteins, whereas the cascade mixing featured in the CPC centrifuge resolved the proteins fully.

It was considered that cascade mixing could be created in the J –type centrifuges if they were fitted with toroidal, rather than multi – layer coils. The Brunel team has now designed and produced such a coil. Preliminary results (Guan *et al*, 2008: paper currently under review, refer to Appendix 3) from work using aqueous two – phase systems have given promising separations of the lysozyme/myoglobin mixture with elution times as predicted from the theoretical partition coefficients.

7.4. Purification of Phosphomannose Isomerase using a CPC Centrifuge (Chapter 6)

One objective of this thesis was to attempt the purification of at least one plant – based protein supplied by the industrial sponsor of the study, Syngenta Limited. Retention of biological activity by the protein during the separation process was critically important, as a separation technique that causes significant loss of biological function cannot be employed by industry.

The superior performance of the CPC centrifuge in resolving a mixture of lysozyme and myoglobin made this instrument the best candidate of the two centrifuges to purify phosphomannose isomerase from a fermentation supernatant. The same phase system used in the previous chapters was applied to the PMI purification, as its behaviour in the CPC centrifuge was known from the lysozyme/myoglobin studies. Thus the phase system was not selected to optimise the distribution ratios of the target protein and the contaminant proteins. A

supernatant containing PMI was prepared from cell paste. Preliminary studies showed that this preparation contained contaminants that were causing emulsification of the two – phase system. An ammonium sulphate precipitation step was introduced, and the resulting supernatant, after appropriate dilution, was loaded onto the CPC centrifuge.

The fractions collected were analysed to detect the presence of active PMI and total protein. This showed that the active PMI eluted in a number of fractions, but these fractions also contained other proteins. SDS-PAGE and gel densitometry was also employed in the analysis of the fractions. This showed that the CPC stage produced a purification of between 11% and 21% in one of the fractions; other fractions had much reduced purity. Importantly, the recovery of active enzyme was 84%, demonstrating that this particular enzyme was not damaged by the CPC process.

It can be concluded that the CPC process produced partial purification of the target protein, but it did not isolate PMI to the high level of purity currently achieved by Syngenta using solid – liquid chromatography. However, the phase system used had not been optimised for protein purification, and it is possible that a phase system designed specifically to isolate and purify PMI from the contaminant proteins contained in the fermentation supernatant would enhance the level of purity beyond what was achieved in this study.

7.5. Concluding Remarks

The aim of this thesis was to develop protein separations in aqueous two – phase systems on the Brunel/DE J – type CCC centrifuges. This study has shown that the wave – like mixing generated by these centrifuges, which works effectively for small molecules in aqueous – organic phase systems, is not sufficient to achieve protein separation in aqueous two – phase systems. Application of another type of countercurrent chromatography (CPC), with its cascade phase mixing, gave good protein separation and theoretical behaviour. This experiment was successfully scaled up from a 0.5 litre column to a 12.5 litre column. The same technology was applied to purifying a protein from a cell paste supernatant; this proved to be only marginally successful, although the biological function of the protein was retained.

This study of the performance of the J – type and CPC centrifuges resulted in the design and production of a toroidal coil that was fitted to a Brunel/DE J – type CCC centrifuge. This type of coil offers the advantages of the J – type centrifuge (the column is constructed from a continuous length of tubing, and therefore relatively easy to clean), and the toroidal design produces cascade mixing for effective protein separation.

The use of aqueous two – phase systems in countercurrent chromatography has, like every technique, both advantages and drawbacks. The ability of these phase systems to retain the biological function of proteins is offset by the limited solubility they offer, and phase systems that allow higher protein concentrations will be required for successful, large – scale protein purification.

Appendices

Appendix 1 – Chromatograms and HPLC Graphs from the Separation of the Proteins Lysozyme and Myoglobin using J – Type CCC Centrifuges (Chapter 4)

The chromatograms and HPLC graphs from all the experiments to separate lysozyme and myoglobin in the J – type CCC centrifuges are shown in Figures 1A-a to 1A-j. In all the experiments:

- Rotational speed = 1800 rpm
- LP = MP
- Sample volume = 2.32 ml (5.0% CV)
- Pumping of the mobile phase commenced at time zero.
- The recording of data began at 1.5 minutes.
- The mobile phase breakthrough point caused mixing of the two phases in the eluent that appears as the first peak on the chromatogram (the operator also observed at this point drops of mobile phase eluting from the column together with the stationary phase).
- The sample was injected onto the column after the MP breakthrough point at the time indicated on each chromatogram (the pre – equilibration method).
- Fraction collected commenced immediately, and continued until the end of the experiment.

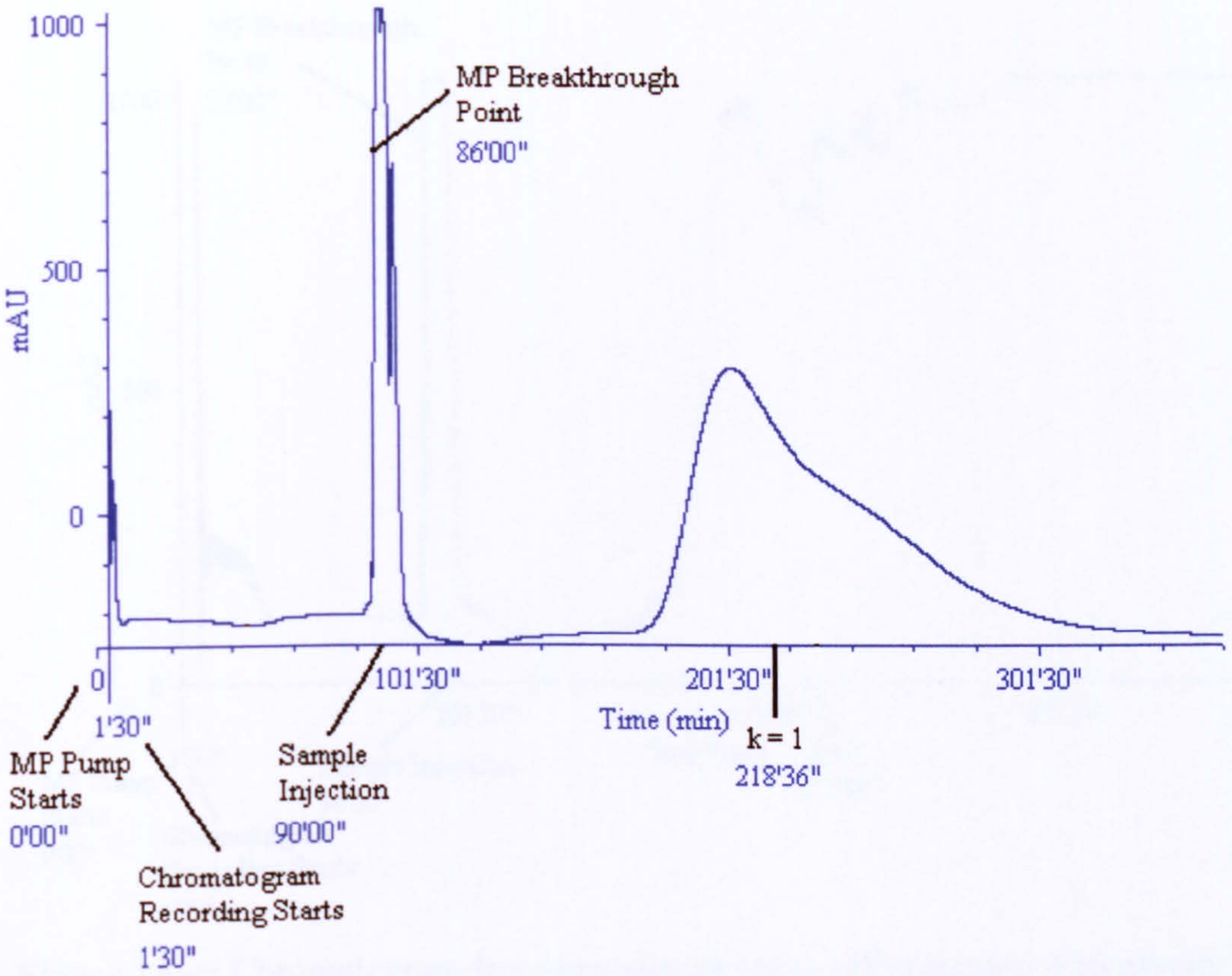

Figure 1A-a (also shown in Figure 4.3.1a): Chromatogram from experiment using MP flow rate 0.36 mlmin^{-1} in the DEM-PRO #1 coil with 2.7 mm bore.

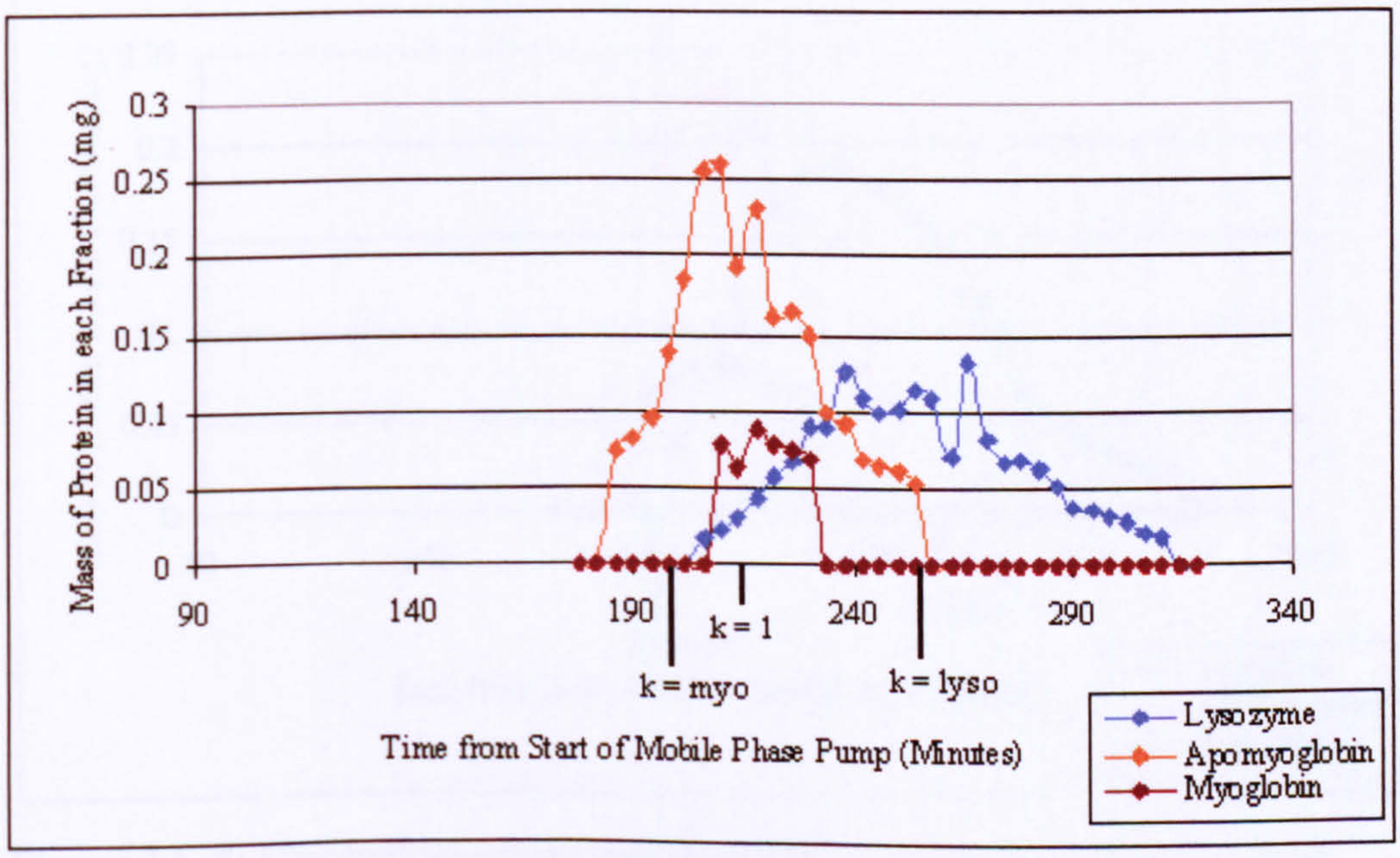

Figure 1A-b (also shown in Figure 4.3.1b): Chromatogram created from HPLC analysis of fractions from experiment using MP flow rate 0.36 mlmin^{-1} in the DEM-PRO #1 coil with 2.7 mm bore.

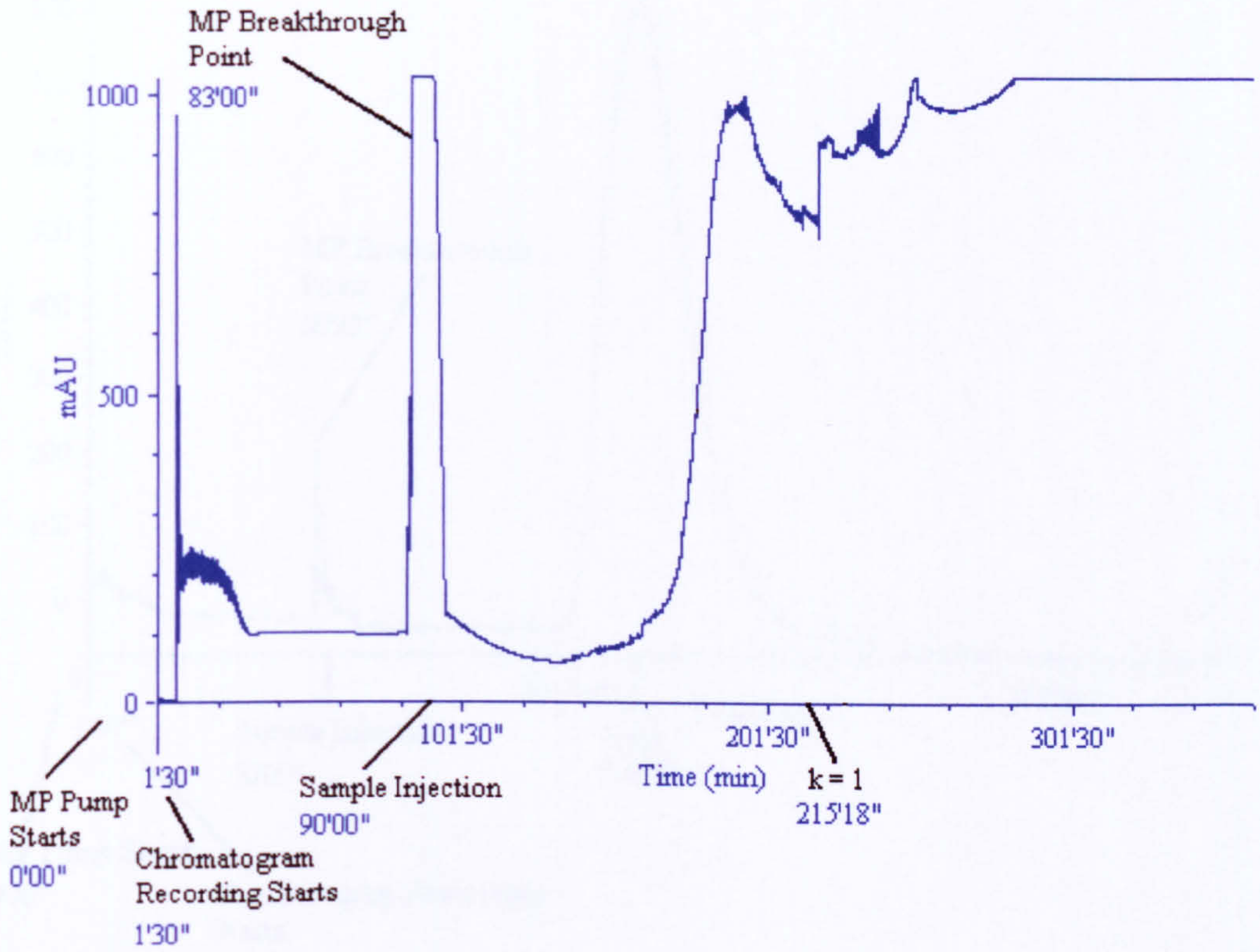

Figure 1A-c: Chromatogram from experiment using MP flow rate 0.36 mlmin^{-1} in the DEM-PRO #2 coil with 2.7 mm bore.

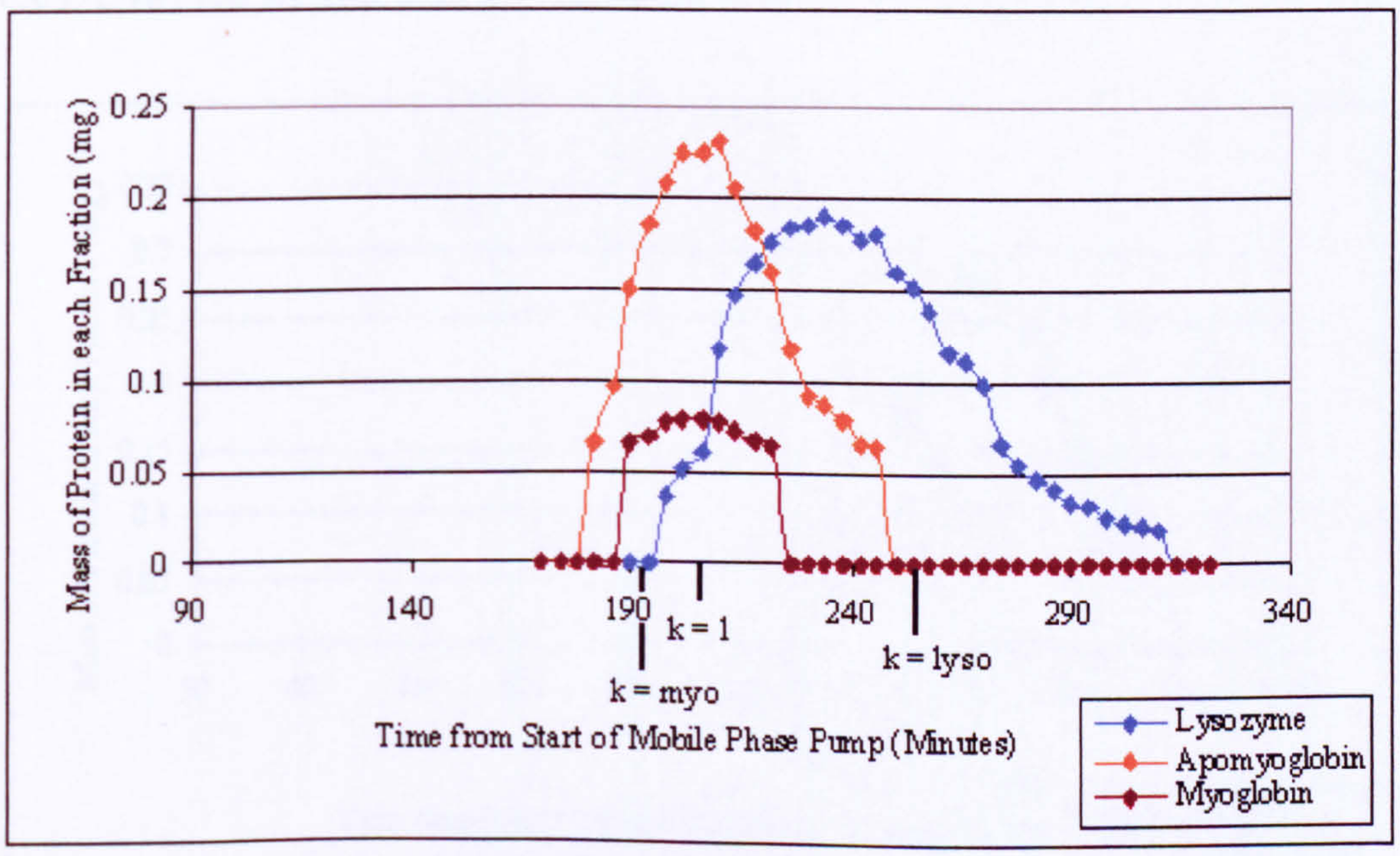

Figure 1A-d: Chromatogram created from HPLC analysis of fractions from experiment using MP flow rate 0.36 mlmin^{-1} in the DEM-PRO #2 coil with 2.7 mm bore.

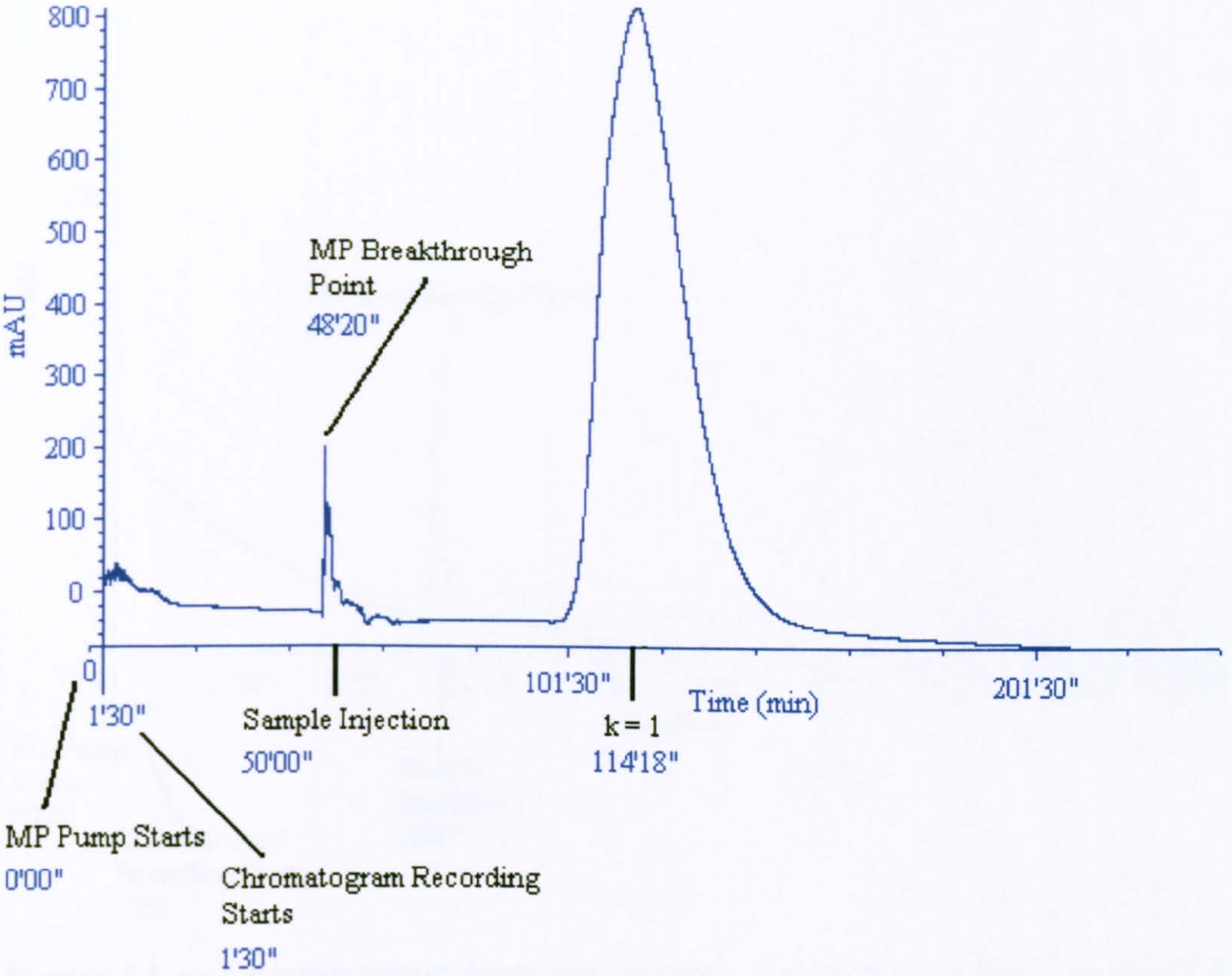

Figure 1A-e: Chromatogram from experiment using MP flow rate 0.72 mlmin^{-1} in the DEM-PRO #1 coil with 2.7 mm bore.

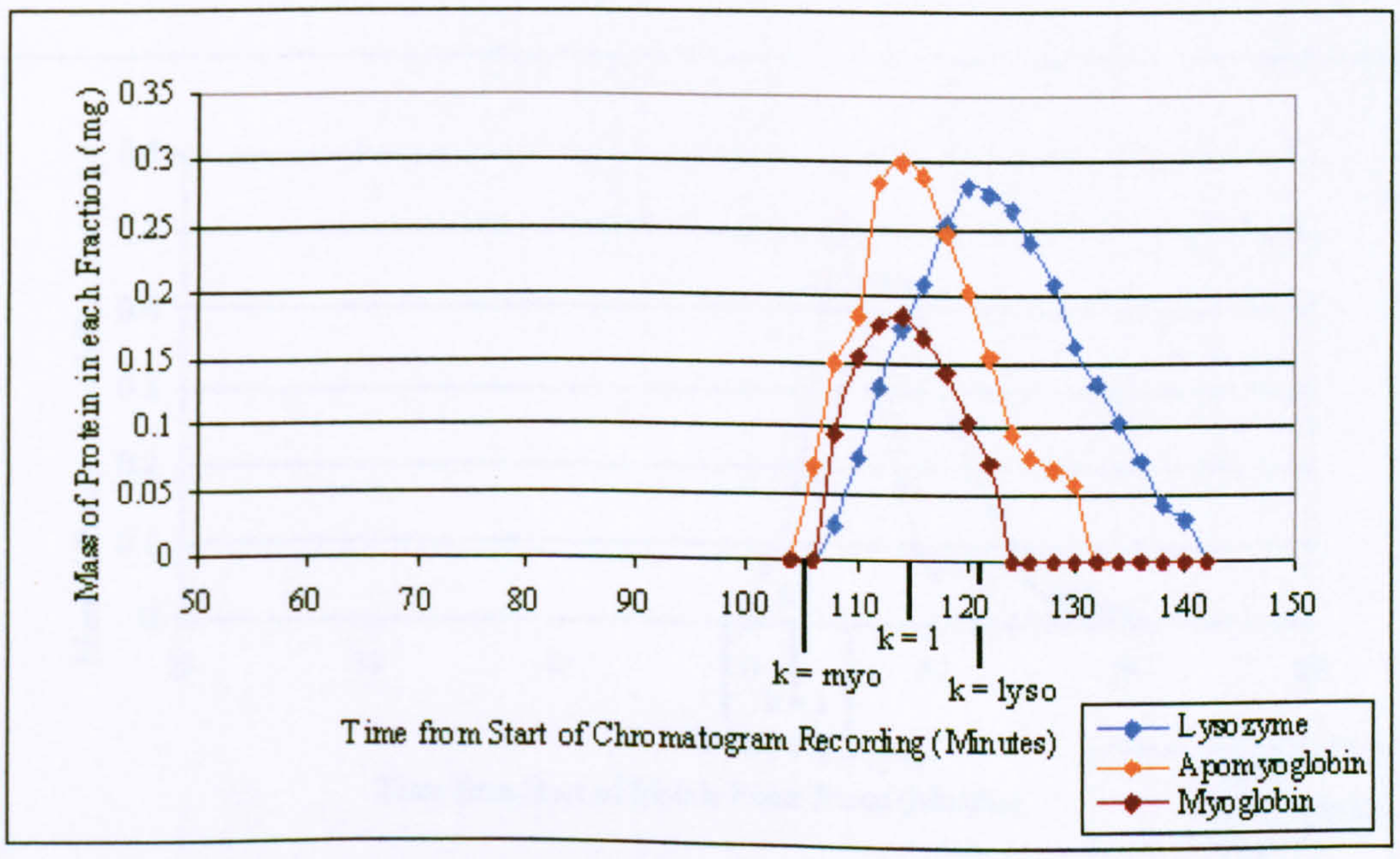

Figure 1A-f: Chromatogram created from HPLC analysis of fractions from experiment using MP flow rate 0.72 mlmin^{-1} in the DEM-PRO #1 coil with 2.7 mm bore.

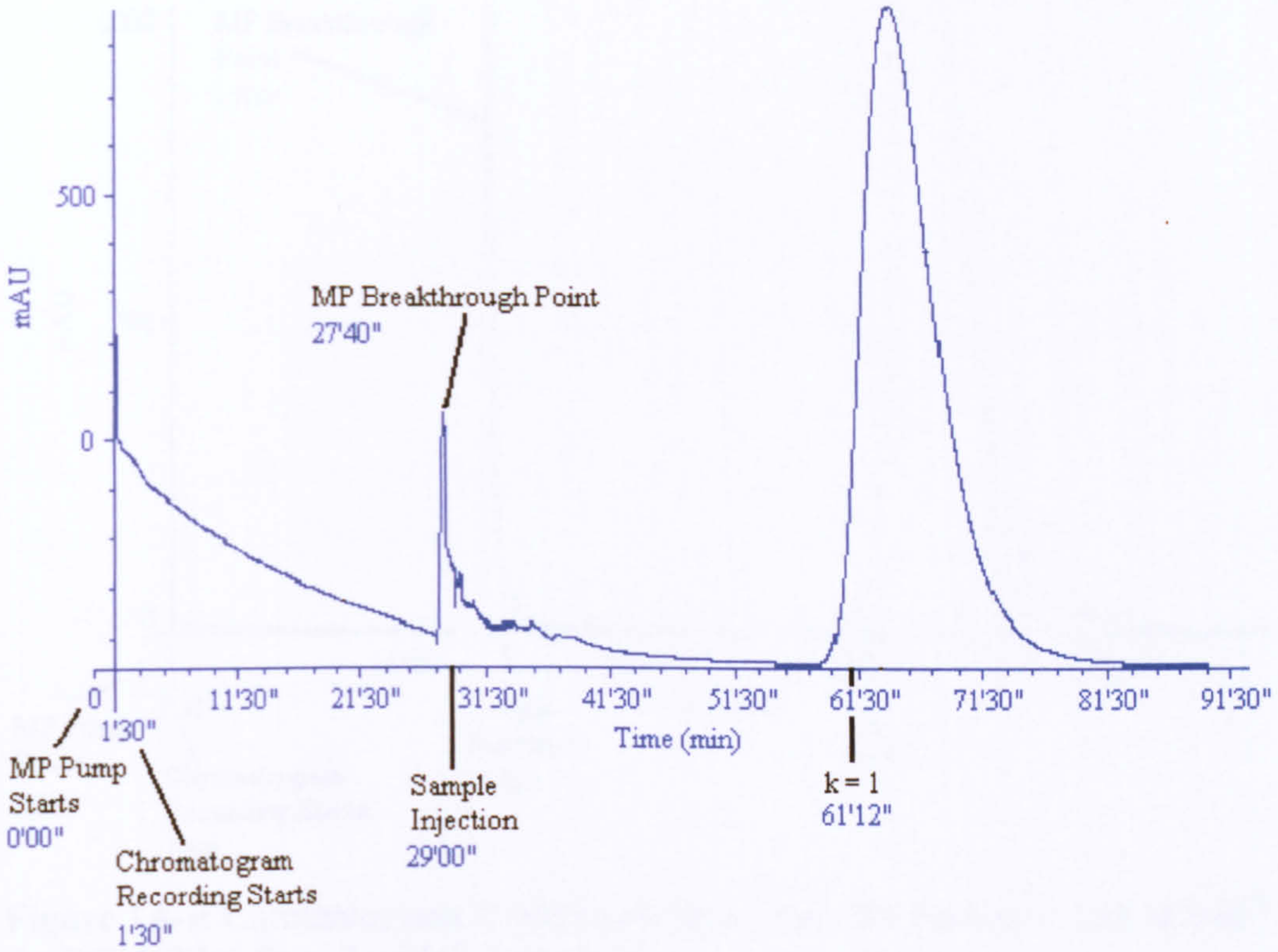

Figure 1A-g: Chromatogram from experiment using MP flow rate 1.44 $mlmin^{-1}$ in the DEM-PRO #1 coil with 2.7 mm bore.

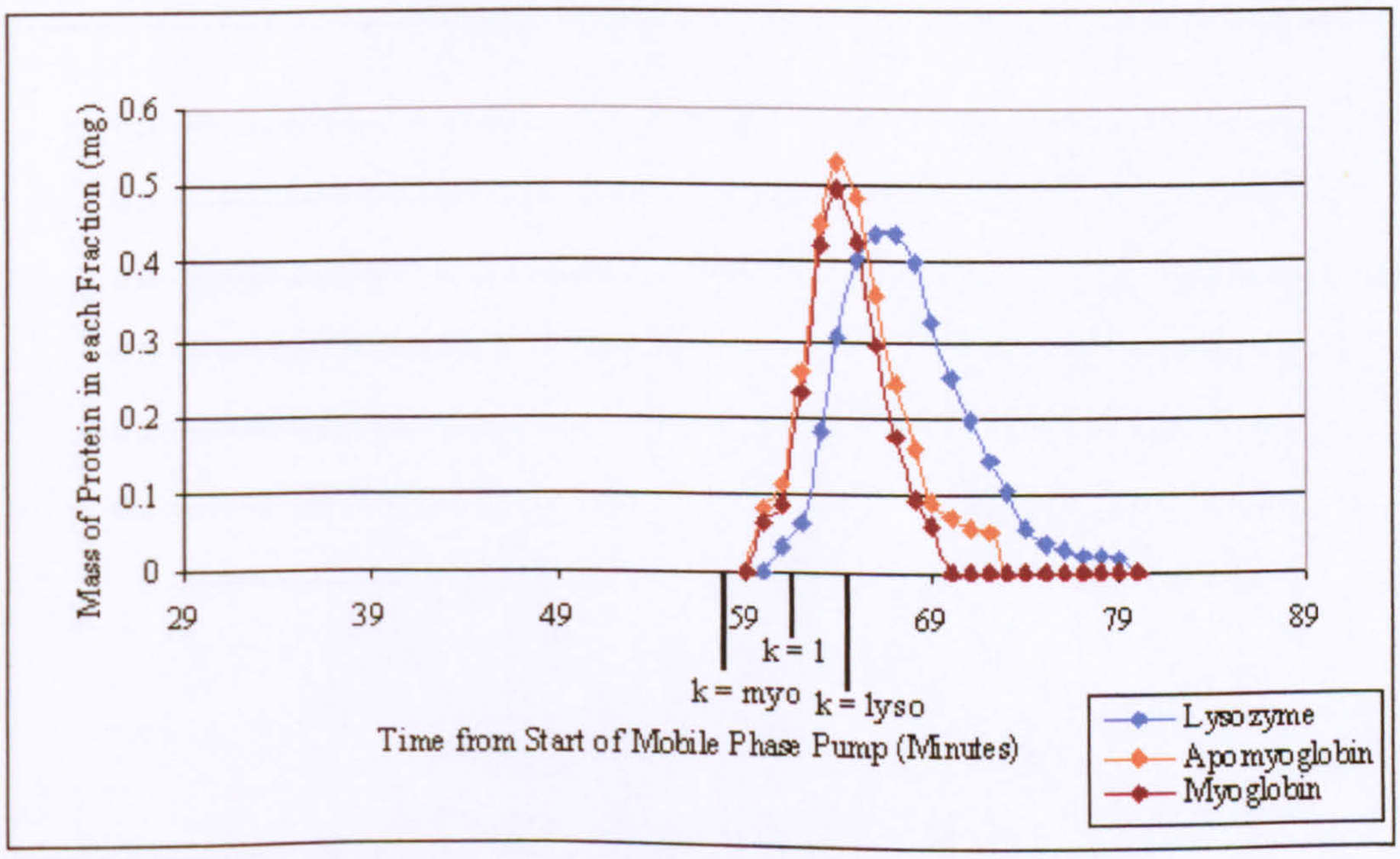

Figure 1A-h: Chromatogram created from HPLC analysis of fractions from experiment using MP flow rate 1.44 $mlmin^{-1}$ in the DEM-PRO #1 coil with 2.7 mm bore.

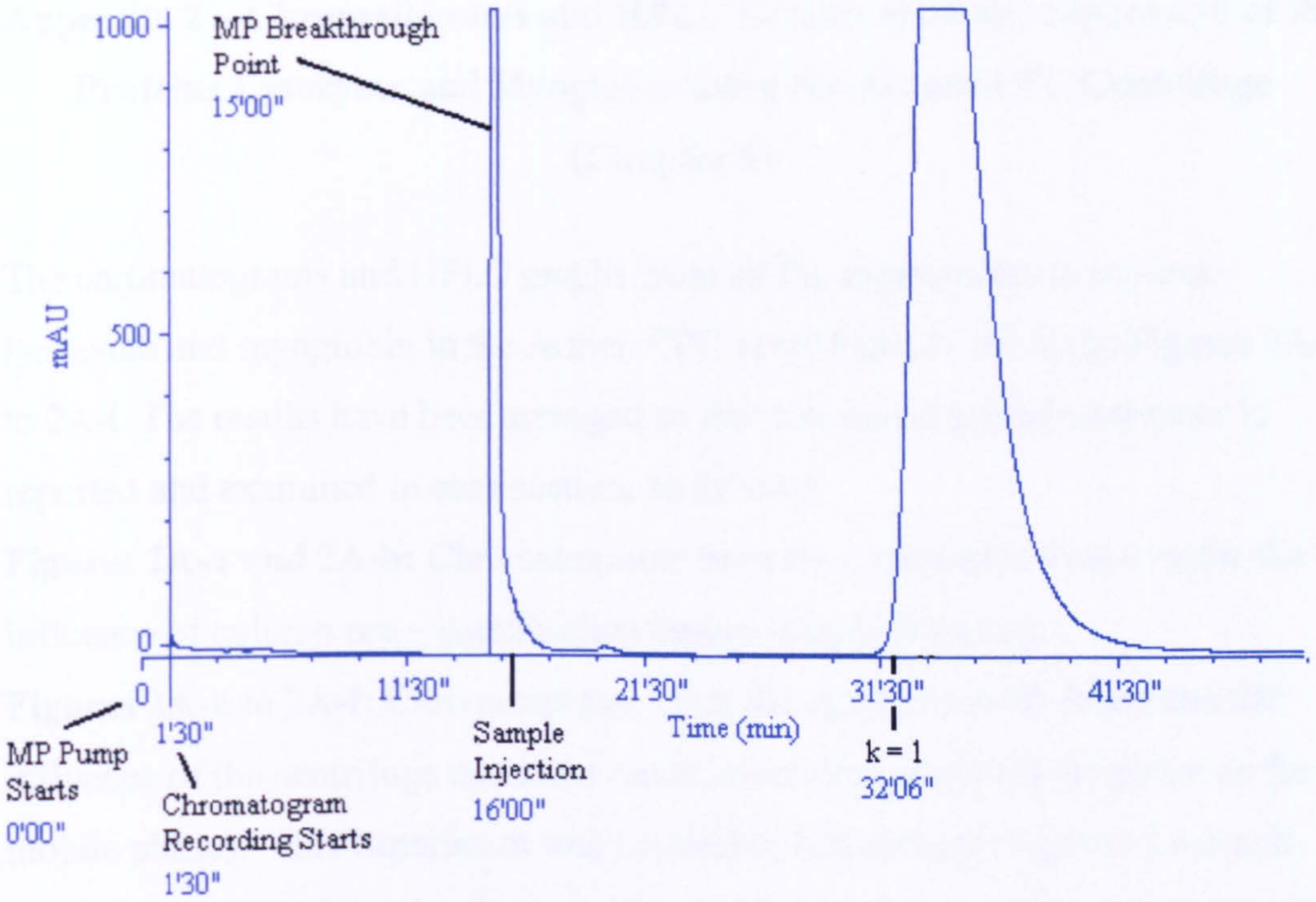

Figure 1A-i: Chromatogram from experiment using MP flow rate 2.88 mlmin^{-1} in the DEM-PRO #1 coil with 2.7 mm bore.

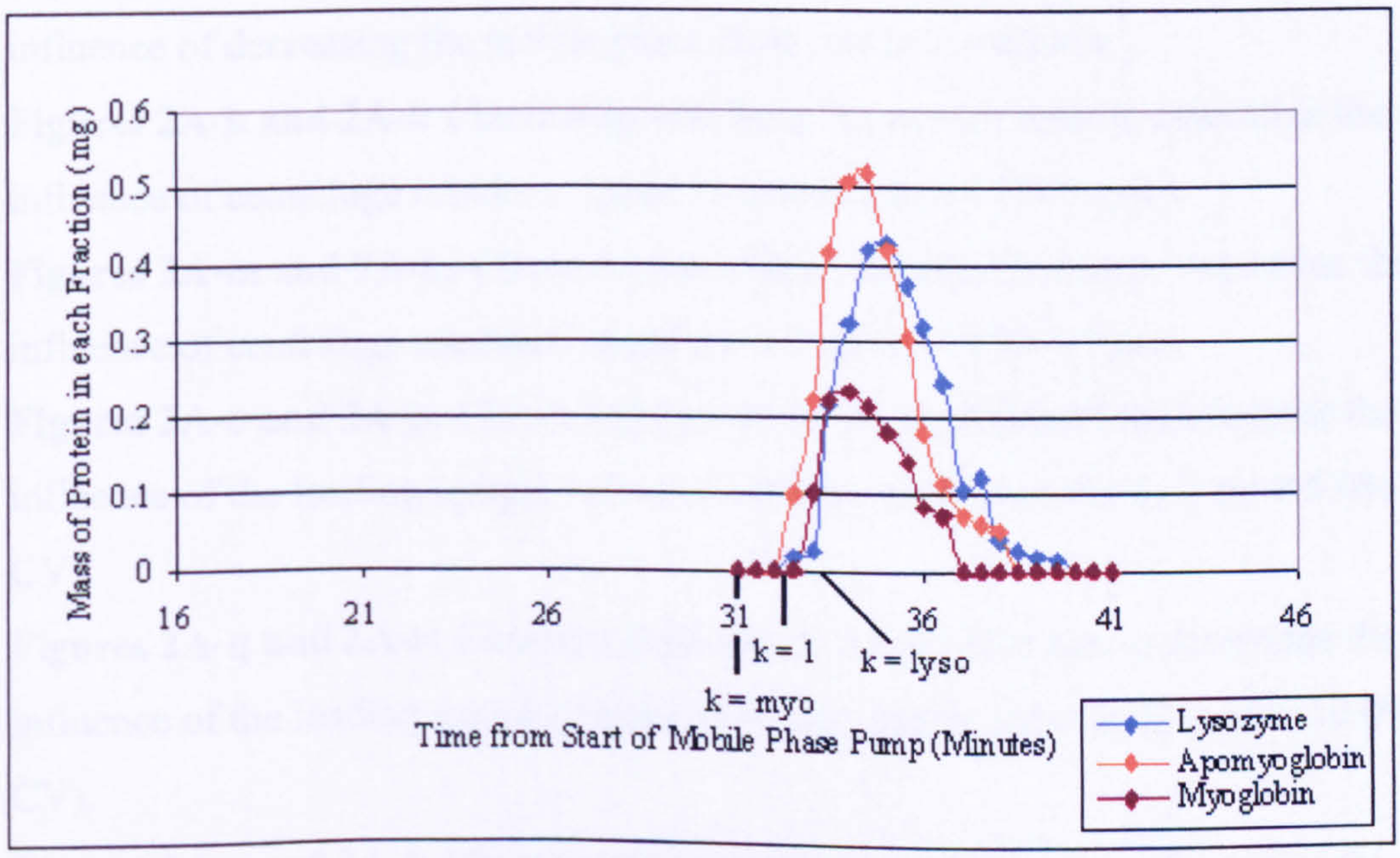

Figure 1A-j: Chromatogram created from HPLC analysis of fractions from experiment using MP flow rate 2.88 mlmin^{-1} in the DEM-PRO #1 coil with 2.7 mm bore.

Appendix 2 – Chromatograms and HPLC Graphs from the Separation of the Proteins Lysozyme and Myoglobin using the Armen CPC Centrifuge (Chapter 5)

The chromatograms and HPLC graphs from all the experiments to separate lysozyme and myoglobin in the Armen CPC centrifuge are shown in Figures 2A-a to 2A-t. The results have been arranged so that one experimental parameter is reported and examined in each section, as follows:

Figures 2A-a and 2A-b: Chromatograms from the experiment to determine the influence of column pre – equilibration before sample injection.

Figures 2A-c to 2A-f: Chromatograms from the experiments to determine the influence of the centrifuge operation mode; ascending mode (upper phase as the mobile phase). This experiment was performed in duplicate: Figures 2A-c and 2A-d show results from the first experiment; Figures 2A-e and 2A-f show results from the second experiment.

Figures 2A-g and 2A-h: Chromatograms from the experiment to determine the influence of the centrifuge operation mode; descending mode (lower phase as the mobile phase).

Figures 2A-i and 2A-j: Chromatograms from the experiment to determine the influence of decreasing the mobile phase flow rate to 5.0 $mlmin^{-1}$.

Figures 2A-k and 2A-l: Chromatograms from the experiments to determine the influence of centrifuge rotational speed (rotational speed 1000 rpm).

Figures 2A-m and 2A-n: Chromatograms from the experiments to determine the influence of centrifuge rotational speed (rotational speed 3000 rpm).

Figures 2A-o and 2A-p: Chromatograms from the experiments to determine the influence of the loading sample volume (loading sample volume 21.5 ml ≡ 5.0% CV).

Figures 2A-q and 2A-r: Chromatograms from the experiments to determine the influence of the loading sample volume (loading sample volume 43.0 ml ≡ 10.0% CV).

Figures 2A-s and 2A-t: Chromatograms from the experiments to determine the influence of the loading sample volume (loading sample volume 86.0 ml ≡ 20.0% CV).

Some graphs could be placed in more than one section, as they show the results of more than one comparable parameter. However, each graph is reported just once to minimise repetition.

In all the experiments:

- The recording of data commenced at time zero.
- The mobile phase breakthrough point caused mixing of the two phases in the eluent that appears as a peak on the chromatogram (the operator also observed at this point drops of mobile phase eluting from the column together with the stationary phase).
- Fraction collected commenced simultaneously with sample injection, and continued until the end of the experiment.

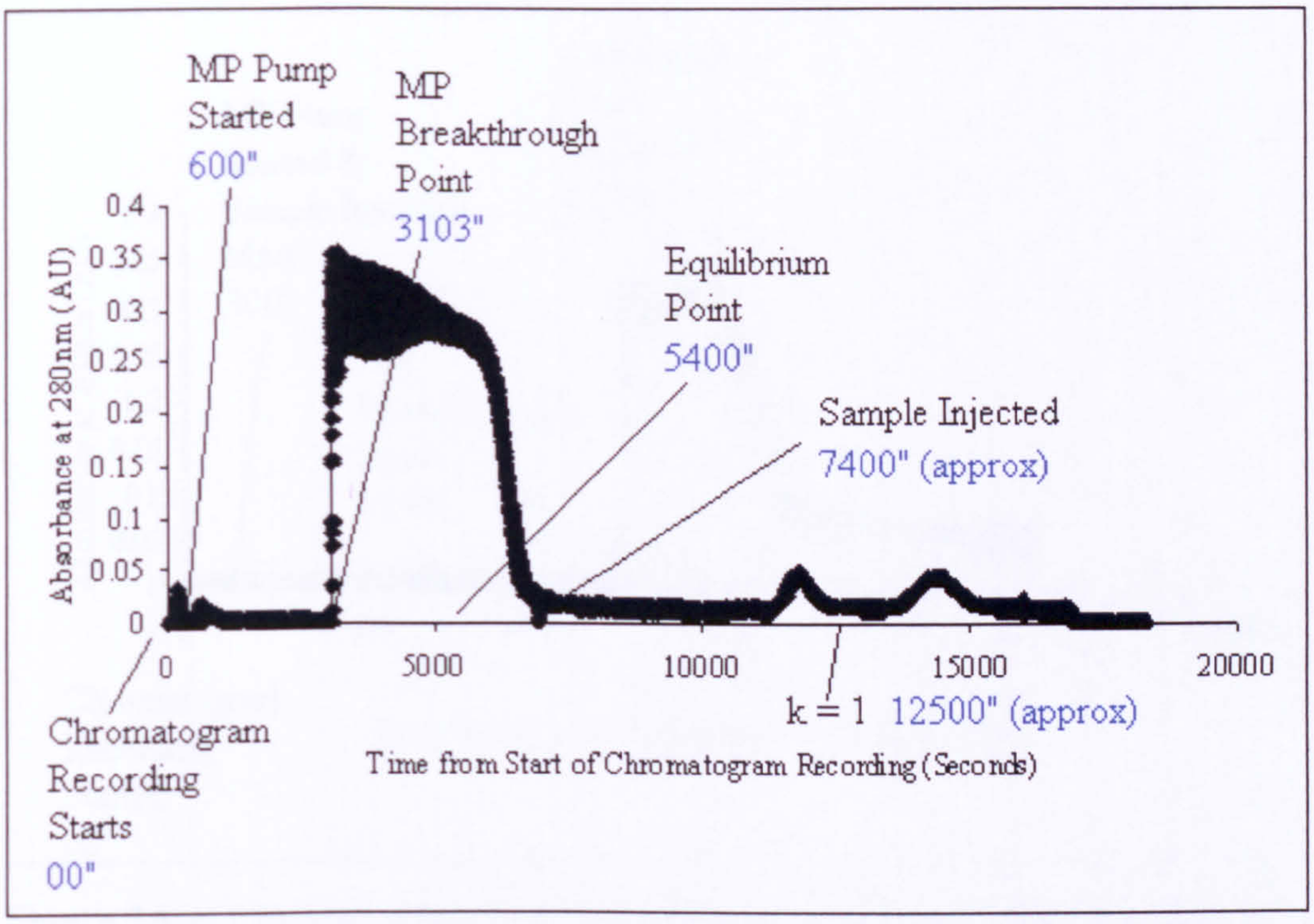

Figure 2A-a: Chromatogram from the experiment to determine the influence of column pre – equilibration before sample injection. The experimental parameters were: rotational speed 2000 rpm; MP flow rate 5.0 $mlmin^{-1}$; LP was the MP (descending mode); sample volume was 8.0 ml (1.86% CV). The column was pre – equilibrated before the sample was injected.

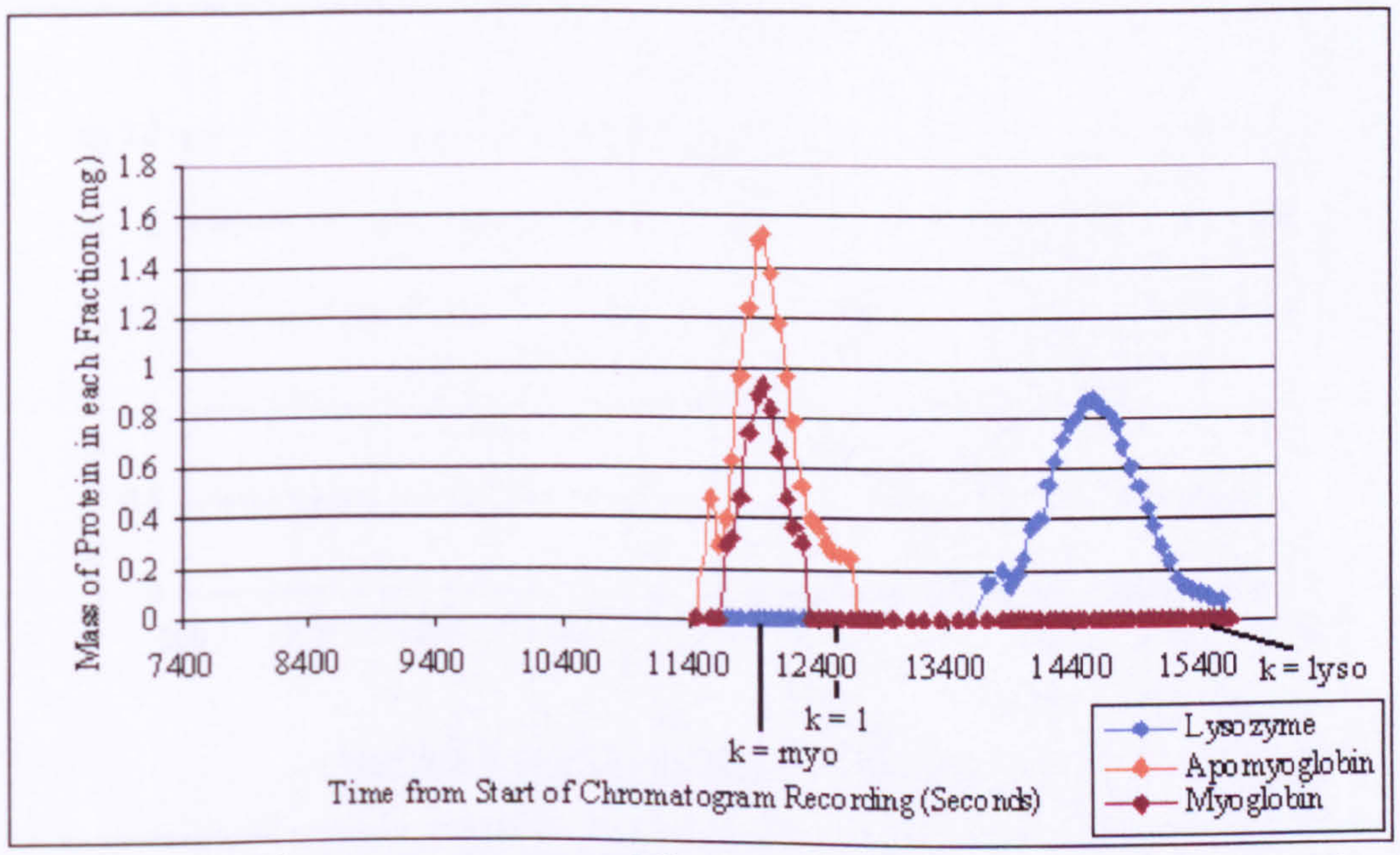

Figure 2A-b: Chromatogram created from HPLC analysis of fractions from the experiment to determine the influence of column pre – equilibration before sample injection. The experimental parameters were: rotational speed 2000 rpm; MP flow rate 5.0 $mlmin^{-1}$; LP was the MP (descending mode); sample volume was 8.0 ml (1.86% CV). The column was pre – equilibrated before the sample was injected.

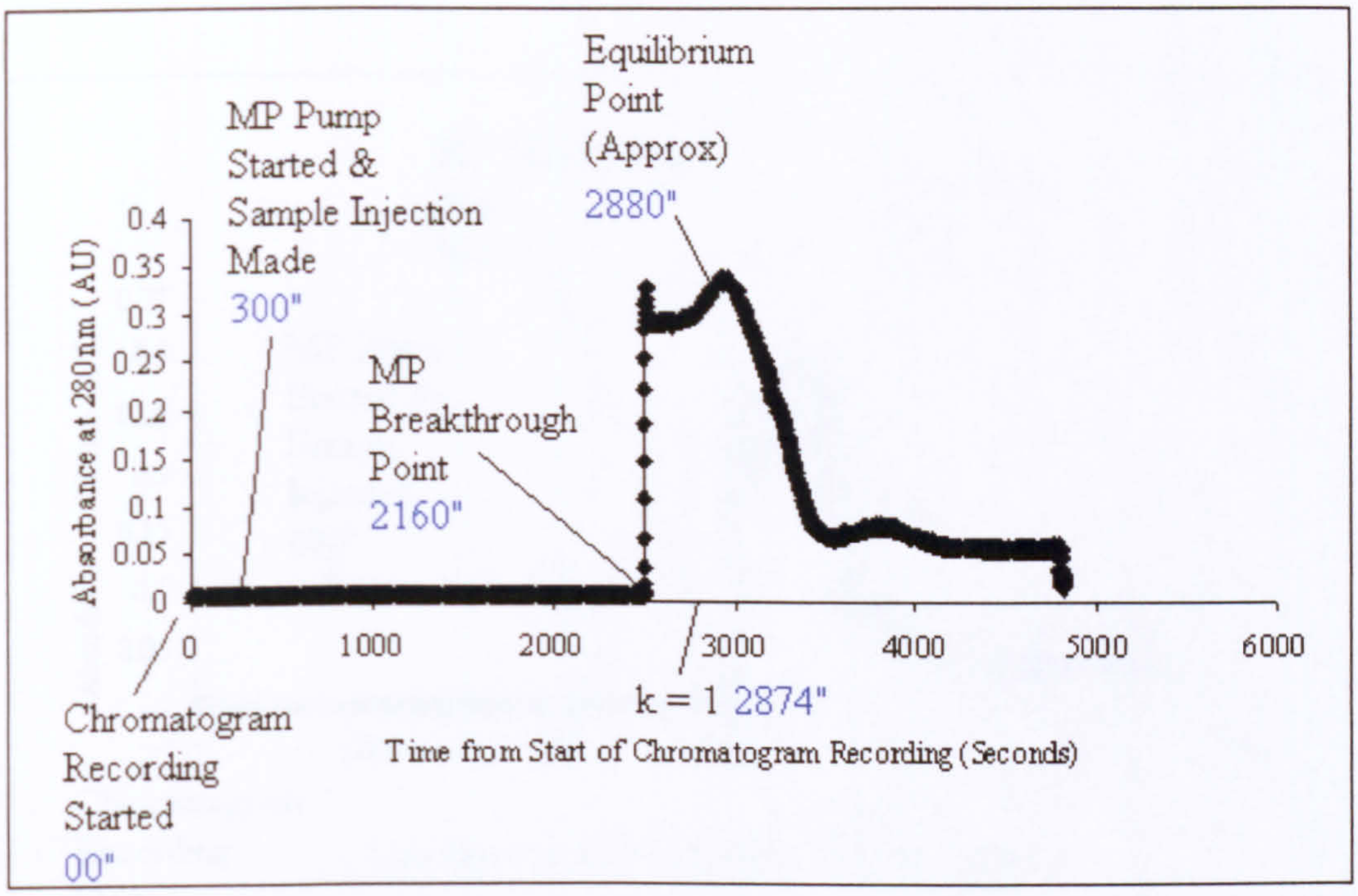

Figure 2A-c: Chromatogram from an experiment to determine the influence of the centrifuge operation mode. The experimental parameters were: rotational speed 2000 rpm; MP flow rate 10.0 $mlmin^{-1}$; sandwich injection; sample volume was 8.0 ml (1.86% CV). The centrifuge was operated in ascending mode, using the UP as the MP.

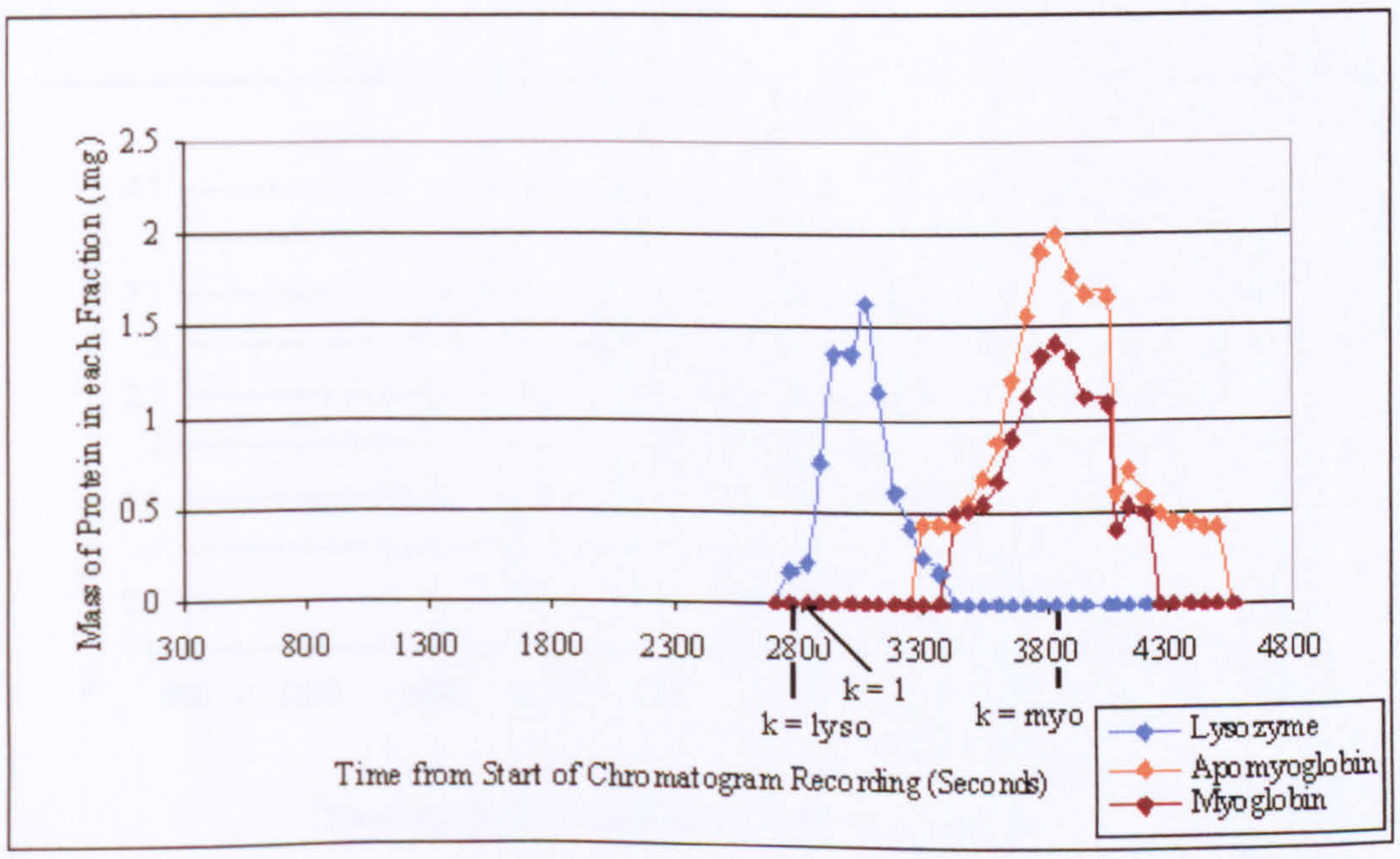

Figure 2A-d: Chromatogram created from HPLC analysis of fractions from the experiment to determine the influence of the centrifuge operation mode. The experimental parameters were: rotational speed 2000 rpm; MP flow rate 10.0 $mlmin^{-1}$; sandwich injection; sample volume was 8.0 ml (1.86% CV). The centrifuge was operated in ascending mode, using the UP as the MP.

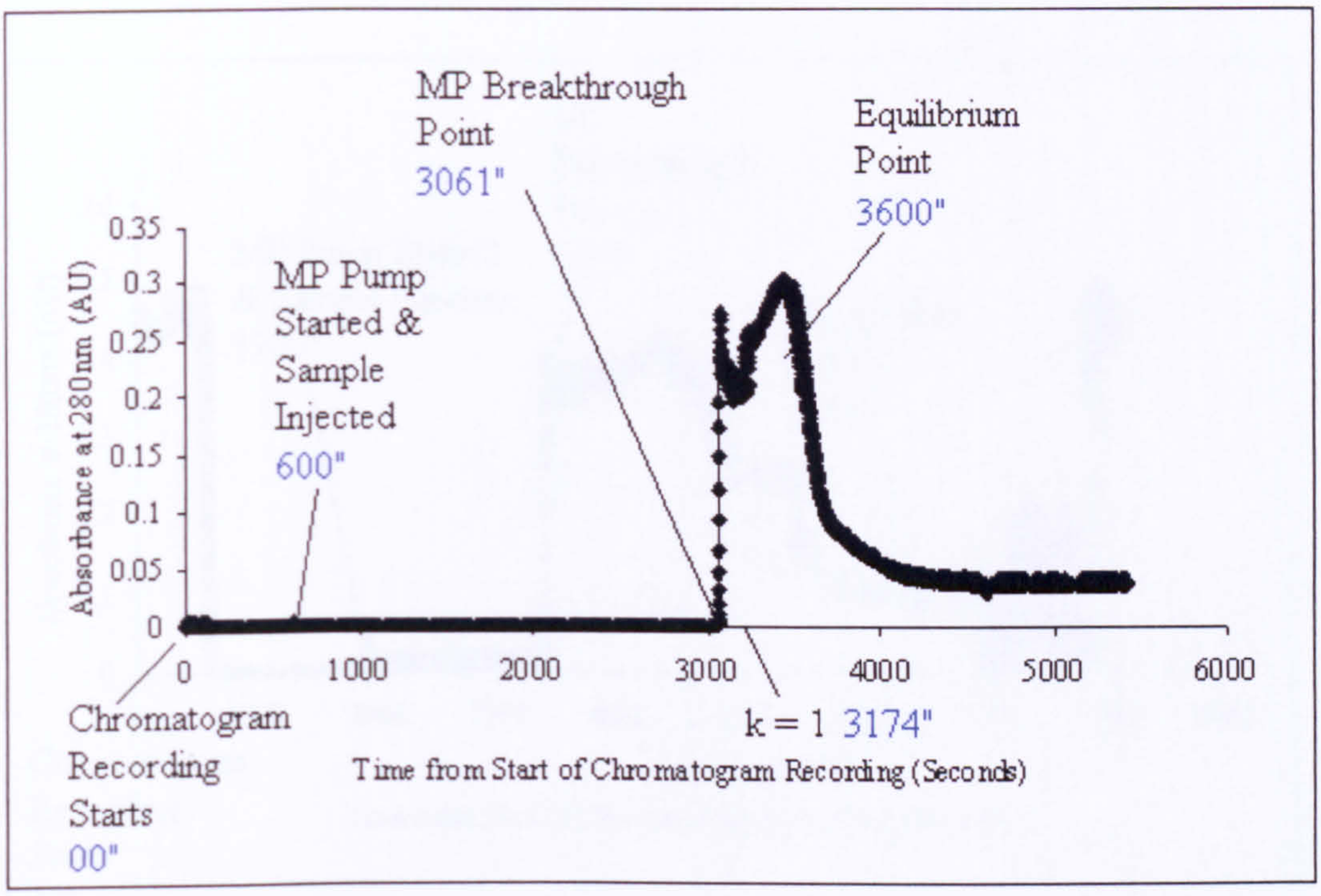

Figure 2A-e: Chromatogram from an experiment to determine the influence of the centrifuge operation mode. The experimental parameters were: rotational speed 2000 rpm; MP flow rate 10.0 $mlmin^{-1}$; sandwich injection; sample volume was 8.0 ml (1.86% CV). The centrifuge was operated in ascending mode, using the UP as the MP.

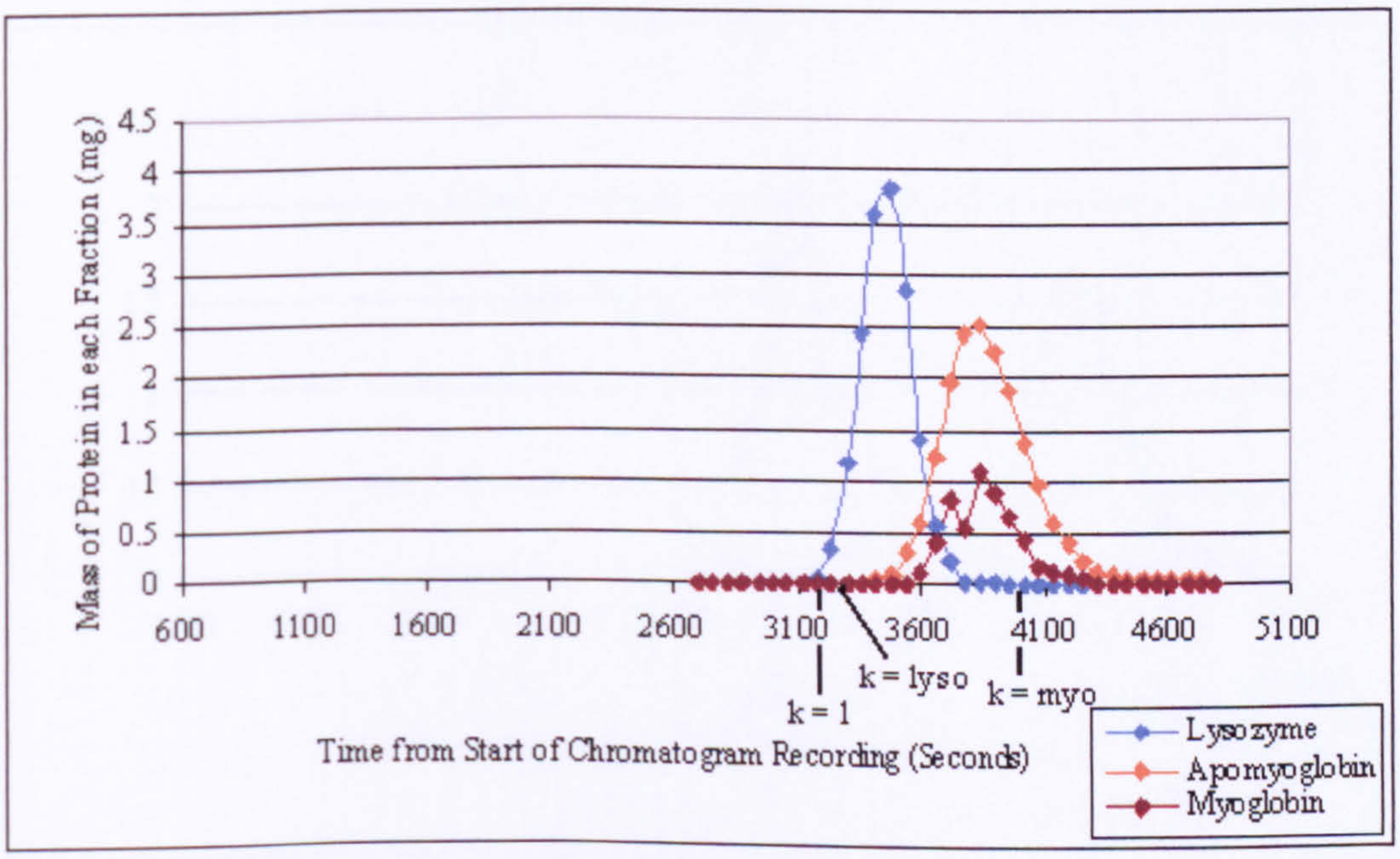

Figure 2A-f: Chromatogram created from HPLC analysis of fractions from the experiment to determine the influence of the centrifuge operation mode. The experimental parameters were: rotational speed 2000 rpm; MP flow rate 10.0 $mlmin^{-1}$; sandwich injection; sample volume was 8.0 ml (1.86% CV). The centrifuge was operated in ascending mode, using the UP as the MP.

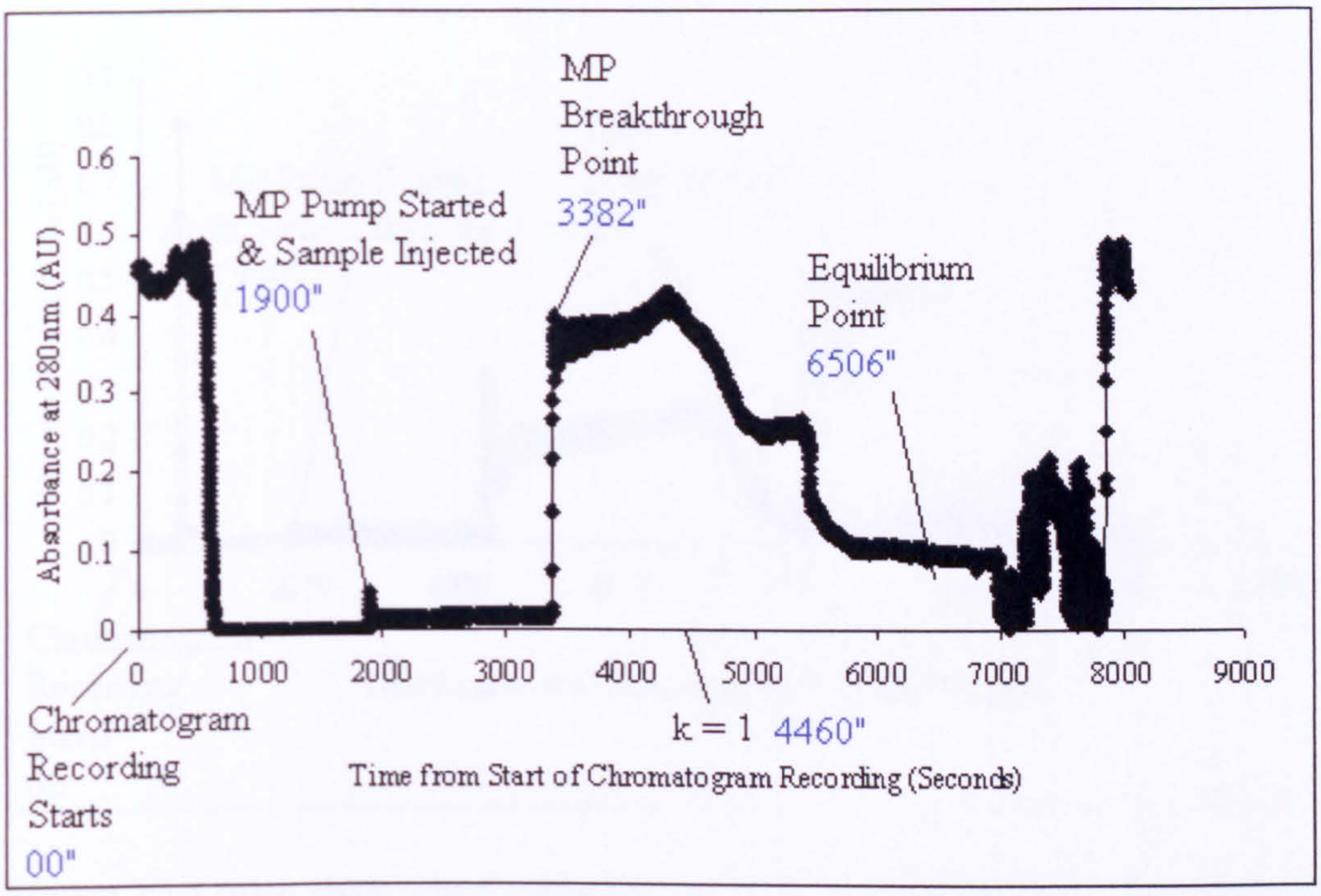

Figure 2A-g: Chromatogram from an experiment to determine the influence of the centrifuge operation mode. The experimental parameters were: rotational speed 2000 rpm; MP flow rate 10.0 $mlmin^{-1}$; sandwich injection; sample volume was 8.0 ml (1.86% CV). The centrifuge was operated in descending mode, using the LP as the MP.

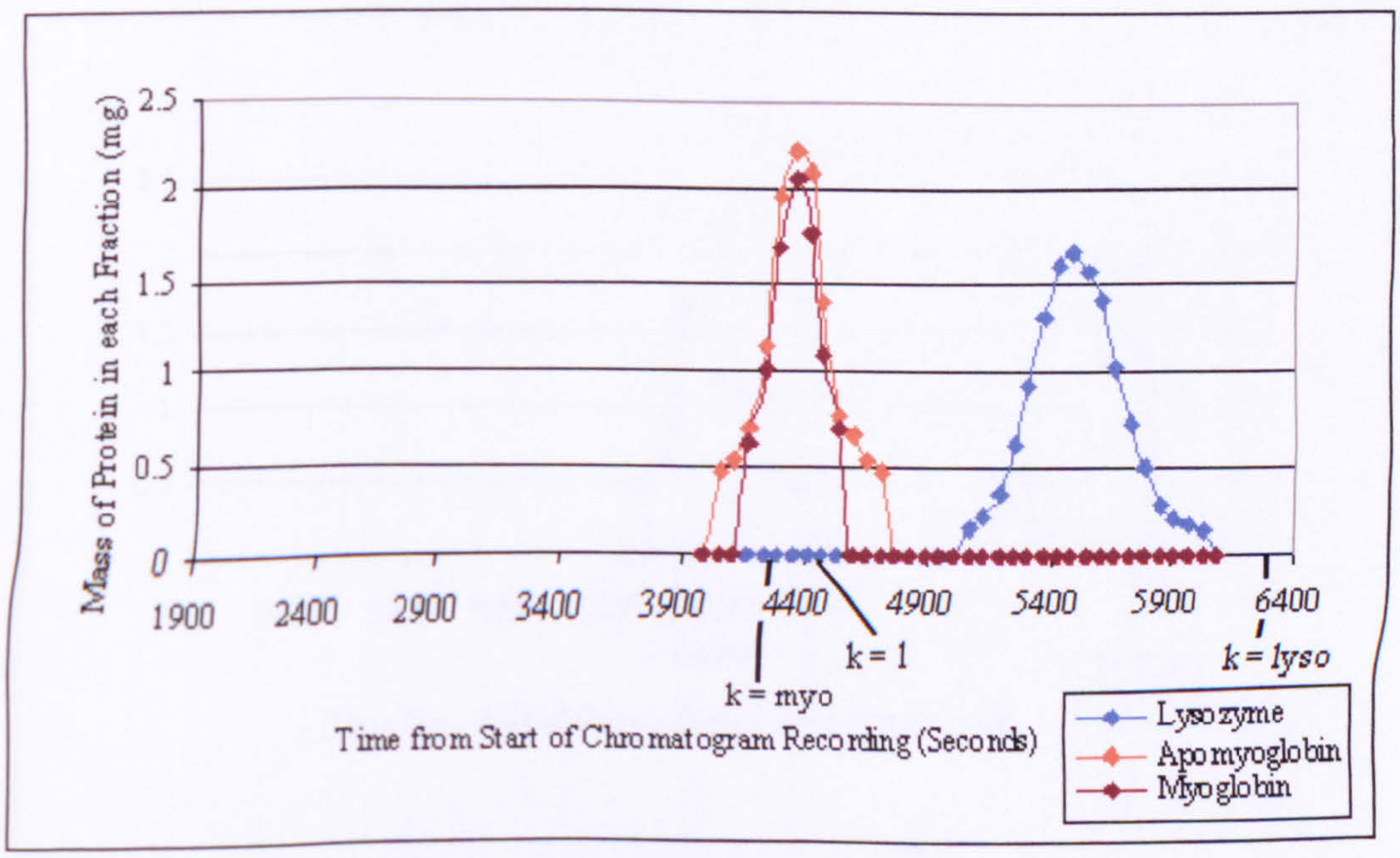

Figure 2A-h: Chromatogram created from HPLC analysis of fractions from an experiment to determine the influence of the centrifuge operation mode. The experimental parameters were: rotational speed 2000 rpm; MP flow rate 10.0 $mlmin^{-1}$; sandwich injection; sample volume was 8.0 ml (1.86% CV). The centrifuge was operated in descending mode, using the LP as the MP.

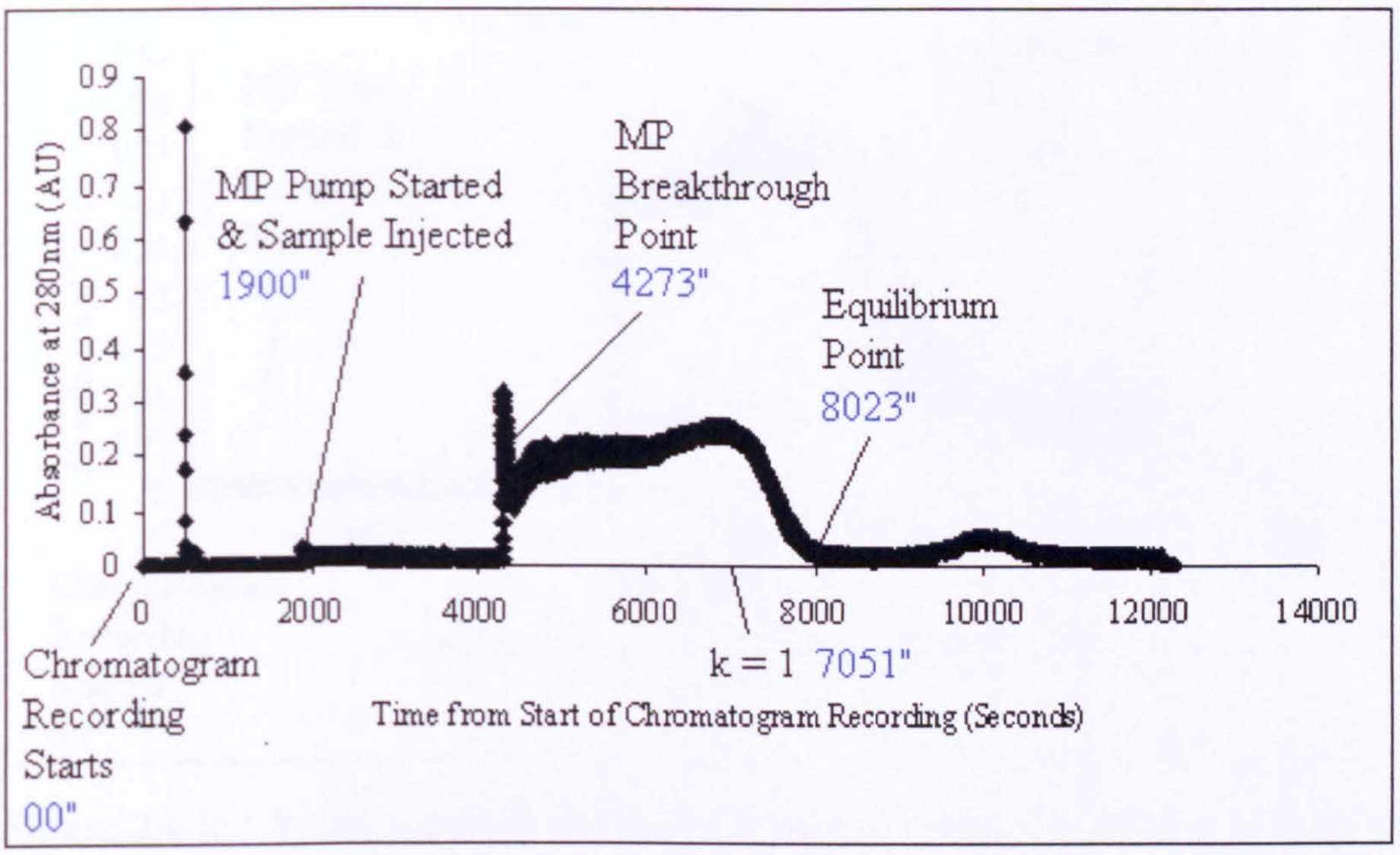

Figure 2A-i (also shown in Figure 5.3.1a): Chromatogram from the experiment to determine the influence of decreasing the MP flow rate to 5.0 mlmin^{-1}. The experimental parameters were: rotational speed 2000 rpm; LP was the MP (descending mode); sandwich injection; sample volume was 8.0 ml (1.86% CV). The MP flow rate was 5.0 mlmin^{-1}.

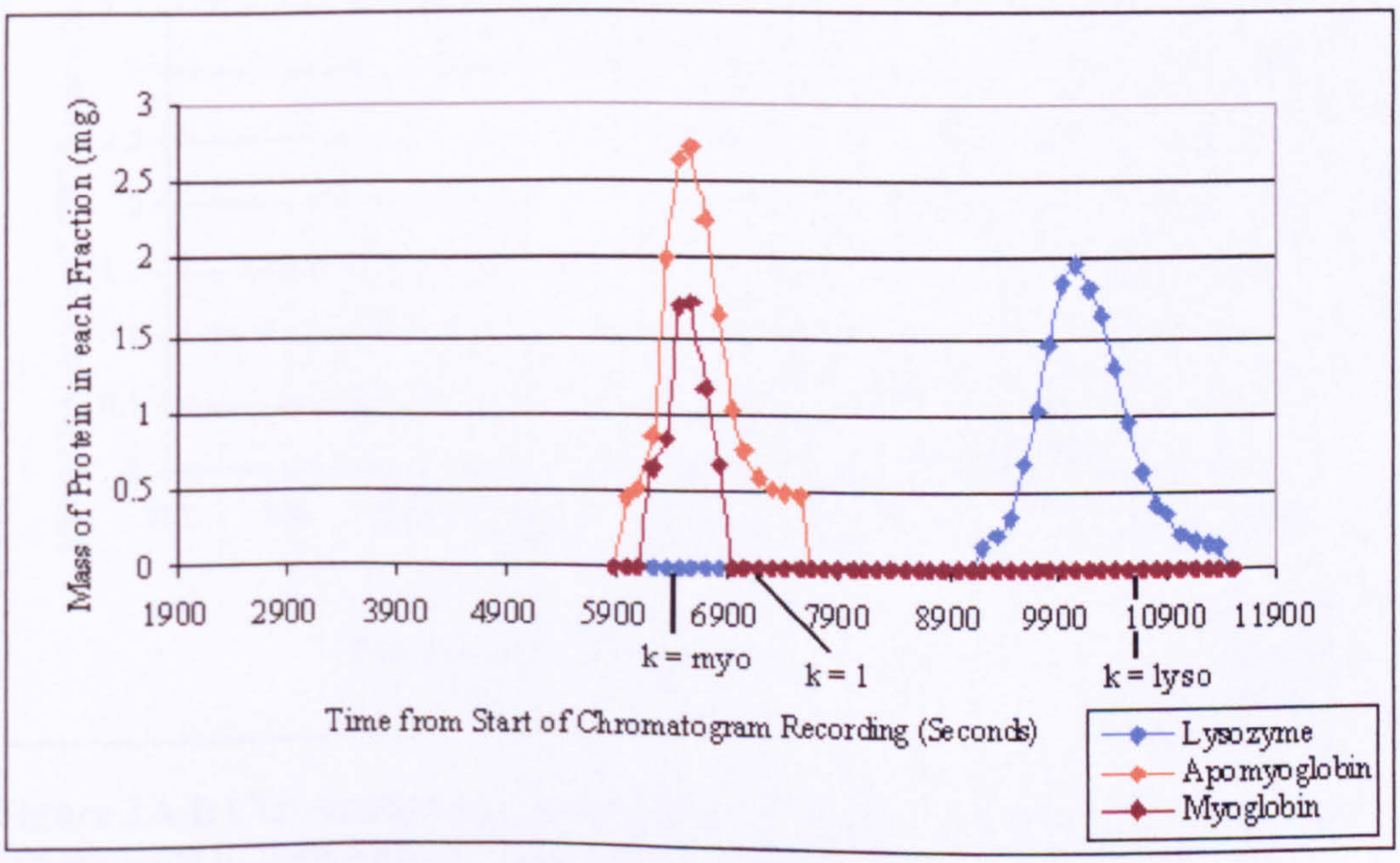

Figure 2A-j (also shown in Figure 5.3.1b): Chromatogram created from HPLC analysis of fractions from the experiment to determine the influence of decreasing the MP flow rate to 5.0 mlmin^{-1}. The experimental parameters were: rotational speed 2000 rpm; LP was the MP (descending mode); sandwich injection; sample volume was 8.0 ml (1.86% CV). The MP flow rate was 5.0 mlmin^{-1}.

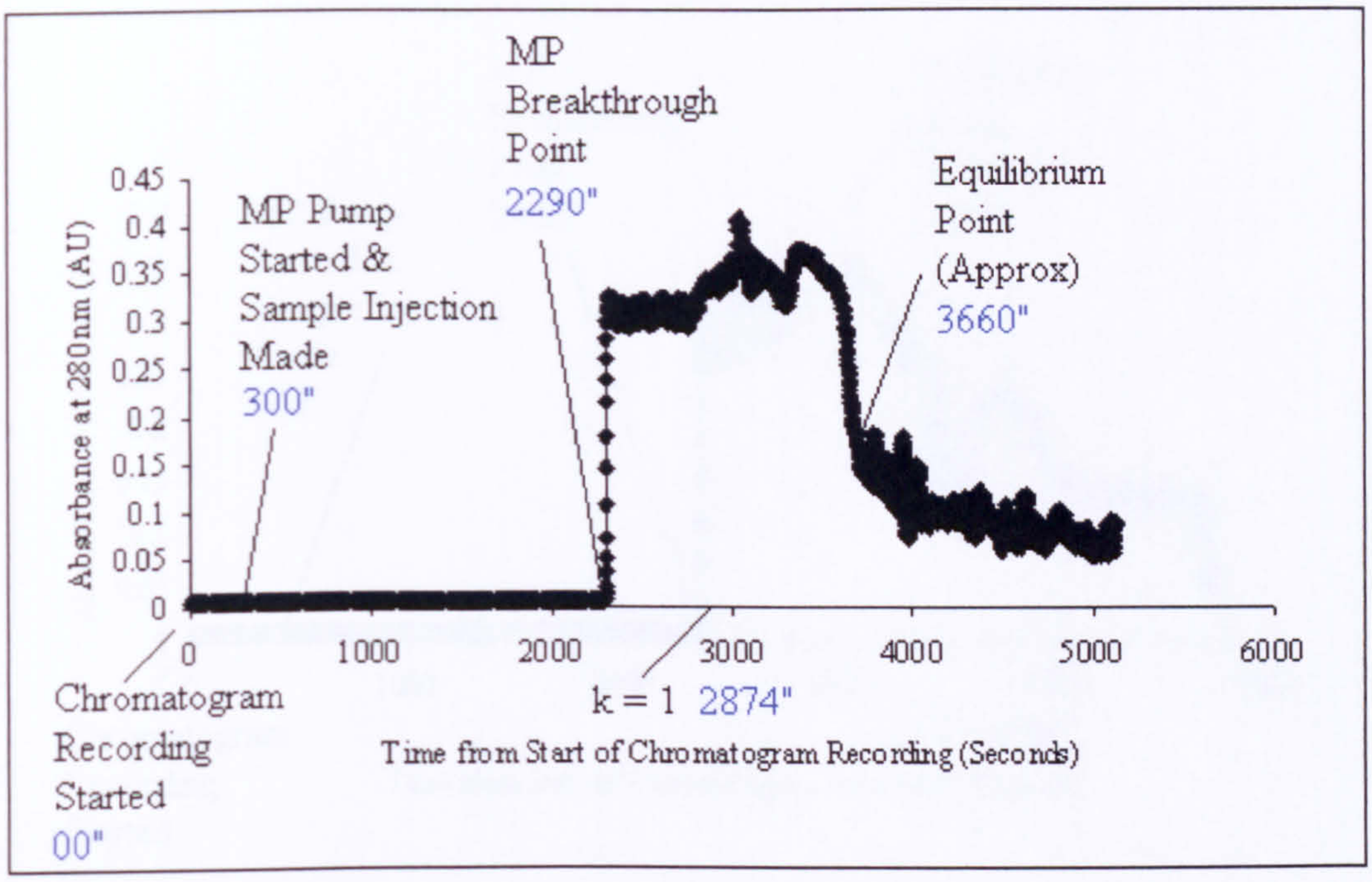

Figure 2A-k: Chromatogram from the experiments to determine the influence of centrifuge rotational speed. The experimental parameters were: MP flow rate 10.0 $mlmin^{-1}$; LP was the MP (descending mode); sandwich injection; sample volume was 8.0 ml (1.86% CV). The rotational speed was 1000 rpm.

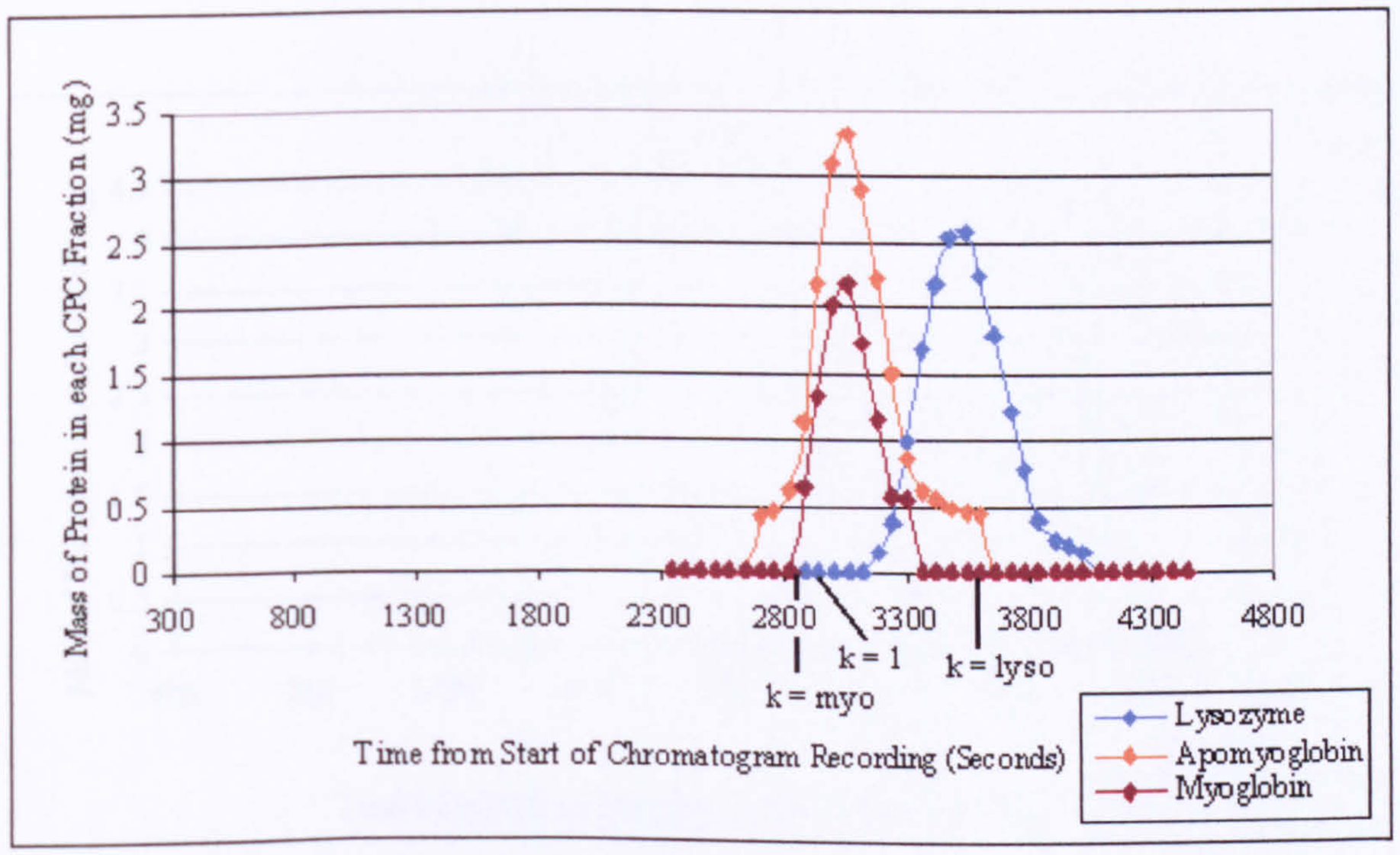

Figure 2A-l: Chromatogram created from HPLC analysis of fractions from the experiments to determine the influence of centrifuge rotational speed. The experimental parameters were: MP flow rate 10.0 $mlmin^{-1}$; LP was the MP (descending mode); sandwich injection; sample volume was 8.0 ml (1.86% CV). The rotational speed was 1000 rpm.

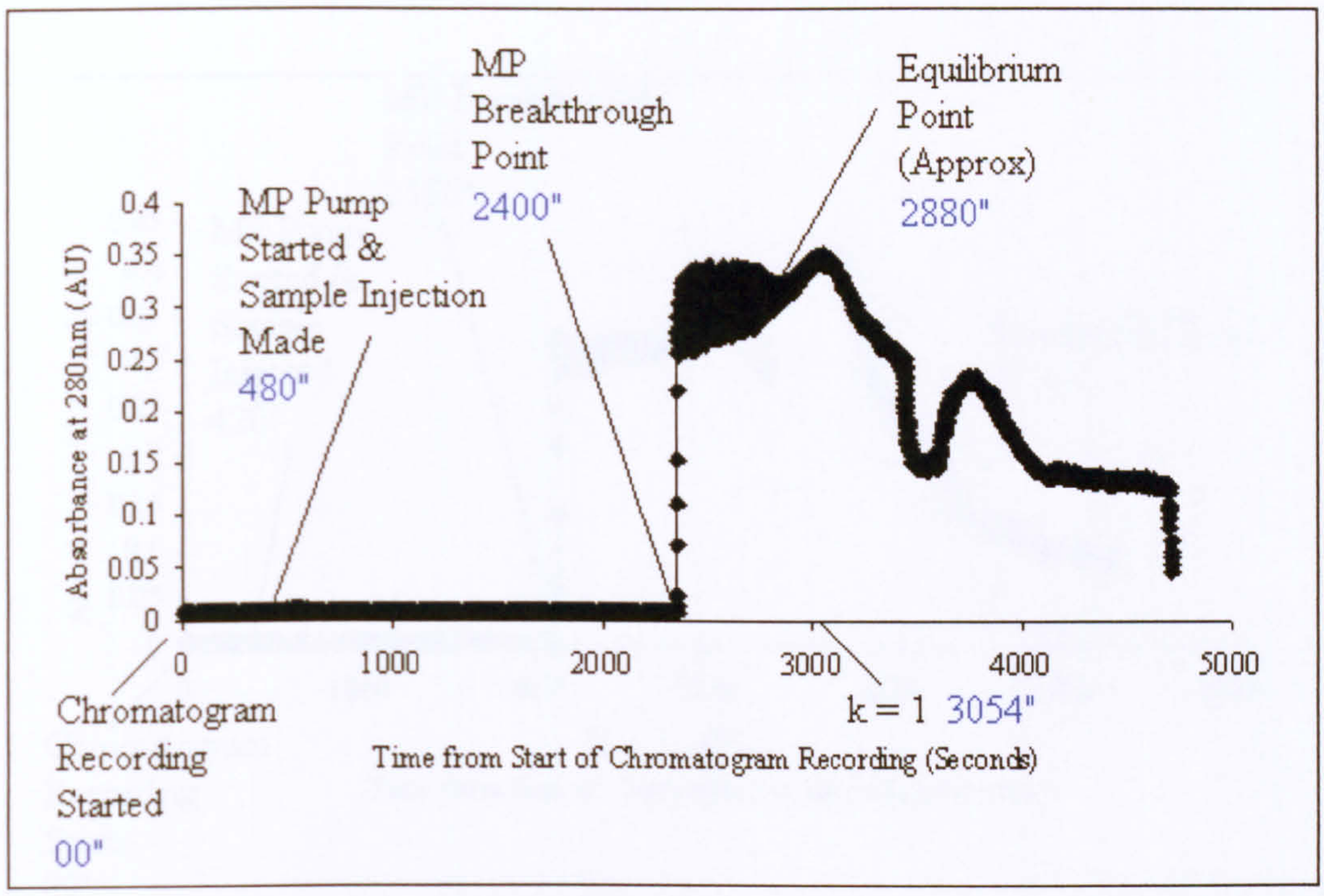

Figure 2A-m: Chromatogram from the experiments to determine the influence of centrifuge rotational speed. The experimental parameters were: MP flow rate 10.0 $mlmin^{-1}$; LP was the MP (descending mode); sandwich injection; sample volume was 8.0 ml (1.86% CV). The rotational speed was 3000 rpm.

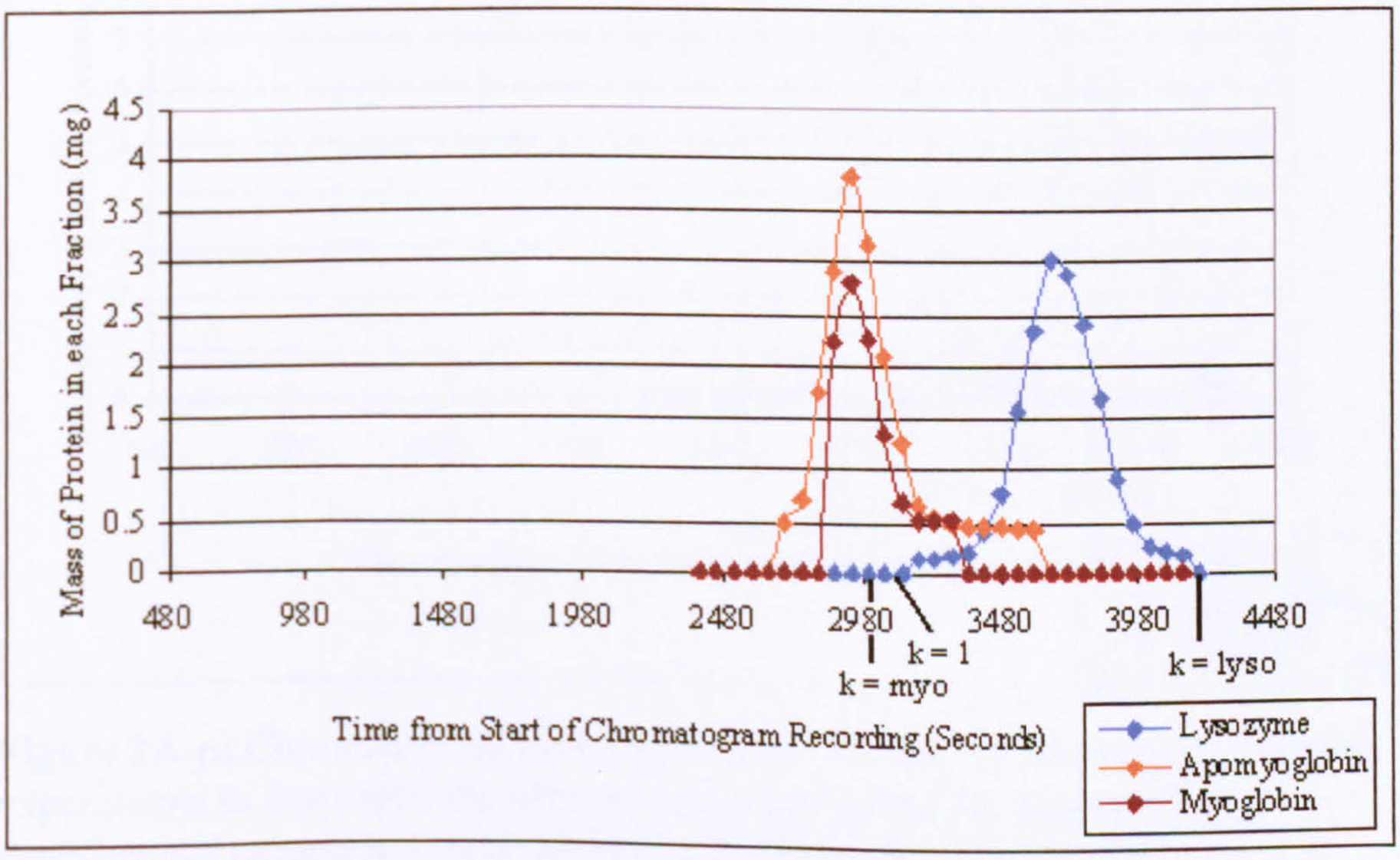

Figure 2A-n: Chromatogram created from HPLC analysis of fractions from the experiments to determine the influence of centrifuge rotational speed. The experimental parameters were: MP flow rate 10.0 $mlmin^{-1}$; LP was the MP (descending mode); sandwich injection; sample volume was 8.0 ml (1.86% CV). The rotational speed was 3000 rpm.

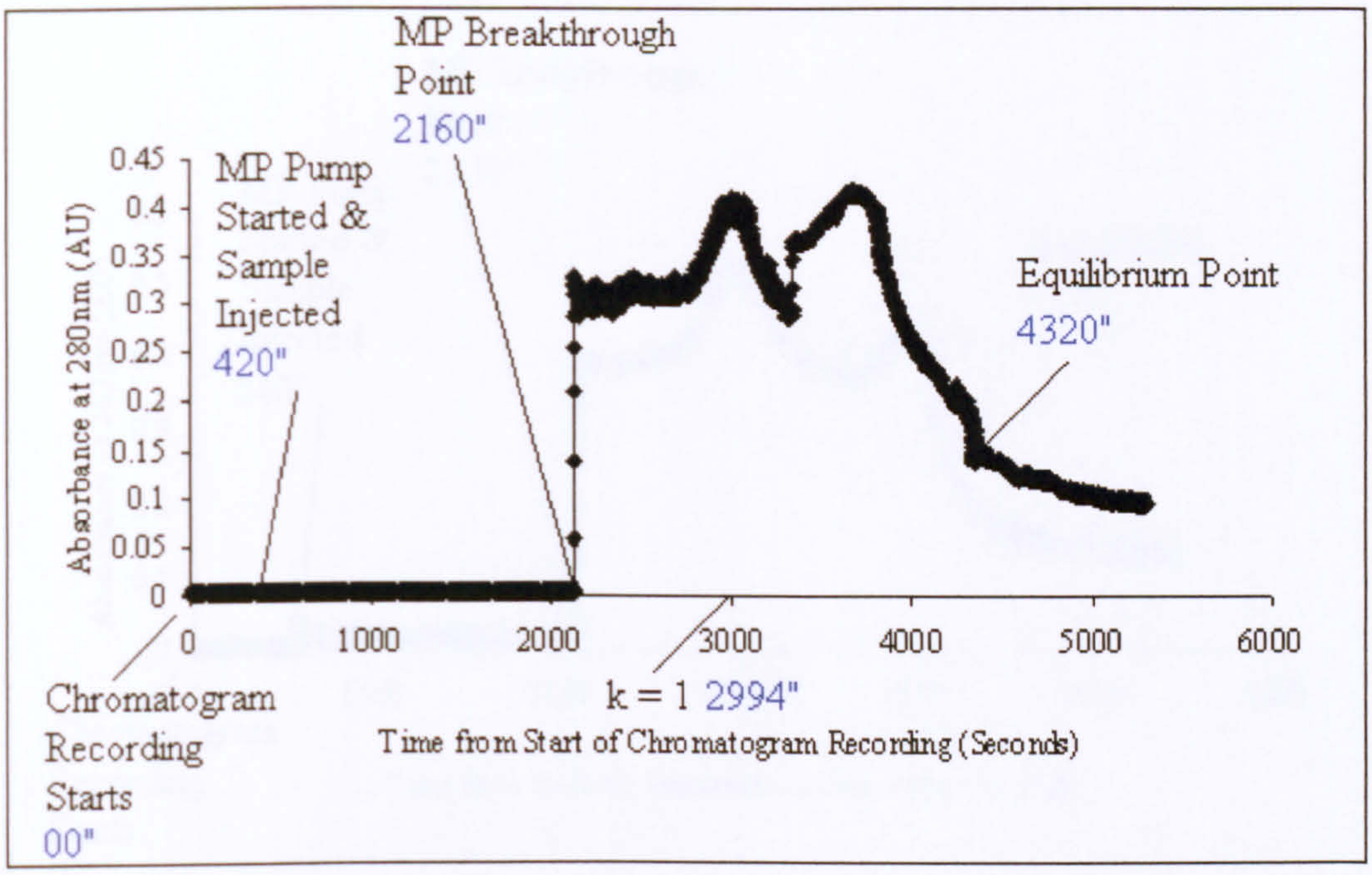

Figure 2A-o: Chromatogram from the experiments to determine the influence of loading sample volume. The experimental parameters were: rotational speed 2000 rpm; MP flow rate 10.0 $mlmin^{-1}$; LP was the MP (descending mode); sandwich injection. The sample volume was 21.5 ml or 5.0% of the column volume.

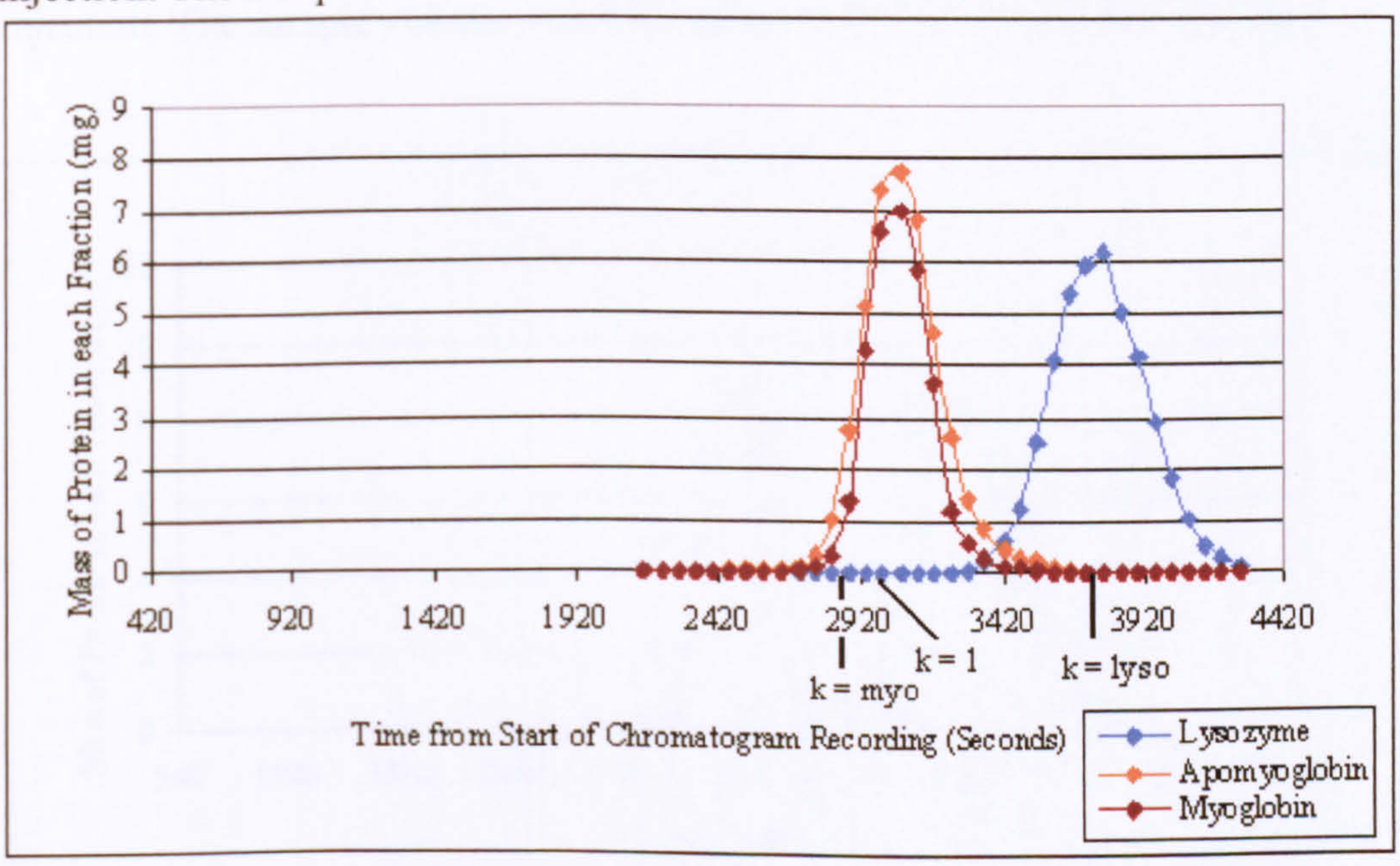

Figure 2A-p: Chromatogram created from HPLC analysis of fractions from the experiments to determine the influence of loading sample volume. The experimental parameters were: rotational speed 2000 rpm; MP flow rate 10.0 $mlmin^{-1}$; LP was the MP (descending mode); sandwich injection. The sample volume was 21.5 ml or 5.0% of the column volume.

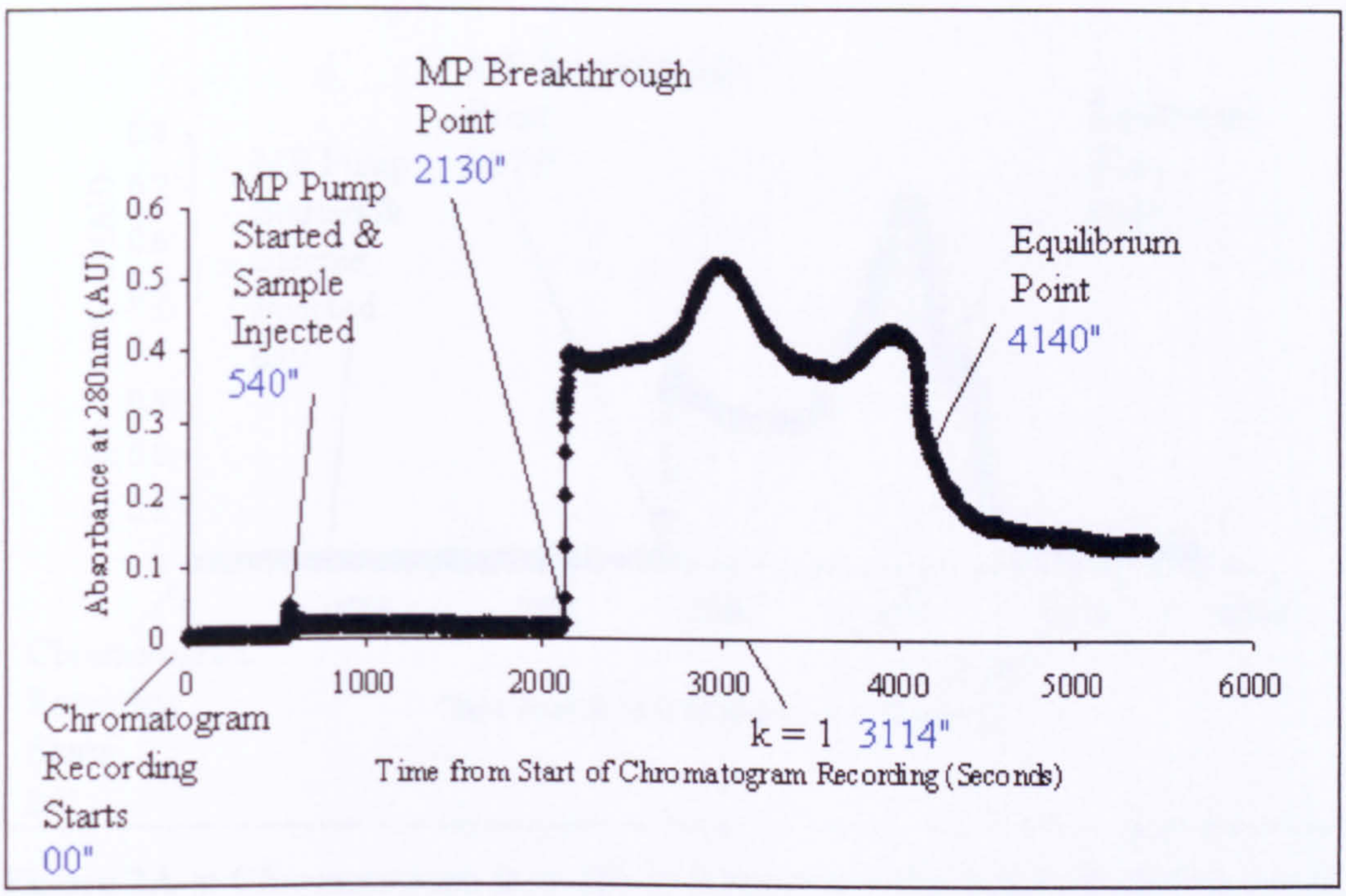

Figure 2A-q: Chromatogram from the experiments to determine the influence of loading sample volume. The experimental parameters were: rotational speed 2000 rpm; MP flow rate 10.0 $mlmin^{-1}$; LP was the MP (descending mode); sandwich injection. The sample volume was 43.0 ml or 10.0% of the column volume.

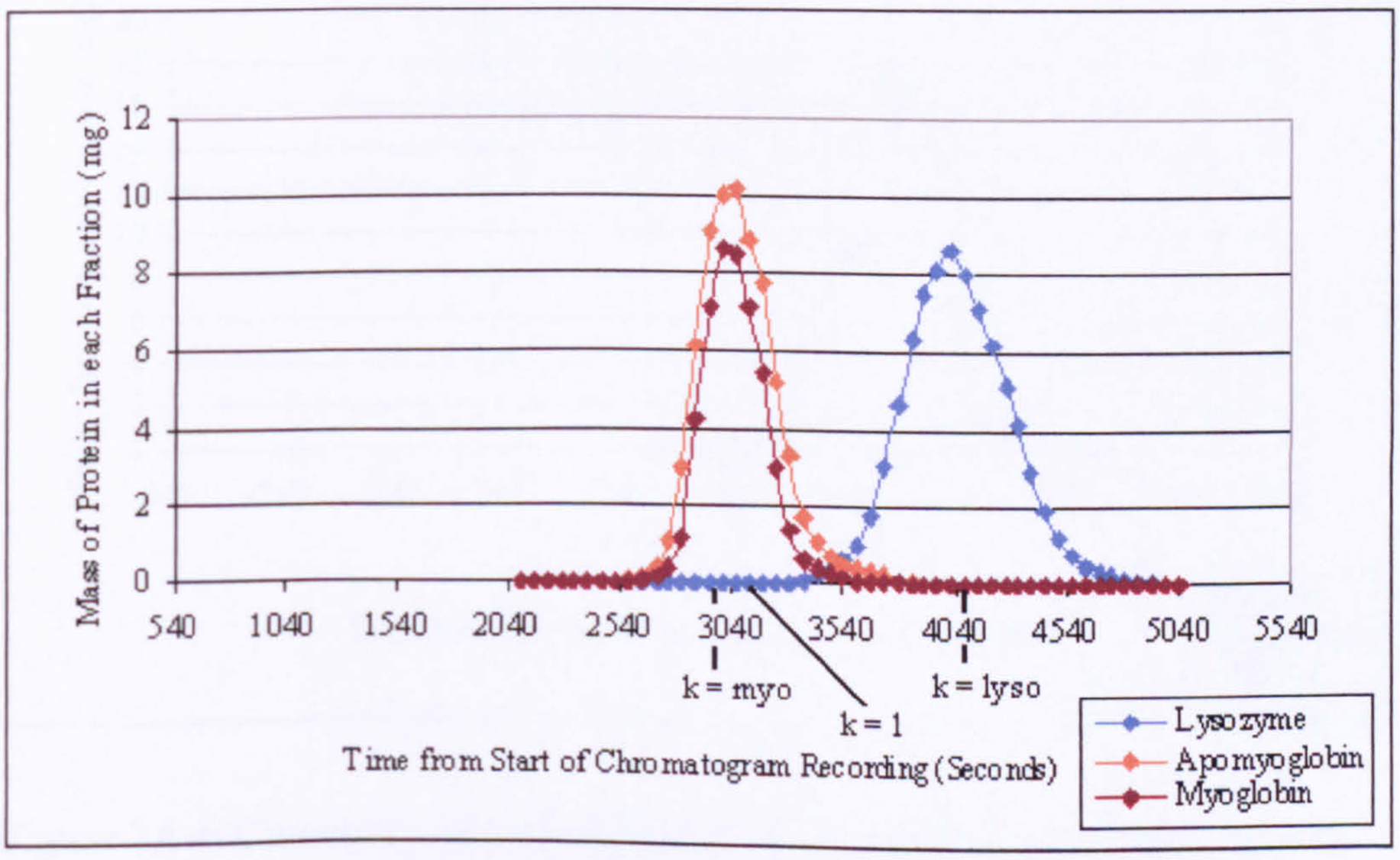

Figure 2A-r: Chromatogram created from HPLC analysis of fractions from the experiments to determine the influence of loading sample volume. The experimental parameters were: rotational speed 2000 rpm; MP flow rate 10.0 $mlmin^{-1}$; LP was the MP (descending mode); sandwich injection. The sample volume was 43.0 ml or 10.0% of the column volume.

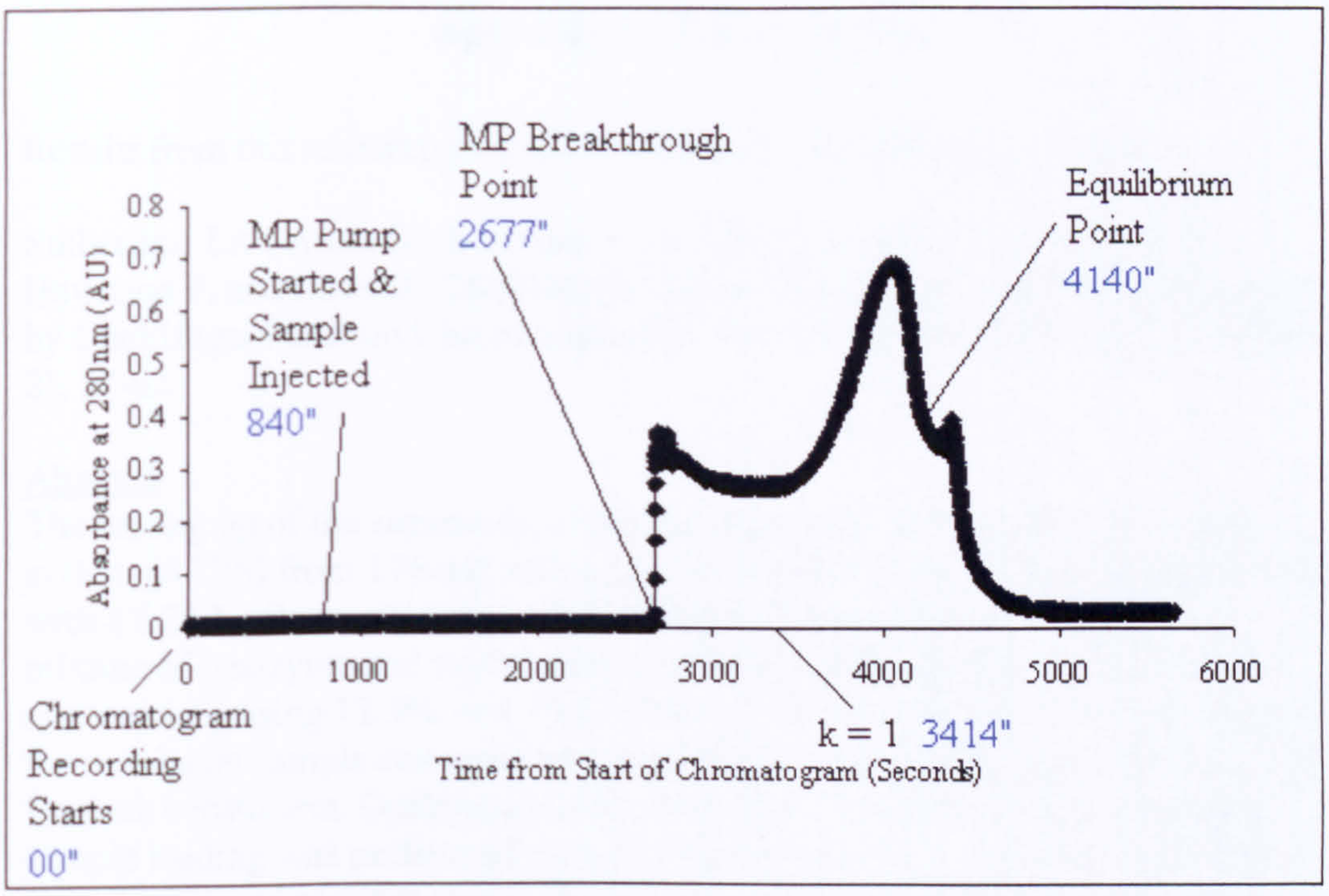

Figure 2A-s: Chromatogram from the experiments to determine the influence of loading sample volume. The experimental parameters were: rotational speed 2000 rpm; MP flow rate 10.0 $mlmin^{-1}$; LP was the MP (descending mode); sandwich injection. The sample volume was 86.0 ml or 20.0% of the column volume.

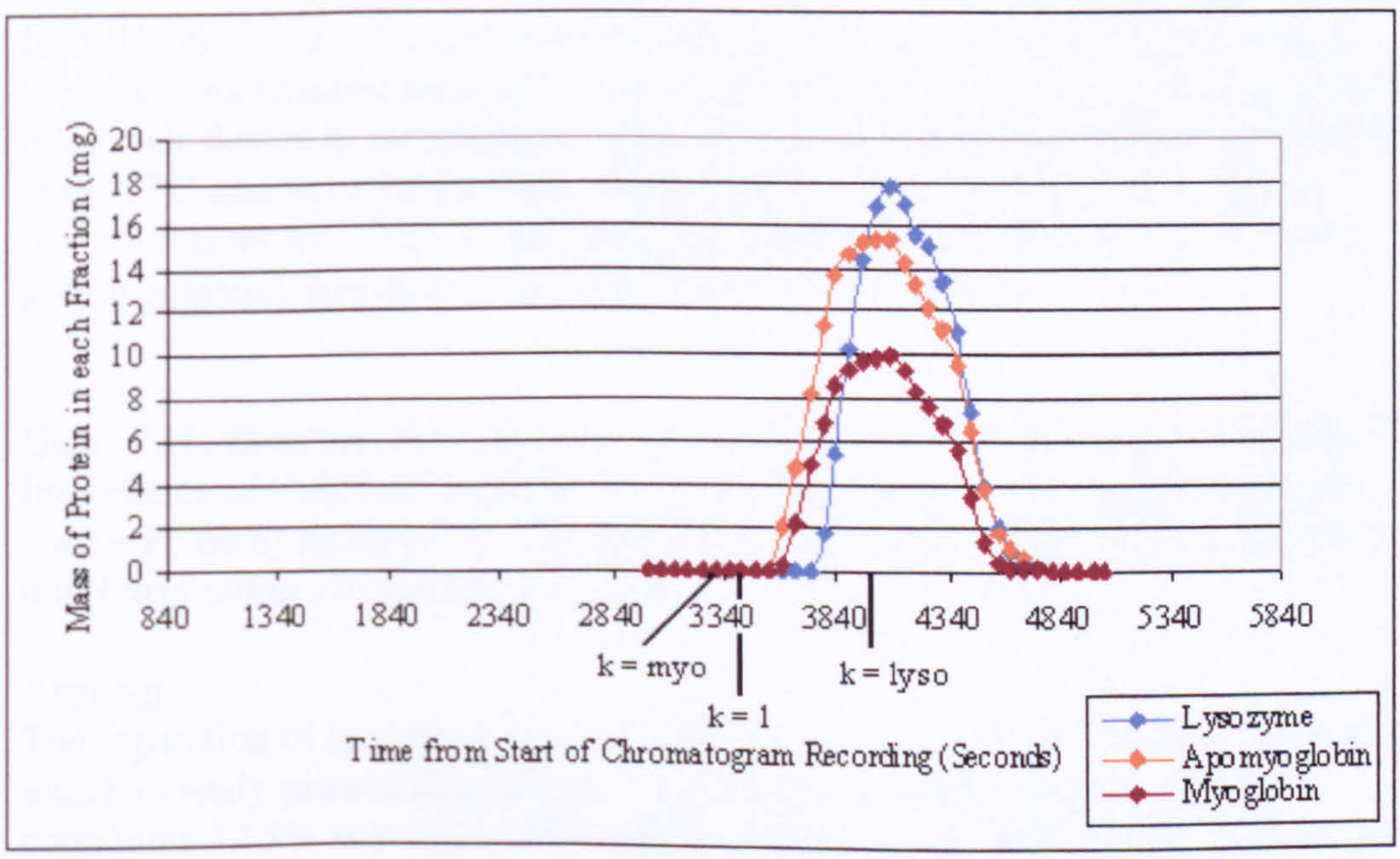

Figure 2A-t: Chromatogram created from HPLC analysis of fractions from the experiments to determine the influence of loading sample volume. The experimental parameters were: rotational speed 2000 rpm; MP flow rate 10.0 $mlmin^{-1}$; LP was the MP (descending mode); sandwich injection. The sample volume was 86.0 ml or 20.0% of the column volume.

Appendix 3 – Papers Written

Results from this research project contributed to the following papers:

Sutherland I.A., Audo G., **Bourton E.**, Couillard F., Fisher D., Garrard I., Hewitson P. and Intes O. (2008) Rapid Linear Scale – Up of a Protein Separation by Centrifugal Partition Chromatography. *Journal of Chromatography A* **1190** (1-2), 57-62.

Abstract

The scaling up of the separation of two proteins with an aqueous two – phase system (ATPS) from 176 mg with a 500 ml laboratory scale CPC column to 2.2 g with a 6.25 L pilot scale column is presented. A model sample system of a mixture of lysozyme and myoglobin was chosen for this study using an ATPS system comprising 12.5% w/w PEG-1000: 12.5% w/w K_2HPO_4. It was found that the maximum sample concentration possible without precipitation was 2.2 $mgml^{-1}$ for each constituent. Optimisation of rotor speed, mobile phase flow rate and sample loading was performed on a laboratory scale device. It was found that a centrifuge speed of 2000 rpm (224 'g'), 10 $mlmin^{-1}$ mobile phase flow rate with a 43 ml (10% of active column volume) sample volume gave optimum operating conditions.

This was linearly scaled up to pilot scale by increasing mobile phase flow rate, fraction size and sample loading in the ratio of the system capacities (*i.e.* 12.5:1). Flow rate was therefore increased from 10 $mlmin^{-1}$ to 125 $mlmin^{-1}$, fraction size from 10 ml to 125 ml and sample loading from 43 ml to 500 ml. Rotor speed however was reduced from 2000 rpm on the laboratory device to 1293 rpm on the pilot scale device to maintain the same 224 'g' field in each chamber, as the pilot scale CPC unit has a larger rotor radius than the laboratory one. Resolution increased from $Rs = 1.28$ on the 500 ml rotor to $Rs = 1.88$ on the 6.25 L rotor, giving potential throughputs in batch mode of over 40 g/day.

Guan Y.H., **Bourton E.C.**, Hewitson P., Sutherland I.A. and Fisher D. (2008) The Importance of Column Design for Scalable Protein Separation using Aqueous Two – Phase Systems on J – Type Countercurrent Chromatography. *Separation and Purification Technology* (Revised version under review).

Abstract

The separation of lysozyme and myoglobin has been used as a model system with which to study protein separation in aqueous two – phase systems (ATPS) containing 12.5% w/w PEG-1000 and 12.5% w/w K_2HPO_4 in Brunel multilayer J – type countercurrent chromatography (CCC) centrifuges, where wave mixing pertains. Poor separations of the proteins with this type of CCC columns were observed in ATPS and the proteins did not elute as predicted from their equilibrium partition coefficients. As mass transfer of the proteins appeared to be a limiting factor, methods of improving mixing of the phases in the J – type CCC were explored. This has led to the design, construction and application of a toroidal column fitted to the Brunel Dynamic Extraction Centrifuge, providing pseudo – hydrostatic CCC in which much improved mixing for the stationary and mobile phases was obtained. In this toroidal column the protein mixture was

separated with the locations of the protein peaks being consistent with those predicted by the partition coefficients. This toroidal coil system will form the basis for optimisation studies and scaling up separations.

Appendix 4 – References

Abbot N.L., Blankschtein D. and Hatton T.A. (1990). On protein partitioning in two – phase aqueous polymer systems. *Bioseparation* **1**, 191-225.

Albertsson P.- Å. (1956a). Chromatography and partition of cells and cell fragments. *Acta Chemica Scandinavica* **10**, 148.

Albertsson P.- Å. (1956b). Chromatography and partition of cells and cell fragments. *Nature* (*London*) **177**, 771-774.

Albertsson P.- Å. (1958a). Particle fractionation in liquid two – phase systems. The composition of some phase systems and the behaviour of some model particles in them. Application to the isolation of cell walls for microorganisms. *Biochimica et Biophysica Acta* **27**, 378-395.

Albertsson P.- Å. (1958b). Partition of proteins in liquid polymer – polymer two – phase systems. *Nature* (*London*) **182**, 709-711.

Albertsson P.- Å. (1962b). Partition methods for fractionation of cell particles and macromolecules. *Methods of Biochemical Analysis* **10**, 229-262.

Albertsson P.- Å. (1971a). Thin – layer countercurrent distribution. *Analytical Biochemistry* **11**, 121-125.

Albertsson P.- Å. (1971b). *Partition of Cell Particles and Macromolecules.* Second Edition. New York: John Wiley & Sons, Inc.

Albertsson P.- Å. (1986). *Partition of Cell Particles and Macromolecules.* Third Edition, New York: John Wiley & Sons, Inc.

Albertsson P.- Å. and Frick G. (1960). Partition of virus particles in a liquid two – phase system. *Biochimica et Biophysica Acta* **37**, 230-237.

Albertsson P.- Å., Johansson G. and Tjerneld F. (1990). *Aqueous Two Phase Separations*. In Asenjo J.A. (ed.) *Separation Processes in Biotechnology.* New York: Marcel Dekker. pp. 287-327.

Albertsson P.- Å. and Nyns E.J. (1959). Counter – current distribution of proteins in aqueous polymer phase systems. *Nature* (*London*) **184**, 1465-1468.

Albertsson P.- Å. and Nyns E.J. (1961). Partition of proteins in an aqueous phase system of dextran and polyethylene glycol. Influence of the electrolyte content. *Arkiv for Kemi* **17**, 197-206.

Al-Marzouqi I. (2006). *Recovery and purification of plasmid DNA gene therapy vectors using aqueous two – phase systems in a J – type countercurrent chromatograph.* Ph.D. Thesis, University College London.

Alred P.A., Kozlowski A., Harris J.M. and Tjerneld F. (1994). Application of temperature – induced phase partitioning at ambient temperature for enzyme purification. *Journal of Chromatography A* **659**, 289-298.

Alves J.G.L.F., Chumpitaz L.D.A., da Silva L.H.M., Franco T.T. and Meirelles A.J.A. (2000). Partitioning of whey proteins, bovine serum albumin and porcine insulin in aqueous two – phase systems. *Journal of Chromatography B* **743**, 235-239.

Ananthapadmanabhan K.P. and Goddard E.D. (1987) Aqueous biphase formation in polyethylene oxide – inorganic salt systems. *Langmuir* **3**, 25-31.

Andrews B.A., Nielson S. and Asenjo J.A. (1996). Partitioning and purification of monoclonal antibodies in aqueous two – phase systems. *Bioseparation* **6**, 303-313.

Andrews A.T., Schmidt A.S. and Asenjo J.A. (2005). Correlation for the partition behavior of proteins in aqueous two – phase systems: Effect of surface hydrophobicity and charge. *Biotechnology and Bioengineering* **90** (3), 380-390.

Attenborough S. (2006). [Discussion on the use of the phosphomannose isomerase gene by Syngenta Limited]. (Personal communication). Syngenta Limited, Jealott's Hill International Research Centre, Bracknell, Berkshire, UK RG42 6EY.

Backman L. (2000). Detection and analysis of interactions by two – phase partition. *In*: Hatti-Kaul R. (ed.) *Aqueous Two – Phase Systems: Methods and Protocols.* New Jersey: Humana Press. Chapter 20.

Beijerinck M.W. (1896). Ueber eine Eigentümlichkeit der löslichen Stärke. *Centralblatt für Bakteriologie, Parasitenkunde u. Infektionskrankheiten. Zweite Abteilung* **22**, 697-699.

de Belval S., le Breton B., Huddleston J. and Lyddiatt A. (1998). Influence of temperature upon protein partitioning in poly(ethylene glycol) – salt aqueous two – phase systems close to the critical point with some observations relevant to the partitioning of particles. *Journal of Chromatography B* **711**, 19-29.

Berggren K., Johansson H.-O. and Tjerneld F. (1995). Effects of salts and the surface hydrophobicity of proteins on partitioning in aqueous two – phase systems containing thermoseparating ethylene oxide – propylene oxide copolymers. *Journal of Chromatography A* **718**, 67-79.

Berggren K., Wolf A., Asenjo J.A., Andrews B.A. and Tjerneld F. (2002). The surface exposed amino acid residues of monomeric proteins determine the partitioning in aqueous two – phase systems. *Biochimica et Biophysica Acta* **1596**, 253-268.

Berthod A. (2002). Fundamentals of countercurrent chromatography. In: Berthod A. (ed.) *Countercurrent Chromatography. The Support – Free Liquid Stationary Phase*. Volume XXXVIII of *Wilson & Wilson's Comprehensive Analytical Chemistry*. First Edition. Amsterdam: Elsevier Science B.V. Chapter 1.

Berthod A. and Talabardon K. (1999). Centrifugal partition chromatography: Operating parameters and partition coefficient determination. *In*: Menet J.-M. and Thiébaut D. (eds.) *Countercurrent Chromatography.* Volume 82 of *Chromatographic Science Series.* New York: Marcel Dekker. Chapter 4.

Björk J., Lundberg S. and Backman L. (1995). Characterization of the binding of calmodulin to non – erythroid spectrin. *European Journal of Cell Biology* **66**, 200-204.

Boaglio A., Bassani G., Picó G. and Nerli B. (2006). Features of the milk whey protein partitioning in polyethyleneglycol – sodium citrate aqueous two – phase systems with the goal of isolating human alpha-1 antitrypsin expressed in bovine milk. *Journal of Chromatography B* **837**, 18-23.

Bolognese B., Nerli B. and Picó G. (2005). Application of the aqueous two – phase systems of ethylene and propylene oxide copolymer – maltodextrin for protein purification. *Journal of Chromatography B* **814**, 347-353.

Booth A.J., Ngiam S.H. and Lye G.J. (2004). Antibiotic purification from fermentation broths by counter – current chromatography: Analysis of product purity and yield trade – offs. *Bioprocess and Biosystems Engineering* **27**, 51-61.

Booth A.J., Sutherland I.A. and Lye G.J. (2003). Modeling the performance of pilot – scale countercurrent chromatograph: Scale – up predictions and experimental verification of erythromycin separation. *Biotechnology and Bioengineering* **81** (6), 640-649.

Bradford M.M. (1976). A rapid and sensitive method for the quantitation of microgram quantities of protein utilizing the principle of protein – dye binding. *Analytical Biochemistry* **72** (1-2), 248-254.

Brooks D.E. and Norris-Jones R. (2000). Measurement of some physical properties of aqueous two – phase systems. *In*: Hatti-Kaul R. (ed.) *Aqueous Two – Phase Systems: Methods and Protocols.* New Jersey: Humana Press. Chapter 4.

Brumbauer A., Johansson G. and Réczey K. (1999). Fractionation of cellulase and β-glucosidase in a *Trichoderma reesei* culture liquid by use of two – phase partitioning. *Bioseparation* **7**, 287-295.

Brumbauer A., Johansson G. and Réczey K. (2000). Study on heterogeneity of β-glucosidase from *Aspergillus* species by using counter – current distribution. *Journal of Chromatography B* **743**, 247-254.

van Buel M.J., van Halsema F.E.D., van der Wielen L.A.M. and Luyben K.Ch.A.M. (1998). Flow regimes in centrifugal partition chromatography. *AIChE Journal* **44** (6), 1356-1362.
Carlsson M., Linse P. and Tjerneld F. (1993). Temperature – dependent protein partitioning in two – phase aqueous polymer systems. *Macromolecules* **26**, 1546-1554.

Cascone O., Andrews B.A. and Asenjo J.A. (1991). Partitioning and purification of thaumatin in aqueous two – phase systems. *Enzyme and Microbial Technology* **13**, 629-635.

Chen J., Ma G.X. and Li D.Q. (1999). HPCPC separation of proteins using polyethylene glycol – potassium phosphate aqueous two – phase. *Preparative Biochemistry and Biotechnology* **29** (4), 371-383.

Conway W.D. (1990). *Countercurrent Chromatography. Apparatus, Theory, and Applications.* First Edition. New York: VCH Publishers Inc.

Conway W.D. and Ito Y. (1984). Phase distribution of liquid – liquid systems in spiral and multilayer helical coils on a centrifugal countercurrent chromatograph. *Presented at Pittsburgh Conference, Atlantic City, NJ, USA, March 1984.*

Dallora N.L.P., Klemz J.G.D. and Filho P. de A. P. (2007). Partitioning of model proteins in aqueous two – phase systems containing polyethylene glycol and ammonium carbamate. *Biochemical Engineering Journal* **34**, 92-97.

Dissing U. and Mattiasson B. (1994). Partition of proteins in polyelectrolyte – neutral polymer aqueous two – phase systems. *Bioseparation* **4**, 335-342.

Engel S., Barak Z., Chipman D.M. and Merchuk J.C. (2000). Purification of acetohydroxy acid synthase by separation in an aqueous two – phase system. *Journal of Chromatography B* **743**, 281-286.

Fahey J.W., Wade K.L., Stephenson K.K. and Chou F.E. (2003). Separation and purification of glucosinolates from crude plant homogenates by high – speed counter – current chromatography. *Journal of Chromatography A* **996**, 85-93.

Fexby S. and Bülow L. (2002). Improved partitioning in aqueous two – phase system of tyrosine – tagged recombinant lactate dehydrogenase. *Protein Expression and Purification* **25**, 263-269.

Fisher D. (1981). The separation of cells and organelles by partitioning in two – polymer aqueous phases. *Biochemical Journal* **196**, 1-10.

Fisher D., Garrard I.J., van den Heuvel R., Sutherland I.A., Chou F.E. and Fahey J.W. (2005). Technology transfer and scale up of a potential cancer – preventive plant secondary metabolite glucoraphanin. *Journal of Liquid Chromatography and Related Technologies* **28**, 1913-1922.

Flanagan S.D., Johansson G., Yost B., Ito Y. and Sutherland I.A. (1984). Toroidal coil countercurrent chromatography in the affinity partitioning of nicotinic cholinergic receptor enriched membranes. *Journal of Liquid Chromatography* **7** (2), 385-402.
Flory P.J. (1953). *Principles of Polymer Chemistry.* New York: Cornell University Press.

Foucault A.P., Bousquet O. and le Goffic F. (1992a). Importance of the parameter Vm/Vc in countercurrent chromatography: Tentative comparison between instrument designs. *Journal of Liquid Chromatography* **15** (15&16), 2691-2706

Foucault A.P., Bousquet O., le Goffic F. and Cazes J. (1992b). Countercurrent chromatography with a new centrifugal partition chromatographic system. *Journal of Liquid Chromatography* **15** (15&16), 2721-2733.

Franco T.T., Andrews A.T. and Asenjo J.A. (1996). Use of chemically modified proteins to study the effect of a single protein property on partitioning in aqueous two – phase systems: Effect of surface hydrophobicity. *Biotechnology and Bioengineering* **49**, 300-308.

Großmann C. and Maurer G. (1995). On the calculation of phase equilibria in aqueous two – phase systems containing ionic solutes. *Fluid Phase Equilibria* **106**, 17-25.

Großmann C., Tintinger R., Zhu J. and Maurer G. (1995). Aqueous two – phase systems of poly(ethylene glycol) and dextran – experimental results and modeling of thermodynamic properties. *Fluid Phase Equilibria* **106**, 111-138.

Grunfeld H., Patel A., Shatzman A. and Nishikawa A.H. (1992). Effector – assisted refolding of recombinant tissue – plasminogen activator produced in *Escherichia coli*. *Applied Biochemistry and Biotechnology* **33**, 117-137.

Guan Y.H., Smulders J., Fisher D. and Sutherland I.A. (2007). Spiral coils for counter – current chromatography using aqueous polymer two – phase systems. *Journal of Chromatography A* **1151** (1-2), 115-120.

Gupta V., Nath S. and Chand S. (2002). Role of water structure on phase separation in polyelectrolyte – polyethylene glycol based aqueous two – phase systems. *Polymer* **43**, 3387-3390.

Haghtalab A., Mokhtarani B. and Maurer G. (2003). Experimental results and thermodynamic modeling of the partitioning of lysozyme, bovine serum albumin, and α-amylase in aqueous two – phase systems of PEG and (K_2HPO_4 or Na_2SO_4). *Journal of Chemical and Engineering Data* **48**, 1170-1177.

Hammar L., Eriksson S., Malm K. and Morein B. (1989). Concentration and purification of feline leukaemia virus (FeLV) and its outer envelope protein gp70 by aqueous two – phase systems. *Journal of Virological Methods* **24**, 91-102.

Hartounian H., Floeter E., Kaler E.W. and Sandler S.I. (1993). Effect of temperature on the phase equilibrium of aqueous two – phase polymer systems. *AIChE Journal* **39** (12), 1976-1984.

Hatti-Kaul R. (2000). Aqueous two – phase systems: A general overview. *In*: Hatti-Kaul R. (ed.) *Aqueous Two – Phase Systems: Methods and Protocols.* New Jersey: Humana Press. Chapter 1.

Heywood-Waddington D., Peters T.J. and Sutherland I.A. (1986). The dynamics of phase partition – a study of parameters affecting rat liver organelle partitioning in aqueous two – polymer phase systems. *Biochemical Journal* **235**, 245-249.

Heywood-Waddington D., Sutherland I.A., Morris W.B. and Peters T.J. (1984). Subcellular fractionation of rat liver homogenates using two – polymer phase systems in a toroidal – coil centrifuge. *Biochemical Journal* **217**, 751-759.

Heywood-Waddington D., Sutherland I.A. and Peters T.J. (1988). Sub – fractionation of rat liver microsomes by two – polymer phase partition in a toroidal coil centrifuge. *Biochemical Society Transactions* **16** (1), 34-35.

Huddleston J., Abelaira J.C., Wang R. and Lyddiatt A. (1996). Protein partition between the different phases comprising poly(ethylene glycol) – salt aqueous two – phase systems, hydrophobic interaction chromatography and precipitation: A generic description in terms of salting – out effects. *Journal of Chromatography B* **680**, 31-41.

Huddleston J., Veide A., Köhler K., Flanagan J., Enfors S.-O. and Lyddiat A. (1991). The molecular basis of partitioning in aqueous two – phase systems. *Trends in Biotechnology* **9**, 381-388.

Hustedt H. (1986). Extractive enzyme recovery with simple recycling of phase forming chemicals. *Biotechnology Letters* **8**, 791-796

Hustedt H., Kroner K.H. and Kula M.-R. (1985). Applications of phase partitioning in biotechnology. *In*: Walter H., Brooks D.E. and Fisher D. (eds.) *Partitioning in Aqueous Two – Phase Systems. Theory, Methods, Uses, and Applications to Biotechnology.* London: Academic Press, Inc. Chapter 15.

Ignatova S., Garrard I.J., Wood P., Janaway L., Fisher D. and Sutherland I.A. [Unpublished results from work conducted in 2005 to purify a 1 kg quantity of glucoraphanin]. (Personal communication). Brunel Institute for Bioengineering, Brunel University, Uxbridge, Middlesex, UK UB8 3PH.

Ikehata J.-I., Shinomiya K., Kobayashi K., Ohshima H., Kitanaka S. and Ito Y. (2004). Effect of Coriolis force on counter – current chromatographic separation by centrifugal partition chromatography. *Journal of Chromatography A* **1025**, 169-175.

Ito Y. (1977). *Toroidal coil planet centrifuge.* US Department Health Education & Welfare. US-04228009.

Ito Y. (1987). Cross – axis synchronous flow – through coil planet centrifuge free of rotary seals for preparative countercurrent chromatography. Part I: Apparatus and analysis of acceleration. *Separation Science and Technology* **22** (8-10), 1971-1987.

Ito Y. (1988). Principles and instrumentation of countercurrent chromatography. *In*: Mandava N.B. and Ito Y. (eds.) *Countercurrent Chromatography. Theory and Practice.* Volume 44 of *Chromatographic Science Series.* New York: Marcel Dekker. Chapter 3.

Ito Y. (1992). Speculation on the mechanism of unilateral hydrodynamic distribution of two immiscible solvent phases in the rotating coil. *Journal of Liquid Chromatography and Related Technologies* **15** (15&16), 2639-2675.

Ito Y., Carmeci P. and Sutherland I.A. (1979). Nonsynchronous flow – through coil planet centrifuge applied to cell separation with physiological solution. *Analytical Biochemistry* **94**, 249-252.

Ito Y., Matsuda K., Ma Y. and Qi L. (1998). Toroidal counter – current chromatography study of the mass transfer rate of proteins in aqueous – aqueous polymer systems. *Journal of Chromatography A* **802** (2), 277-283.

Ito Y. and Oka H. (1988). Horizontal flow – through coil planet centrifuge equipped with a set of multilayer coils around the column holder. *Journal of Chromatography* **457**, 393-397.

Ito Y., Weinstein M.A., Aoki I., Harada R., Kimura E. and Nunogaki K. (1966) The coil planet centrifuge. *Nature* **212** (5066), 985-987.

Ito Y., Yang F., Fitze P.E. and Sullivan J.V. (2003). Spiral disk assembly for HSCCC: Column design and basic studies on chromatographic resolution and stationary phase retention. *Journal of Liquid Chromatography and Related Technologies* **26** (9&10), 1355-1372.

Jayapal M., Regupathi I. and Murugesan T. (2007). Liquid – liquid equilibrium of poly(ethylene glycol)-2000 + potassium citrate + water at (25, 35, and 45)°C. *Journal of Chemical and Engineering Data* **52**, 56-59.

Johansson G. (1970a). Partition of salts and their effects on partition of proteins in a dextran – poly(ethylene glycol) – water two – phase system. *Biochimica et Biophysica Acta* **221**, 387-390.

Johansson G. (1985). Partitioning of proteins. *In*: Walter H., Brooks D.E. and Fisher D. (eds.) *Partitioning in Aqueous Two – Phase Systems. Theory, Methods, Uses, and Applications to Biotechnology.* London: Academic Press, Inc. Chapter 6.

Johansson G., Andersson M. and Åkerlund H.-E. (1984). Counter – current distribution of yeast enzymes with polymer – bound triazine dye affinity ligands. *Journal of Chromatography* **298**, 483-493.

Johansson H.-O., Karlström G., Tjerneld F. and Haynes C.A. (1998). Driving forces for phase separation and partitioning in aqueous two – phase systems. *Journal of Chromatography B* **711**, 3-17.

Johansson H.-O., Lundh G., Karlström G. and Tjerneld F. (1996). Effects of ions on partitioning of serum albumin and lysozyme in aqueous two – phase systems containing ethylene oxide/propylene oxide co – polymers. *Biochimica et Biophysica Acta* **1290**, 289-298.

Johansson G. and Reczey K. (1998). Concentration and purification of β-glucosidase from *Aspergillus niger* by using aqueous two – phase partitioning. *Journal of Chromatography B* **711**, 161-172.

Kajiuchi T., Shin-Ya Y., Nagai H. and Fujiwara K. (2002). Partitioning of chicken egg white proteins in polyelectrolyte/salt aqueous two – phase systems composed of polyethyleneoxide – maleic acid copolymer and potassium phosphate. *Journal of Chemical Technology and Biotechnology* **77**, 495-499.

Kaul A. (2000). The phase diagram. *In*: Hatti-Kaul R. (ed.) *Aqueous Two – Phase Systems: Methods and Protocols.* New Jersey: Humana Press. Chapter 2.

Kaul A., Pereira R.A.M., Asenjo J.A. and Merchuk J.C. (1995). Kinetics of phase separation for polyethylene glycol – phosphate two – phase systems. *Biotechnology and Bioengineering* **48**, 246-256.

Kuhlmann W., Halwachs W. and Schügerl K. (1980). Racemat – Spaltung von Aminosäuren durch Immobilisierung von Acylase im wäßrigen Zweiphasensystem. *Chemie Ingenieur Technik* **52**, 607 and *MS* 821/80.

Li M. and Peeples T.L. (2004). Purification of hyperthermophilic archaeal amylolytic enzyme (MJA1) using thermoseparating aqueous two – phase systems. *Journal of Chromatography B* **807**, 69-74.

Magri M.L., Cabrera R.B., Miranda M.V., Fernández-Lahore H.M. and Cascone O. (2003). Performance of an aqueous two – phase – based countercurrent chromatographic system for horseradish peroxidase purification. *Journal of Seperation Science* **26**, 1701-1706.

Marchal L., Foucault A., Patissier G., Rosant J.M. and Legrand J. (2000). Influence of flow patterns on chromatographic efficiency in centrifugal partition chromatography. *Journal of Chromatography A* **869**, 339-352.

Marchal L., Foucault A.P., Patissier G., Rosant J.-M. and Legrand J. (2002a). *Centrifugal Partition Chromatography: An Engineering Approach.* In Berthod A. (ed.) *Countercurrent Chromatography. The Support – Free Liquid Stationary Phase.* Volume XXXVIII of *Wilson & Wilson's Comprehensive Analytical Chemistry.* Amsterdam: Elsevier Science B.V. pp. 115-157.

Marchal L., Legrand J. and Foucault A. (2002b). Mass transport and flow regimes in centrifugal partition chromatography. *AIChE Journal* **48** (8), 1692-1704.

Marcos J.C., Fonseca L.P., Ramalho M.T. and Cabral J.M.S. (1998). Variation of penicillin acylase partition coefficient with phase volume ratio in poly(ethylene glycol) – sodium citrate aqueous two – phase systems. *Journal of Chromatography B* **711**, 295-299.

Margraff R., Intes O., Renault J.-H. and Garret P. (2005). Partitron 25, a multi – purpose industrial centrifugal partition chromatograph: Rotor design and preliminary results on efficiency and stationary phase retention. *Journal of Liquid Chromatography and Related Technologies* **28**, 1893-1902.

Maryutina T.A., Ignatova S.N. and Sutherland I.A. (2003). Organic phase retention in CCC: Effect of temperature, tubing material, tubing bore, mobile phase flow, and the addition of an extraction agent. *Journal of Liquid Chromatography and Related Technologies* **26** (9&10), 1537-1550.

Menet J.-M., Thiébaut D., Rosset R., Wesfreid J.E. and Martin M. (1994). Classification of countercurrent chromatography solvent systems on the basis of the capillary wavelength. *Analytical Chemistry* **66**, 168-176.

Miranda M.V., Lahore H.M.F. and Cascone O. (1996). Partition behaviour of thaumatin derivatives in poly(ethyleneglycol)/salt aqueous two – phase systems. *Bioseparation* **6**, 315-321.

Mishima K., Matsuyama K., Ezawa M., Taruta Y., Takarabe S. and Nagatani M. (1998). Interfacial tension of aqueous two – phase systems containing poly(ethylene glycol) and dipotassium hydrogen phosphate. *Journal of Chromatography B* **711**, 313-318.

Murayama W., Kobayashi T., Kosuge Y., Yano H., Nunogaki Y. and Nunogaki K. (1982). A new centrifugal counter – current chromatograph and its application. *Journal of Chromatography* **239**, 643-649.

Okazaki T. and Kornberg A. (1964). Enzymatic synthesis of deoxyribonucleic acid. XV. Purification and properties of a polymerase from *Bacillus subtilis*. *Journal of Biological Chemistry* **239**, 259-268.

Pan I.-H. and Li Y.-K. (2001). Rapid process for purification of an extracellular β-xylosidase by aqueous two – phase extraction. *Journal of Chromatography B* **754**, 179-184.

Pan I.-H., Yao H.-J. and Li Y.-K. (2001). Effective extraction and purification of β-xylosidase from *Trichoderma koningii* fermentation culture by aqueous two – phase partitioning. *Enzyme and Microbial Technology* **28**, 196-201.

Papamichael N., Börner B. and Hustedt H. (1992). Continuous aqueous phase extraction of proteins: Automated processing and recycling of process chemicals. *Journal of Chemical Technology and Biotechnology* **54**, 47-55.

Pereira M., Wu Y.-T., Venâncio A. and Teixeira J. (2003). Aqueous two – phase extraction using thermoseparating polymer: A new system for the separation of endo – polygalacturonase. *Biochemical Engineering Journal* **15**, 131-138.

Persson J., Johansson H.-O. and Tjerneld F. (1999). Purification of protein and recycling of polymers in a new aqueous two – phase system using two thermoseparating polymers. *Journal of Chromatography A* **864**, 31-48.

Privalle L.S., Wright M., Reed J., Hansen G., Dawson J., Dunder E.M., Chang Y.-F., Luann Powell M. and Meghji M. (2000). Phosphomannose isomerase, a novel selectable plant selection system: Mode of action and safety assessment. *In*: Fairbairn C., Scoles G. and McHughen A. (eds.) *Proceedings of the 6th International Symposium on the Biosafety of Genetically Modified Organisms, Saskatoon, Canada.* University of Saskatchewan: University Extension Press. pp. 171-178.

Ryden J. and Albertsson P.- Å. (1971). Interfacial tension of dextran – polyethylene glycol – water two – phase systems. *Journal of Colloid and Interface Science* **37** (1), 219-222.

Reh G., Nerli B. and Picó G. (2002). Isolation of alpha-1-antitrypsin from human plasma by partitioning in aqueous biphasic systems of polyethyleneglycol – phosphate. *Journal of Chromatography B* **780**, 389-396.
Rito-Palomares M. and Lyddiatt A. (2000). Practical implementation of aqueous two – phase processes for protein recovery from yeast. *Journal of Chemical Technology and Biotechnology* **75**, 632-638.

Rodenbrock A., Selber K., Egmond M.R. and Kula M.-R. (2001). Extraction of peptide tagged cutinase in detergent – based aqueous two – phase systems. *Bioseparation* **9**, 269-276.

Rydén J. and Albertsson P.- Å. (1971). Interfacial tension of dextran – polyethylene glycol – water two – phase systems. *Journal of Colloid and Interface Science* **37**, 219-222.

Schmidt A.S., Ventom A.M. and Asenjo J.A. (1994). Partition and purification of α-amylase in aqueous two – phase systems. *Enzyme and Microbial Technology* **16**, 131-142.

Shibusawa Y. and Ito Y. (1991). Protein separation with aqueous – aqueous polymer systems by two types of counter – current chromatographs. *Journal of Chromatography* **550**, 695-704.

Shibusawa Y., Takeuchi N., Tsutsumi K., Nakano S., Yanagida A., Shindo H. and Ito Y. (2007). One – step purification of histone deacetylase from *Escherichia coli* cell – lysate by counter – current chromatography using aqueous two – phase system. *Journal of Chromatography A* **1151** (1-2), 158-163.

Shinomiya K., Hirozane S., Kabasawa Y. and Ito Y. (2000). Protein separation by cross – axis coil planet centrifuge with two different positions of eccentric coil assemblies using polyethylene glycol – dextran solvent system. *Journal of Liquid Chromatography and Related Technologies* **27** (7), 1119-1129.

Shinomiya K., Inokuchi N., Gnabre J.N., Muto M., Kabasawa Y., Fales H.M. and Ito Y. (1996a). Countercurrent chromatographic analysis of ovalbumin obtained from various sources using the cross – axis coil planet centrifuge. *Journal of Chromatography A* **724**, 179-184.

Shinomiya K. and Ito Y. (2004). Effects of the planetary motion of a coiled column on protein separation by the nonsynchronous coil planet centrifuge. *Journal of Liquid Chromatography and Related Technologies* **27** (20), 3243-3255.

Shinomiya K., Kabasawa Y. and Ito Y. (1998). Protein separation by cross – axis coil planet centrifuge with two different types of coiled columns. *Journal of Liquid Chromatography and Related Technologies* **21** (1&2), 111-120.

Shinomiya K., Kabasawa Y. and Ito Y. (1999). Effect of elution modes on protein separation by cross – axis coil planet centrifuge with two different types of coiled columns. *Preparative Biochemistry and Biotechnology* **29** (2), 139-150.

Shinomiya K., Kabasawa Y. and Ito Y. (2002). Protein separation by cross – axis coil planet centrifuge with spiral column assemblies. *Journal of Liquid Chromatography and Related Technologies* **25** (17), 2665-2678.

Shinomiya K., Kabasawa Y., Yanagidaira K., Sasaki H., Muto M., Okada T. and Ito Y. (2003). Protein separation by nonsynchronous coil planet centrifuge with aqueous – aqueous polymer phase systems. *Journal of Chromatography A* **1005** (1-2), 103-112.

Shinomiya K., Menet J.-M., Fales H.M. and Ito Y. (1993). Studies on a new cross – axis coil planet centrifuge for performing counter – current chromatography. I. Design of the apparatus, retention of the stationary phase, and efficiency in the separation of proteins with polymer phase systems. *Journal of Chromatography* **644**, 215-229.

Shinomiya K., Muto M., Kabasawa Y., Fales H.M. and Ito Y. (1996b). Protein separation by improved cross – axis coil planet centrifuge with eccentric coil assemblies. *Journal of Liquid Chromatography and Related Technologies* **19** (3), 415-425.

Skoog D.A., West D.M. and Holler F.J. (1994). *Analytical Chemistry. An Introduction.* Sixth Edition. Saunders College Publishing.

Snyder S.M., Cole K.D. and Sziag D.C. (1992). Phase compositions, viscosities, and densities for aqueous two – phase systems composed of polyethylene glycol and various salts at 25°C. *Journal of Chemical and Engineering Data* **37**, 268-274.

Solano-Castillo C. and Rito-Palomares M. (2000). Kinetics of phase separation under different process and design parameters in aqueous two – phase systems. *Journal of Chromatography B* **743**, 195-201.

Su C.-K. and Chiang B.H. (2006). Partitioning and purification of lysozyme from chicken egg white using aqueous two – phase system. *Process Biochemistry* **41**, 257-263.

Sutherland I.A. (2007). Review of centrifugal liquid – liquid chromatography using aqueous two – phase solvent systems: Its scale – up and prospects for the future production of high – value biologicals. *Current Opinion in Drug Discovery & Development*. **10** (5), 540-549.

Sutherland I.A., Audo G., Bourton E.C., Couillard F., Fisher D., Garrard I., Hewitson P. and Intes O. (2008). Rapid linear scale – up of a protein separation by centrifugal partition chromatography. *Journal of Chromatography A* (In press).

Sutherland I.A., Booth A.J., Brown L., Kemp B., Kidwell H., Games D., Graham A.S., Guillon G.G., Hawes D., Hayes M., Janaway L., Lye G.J., Massey P., Preston C., Shering P., Shoulder T., Strawson C. and Wood P. (2001b). Industrial scale – up of countercurrent chromatography. *Journal of Liquid Chromatography and Related Technologies* **24** (11&12), 1533-1553.

Sutherland I.A., Brown L., Graham A.S., Guillon G.G., Hawes D., Janaway L., Whiteside R. and Wood P. (2001a). Industrial scale – up of countercurrent chromatography: Predictive scale – up. *Journal of Chromatographic Science* **39**, 21-28.

Sutherland I.A., de Folter J. and Wood P.L. (2003). Modelling CCC using an eluting countercurrent distribution model. *Journal of Liquid Chromatography and Related Technologies* **26** (9&10), 1449-1474.

Sutherland I.A., Hawes D., Ignatova S., Janaway L. and Wood P. (2005). Review of progress toward the industrial scale – up of CCC. *Journal of Liquid Chromatography and Related Technologies* **28**, 1877-1891.

Sutherland I.A., Hawes D., Janaway L., Tinnion E., Kidwell H. and Wood P. (2001c). From analytical to process scale liquid – liquid countercurrent chromatography (CCC) with 100% sample recovery – Is it feasible? *Analytical Sciences* **17** Supplement, i765-i767.

Sutherland I.A., Heywood-Waddington D. and Ito Y. (1987). Counter – current chromatography: Applications to the separation of biopolymers, organelles and cells using either aqueous – organic or aqueous – aqueous phase systems. *Journal of Chromatography* **384**, 197-207.

Sutherland I.A., Heywood-Waddington D. and Peters T.J. (1984). Toroidal coil countercurrent chromatography: A fast simple alternative to countercurrent distribution using aqueous two phase partition. *Journal of Liquid Chromatography* **7** (2), 363-384.

Sutherland I.A., Heywood-Waddington D. and Peters T.J. (1985). Countercurrent chromatography using a toroidal coil planet centrifuge: A comparative study of the separation of organelles using aqueous two – phase partition. *Journal of Liquid Chromatography* **8** (12), 2315-2335.

Sutherland I.A. and Ito Y. (1978). Toroidal coil chromatography. A new high – speed, high – resolution method of separating cells and cell organelles on their distribution in two – phase polymer systems. *Journal of High Resolution Chromatography & Chromatography Communications* **1** (3), 171-172.

Sutherland I.A., Muytjens J., Prins M. and Wood P. (2000). A new hypothesis on phase distribution in countercurrent chromatography. *Journal of Liquid Chromatography and Related Technologies* **23** (15), 2259-2276.

Sutherland I.A. and Wood P.L. (1999). A new perspective on the mechanism of mixing and settling in countercurrent chromatography using a J – type coil planet centrifuge. *In: Proceedings of Pittsburgh Conference CCC Session, Orlando, Florida, March 10th 1999.*

Tanimura T., Pisano J.J., Ito Y. and Bowman R.L. (1970). Droplet countercurrent chromatography. *Science* **169**, 54-56.

Tjerneld F., Berner S., Cajarville A. and Johansson G. (1986). New aqueous two – phase system based on hydroxypropyl starch useful in enzyme purification. *Enzyme and Microbial Technology* **8**, 417-423.

Tubío G., Nerli B. and Picó G. (2007). Partitioning features of bovine trypsin and α-chymotrypsin in polyethyleneglycol – sodium citrate aqueous two – phase systems. *Journal of Chromatography B* **852**, 244-249.

Veide A., Smeds A.-L. and Enfors S.-O. (1983). A process for large – scale isolation of β-galactosidase from *E. coli* in an aqueous two – phase system. *Biotechnology and Bioengineering* **25**, 1789-1800.

Vernau J. and Kula M.-R. (1990). Extraction of proteins from biological raw material using aqueous polyethylene glycol – citrate phase systems. *Biotechnology and Applied Biochemistry* **12**, 397-404.

Vonnegut B. (1942). Rotating bubble method for the determination of surface and interfacial tensions. *Review of Scientific Instruments* **13**, 6.

Walter H., Brooks D.E. and Fisher D. (eds.) (1985). *Partitioning in Aqueous Two – Phase Systems. Theory, Methods, Uses, and Applications to Biotechnology.* London: Academic Press, Inc.

Walter H. and Johansson G. (eds.) (1994). *Methods in Enzymology: Aqueous Two – Phase Systems.* San Diego: Academic Press Inc.

Wood P.L. (2002). *The hydrodynamics of countercurrent chromatography in J – type centrifuges.* Ph.D. Thesis, Brunel University.

Yamazaki Y. and Suzuki H. (1979). An attempt of new enzyme reactor based on aqueous two – phase systems. *Report of the Fermentation Research Institute (Chiba, Japan)* **52**, 33-40.

Yanagida A., Isozaki M., Shibusawa Y., Shindo H. and Ito Y. (2004). Purification of glucosyltransferase from cell – lysate of *Streptococcus mutans* by counter – current chromatography using aqueous polymer two – phase system. *Journal of Chromatography B* **805**, 155-160.

Zafarani-Moattar M.T. and Sadeghi R. (2001). Liquid – liquid equilibria of aqueous two – phase systems containing polyethylene glycol and sodium dihydrogen phosphate or disodium hydrogen phosphate. Experiment and correlation. *Fluid Phase Equilibria* **181**, 95-112.

Zhi W., Deng Q., Song J., Gu M. and Ouyang F. (2005). One – step purification of α-amylase from the cultivation supernatant of recombinant *Bacillus subtilis* by high – speed counter – current chromatography with aqueous polymer two – phase systems. *Journal of Chromatography A* **1070**, 215-219.